In vitro studies and in vivo evaluation of novel diamidines for 2nd stage sleeping sickness

INAUGURALDISSERTATION

zur

Erlangung der Würde eines Doktors der Philosophie

vorgelegt der

Philosophisch-Naturwissenschaftlichen Fakultät

der Universität Basel

von

Tanja Wenzler

aus Deutschland

Basel, 2014

Genehmigt von der Philosophisch-Naturwissenschaftlichen Fakultät
auf Antrag von
Prof. Dr. Reto Brun und Prof. Dr. Simon Croft

Basel, den 10. Dezember 2013

Prof. Dr. Jörg Schibler
Dekan

Table of Contents

Abbreviations 1

Summary 3

Zusammenfassung 5

Chapter 1 9
Introduction

Chapter 2 29
Antiparasitic agents: new drugs on the horizon.

Chapter 3 35
New treatment option for second-stage African sleeping sickness:
in vitro and in vivo efficacy of aza analogs of DB289.

Chapter 4 43
Synthesis and antiprotozoal activity of dicationic 2,6-diphenylpyrazines and
aza-analogues.

Chapter 5 53
Aquaporin 2 mutations in *Trypanosoma brucei gambiense* field isolates correlate
with decreased susceptibility to pentamidine and melarsoprol,

Chapter 6 61
Isothermal Microcalorimetry, a New Tool to Monitor Drug Action against
Trypanosoma brucei and *Plasmodium falciparum*.

Chapter 7 69
Pharmacokinetics, *T. b. gambiense* efficacy and time of drug action of DB829,
a preclinical candidate for treatment of second stage human African trypanosomiasis.

Chapter 8 83
Synthesis and Antiprotozoal Activity of Dicationic m-Terphenyl and 1,3-Dipyridylbenzene Derivatives

Chapter 9 105
In vitro and in vivo evaluation of 28DAP010, a novel diamidine for the treatment of second stage African sleeping sickness

Chapter 10 117
General Discussion and Conclusion

Acknowledgments 135

Curriculum vitae 137

Abbreviations

AT1	adenosine transporter 1
AUC	area under the curve
AQP	aquaporin
BBB	blood brain barrier
BID	dosing twice a day
BSF	blood stream forms
CATT	Card Agglutination Test for Trypanosomiasis
CL	total body clearance
C_{max}	peak concentration
CNS	central nervous system
CPDD	Consortium for Parasitic Drug Development
CSF	cerebrospinal fluid
DB75	furamidine
DB289	pafuramidine maleate
DMSO	dimethylsulfoxid
DNA	deoxyribonucleic acid
FDA	Food and Drug Administration
$F_{u,P}$	unbound fraction in plasma
h	hour
HAT	Human African trypanosomiasis
IC_{50}	50% inhibitory concentration
I.M	intramuscular (injection into a muscle)
I.P.	intraperitoneal (injection into the peritoneum)
I.V.	intravenous (injection into the vein)
kDNA	kinetoplast deoxyribonucleic acid
KO	knock-out
Mel	melarsoprol
MRD	mean relapse day
MSD	mean survival day
NECT	nifurtimox eflornithine combination therapy
P2	purine transporter 2
Pent	pentamidine

PK	pharmacokinetics
P.O.	oral
RF	resistance factor
SD	standard deviation
SI	selectivity index ($IC_{50\ parasite}/IC_{50\ mamalian\ cells}$)
spp	subspecies
STIB	Swiss Tropical Institute, Basel
T. b.	*Trypanosoma brucei*
$t_{1/2}$	half-life
t_{max}	time to maximum concentration
UNC	University of North Carolina
Vs.	versus
VSG	variant surface glycoprotein
Vz	volume of distribution
WBC	white blood cells
WHO	World Health Organisation
μ	growth rate
Yr	Year

Summary

African sleeping sickness is one of the most neglected tropical diseases. Transmitted by the tsetse fly it exclusively occurs in sub-Saharan Africa. It is caused by two different parasite subspecies causing two different forms of African sleeping sickness. *Trypanosoma brucei gambiense* is prevalent in West and Central Africa while *Trypanosoma brucei rhodesiense* is prevalent in East and South Africa. Sleeping sickness is classified in two main stages. In the first stage, the parasites reside in the lymph and blood system. In the second stage, the parasites additionally infect the brain. Untreated sleeping sickness is fatal. Drugs are available for this fearsome disease, however, most of them are old and have many drawbacks, such as severe adverse effects, treatment failures and complicated treatment schedules, which is a problem in remote rural areas where the disease primarily occurs.

African sleeping sickness is a communicable disease that can be controlled. In 1998, there were an estimated 300,000 cases. By 2012 the prevalence has decreased to about 30,000, by different control measures such as vector control, improved surveillance and free drug distribution. Elimination seems possible, but safe and effective drugs are needed to reach this goal. One of the current drugs is the diamidine pentamidine which is in use since the early 1940s. However, it works only in patients with first stage disease and it has to be injected.

The Consortium for Parasitic Drug Development (CPDD) was founded in the year 2000 to find novel diamidines with better characteristics than the existing drugs. We improved oral absorption, which makes it possible to use pills instead of injections, and central nervous system (CNS) penetration. One compound (pafuramidine) has been tested in patients with first stage infections. It was the first compound that cured sleeping sickness orally, which is of great help for rural areas. Unfortunately, pafuramidine caused kidney and liver problems, and it did not cure second stage infections. In the meantime, we have identified superior compounds especially for the second stage.

As described in Chapter 3, two compounds, the prodrugs DB868 and DB844, given orally, cured all mice with CNS infections. However, both prodrugs were too toxic at the high doses required to cure both stages in monkeys. Nevertheless, DB868 is a good candidate drug to cure first stage sleeping sickness by an oral treatment, as demonstrated in mice and monkeys with first stage infections. Chapter 4 shows data of another CNS potent prodrug, DB1227 which was, however, less effective than DB868 in CNS infected mice.

Chapters 3, 7, 8 and 9 deal with two unmasked diamidines, DB829 and 28DAP010, which were highly effective in mice with second stage infections after i.p. injection. This was unexpected since diamidines are rather unlikely to cross the blood brain barrier in sufficient concentrations by diffusion. These two diamidines may penetrate into the brain by specific transporter proteins. The advantage of the two diamidines is that both cure with a short treatment course which could shorten the time of hospitalization of the patients. We have already tested DB829 in monkeys with promising results. It was safe and effective at low doses and a short treatment schedule in monkeys with second stage disease. 28DAP010 seems to be similarly effective as DB829 on both *T. brucei* subspecies in vitro and in mouse models.

In Chapter 6 we established a new in vitro method to measure the kinetics of drug action on pathogenic protozoa on a real time basis. We exploited the capacity of viable cells to produce heat and measured the heat flow using microcalorimetry. 28DAP010 inhibited the heat production of trypanosome cultures faster than DB829. The parasite clearance time of 28DAP010 was also faster than of DB829 in mice. The required effective treatment duration was still similar in mice with single dose for first stage and 5 days for second stage infections.

Upcoming efficacy studies will reveal if 28DAP010 is as curative in monkeys as DB829 and toxicity studies of 28DAP010 and DB829 side by side will shed light on their toxicity profile. These studies will help to select the better of these two compounds as a clinical drug candidate for the treatment of second stage sleeping sickness.

Zusammenfassung

Die Afrikanische Schlafkrankheit ist eine Tropenkrankheit, welche durch die Tsetsefliege übertragen wird und daher ausschliesslich im tropischen Afrika vorkommt. Sie gehört zu den vernachlässigsten Krankheiten überhaupt und wird deshalb auch "vergessene Seuche" genannt. Der Erreger ist ein einzelliger Parasit. Es gibt zwei verschiedene Unterarten, die zu etwas unterschiedlichen Schlafkrankheitsformen führen. Ohne wirksame Medikamentenbehandlung sind beide Formen tödlich. *Trypanosoma brucei gambiense* kommt nur in West- und Zentralafrika vor, während *Trypanosoma brucei rhodesiense* in Ost- und Südafrika zu finden ist. Der Krankheitsverlauf kann in zwei Stadien unterteilt werden. Im ersten Stadium findet man die Parasiten im Blut- und Lymphsystem und im zweiten Stadium zusätzlich im Gehirn. Zwar gibt es für diese Krankheit Medikamente, jedoch sind die meisten davon veraltet, haben ausgeprägte Nebenwirkungen und sind wegen Rückfällen oder der komplizierten und aufwendigen Behandlung problematisch.

Die Bekämpfung der Afrikanischen Schlafkrankheit ist möglich. 1998 gab es geschätzt etwa 300.000 Krankheitsfälle. Durch verbesserte Überwachung mit anschliessender medizinischer Behandlung der Infizierten, kostenlose Medikamentenverteilung und Vektorkontrolle, liess sich die Krankheit auf etwa 30.000 Krankheitsfälle im Jahr 2012, eindämmen. Für eine Eliminierung sind wirksame und verträgliche Medikamente notwendig. Ein Diamidin, das schon seit den frühen 40-er Jahren eingesetzt wird ist Pentamidin. Es wirkt noch heute, aber nur in Patienten die sich im ersten Stadium befinden, zudem muss es injiziert werden.

Im Jahr 2000 wurde das Konsortium CPDD, für die Entwicklung neuer Wirkstoffe zur Behandlung parasitärer Erkrankungen, vor allem für die Schlafkrankheit, gegründet. Neuartige Diamidine mit verbesserten Eigenschaften wurden gesucht und es war uns möglich, die orale Bioverfügbarkeit und die Bluthirnschrankengängigkeit, chemisch zu verbessern. Pafuramidin, war einer der neuen Wirkstoffe, das erste oral einzunehmende Medikament gegen Schlafkrankheit, das im Menschen getestet wurde. Ein orales

Medikament hat grosse Vorteile für diese Krankheit, die hauptsächlich in abgelegenen Gebieten Afrikas vorkommt, wo ein ausgebautes Gesundheitssystem oft fehlt.

Pafuramidin heilte nur das erste Schlafkrankheitsstadium und dabei wurden Leber- und Nieren-Unverträglichkeiten festgestellt. Während der klinischen Studie testeten wir weitere Diamidine und fanden verbesserte Substanzen, vor allem bezüglich der Wirksamkeit des zweiten Krankheitsstadiums. Kapitel 3 und 4 beschreibt die wirksamsten Moleküle, die das Zweitstadium bei oraler Verabreichung heilten. Diese Moleküle, DB844, DB868, DB1227, aber auch das Pafuramidin sind Medikamenten-vorstufen (Prodrugs). Diese wurden entwickelt, um die orale Aufnahme und Gehirn-gängigkeit zu verbessern. Die aktivsten waren DB868 und DB844 in Mäusen, jedoch zeigten beide Moleküle toxische Wirkungen im Affen ohne dabei ausreichend die Gehirninfektion zu heilen. Dennoch war DB868 im Affenmodell deutlich besser verträglich als Pafuramidin und ist somit ein guter Ersatzkandidat für eine orale Wirkstoffentwicklung fürs erste Stadium.

Unerwartet konnten wir jedoch zwei Diamidine (ohne Vorstufenergänzung) identifizieren, die ebenfalls Mäuse mit Gehirninfektionen heilten. Da Diamidine unter physiologischen Bedingungen protoniert sind, ist es unwahrscheinlich, dass sie durch die Bluthirnschranke diffundieren. Möglicherweise werden sie über spezifische Mechanismen ins Gehirn transportiert. Kapitel 3, 7, 8 und 9 befassen sich mit den beiden aktivsten Diamidinen, DB829 und 28DAP010. Ihre hohe Wirkung und die kurze Behandlungszeit nach parenteraler Verabreichung (i.p. oder i.m) sind vielversprechend. DB829 war gut verträglich und wirksam bei niedrigen Dosen und heilte die infizierten Affen mit dem zweiten Krankheitsstadium bereits bei einer 5-tägigen Behandlung. In vitro und im Mausmodel war 28DAP010 auf beide Trypanosomen Unterarten ähnlich wirksam wie DB829.

Um die Wirkungszeit neuer Substanzen auf Trypanosomen zu testen, entwickelten wir eine neue Methode, die in Kapitel 6 beschrieben wird. Dabei nutzten wir die Eigenschaft der Zellen, Wärme zu produzieren und massen diese mit einem Kalorimeter auf Echtzeit.

28DAP010 reduzierte die Wärmeentwicklung einer Trypanosomenkultur deutlich schneller als DB829. Auch in infizierten Mäusen wirkte 28DAP010 schneller. Die Behandlungsdauer und Dosierung war bei beiden Diamidinen trotzdem vergleichbar. Eine Einzeldosis heilte das erste und eine 5-tägige Behandlung das zweite Stadium in Mäusen.

Weitere Studien sind nötig, um die Wirksamkeit von 28DAP010 im Affenmodel zu überprüfen und die Verträglichkeit beider Diamidine zu analysieren. Diese Ergebnisse werden zeigen, welches der bessere klinische Kandidat für die Behandlung des zweiten Schlafkrankheitsstadiums sein wird.

Introduction

African sleeping sickness, also known as Human African Trypanosomiasis (HAT), is a parasitic disease in humans. Since it is prevalent only in sub-Saharan Africa, it is neglected, even though it is a fatal disease. HAT is currently endemic in 23 countries with about 70 million people at risk of infection (Simarro et al., 2012, 2010). The illness is caused by flagellated protozoans of the genus *Trypanosoma,* and by two different subspecies of *Trypanosoma brucei*, *T. b. gambiense* and *T. b. rhodesiense* belonging to the order Kinetoplastida, family Trypanosomatidae. These parasites are 20 to 30 µm long and 1.5 to 3.5 µm wide and live and multiply extracellularly in the blood and tissue fluids of the infected patients. The different subspecies cause slightly different diseases. *T. b. gambiense*, prevalent in west and central Africa cause West African Sleeping sickness or Gambian Trypanosomiasis which is a more chronic disease killing the patient in around three years (Checchi et al., 2008). *T. b. rhodesiense* prevalent in east Africa causes East African Sleeping sickness, also known as Rhodesian Trypanosomiasis, which is usually an acute disease causing death within several months unless treated (Brun et al., 2010; Odiit et al., 1997). HAT is classified in two stages. In the first, also known as hemolymphatic stage, the parasites reside in the blood and lymph system. In the second, cerebral or meningo-encephalitic stage, the parasites have crossed the blood brain barrier (BBB) and invaded additionally the cerebrospinal fluid (CSF) and the central nervous system (CNS).

The symptoms of HAT vary and differ between *T. b. gambiense* and *T. b. rhodesiense* infected patients and the different disease stages (Chappuis et al., 2005). The absence of specific signs hamper the screening and the diagnosis of the disease, especially of the early stage of the HAT (Maurice, 2013). One symptom is the trypanosome chancre of 2 to 5 cm in diameter. It is a red sore skin lesion caused by an inflammatory reaction at the site of the bite of the tsetse where the trypanosomes multiply locally before entering the lymphatic system. Unfortunately, it is mostly observed only in *T. b. rhodesiense* infected patients and even there only occasionally (≈ 19%) (Brun et al., 2010). Winterbottom's sign (posterior cervical lymphadenopathy), a swelling of lymph nodes along the back of

the neck is another symptom for HAT (Chappuis et al., 2005). It is caused by trypanosomes in the lymphatic fluid causing inflammation. Winterbottom's sign is seen in the first stage of HAT, more often in *T. b. gambiense* than in *T. b. rhodesiense* infected patients. Other symptoms are less specific, e.g. irregular fever, headache, myalgia, fatigue, adenopathy, and pruritus or a relatively asymptotic phase that can last for several months or sometimes even years in *T. b. gambiense* (Chappuis et al., 2005; Stuart et al., 2008). The second stage is a result of a chronic meningo-encephalitis. It starts with progressive mental deteriorations proceeding to coma and finally death if untreated. The sleep disorder, a dysregulation of the circadian rhythm and a fragmentation of the sleep/wake cycle, are characteristic symptoms, especially in *T. b. gambiense* infected patients, which gave HAT its name sleeping sickness (Brun et al., 2010). Severe psychiatric and neurological symptoms accompany the second stage such as psychological and behavioral changes and sensory disturbances. Motor weakness, walking difficulties and speech disorders increase also with the number of white blood cells (WBC) in the CSF (Blum et al., 2006). As the symptoms for HAT are not specific enough to diagnose the disease, blood and lymph is analyzed for a parasitological confirmation (direct observation of trypanosomes) of suspected HAT patients, and in case of positive, a CSF examination for the stage determination (Chappuis et al., 2005).

Trypanosoma brucei spp are transmitted by the bite of an infected tsetse fly (*Glossina spp.*). There are nearly 30 *Glossina* species and subspecies of which *G. palpalis* is the main group transmitting *T. b. gambiense* and *G. morsitans* and *G. fuscipes* mainly are responsible for transmitting *T. b. rhodesiense*. The vector is the reason why HAT only occurs in Africa as the tsetse fly habitats are restricted to sub-Saharan Africa (Brun et al., 2010) (Figure 1). Transmission is not easy. The developmental cycle in the tsetse fly is complex and involves different parasite stages or forms with morphological and biochemical changes until the fly becomes infective with metacyclic trypanosome forms in the lumen of the salivary glands. The process takes around 3 to 4 weeks from the infectious blood meal until the fly is able to transmit. In addition the infection rate in tsetse is very low, usually below 1% (Solano et al., 2013). Therefore vector control is an efficient means to reduce the prevalence of the disease (Solano et al., 2013).

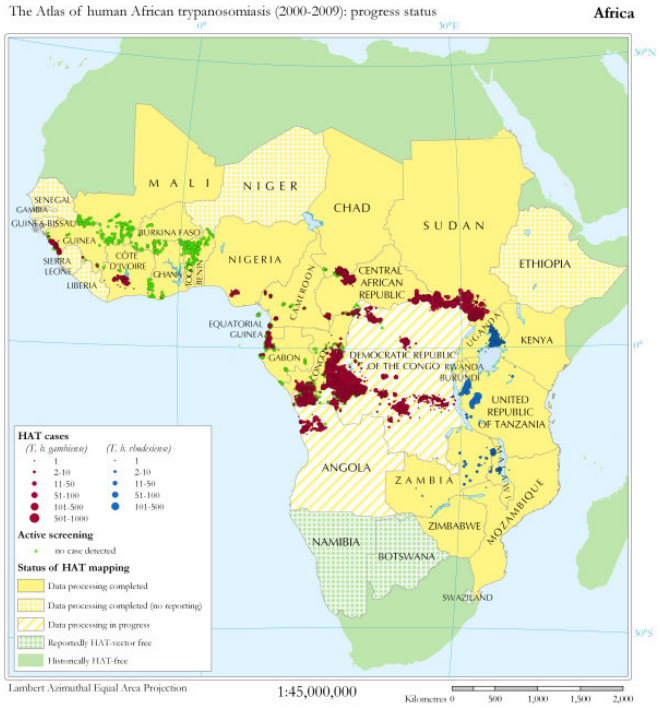

Figure 1: **The Atlas of human African trypanosomiasis** (Simarro et al., 2010). Sleeping sickness transmission takes place in sub-Saharan Africa, in discrete 'foci' within the geographic distribution of the tsetse fly. Several of the 36 countries considered as endemic have not reported any cases in recent years. In the last 10 years, HAT was reported in 23 African countries (Simarro et al., 2010).

The prevalence of HAT has dropped over 10-fold since the end of the last century (Simarro et al., 2008). However, it is estimated by the World Health Organisation (WHO) that there are still around 30,000 infected patients as 7197 new cases were reported in 2012 despite the sustained control efforts (World Health Organisation, 2013). It is not the first time that HAT has been diminished. By the end of the 1960s, the disease had been almost eliminated by large-scale screening and different intervention programs. Then – just over one decade ago - by the end of the 1990s, the numbers were again alarmingly high with about 300,000 to 450,000 estimated patients (Barrett, 2006, 1999) (Figure 2). The main reason for the "rise and falls" of the numbers of the HAT patients are the level of interventions taken to control the disease. Active case finding by systematic screening in at-risk populations followed by an effective treatment of the patients is most important, for the individual but also to reduce the disease reservoir (Simarro et al., 2008). Vector control is complementary approach to reduce the prevalence and to contribute to the elimination of the disease.

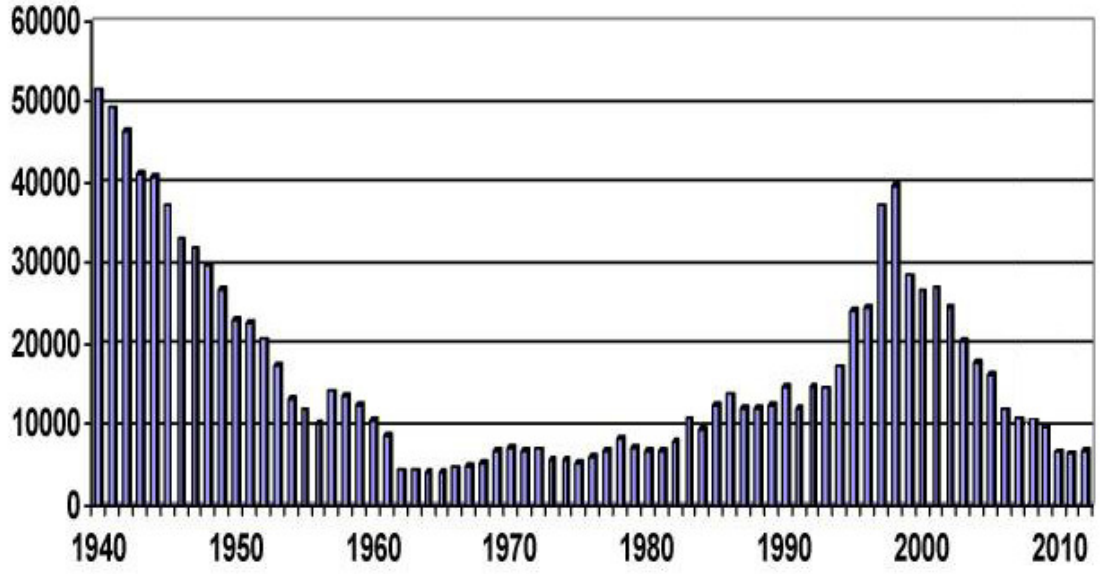

Figure 2: Rise and fall of sleeping sickness with reported HAT cases per year. In times of low surveillance (1990s) the estimated prevalence was about twelve-fold the reported number of cases. Today a factor of 3 is sufficient to reach credible estimates as the surveillance rate has been increased. Diagram adapted from (Schofield and Kabayo, 2008; Simarro et al., 2008).

Better diagnostics and better drugs are still important prerequisites to control HAT. The parasite numbers are low, especially in *T. b. gambiense* infected patients. Therefore a parasitological confirmation (in large scale) is still a challenge. A three step approach is used to diagnose suspected *T. b. gambiense* patients: screening, parasitological confirmation, and staging (Brun et al., 2010; Chappuis et al., 2005; Wastling and Welburn, 2011). A serological test for the presence of antibodies (Card Agglutination Test for Trypanosomiasis, CATT) that is cheap and easy to use is available for the screening of *T. b. gambiense* HAT but not yet for *T. b. rhodesiense.* For both subspecies and especially for *T. b. rhodesiense,* a parasitological confirmation is required for HAT diagnosis. Different parasitological methods, which rely on microscopic search for parasites, are available to analyze samples from blood or enlarged lymph nodes (or CSF for second stage diagnosis) (Wastling and Welburn, 2011). The most sensitive is the mini-anion exchange centrifugation technique (mAECT), a concentration technique, yielding in an analytical sensitivity of 50 parasites per mL of blood (Büscher et al., 2009) Sensitivity might still not be sufficient in some *T. b. gambiense* HAT patients with low

parasite loads, and it is tedious and time-consuming. A first rapid test kit (SD BIOLINE HAT test) using parasite antigens has been developed with support of FIND. An evaluation of its performance is ongoing (FIND, 2013). The LAMP test, a diagnostic kit for qualitative detection of the parasite's DNA by loop-mediated isothermal amplification, seems to be promising. But this test is also not 100% specific and it has not been evaluated yet under field conditions (Mitashi et al., 2013). There is still need for a confirmed ideal diagnostic test for HAT that is affordable, user-friendly, without the need of special equipment, fast, and accurate (Lejon et al., 2013). The staging of HAT is far from optimal. Since a second stage treatment is more toxic (especially melarsoprol) and the treatment more expensive or complicated (NECT), the stage of the disease has to be determined prior to treatment. Currently, cerebrospinal fluid (CSF) is taken from the patient by lumbar puncture, which is very painful for the patient. Second stage is determined either if parasites are observed in the CSF and/or if the leukocyte count (white blood cells) exceeds 5 cells per µL (Chappuis et al., 2005; Wastling and Welburn, 2011). Studies to improve diagnostic tools are ongoing.

Vaccines are not available for HAT and it is highly unlikely that they can be developed due to the antigenic variation of the parasite (Stuart et al., 2008). This mechanism enables the parasites to evade the immune response of the mammalian host. The trypomastigote blood-stream forms are completely covered by identical copies of glycoproteins that protect the parasite against lysis by serum components. Specific antibodies can kill the cells after recognition. However, the parasite is able to switch (in 0.1% of the trypanosome divisions) to new antigenically distinct glycoproteins (variable surface glycoproteins, VSG) (Morrison et al., 2009; Turner and Barry, 1989). The parasites with a new VSG cannot be detected and neutralized by the humoral immune response to the previous VSG and will proliferate in the patient until the next generation of specific antibodies is generated. This leads to a fluctuating number of trypanosomes (parasitemia waves) that can be observed in the blood of patients or animals (Stuart et al., 2008).

Drugs are available for HAT. Treatment recommendations vary according to the trypanosome subspecies and the stage of the disease. Drugs for first stage disease are

pentamidine for *T. b. gambiense* and suramin for *T. b. rhodesiense* infections (Table 1). Both are still successful as treatment failures are rare (≈ 95% cures). However, both have to be administered parenterally as both drugs have a low oral bioavailability. First-line treatments for second stage disease are a combination of nifurtimox and eflornithine (NECT) for *T. b. gambiense* and melarsoprol for *T. b. rhodesiense* patients (Table 1). Especially melarsoprol, an arsenical compound, is highly toxic. About 8% of the patients are killed by its adverse reactions. Additionally, treatment failures have been reported to levels up to around 30% in some HAT foci (Barrett et al., 2007). The treatment is painful, as melarsoprol is a 3.6% solution in propylene glycol which irritates at the site of injection, and the drug has to be administered by slow intravenous (i.v.) injections over 10 days (Kuepfer et al., 2012). Melarsoprol treatment is difficult to bear. NECT is less toxic and more effective than melarsoprol. However, eflornithine is very expensive and only effective on *T. b. gambiense* (Iten et al., 1995). The combination therapy is half oral since nifurtimox can be taken orally, but the partner drug, eflornithine, has to be administered intravenously by infusion. So all treatments require good health systems including skilled staff, which can be a problem in remote rural areas where African sleeping sickness is primarily found.

Table 1: HAT first-line treatment recommendations

	T. b. gambiense	*T. b. rhodesiense*
1st stage	Pentamidine	Suramin
2nd stage	Nifurtimox + Eflornithine (NECT)	Melarsoprol

Drug resistance is an issue and one of the reasons why drug discovery should continue especially for the treatment of second stage disease. NECT, which was introduced in 2009, is still effective. However, treatment failures have been reported already for eflornithine when it was used as a monotherapy (Balasegaram et al., 2009), and nifurtimox is not very effective in its own against African trypanosomes (Kaiser et al.,

2011). Resistance may develop in the near future also to NECT - the currently best treatment option for second stage *T. b. gambiense* HAT. Therefore, drug discovery should continue to avoid a revival of HAT after loss of efficacy of one of the current drugs.

Two potential new candidate drugs have entered clinical testing for HAT. Fexinidazole, a nitroimidazole entered clinical testing phase II/III and the benzoxaborole SCYX-7158 entered phase I. Both compounds can be administered by an oral route and are being developed for a new treatment for second stage disease. This is a great improvement compared to the situation 10 years ago (Mäser et al., 2012). However, two compounds entering the clinical trials might not be enough to ensure a new treatment option for second stage sleeping sickness, since about 75% of candidate drugs do not complete drug development (DiMasi and Grabowski, 2007).

Diamidines have a long history in drug development for treatment of African sleeping sickness. Trypanocidal activity of the first diamidine, the hypoglycaemic drug synthalin (Figure 2), has been shown in rodents already in 1935 (Steverding, 2010). Since blood-stream trypanosomes consume enormous amount of sugar for their metabolism, the activity of synthalin was thought to be due to starving of the parasites. In 1937, Yorke and Lourie discovered that synthalin itself is trypanocidal and its activity is not attributed to its hypoglycaemic effect (Lourie and Yorke, 1937; Steverding, 2010). Thereafter, a large number of aromatic diamidines were prepared among which were the two phenyl containing diamidines, stilbamidine and pentamidine (Steverding, 2010). Both were highly active against HAT. Pentamidine is still in use as first stage drug in *T. b. gambiense* patients since the 1940s. Interestingly, one of its adverse reactions is still hypoglycaemia – related to its previous rational. The use of Stilbamidine has been abandoned due to neurological toxicity in some patients (Steverding, 2010).

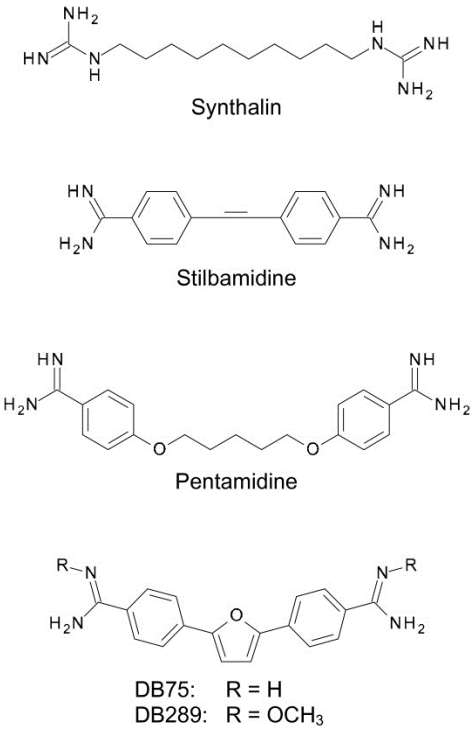

Figure 2: Development of diamidines for HAT. Synthalin was the first diamidine discovered with trypanocidal activity. The aromatic diamidines, Stilbamidine and pentamidine are both highly active against first stage HAT. DB75 is a novel diamidine and the active molecule of the methamidoxime prodrug DB289, which was the first oral drug for treatment of first stage sleeping sickness tested in clinical trials (Figure adapted from Steverding (2010)).

Pentamidine is an interesting compound. No increased treatment failures have been reported so far though it has been in use for first stage *T. b. gambiense* HAT since the end 1930s (Baker et al., 2013). Pentamidine is not only active on African trypanosomes but has a broad spectrum of antimicrobial activities (Werbovetz, 2006). It is also in clinical use for antimony-resistant leishmaniasis and *Pneumocystis jirovecii* pneumonia (a fungus) (Croft et al., 2005; Sands et al., 1985; Sattler et al., 1988; Soeiro et al., 2008; Werbovetz, 2006). Pentamidine was shown to be active also on other pathogens such as *Plasmodium falciparum* (Bell et al., 1990), even on chloroquine resistant *P. falciparum* parasites in vitro (Stead et al., 2001), but is not in clinical use for malaria due to its poor oral bioavailability (Werbovetz, 2006).

The mechanism of action is still unclear and it may differ in different organisms (Mathis et al., 2007; Werbovetz, 2006). It has been shown that pentamidine, Furamidine and several other diamidines are transported into trypanosomes and plasmodia to high intracellular concentrations and these compounds bind to the minor groove at AT-rich sites of the parasite DNA (Bray et al., 2003; Mathis et al., 2007; Wilson et al., 2008) (Figure 3). The trypanosomes' kinetoplast minicircles are particularly AT rich and hence

a good target for diamidine binding. Kinetoplast destruction within 24 h of exposure has been observed with pentamidine and furamidine and the loss of the kinetoplast precedes trypanosome death. DNA binding correlates to some extent with trypanocidal activity but it is probably not the primary or exclusive drug target (Barrett et al., 2013; Werbovetz, 2006; Wilson et al., 2008). The mitochondrion as drug target in blood-stream form trypanosomes was questioned as blood-stream forms depend for energy generation only on glycolysis and because dyskinetoplastic trypanosomes exist (Schnaufer et al., 2002; Soeiro et al., 2013; Werbovetz, 2006). However, inhibition of the mitochondrial topoisomerase II, which is involved in kDNA expression and replication, seems to be involved in the trypanocidal activity against blood-stream form *T. brucei*. Blockage of topoisomerase II expression by RNA interference was lethal also in blood-stream trypanosomes (Soeiro et al., 2013; Wang and Englund, 2001). The mode of action of diamidines has still not been revealed. It is most likely that diamidines have multiple targets rather than a single bioreceptor to kill the parasite. That would explain also why resistance to pentamidine has been linked so far only to transporters involved in accumulation of the drug (Baker et al., 2013).

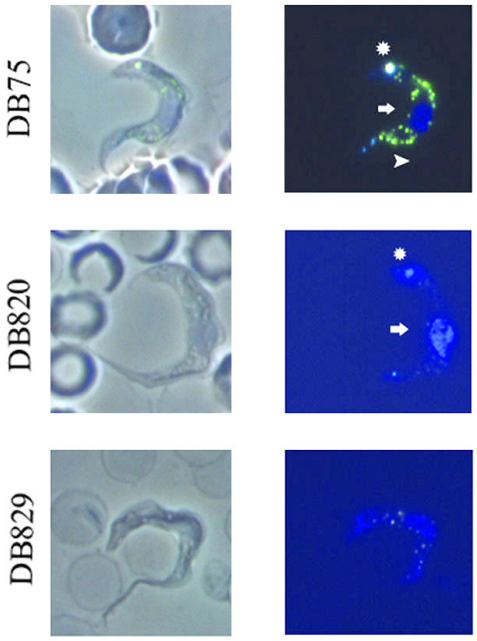

Figure 3: Fluorescence microscopy after uptake of novel diamidines with innate fluorescence properties. DB75 and its aza-analogues DB820 and DB829 have been shown to localize not only to the DNA-containing nucleus and kinetoplast of trypanosomes but also to acidocalcisomes. DB829 is also accumulating to high concentrations in the trypanosomes. However, its fluorescence is quenched after binding (by 86%), making it more difficult to study its uptake rate and its intracellular distribution by fluorescence microscopy. Arrows: nucleus, circle: kinetoplast, arrowhead: acidocalcisomes. (Figure adapted from Mathis et al., (2007).

Other diamidines with antiprotozoal activity are diminazene (Peregrine and Mamman, 1993) and isometamidium (a monoamidine) which are used to treat animal trypanosomiasis (nagana) and propamidine, effective against *Acanthamoeba* species (Seal, 2003). The continuing interest in aromatic diamidines with improved properties to find new drug candidates for HAT is therefore of no surprise.

Over 2000 novel diamidines have been synthesized since the 1970s alone by Boykin *et al* at the Georgia State University and by Tidwell *et al* at the University of North Carolina. Interest in pentamidine analogues and their prodrugs has spread beyond these two groups (Kotthaus et al., 2011; Porcheddu et al., 2012; Rodríguez et al., 2008). But so far nobody else has identified compounds that were more effective in animal models than the ones synthesized by Boykin et al or Tidwell et al., in particular for the treatment of second stage infections.

In 1977, Das and Boykin reported the antitrypanosomal activity of DB75, also named furamidine (Figure 2), and started with this the era of novel diamidines for HAT (Das and Boykin, 1977). This compound is highly active in vitro against African trypanosomes and in infected mice by parenteral administration. However, since diamidines are positively charged at physiological pH, their predicted membrane permeability is low (Ansede et al., 2004). This reduces their ability to cross sufficiently i) the gastrointestinal tract (leading to a poor oral absorption) and ii) the blood brain barrier (BBB), which is required to cure second stage disease. To enhance the oral bioavailability and central nervous system (CNS) penetration, prodrugs of diamidines were synthesized. These prodrugs had the cationic moiety masked which decreases its pKa value (acid dissociation constant) (Werbovetz, 2006). The prodrugs are inactive in vitro, but after absorption, are metabolized to the active molecule by the body's own enzymes (Midgley et al., 2007). The prodrug approach indeed improved the desired characteristics especially when methamidoxime groups were attached to the molecule. DB289, also named pafuramidine maleate, is a methamidoxime prodrug of DB75 and the most prominent example of this approach. Pafuramidine has shown good oral bioavailability and good efficacy in vivo (Wenzler et al., 2009). In the year 2000, pafuramidine was selected by

the Consortium for Parasitic Drug Development (CPDD) and entered clinical trials to be tested for the treatment of first stage *T. b. gambiense* HAT as the first oral drug developed (ever) for this disease (Burri, 2010).

A good, new drug has to fulfill two requirements. First, it has to be effective and second, safe. On the one hand, pafuramidine was very successful. It cured many patients during the clinical trials with the advantage of its oral administration route. Pafuramidine was as effective as pentamidine in the phase III clinical trial, and its safety profile was inconspicuous (Burri, 2010). However, during a phase III trial, an additional supportive Phase I study was conducted for registration with the Food and Drug Administration (FDA). This additional safety assessment was required because the treatment was extended during phase IIb, from 5 days to 10 days to enhance its efficacy. To cover safety not only for first stage HAT but also for a 2nd disease (*Pneumocystis* pneumonia), the additional phase I was conducted not only for 10 days, as necessary for HAT, but for 14 days as necessary for *Pneumocystis* pneumonia (Burri, 2010). During the supportive phase I study, severe hepato- and a delayed renal-toxicity that appeared several days after the last drug administration, was discovered in healthy volunteers. As a consequence, the clinical development program for this promising prodrug, pafuramidine, was discontinued (Burri, 2010; Harrill et al., 2012; Paine et al., 2010).

Efficacy of pafuramidine was not only assessed in humans in *T. b. gambiense* (Burri, 2010) and *Pneumocystis jirovecii* infected patients (Chen et al., 2007) but also in an open-label, pilot phase II trial in malaria patients infected with *P. falciparum* or *P. vivax* (Yeramian et al., 2005). Pafuramidine cured orally 90% of the patients (9/10) with *P. vivax* and 96% (22/23) with acute, uncomplicated *P. falciparum* infections when treated with 100 mg orally twice a day for 5 days in Thailand (Yeramian et al., 2005). These examples show that the prodrug approach with methamidoxime is working well in principle.

Within this PhD thesis, we searched for new backup compounds among the diamidine series for sleeping sickness, in particular compounds that cure second stage HAT. Second stage efficacy of a new sleeping sickness drug is important as the current second stage drugs have more disadvantages than the first stage drugs and because the majority of patients are diagnosed when they already have developed CNS infections (Pépin and Mpia, 2005). In particular a treatment that is simpler to implement and cheaper than the first-line therapy NECT (Simarro et al., 2012) will be of great help.

We screened for prodrugs that are effective orally in first and second stage mouse models. Additionally we assessed if active diamidines could be used directly to treat second stage disease without the need of a prodrug substitution. Further biological characterization of the best novel diamidines included activity against different *T. brucei* trypanosome subspecies, especially different *T. b. gambiense* strains since the majority of patients (≥ 98%) are due to *T. b. gambiense* infections (World Health Organisation, 2013).

Cross resistance between diamidines and melamine-based arsenicals such as melarsoprol has been observed already since the 1950s (Williamson and Rollo, 1959) and seems to be linked to drug uptake by common transporters located at the trypanosome surface. Melarsoprol treatment failures in the field and loss of pentamidine susceptibility in vitro have been observed. Therefore, cross resistance of novel diamidines with pentamidine or with melarsoprol had to be explored.

Another aim was to establish a new methodology to monitor the kinetics of drug action in vitro on a real-time basis. All these studies are important as their information will be considered for deciding which compound should be pursued to preclinical or clinical testing for the treatment of second stage HAT.

References

Ansede, J.H., Anbazhagan, M., Brun, R., Easterbrook, J.D., Hall, J.E., Boykin, D.W., 2004. O-alkoxyamidine prodrugs of furamidine: in vitro transport and microsomal metabolism as indicators of in vivo efficacy in a mouse model of *Trypanosoma brucei rhodesiense* infection. J. Med. Chem. 47, 4335–4338.

Baker, N., de Koning, H.P., Mäser, P., Horn, D., 2013. Drug resistance in African trypanosomiasis: the melarsoprol and pentamidine story. Trends Parasitol. 29, 110–118.

Balasegaram, M., Young, H., Chappuis, F., Priotto, G., Raguenaud, M.-E., Checchi, F., 2009. Effectiveness of melarsoprol and eflornithine as first-line regimens for gambiense sleeping sickness in nine Médecins Sans Frontières programmes. Trans. R. Soc. Trop. Med. Hyg. 103, 280–290.

Barrett, M.P., 1999. The fall and rise of sleeping sickness. Lancet 353, 1113–1114.

Barrett, M.P., 2006. The rise and fall of sleeping sickness. Lancet 367, 1377–1378.

Barrett, M.P., Boykin, D.W., Brun, R., Tidwell, R.R., 2007. Human African trypanosomiasis: pharmacological re-engagement with a neglected disease. Br. J. Pharmacol. 152, 1155–1171.

Barrett, M.P., Gemmell, C.G., Suckling, C.J., 2013. Minor groove binders as anti-infective agents. Pharmacol. Ther. 139, 12–23.

Bell, C.A., Hall, J.E., Kyle, D.E., Grogl, M., Ohemeng, K.A., Allen, M.A., Tidwell, R.R., 1990. Structure-activity relationships of analogs of pentamidine against *Plasmodium falciparum* and *Leishmania mexicana amazonensis*. Antimicrob. Agents Chemother. 34, 1381–1386.

Blum, J., Schmid, C., Burri, C., 2006. Clinical aspects of 2541 patients with second stage human African trypanosomiasis. Acta Trop. 97, 55–64.

Bray, P.G., Barrett, M.P., Ward, S.A., de Koning, H.P., 2003. Pentamidine uptake and resistance in pathogenic protozoa: past, present and future. Trends Parasitol. 19, 232–239.

Brun, R., Blum, J., Chappuis, F., Burri, C., 2010. Human African trypanosomiasis. The Lancet 375, 148–159.

Burri, C., 2010. Chemotherapy against human African trypanosomiasis: is there a road to success? Parasitology 137, 1987–1994.

Büscher, P., Mumba Ngoyi, D., Kaboré, J., Lejon, V., Robays, J., Jamonneau, V., Bebronne, N., Van der Veken, W., Biéler, S., 2009. Improved Models of Mini Anion Exchange Centrifugation Technique (mAECT) and Modified Single Centrifugation (MSC) for Sleeping Sickness Diagnosis and Staging. PLoS Negl Trop Dis 3, e471.

Chappuis, F., Loutan, L., Simarro, P., Lejon, V., Büscher, P., 2005. Options for field diagnosis of human african trypanosomiasis. Clin. Microbiol. Rev. 18, 133–146.

Checchi, F., Filipe, J.A.N., Haydon, D.T., Chandramohan, D., Chappuis, F., 2008. Estimates of the duration of the early and late stage of *gambiense* sleeping sickness. BMC Infect. Dis. 8, 16.

Chen, D., Marsh, R., Aberg, J.A., 2007. Pafuramidine for *Pneumocystis jiroveci* pneumonia in HIV-infected individuals. Expert Rev. Anti Infect. Ther. 5, 921–928.

Croft, S.L., Barrett, M.P., Urbina, J.A., 2005. Chemotherapy of trypanosomiases and leishmaniasis. Trends Parasitol. 21, 508–512.

Das, B.P., Boykin, D.W., 1977. Synthesis and antiprotozoal activity of 2,5-bis(4-guanylphenyl)furans. J Med Chem 20, 531–536.

DiMasi, J.A., Grabowski, H.G., 2007. The cost of biopharmaceutical R&D: is biotech different? Manag. Decis. Econ. 28, 469–479.

FIND, 2013. FIND - Developing new diagnostic tests for human African trypanosomiasis [WWW Document]. URL http://www.finddiagnostics.org/resource-centre/reports_brochures/developing_new_diagnostic_tests_for_hat_may2013.html (accessed 11.12.13).

Harrill, A.H., Desmet, K.D., Wolf, K.K., Bridges, A.S., Eaddy, J.S., Kurtz, C.L., Hall, J.E., Paine, M.F., Tidwell, R.R., Watkins, P.B., 2012. A mouse diversity panel approach reveals the potential for clinical kidney injury due to DB289 not predicted by classical rodent models. Toxicol. Sci. Off. J. Soc. Toxicol. 130, 416–426.

Iten, M., Matovu, E., Brun, R., Kaminsky, R., 1995. Innate lack of susceptibility of Ugandan *Trypanosoma brucei rhodesiense* to DL-alpha-difluoromethylornithine (DFMO). Trop. Med. Parasitol. Off. Organ Dtsch. Tropenmedizinische Ges. Dtsch. Ges. Für Tech. Zusammenarbeit GTZ 46, 190–194.

Kaiser, M., Bray, M.A., Cal, M., Bourdin Trunz, B., Torreele, E., Brun, R., 2011. Antitrypanosomal Activity of Fexinidazole, a New Oral Nitroimidazole Drug Candidate for Treatment of Sleeping Sickness. Antimicrob. Agents Chemother. 55, 5602–5608.

Kotthaus, Joscha, Kotthaus, Jürke, Schade, D., Schwering, U., Hungeling, H., Müller-Fielitz, H., Raasch, W., Clement, B., 2011. New prodrugs of the antiprotozoal drug pentamidine. ChemMedChem 6, 2233–2242.

Kuepfer, I., Schmid, C., Allan, M., Edielu, A., Haary, E.P., Kakembo, A., Kibona, S., Blum, J., Burri, C., 2012. Safety and Efficacy of the 10-Day Melarsoprol Schedule for the Treatment of Second Stage *Rhodesiense* Sleeping Sickness. PLoS Negl. Trop. Dis. 6.

Lejon, V., Jacobs, J., Simarro, P.P., 2013. Elimination of sleeping sickness hindered by difficult diagnosis. Bull. World Health Organ. 91, 718.

Lourie, E., Yorke, W., 1937. Studies in chemotherapy. XVI. The trypanocidal action of synthalin. Ann Trop Med Parasitol 31, 435–445.

Mäser, P., Wittlin, S., Rottmann, M., Wenzler, T., Kaiser, M., Brun, R., 2012. Antiparasitic agents: new drugs on the horizon. Curr. Opin. Pharmacol.

Mathis, A.M., Bridges, A.S., Ismail, M.A., Kumar, A., Francesconi, I., Anbazhagan, M., Hu, Q., Tanious, F.A., Wenzler, T., Saulter, J., Wilson, W.D., Brun, R., Boykin, D.W., Tidwell, R.R., Hall, J.E., 2007. Diphenyl Furans and Aza Analogs: Effects of Structural Modification on In Vitro Activity, DNA Binding, and Accumulation and Distribution in Trypanosomes. Antimicrob. Agents Chemother. 51, 2801–2810.

Maurice, J., 2013. New WHO plan targets the demise of sleeping sickness. The Lancet 381, 13–14.

Midgley, I., Fitzpatrick, K., Taylor, L.M., Houchen, T.L., Henderson, S.J., Wright, S.J., Cybulski, Z.R., John, B.A., McBurney, A., Boykin, D.W., Trendler, K.L., 2007. Pharmacokinetics and Metabolism of the Prodrug DB289 (2,5-Bis[4-(N-Methoxyamidino)phenyl]furan Monomaleate) in Rat and Monkey and Its Conversion to the Antiprotozoal/Antifungal Drug DB75 (2,5-Bis(4-Guanylphenyl)furan Dihydrochloride). Drug Metab. Dispos. 35, 955–967.

Mitashi, P., Hasker, E., Ngoyi, D.M., Pyana, P.P., Lejon, V., Van der Veken, W., Lutumba, P., Büscher, P., Boelaert, M., Deborggraeve, S., 2013. Diagnostic Accuracy of Loopamp *Trypanosoma brucei* Detection Kit for Diagnosis of Human African Trypanosomiasis in Clinical Samples. PLoS Negl Trop Dis 7, e2504.

Morrison, L.J., Marcello, L., McCulloch, R., 2009. Antigenic variation in the African trypanosome: molecular mechanisms and phenotypic complexity. Cell. Microbiol. 11, 1724–1734.

Odiit, M., Kansiime, F., Enyaru, J.C., 1997. Duration of symptoms and case fatality of sleeping sickness caused by *Trypanosoma brucei rhodesiense* in Tororo, Uganda. East Afr. Med. J. 74, 792–795.

Paine, M.F., Wang, M.Z., Generaux, C.N., Boykin, D.W., Wilson, W.D., De Koning, H.P., Olson, C.A., Pohlig, G., Burri, C., Brun, R., Murilla, G.A., Thuita, J.K., Barrett, M.P., Tidwell, R.R., 2010. Diamidines for human African trypanosomiasis. Curr. Opin. Investig. Drugs Lond. Engl. 2000 11, 876–883.

Pépin, J., Mpia, B., 2005. Trypanosomiasis relapse after melarsoprol therapy, Democratic Republic of Congo, 1982-2001. Emerg. Infect. Dis. 11, 921–927.

Peregrine, A.S., Mamman, M., 1993. Pharmacology of diminazene: a review. Acta Trop. 54, 185–203.

Porcheddu, A., Giacomelli, G., De Luca, L., 2012. New pentamidine analogues in medicinal chemistry. Curr. Med. Chem. 19, 5819–5836.

Rodríguez, F., Rozas, I., Kaiser, M., Brun, R., Nguyen, B., Wilson, W.D., García, R.N., Dardonville, C., 2008. New Bis(2-aminoimidazoline) and Bisguanidine DNA Minor Groove Binders with Potent in Vivo Antitrypanosomal and Antiplasmodial Activity. J. Med. Chem. 51, 909–923.

Sands, M., Kron, M.A., Brown, R.B., 1985. Pentamidine: a review. Rev. Infect. Dis. 7, 625–634.

Sattler, F.R., Cowan, R., Nielsen, D.M., Ruskin, J., 1988. Trimethoprim-sulfamethoxazole compared with pentamidine for treatment of *Pneumocystis carinii* pneumonia in the acquired immunodeficiency syndrome. A prospective, noncrossover study. Ann. Intern. Med. 109, 280–287.

Schnaufer, A., Domingo, G.J., Stuart, K., 2002. Natural and induced dyskinetoplastic trypanosomatids: how to live without mitochondrial DNA. Int. J. Parasitol. 32, 1071–1084.

Schofield, C.J., Kabayo, J.P., 2008. Trypanosomiasis vector control in Africa and Latin America. Parasit. Vectors 1, 24.

Seal, D., 2003. Treatment of Acanthamoeba keratitis. Expert Rev. Anti Infect. Ther. 1, 205–208.

Simarro, Pere P., Cecchi, G., Franco, J.R., Paone, M., Diarra, A., Ruiz-Postigo, J.A., Fevre, E.M., Mattioli, R.C., Jannin, J.G., 2012. Estimating and Mapping the Population at Risk of Sleeping Sickness. PLoS Negl. Trop. Dis. 6.

Simarro, P.P., Cecchi, G., Paone, M., Franco, J.R., Diarra, A., Ruiz, J.A., Fèvre, E.M., Courtin, F., Mattioli, R.C., Jannin, J.G., 2010. The Atlas of human African trypanosomiasis: a contribution to global mapping of neglected tropical diseases. Int. J. Heal. Geogr. 9, 57.

Simarro, P P, Franco, J., Diarra, A., Postigo, J.A.R., Jannin, J., 2012. Update on field use of the available drugs for the chemotherapy of human African trypanosomiasis. Parasitology 139, 842–846.

Simarro, P.P., Jannin, J., Cattand, P., 2008. Eliminating human African trypanosomiasis: where do we stand and what comes next? PLoS Med. 5, e55.

Soeiro, M.N.C., de Castro, S.L., de Souza, E.M., Batista, D.G.J., Silva, C.F., Boykin, D.W., 2008. Diamidine activity against trypanosomes: the state of the art. Curr. Mol. Pharmacol. 1, 151–161.

Soeiro, M.N.C., Werbovetz, K., Boykin, D.W., Wilson, W.D., Wang, M.Z., Hemphill, A., 2013. Novel amidines and analogues as promising agents against intracellular parasites: a systematic review. Parasitology 1–23.

Solano, P., Torr, S.J., Lehane, M.J., 2013. Is vector control needed to eliminate *gambiense* human African trypanosomiasis? Front. Cell. Infect. Microbiol. 3, 33.

Stead, A.M.W., Bray, P.G., Edwards, I.G., DeKoning, H.P., Elford, B.C., Stocks, P.A., Ward, S.A., 2001. Diamidine Compounds: Selective Uptake and Targeting in *Plasmodium falciparum*. Mol. Pharmacol. 59, 1298–1306.

Steverding, D., 2010. The development of drugs for treatment of sleeping sickness: a historical review. Parasit. Vectors 3, 15.

Stuart, K., Brun, R., Croft, S., Fairlamb, A., Gurtler, R.E., McKerrow, J., Reed, S., Tarleton, R., 2008. Kinetoplastids: related protozoan pathogens, different diseases. J. Clin. Invest. 118, 1301–1310.

Turner, C.M., Barry, J.D., 1989. High frequency of antigenic variation in *Trypanosoma brucei rhodesiense* infections. Parasitology 99 Pt 1, 67–75.

Wang, Z., Englund, P.T., 2001. RNA interference of a trypanosome topoisomerase II causes progressive loss of mitochondrial DNA. EMBO J. 20, 4674–4683.

Wastling, S.L., Welburn, S.C., 2011. Diagnosis of human sleeping sickness: sense and sensitivity. Trends Parasitol. 27, 394–402.

Wenzler, T., Boykin, D.W., Ismail, M.A., Hall, J.E., Tidwell, R.R., Brun, R., 2009. New treatment option for second-stage African sleeping sickness: in vitro and in vivo efficacy of aza analogs of DB289. Antimicrob. Agents Chemother. 53, 4185–4192.

Werbovetz, K., 2006. Diamidines as antitrypanosomal, antileishmanial and antimalarial agents. Curr. Opin. Investig. Drugs Lond. Engl. 2000 7, 147–157.

Williamson, J., Rollo, I.M., 1959. Drug resistance in trypanosomes; cross-resistance analyses. Br. J. Pharmacol. Chemother. 14, 423–430.

Wilson, W.D., Tanious, F.A., Mathis, A., Tevis, D., Hall, J.E., Boykin, D.W., 2008. Antiparasitic compounds that target DNA. Biochimie 90, 999–1014.

World Health Organisation, 2013. African trypanosomiasis (sleeping sickness). Fact sheet N°259. http://www.who.int/mediacentre/factsheets/fs259/en/#

Yeramian, P., Meshnick, S.R., Krudsood, S., Chalermrut, K., Silachamroon, U., Tangpukdee, N., Allen, J., Brun, R., Kwiek, J.J., Tidwell, R., Looareesuwan, S., 2005. Efficacy of DB289 in Thai patients with *Plasmodium vivax* or acute, uncomplicated Plasmodium falciparum infections. J. Infect. Dis. 192, 319–322.

Available online at www.sciencedirect.com

SciVerse ScienceDirect

Current Opinion in Pharmacology

Antiparasitic agents: new drugs on the horizon

Pascal Mäser[1,2], Sergio Wittlin[1,2], Matthias Rottmann[1,2], Tanja Wenzler[1,2], Marcel Kaiser[1,2] and Reto Brun[1,2]

The need for new drugs against tropical parasites such as *Plasmodium falciparum* and *Trypanosoma brucei* is persistent since problems with resistance and toxicity are jeopardizing the currently available medicines. Public-private partnerships aiming to develop new medicines for malaria and sleeping sickness have, over the past 12 years, brought forward several drug candidates that have entered clinical trials. These are the synthetic peroxide OZ439 and the spiroindolone NITD609 against *P. falciparum*, fexinidazole and the oxaborole SCYX-7158 against *T. brucei*. A further class of high chemotherapeutic potential are the diamidines, novel members of which may serve as back-up compounds against trypanosomes and other parasites. Thus, finally, new therapeutic agents against malaria and sleeping sickness are within reach.

Addresses
[1] Swiss Tropical and Public Health Institute, 4003 Basel, Switzerland
[2] University of Basel, 4000 Basel, Switzerland

Corresponding author: Mäser, Pascal (pascal.maeser@unibas.ch)

Current Opinion in Pharmacology 2012, **12**:562–566

This review comes from a themed issue on **Anti-infectives**

Edited by **Laurenz Kellenberger** and **Malcolm GP Page**

For a complete overview see the Issue and the Editorial

Available online 29th May 2012

http://dx.doi.org/10.1016/j.coph.2012.05.001

Introduction

The future looked grim for antiparasitic drug development at the end of the last century, with pharma having withdrawn since decades for want of return and academia lacking the means to develop new compounds themselves. The crisis was resolved by the creation of product-development-partnerships dedicated to the discovery and development of new drugs, such as the Medicines for Malaria Venture (www.mmv.org) or the Drugs for Neglected Diseases initiative (www.dndi.org). A substantial role was played by the Bill and Melinda Gates Foundation (http://www.gatesfoundation.org). So far, these initiatives have successfully brought to market new formulations and combinations of existing drugs. Here we focus on the development of new drugs, reviewing the compounds that are currently in clinical trials against *Plasmodium falciparum*, the causative agent of malaria tropica, and *Trypanosoma brucei* spp., causative agents of sleeping sickness. Both are vector-borne blood parasites, transmitted by *Anopheles* mosquitoes and tsetse flies, respectively.

Drug candidates for malaria

The need for new antimalarials is persistent in spite of the comparably large number of available drugs [1•], owing to the propensity of *P. falciparum* to become drug resistant. Activity against drug-resistant *P. falciparum* isolates is therefore a must for a new lead compound. Further requirements in the target product profile of a new antimalarial are oral bioavailability, low price, activity against *P. vivax* and other human-pathogenic species of *Plasmodium*, and ideally cure by a single dose. Ability to block transmission (i.e. activity against the gametocyte stages) is another important point in line with the malaria eradication agenda [2].

Synthetic peroxides

Artemisinin (Figure 1) from *Artemisia annua* and its semisynthetic derivatives are amongst the most effective and rapidly acting antimalarials available to date. They are sesquiterpene lactones containing an endoperoxide bridge that, when opened by chemical reduction, is thought to react with and alkylate heme and target proteins in the parasite. The extremely short half-life of artemisinins in the human body requires application twice daily. In the quest for fully synthetic peroxides with better pharmacokinetics, a research team from the University of Nebraska Medical Center, the Swiss Tropical and Public Health Institute, and the Centre for Drug Candidate Optimisation (Melbourne), created a series of over 700 adamantane-based ozonides, most of which had low nanomolar activity and striking antiplasmodial selectivity *in vitro*. The first clinical candidate, OZ277 (Arterolane, Figure 1), was recently registered by Ranbaxy Laboratories Ltd. for antimalarial combination therapy in India. The next-generation ozonide OZ439 (Figure 1) combined excellent activity with a longer half-life of elimination. In established preclinical models of malaria, OZ439 was more effective than the semisynthetic artemisinin artesunate and other comparator drugs, resulting in cures of *P. berghei* infected mice with a single oral dose of 20 mg/kg [3••]. Since OZ439 and other peroxide antimalarials have similar *in vitro* potencies, the outstanding efficacy of OZ439 is thought to be the result of its prolonged plasma exposure, which has been demonstrated in both preclinical animal models and in human volunteers. OZ439 recently completed Phase I clinical trials, where it was shown to be safe and well-tolerated.

Figure 1

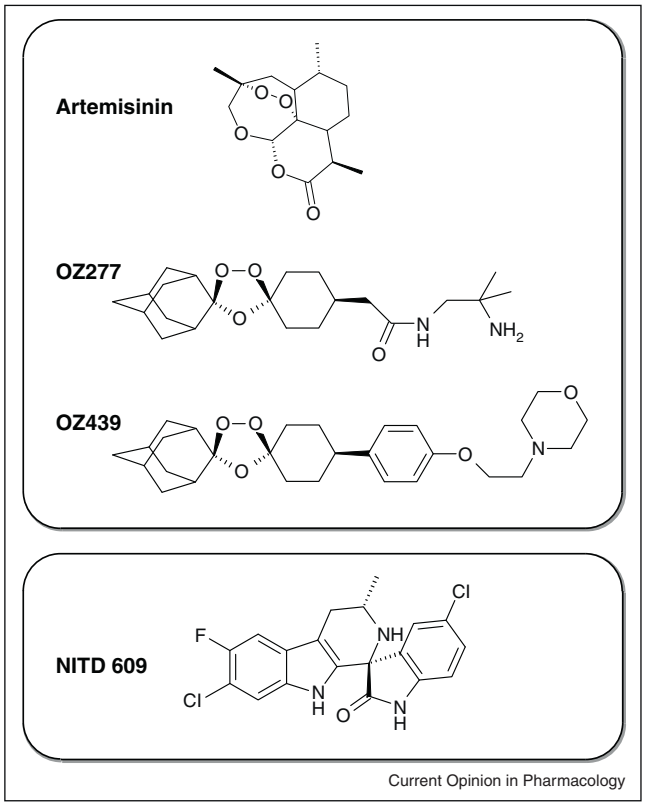

Structures of the discussed antimalarial drugs and candidates.

A phase IIa trial is running (www.mmv.org/research-development/science-portfolio) and OZ439 has demonstrated equally good efficacy in the treatment of *P. falciparum* and *P. vivax* patients. Owing to its safety and exceptional pharmacokinetic properties, the synthetic OZ439 has the potential to achieve MMV's goal of a single-dose oral cure. Apart from the peroxide bond, OZ439 has no similarity to the artemisinins (Figure 1), which raises hopes that it will be active against artemisinin-resistant parasites. This, however, remains to be tested.

Spiroindolones

In search of completely new antimalarial chemotypes the NGBS Consortium consisting of the Novartis Institute for Tropical Diseases (Singapore), the Genomics Institute of the Novartis Research Foundation, the Biomedical Primate Research Centre (Netherlands), and the Swiss Tropical and Public Health Institute screened a library of about 12 000 natural products, and synthetic compounds with structural features of natural products, against *P. falciparum in vitro*. This yielded 275 hits with submicromolar activity, of which the spirotetrahydro-β-carbolines (or spiroindolones) were selected for further development [4••,5]. The optimized candidate NITD609 (Figure 1) had IC_{50} values around 1 nM against all tested *P. falciparum* strains, including resistant isolates. An incorporation assay with radiolabeled methionine and cysteine revealed that NITD609, in contrast to other antimalarials, blocked protein synthesis in *P. falciparum* parasites within 1 h of exposure, suggesting a distinct mode of action. The P-type ATPase PfATP4 had been implicated based on drug resistance studies, but the exact mechanism of action of NITD609 remains unknown. NITD609 has excellent oral bioavailability and was curative in the *P. berghei* mouse model at a single dose of 100 mg/kg [4••]. The compound displays a promising early safety profile and no cardiotoxicity or genotoxicity liabilities. NITD609 has successfully passed first testing in man and is the first molecule with a novel mechanism of action to enter Phase IIa studies for malaria in the last 20 years (www.mmv.org/research-development/science-portfolio), nourishing the hope for a next generation treatment (Table 1).

Drug candidates for sleeping sickness

The need for new drugs against sleeping sickness, also called human African trypanosomiasis (HAT), stems mainly from the toxicity and unfavorable pharmacologic properties of the available drugs. This in turn raises an ethical dilemma: does a new drug merely need to be

Table 1

Overview on the discussed drug candidates

	Malaria drug candidates		HAT drug candidates		
	OZ439	NITD609	Fexinidazole	SCYX-7518	DB829
In vitro IC_{50}[a]	3 nM	0.5–1.4 nM	0.7–3.3 μM	0.2–1 μM	19 nM
In vitro selectivity[b]	>10 000	>10 000	>100	>100	>10 000
Oral bioavailability	76% (rat)	100% (mouse)	41% (mouse)	55% (mouse)	presumably very low
Curative dose in the mouse model (mg/kg)	20 oral, 1 day	100 oral, 1 day	100 bid oral, 5 days CNS model	25 bid oral, 7 days CNS model	20 ip, 10 days CNS model
State of development	Phase II	Phase IIa	Phase I	Phase I	Preclinical

[a] Against *P. falciparum* (malaria candidates) or *T. brucei* (HAT candidates).
[b] Compared to mammalian fibroblasts.

substantially safer than the currently used ones, or will it have to meet the highest safety standards? The latter will be particularly difficult to attain for the treatment of the second stage of the disease, when the parasites have invaded the CNS, for this requires drugs to pass the blood–brain barrier as well.

Nitroimidazoles

DNDi undertook a systematic review and profiling of nitroheterocyclic molecules at a time when most pharma had abandoned this old and proven class of antimicrobials. Metronidazole, tinidazole or ornidazole are some nitroimidazoles on the market, and nifurtimox (Figure 2) in combination with eflornithine is used to treat second-stage HAT [6]. Screening of more than 700 nitroheterocyclics against *T. brucei* rediscovered fexinidazole (Figure 2) as a drug candidate [7••]. Originally developed as an antimicrobial by Hoechst, fexinidazole had been shown to be active against trypanosomes in the 1980s [8,9] but never made it to clinical testing. Fexinidazole has a positive Ames test; to mammalian cells, however, it is not mutagenic [7••]. In mammals, fexinidazole is rapidly absorbed and metabolized to fexinidazole-sulfoxide and fexinidazole-sulfone. All three compounds cross the blood brain barrier and possess trypanocidal activity, with IC_{50} ranging from 0.7 to 3.3 μM against both drug-sensitive and drug-resistant *T. brucei* spp. isolates [10]. Fexinidazole cures the *T. b. rhodesiense* and *T. b. gambiense* acute mouse models at a daily oral dose of 100 mg/kg given on 4 consecutive days, and the CNS model at an intraperitoneal dose of 50 mg/kg bid or an oral dose of 100 mg/kg bid, both given for five consecutive days [7••]. A phase I clinical trial was performed in 2009 without specific issues of concern. A phase II/III study to investigate the efficacy and safety of fexinidazole will start mid 2012. Patients will be treated orally for 10 days with a daily single dose (www.dndi.org/portfolio/fexinidazole.html).

Benzoxaboroles

The oxaboroles are a promising new class of antimicrobials developed by Anacor Pharmaceuticals (Palo Alto, CA), a company specialized in boron chemistry. Screening an oxaborole library against *T. brucei* at Scynexis (Research Triangle Park, NC) brought forward benzoxaborole 6-carboxamides as new leads [11••]. The compound SCYX-6759 was the most potent in this first screening campaign. It showed good *in vitro* potency and cured the acute and the CNS mouse models. Further optimization was focused on improvement of brain permeability and pharmacokinetics, yielding SCYX-7158 (Figure 2) as a clinical drug candidate [12]. It is a fast acting compound with IC_{50} against *T. b. rhodesiense* and *T. b. gambiense* strains between 0.2 and 1 μM. SCYX-7158 has a good oral bioavailability and blood–brain-barrier permeability. It cures the acute *T. brucei* mouse model

Figure 2

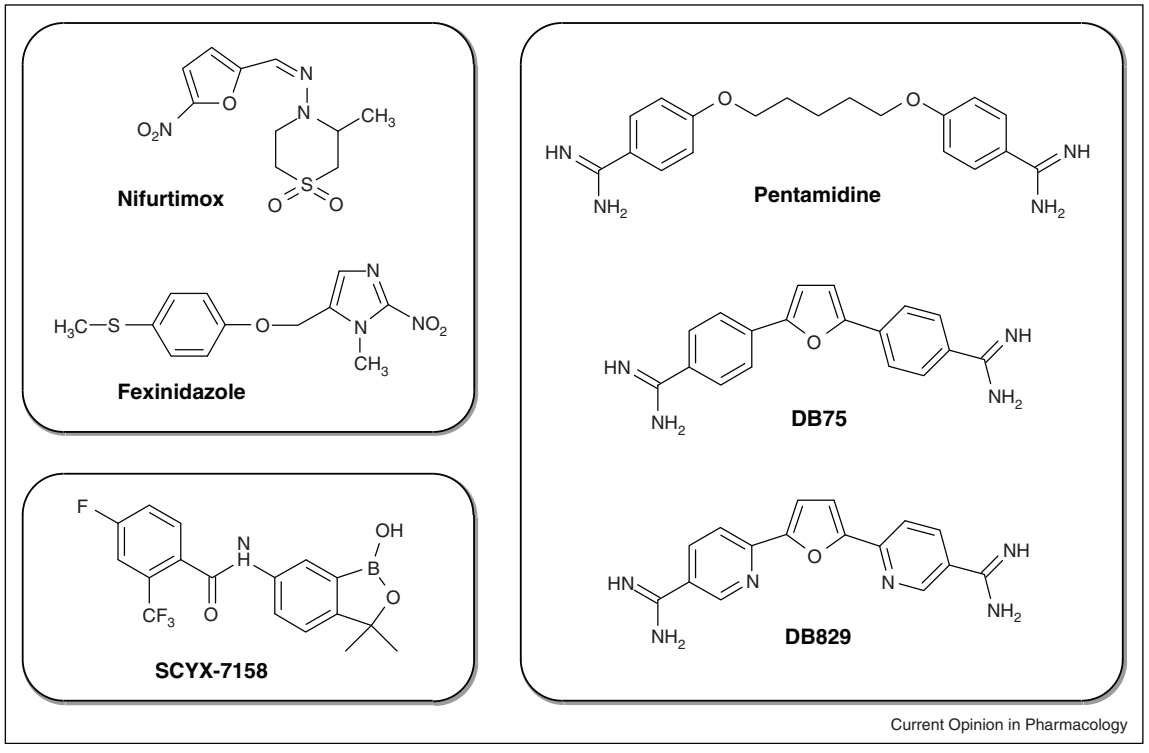

Structures of the discussed sleeping sickness drugs and candidates.

at an oral dose of 5 mg/kg given for 4 days and the second stage model at an oral dose of 25 mg/kg given for 7 consecutive days [12]. Toxicity and ADME investigations were unproblematic and SCYX-7158 got the clearance for a Phase I clinical trial that started in March 2012 (press release DNDi March 12th 2012).

Diamidines

The trypanocidal potential of aromatic diamidines has long been known and pentamidine (Figure 2), introduced in 1941, is still the drug of choice to treat 1st stage *T. b. gambiense* infections [13•,14]. The Consortium for Parasitic Drug Development (www.thecpdd.org) has screened over 2000 new diamidines against *T. brucei*, 517 of which had an IC_{50} below 200 nM and an *in vitro* selectivity above 1000. An initial lead, DB75 (furamidine, Figure 2) synthesized by David Boykin (Georgia State University, USA), had excellent efficacy but lacked oral bioavailability and blood–brain barrier penetration [15••]. These limitations were overcome by the corresponding methoxime prodrug DB289 (pafuramidine [16]), which became the first trypanocide to enter clinical trials as an oral drug. In a phase III clinical trial for 1st stage HAT, oral pafuramidine for 10 consecutive days was almost as effective as pentamidine injected *i.m.*, and the safety profile was inconspicuous [17]. But when an additional phase I trial was conducted testing a 14 days schedule that would cover the treatment of pneumocystosis, renal toxicity was observed about 8 weeks post treatment. This stopped pafuramidine for HAT and other indications. However, the pafuramidine backup program revealed several even more potent diamidines, especially against the 2nd stage of the disease. DB868, an aza analogue of DB289, cures mice with CNS infections [15••] and is well tolerated in monkeys. Surprisingly, two diamidines were able to cure CNS infections without prior masking of the amidine groups. The parent compound DB829 (Figure 2) was the first diamidine that cured the acute as well as the late-stage mouse model [15••], and also cured CNS-infected vervet monkeys [18].

Conclusion

The last novel chemotypes introduced into the clinics were atovaquone/proguanil for malaria in 1996, and eflornithine for sleeping sickness in 1990. Now there is reason for hope that new drugs will become available within the next three to five years. The process is more straightforward for sleeping sickness that can be treated by monotherapy. New antimalarials should always be administered as combinations to reduce the risk of drug resistance development [19], and hence the identification of suitable partners may complicate drug development and registration. Nevertheless, new drugs against malaria and sleeping sickness are finally tangible and we are confident that some of the drug candidates described above will make it to the market. Considering, however, how difficult it has become for a drug to obtain FDA approval and how little it takes to kill it, it is pivotal to keep full drug development pipelines and sustain early drug discovery programs against *P. falciparum* and *T. brucei*.

Acknowledgements

We are grateful to Bryan Yeung and Jonathan Vennerstrom for critical reading of the manuscript. Special thanks to Marcel Tanner for his unresting encouragement and support of our drug R & D activities.

References and recommended reading

Papers of particular interest, published within the period of review, have been highlighted as:

- • of special interest
- •• of outstanding interest

1. • Delves M, Plouffe D, Scheurer C, Meister S, Wittlin S, Winzeler EA, Sinden RE, Leroy D: **The activities of current antimalarial drugs on the life cycle stages of Plasmodium: a comparative study with human and rodent parasites**. *PLoS Med* 2012, **9**:e1001169.
In addition to standardized drug sensitivity data, this paper also provides a good overview on the current antimalarials.

2. Alonso PL, Brown G, Arevalo-Herrera M, Binka F, Chitnis C, Collins F, Doumbo OK, Greenwood B, Hall BF, Levine MM *et al.*: **A research agenda to underpin malaria eradication**. *PLoS Med* 2011, **8**:e1000406.

3. •• Charman SA, Arbe-Barnes S, Bathurst IC, Brun R, Campbell M, Charman WN, Chiu FC, Chollet J, Craft JC, Creek DJ *et al.*: **Synthetic ozonide drug candidate OZ439 offers new hope for a single-dose cure of uncomplicated malaria**. *Proc Natl Acad Sci USA* 2011, **108**:4400-4405.
Discovery and characterization of OZ439 as an antimalarial drug candidate.

4. •• Rottmann M, McNamara C, Yeung BK, Lee MC, Zou B, Russell B, Seitz P, Plouffe DM, Dharia NV, Tan J *et al.*: **Spiroindolones, a potent compound class for the treatment of malaria**. *Science* 2010, **329**:1175-1180.
Discovery and characterization of NITD609 as an antimalarial drug candidate.

5. Yeung BK, Zou B, Rottmann M, Lakshminarayana SB, Ang SH, Leong SY, Tan J, Wong J, Keller-Maerki S, Fischli C *et al.*: **Spirotetrahydro beta-carbolines (spiroindolones): a new class of potent and orally efficacious compounds for the treatment of malaria**. *J Med Chem* 2010, **53**:5155-5164.

6. Priotto G, Kasparian S, Mutombo W, Ngouama D, Ghorashian S, Arnold U, Ghabri S, Baudin E, Buard V, Kazadi-Kyanza S *et al.*: **Nifurtimox-eflornithine combination therapy for second-stage African Trypanosoma brucei gambiense trypanosomiasis: a multicentre, randomised, phase III, non-inferiority trial**. *Lancet* 2009, **374**:56-64.

7. •• Torreele E, Bourdin Trunz B, Tweats D, Kaiser M, Brun R, Mazue G, Bray MA, Pecoul B: **Fexinidazole – a new oral nitroimidazole drug candidate entering clinical development for the treatment of sleeping sickness**. *PLoS Negl Trop Dis* 2011, **4**:e923.
Re-discovery and characterization of fexinidazole as a HAT drug candidate.

8. Raether W, Seidenath H: **The activity of fexinidazole (HOE 239) against experimental infections with *Trypanosoma cruzi*, trichomonads and *Entamoeba histolytica***. *Ann Trop Med Parasitol* 1983, **77**:13-26.

9. Jennings FW, Urquhart GM: **The use of the 2 substituted 5-nitroimidazole, Fexinidazole (Hoe 239) in the treatment of chronic *T. brucei* infections in mice**. *Z Parasitenkd* 1983, **69**:577-581.

10. Kaiser M, Bray MA, Cal M, Bourdin Trunz B, Torreele E, Brun R: **Antitrypanosomal activity of fexinidazole, a new oral nitroimidazole drug candidate for treatment of sleeping sickness**. *Antimicrob Agents Chemother* 2011, **55**:5602-5608.

11. •• Nare B, Wring S, Bacchi C, Beaudet B, Bowling T, Brun R, Chen D, Ding C, Freund Y, Gaukel E *et al.*: **Discovery of novel orally bioavailable oxaborole 6-carboxamides that demonstrate**

cure in a murine model of late stage central nervous system African Trypanosomiasis. *Antimicrob Agents Chemother* 2010, **54**:4379-4388.
Discovery and characterization of benzoxaboroles as new leads against HAT.

12. Jacobs RT, Nare B, Wring SA, Orr MD, Chen D, Sligar JM, Jenks MX, Noe RA, Bowling TS, Mercer LT *et al.*: **SCYX-7158, an orally-active benzoxaborole for the treatment of stage 2 human African trypanosomiasis**. *PLoS Negl Trop Dis* 2011, **5**:e1151.

13. Brun R, Blum J, Chappuis F, Burri C: **Human African**
• **trypanosomiasis**. *Lancet* 2010, **375**:148-159.
Review on the current situation of sleeping sickness.

14. WHO: **Human African trypanosomiasis (sleeping sickness)**. *WHO Fact sheet* 2012, **259**.

15. Wenzler T, Boykin DW, Ismail MA, Hall JE, Tidwell RR, Brun R:
•• **New treatment option for second-stage African sleeping sickness: in vitro and in vivo efficacy of aza analogs of DB289**. *Antimicrob Agents Chemother* 2009, **53**:4185-4192.
First description of a diamidine that is able to cure the *T. brucei* CNS model.

16. Mdachi RE, Thuita JK, Kagira JM, Ngotho JM, Murilla GA, Ndung'u JM, Tidwell RR, Hall JE, Brun R: **Efficacy of the novel diamidine compound 2,5-Bis(4-amidinophenyl)-furan-bis-O-Methlylamidoxime (Pafuramidine, DB289) against *Trypanosoma brucei rhodesiense* infection in vervet monkeys after oral administration**. *Antimicrob Agents Chemother* 2009, **53**:953-957.

17. Burri C: **Chemotherapy against human African trypanosomiasis: is there a road to success?** *Parasitology* 2010, **137**:1987-1994.

18. Brun R, Don R, Jacobs RT, Wang MZ, Barrett MP: **Development of novel drugs for human African trypanosomiasis**. *Future Microbiol* 2011, **6**:677-691.

19. WHO: **Guidelines for the treatment of malaria**. *WHO Library*. 2010.

ANTIMICROBIAL AGENTS AND CHEMOTHERAPY, Oct. 2009, p. 4185–4192 Vol. 53, No. 10
0066-4804/09/$08.00+0 doi:10.1128/AAC.00225-09

New Treatment Option for Second-Stage African Sleeping Sickness: In Vitro and In Vivo Efficacy of Aza Analogs of DB289▽

Tanja Wenzler,[1]* David W. Boykin,[2] Mohamed A. Ismail,[2] James Edwin Hall,[3] Richard R. Tidwell,[3] and Reto Brun[1]

Department of Medical Parasitology and Infection Biology, Swiss Tropical Institute, Basel, Switzerland[1]; Department of Chemistry, Center for Biotechnology and Drug Design, Georgia State University, Atlanta, Georgia[2]; and Department of Pathology and Laboratory Medicine, School of Medicine, The University of North Carolina, Chapel Hill, North Carolina[3]

Received 18 February 2009/Returned for modification 14 May 2009/Accepted 10 July 2009

African sleeping sickness is a fatal parasitic disease, and all drugs currently in use for treatment have strong liabilities. It is essential to find new, effective, and less toxic drugs, ideally with oral application, to control the disease. In this study, the aromatic diamidine DB75 (furamidine) and two aza analogs, DB820 and DB829 (CPD-0801), as well as their methoxyamidine prodrugs and amidoxime metabolites, were evaluated against African trypanosomes. The active parent diamidines showed similar in vitro profiles against different *Trypanosoma brucei* strains, melarsoprol- and pentamidine-resistant lines, and a P2 transporter knockout strain (AT1KO), with DB75 as the most trypanocidal molecule. In the *T. b. rhodesiense* strain STIB900 acute mouse model, the aza analogs DB820 and DB829 demonstrated activities superior to that of DB75. The aza prodrugs DB844 and DB868, as well as two metabolites of DB844, were orally more potent in the *T. b. brucei* strain GVR35 mouse central nervous system (CNS) model than DB289 (pafuramidine maleate). Unexpectedly, the parent diamidine DB829 showed high activity in the mouse CNS model by the intraperitoneal route. In conclusion, DB868 with oral and DB829 with parenteral application are potential candidates for further development of a second-stage African sleeping sickness drug.

Sleeping sickness, also called *h*uman *A*frican *t*rypanosomiasis (HAT), is a vector-borne parasitic disease caused by *Trypanosoma brucei* subspecies, which are unicellular flagellated protozoans. Depending on the subspecies, there are two different forms of the disease which show different clinical features. West African sleeping sickness, a more chronic disease caused by *T. b. gambiense*, is prevalent in West and Central Africa. East African sleeping sickness, a more acute and virulent disease caused by *T. b. rhodesiense*, is endemic in East and Southern Africa (7). The disease is transmitted by the bite of an infected tsetse fly. Tsetse flies and, consequently, the disease are found in remote rural areas of sub-Saharan Africa. The number of sleeping sickness cases decreased in recent years to <12,000 reported cases (28) and 50,000 to 70,000 estimated cases (35) due to improved HAT control.

There are two stages of the disease. In the first stage, the parasites reside and proliferate in the hemolymphatic system. In the second, encephalitic stage, the parasites cross the blood-brain barrier (BBB) and infect the central nervous system (CNS) and the cerebrospinal fluid. The second stage is difficult to treat, as the BBB is a barrier for most drugs, preventing trypanocidal levels of those agents in the CNS and cerebrospinal fluid. If untreated, the disease is invariably fatal. HAT exclusively affects the world's poorest populations, making drug development against this tropical disease economically unattractive for pharmaceutical industries (7, 30, 33). As a consequence, HAT has become one of the most neglected tropical diseases. The drugs currently in use against HAT are unsatisfactory, especially those for the second stage. All drugs suffer from poor oral bioavailability and must be administered parenterally, causing compliance problems in rural areas where health systems are poorly developed or nonexistent. Additionally, the treatment schedule is long and laborious and the adverse events severe or even lethal. Up to 5% of the patients treated with the second-stage drug melarsoprol die of a reactive encephalopathy (18). Drug resistance is also of growing concern and, especially for the encephalitic stage, there are no appropriate treatment options available after treatment failures. Consequently, new drugs are desperately needed to combat this disease.

One of the drugs currently in use for the hemolymphatic stage is the aromatic diamidine pentamidine. It has a broad spectrum of antiparasitic activities and is also used clinically against antimony-resistant leishmaniasis and against *Pneumocystis jiroveci* infection, mostly in AIDS patients (29). This old drug has been used since the early 1940s for the treatment of first-stage *T. b. gambiense* HAT (13). The use of pentamidine is partially restricted due to its lack of oral bioavailability and its toxicity.

The aim of this work was to develop novel aromatic diamidines that are effective for first-stage disease (oral administration) or are effective for second-stage HAT (oral or parenteral administration). A leading structure is DB75 [furamidine; 2,5-bis(4-aminophenyl)-furan], which has a broad spectrum of antiparasitic activity covering *P. jiroveci*, *Leishmania* spp., *Giardia intestinalis*, *Plasmodium falciparum*, and *Trypanosoma* spp. The diphenylfuran diamidines represent an important class of DNA minor groove binders (32, 34). The selective and rapid uptake leads to high drug accumulation in the parasite (21, 22). However, like most of the aromatic diamidines, furamidine and its analogs have low oral bioavailability due to their pos-

* Corresponding author. Mailing address: Swiss Tropical Institute, Socinstrasse 57, P.O. Box, CH-4002 Basel, Switzerland. Phone: 41 612848165. Fax: 41 612848101. E-mail: tanja.wenzler@unibas.ch.

▽ Published ahead of print on 20 July 2009.

itively charged amidine groups and are therefore orally not effective. To improve the oral bioavailability, prodrugs were synthesized. After oral absorption through the gastrointestinal barrier, they are metabolized to their active trypanocidal parent drugs. This approach was successful for DB75 and its prodrug DB289 [pafuramidine maleate; 2,5-bis(4-amidinophenyl)-furan-bis-*O*-methylamidoxime], which became the first oral drug for sleeping sickness to enter clinical trials for the first stage. In a pivotal phase III trial, 273 patients were enrolled between August 2005 and March 2007. In October 2008, an additional phase I study of healthy volunteers was initiated to complete the safety assessment for registration of DB289 for sleeping sickness and *Pneumocystis jiroveci*. In the extended phase I trial, more severe liver toxicity and delayed renal insufficiency were observed in a number of participants and, as a consequence, the DB289 development program was discontinued (25). The mechanism of toxicity of DB289, particularly the delayed renal toxicity, is currently being further studied in animal models.

Many analogs of DB75/DB289 have been synthesized and tested in vitro and in vivo to find a new clinical candidate, especially for second-stage disease. Several of those analogs were effective in our stringent *T. b. rhodesiense* strain STIB900 acute mouse model (2). However, only a very few have shown good activity in the *T. b. brucei* strain GVR35 mouse CNS model. DB289 resulted in cures of 60% of GVR35-infected mice, but it was not effective in the vervet monkey CNS model (24). Though it was able to cure one-third of monkeys with an early CNS infection when treatment was initiated on day 14 postinfection, it was not curative when treatment was delayed to day 28 postinfection, a time point when brain infection is well established (24). DB289 can therefore not be considered a clinical candidate for second-stage disease, but its aza analogs have more potential and were evaluated in this study.

MATERIALS AND METHODS

Materials. Pentamidine isethionate and diminazene aceturate were purchased from Sigma-Aldrich; melarsoprol (Aventis) was provided by WHO; and DB75 and DB289 were provided by Immtech Pharmaceuticals. DB820, DB844, DB829, and DB868 were provided by David Boykin; their synthesis has been reported (16). The intermediates DB290, DB775, DB821, DB840, DB1058, DB1284, and DB1679 were also provided by David Boykin. Synthesis has been reported for DB290 (10), DB775 (1), DB821 (16), DB840 (16), and DB1058 and DB1284 (15). The synthesis of DB1679 has not been published yet.

Preparation of compounds. Compounds were dissolved in 100% dimethyl sulfoxide (DMSO) and finally diluted in culture medium prior to the assay. The DMSO concentration never exceeded 1% in the in vitro assays. For in vivo experiments, the compounds were dissolved in DMSO and further diluted with distilled H_2O to a final DMSO concentration of 10% prior to administration to animals.

Parasites. (i) *T. b. rhodesiense*. *T. b. rhodesiense* strain STIB900 is a derivative of strain STIB704. The strain was isolated from a patient in Ifakara, Tanzania, in 1982. STIB900 is used for routine in vitro screening and for the acute mouse model which mimics the first stage of HAT (31). STIB900mel and STIB900pent are melarsoprol- and pentamidine-resistant populations, respectively. When tested along with these drug-resistant lines, STIB900 was named STIB900wt. These resistant lines were generated by growing STIB900 in increasing subcurative drug concentrations (8).

(ii) *T. b. gambiense*. The *T. b. gambiense* strains used include STIB930, a derivate of strain TH1/78E(031), which was isolated from a patient in Côte d'Ivoire in 1978 (14); strain ITMAP141267, which was isolated from a patient in the Democratic Republic of Congo in 1960 (5); and strain K03048, which was isolated from a patient in South Sudan in 2003 (20).

(iii) *T. b. brucei*. The *T. b. brucei* strains used include BS221, a derivative of strain S427 that was isolated in Uganda in 1960; strain AT1KO, a P2 transporter knockout of the *T. b. brucei* strain BS221 (23); and strain GVR35, isolated from a wildebeest in the Serengeti in 1966 (primary isolate S10) (17).

In vitro growth inhibition assays using *T. brucei* subspecies. The 50% inhibitory concentrations (IC_{50}s) were determined by using the Alamar blue assay (27) and were carried out three times independently and in duplicate. Briefly, the compounds were tested in minimum essential medium with Earle's salts, supplemented according to the protocol of Baltz et al. (6) with the following modifications: 0.2 mM 2-mercaptoethanol, 1 mM Na-pyruvate, 0.5 mM hypoxanthine, and 15% heat-inactivated horse serum for *T. b. rhodesiense* and *T. b. brucei* and 15% human serum plus 5% fetal calf serum for *T. b. gambiense*. Serial drug dilutions were prepared in 96-well microtiter plates, and each well was inoculated with 2,000 bloodstream forms for *T. b. rhodesiense* or *T. b. brucei* assay and with 5,000 trypanosomes for *T. b. gambiense* assay. The drug exposure was at 37°C under a humidified 5% CO_2 atmosphere for 70 h. Ten microliters of the viability marker Alamar blue (12.5 mg resazurin [Sigma] dissolved in 100 ml phosphate-buffered saline) was then added to each well, and the plates incubated for an additional 2 to 6 h until the signal/background fluorescence ratio was about 10 for *T. b. rhodesiense* and *T. b. brucei* or about 5 for *T. b. gambiense* isolates. The plates were read in a Spectramax Gemini XS microplate fluorescence scanner (Molecular Devices) using an excitation wavelength of 536 nm and an emission wavelength of 588 nm. The IC_{50}s were calculated from the sigmoidal inhibition curves using SoftmaxPro software.

In vivo experiments. Adult female NMRI mice were obtained from RCC, Ittingen, Switzerland. They weighed between 20 and 25 g at the beginning of the study and were housed under standard conditions with food pellets and water ad libitum. All protocols and procedures used in the current study were reviewed and approved by the local veterinary authorities of the Canton Basel-Stadt, Switzerland.

STIB900 acute mouse model. The STIB900 acute mouse model mimics the first stage of the disease. Experiments were performed as previously reported (31), with minor modifications. Briefly, female NMRI mice were infected intraperitoneally (i.p.) with 2×10^4 STIB900 bloodstream forms. Experimental groups of four mice were treated i.p. with parent diamidines or orally (per os [p.o.]) with prodrugs on four consecutive days from day 3 to 6 postinfection. A control group was infected but remained untreated. The tail blood of all mice was checked for parasitemia until 60 days after infection. Surviving and aparasitemic mice at day 60 were considered cured and then euthanized. The day of death of the animals was recorded (including the cured mice, as >60) to calculate the mean survival time in days (MSD).

GVR35 mouse CNS model. The GVR35 mouse CNS model mimics the second stage of the disease. Five female NMRI mice per experimental group were used. Each mouse was inoculated i.p. with 2×10^4 bloodstream forms. The treatment was i.p. for parent compounds and p.o. for prodrugs on five consecutive days from day 21 to 25 postinfection. Some experimental groups were treated for 10 consecutive days (day 21 to 30 postinfection). A control group was treated on day 21 with a single dose of diminazene aceturate at 40 mg/kg of body weight i.p., which is subcurative since it clears the trypanosomes only in the hemolymphatic system and not in the CNS, leading to a subsequent reappearance of trypanosomes in the blood (17). Parasitemia was monitored twice in the first week after treatment followed by once a week until 180 days postinfection. Mice were considered cured when there was no parasitemia relapse detected in the tail blood over the 180-day observation period. Surviving mice were euthanized on day 180, and the day of death of the animals recorded (including the cured mice, as >180) to calculate the MSD.

RESULTS

In vitro results. The standard drugs melarsoprol, pentamidine, and DB75 (furamidine) were tested along with DB820 and DB829 against different *T. brucei* subspecies isolates in vitro (Table 1). In vitro data for the prodrugs are not included, but all were tested against *T. b. rhodesiense* STIB900wt and it was confirmed that all prodrugs were inactive ($IC_{50} > 3{,}000$ ng/ml). All other compounds were highly active, with IC_{50}s of ≤6.5 ng/ml (≤14 nM) against the reference strain STIB900wt. DB829 was less active than DB75 and DB820 or the two standard drugs. The activity ranking was confirmed repetitively by several additional in vitro experiments.

All compounds were found to be highly active against three different *T. b. gambiense* isolates ($IC_{50} < 40$ ng/ml [<85 nM]), with the activity ranking seen before (DB75 > DB820 >

TABLE 1. In vitro antitrypanosomal activity against different trypanosome subspecies and a P2 transporter knockout (AT1KO)

Compound	IC_{50} (ng/ml) for indicated strain							
	T. b. rhodesiense			*T. b. gambiense*			*T. b. brucei*	
	STIB900wt	STIB900pent	STIB900mel	K03048	ITMAP141267	STIB930	BS221	AT1KO
Melarsoprol	1.4	28.2	56.7	3.1	2.7	5.3	3.6	18.7
Pentamidine	1.2	133.6	124.5	15.5	4.2	1.1	0.9	4.1
DB75	1.0	14.3	19.0	4.2	3.1	5.1	1.2	15.8
DB820	2.4	22.5	29.2	8.4	5.7	8.4	2.8	42.9
DB829	6.5	67.9	64.3	39.5	16.2	35.1	6.0	106.4

DB829). The sensitivities of the *T. b. gambiense* isolates were similar for the drugs used, except for pentamidine. K03048 showed an elevated IC_{50} of 15.5 ng/ml, which is 14 times higher than the IC_{50} for STIB930. The in vitro susceptibilities of *T. b. brucei* BS221 were comparable to those of STIB900 for all compounds tested. AT1KO, the P2 transporter knockout of BS221, was less susceptible than the wild type. Pentamidine and melarsoprol demonstrated 4- to 5-fold losses of activity, while the three diphenylfuran diamidines revealed losses of activity of 13- to 18-fold (Table 2). The drug susceptibilities of the melarsoprol- and pentamidine-resistant STIB900 lines to all tested compounds were strongly reduced, but the highest cross-resistance was observed between melarsoprol and pentamidine. The melarsoprol-resistant trypanosomes showed a high level of resistance to pentamidine (resistance index, >100), as high as that of the pentamidine-resistant line. Melarsoprol resistance was high (42-fold) in the melarsoprol-resistant trypanosomes but lower than their pentamidine resistance and lower than in the pentamidine-resistant line. Levels of cross-resistance to the three diphenylfuran diamidines were significantly lower and comparable for the pentamidine- and the melarsoprol-resistant lines, with ratios of activities against STIB900pen/STIB900wt and STIB900mel/STIB900wt of 10 to 20. All three diphenylfuran diamidines were still highly active against both resistant lines, with IC_{50}s of 15 to 68 ng/ml. Again, DB829 was less potent than DB75.

In vivo STIB900 acute model results. Furamidine and pentamidine showed similar efficacies at doses of 20 mg/kg i.p. on four consecutive days in the in vivo STIB900 acute model, with three/four and two/four mice cured, respectively (Table 3). The aza analogs, DB820 and DB829, were both substantially more potent in this acute model than pentamidine and furamidine, although their levels of activity in vitro were lower. We obtained good dose responses and comparable efficacies of both aza compounds with i.p. administration despite the in vitro activity of DB829 being lower than that of DB820. The dimethoxyamidine prodrugs DB844, DB868, and DB289 (Fig. 1) were all able to cure four/four mice when tested orally in the STIB900 mouse model (Table 3). DB844 was also tested at a single dose of 20 mg/kg p.o. and gave three/four cures (data not presented). Dose responses clearly show that DB844 was more active than DB868, although their parent drugs had comparable in vivo efficacies.

In vivo GVR35 CNS model results. The prodrug DB289 showed good CNS activity in the in vivo GVR35 CNS model, with three/five mice cured at a dose of 100 mg/kg p.o. on five consecutive days (Table 4). Treatment for 10 days at 50 mg/kg represents an identical total dose but was less effective. DB844 was the first prodrug that cured all mice in the GVR35 mouse CNS model, at a dose of 100 mg/kg on five consecutive days administered by the oral route. It was additionally evaluated with 10-day treatments at different dosages. At 50 mg/kg p.o. on 10 consecutive days, cures of three/five mice were achieved; at 25 mg/kg, one/five was cured; and at 10 mg/kg, all mice relapsed with an MSD comparable to that of diminazene aceturate-treated control mice. DB868 had a similar efficacy and also cured all mice at a dose of 100 mg/kg p.o on five consecutive days. The extended 10-day treatment with four different doses resulted in good dose responses, highlighting the high CNS activity of DB868. At 100 mg/kg p.o. on 10 consecutive days, all mice were cured; at 50 mg/kg, four/five mice were cured; at 25 mg/kg, one/five mice was cured; and at 10 mg/kg, all mice relapsed, with an MSD similar to that of the control mice. The data show that although DB844 was more active than DB868 in the STIB900 acute mouse model, they were equally active in the mouse CNS model.

The parent compounds DB75, DB820, and DB829 were also evaluated in the GVR35 mouse CNS model. DB75 did not cure mice at 20 mg/kg i.p. on five consecutive days, but it did extend the survival to 92.25 days postinfection, which is a slight improvement over the survival in the control group treated at 40 mg/kg on one day with diminazene aceturate. DB75 administered for 10 days at 25 mg/kg i.p. was toxic and killed all mice.

TABLE 2. In vitro activity indices of different isolates versus that of reference strain STIB900 or BS221

Compound	Activity index against indicated strain pair						
	STIB900wt/ STIB900wt	STIB900pent/ STIB900wt	STIB900mel/ STIB900wt	K03048/ STIB900wt	ITMAP141267/ STIB900wt	STIB930/ STIB900wt	AT1KO/BS221
Melarsoprol	1	20.9	42.0	2.3	2.0	3.9	5.2
Pentamidine	1	113.1	105.4	13.1	3.6	0.9	4.3
DB75	1	14.7	19.5	4.3	3.2	5.3	13.1
DB820	1	9.6	12.4	3.5	2.4	3.5	15.4
DB829	1	10.5	10.0	6.1	2.5	5.4	17.8

TABLE 3. In vivo antitrypanosomal activity in the STIB900 acute mouse model

Type of compound (method of administration)	Dose[a]	Result[b] for indicated compound							
		No. of mice cured	MSD	No. of mice cured	MSD	No. of mice cured	MSD	No. of mice cured	MSD
Parent (i.p.)		DB75		DB820		DB829		Pentamidine	
	20	3/4	>57.75	4/4	>60	4/4	>60	2/4	>57.5
	10	ND		4/4	>60	4/4	>60	ND	
	5	1/4	>46	3/4	>54.5	3/4	>49.5	2/4	>45
	2.5	ND		2/4	>49	2/4	>60	ND	
	0.5	ND		0/4	29	1/4	>31	ND	
Prodrug (p.o.)		DB289		DB844		DB868			
	50	4/4	>60	ND		4/4	>60		
	25	4/4	>60	4/4	>60	2/4	>42		
	5	3/4	ND	3/4	>50.25	1/4	>40.25		
	2.5	1/4	ND	0/4	19.5	ND			

[a] Dose (mg/kg) was administered on four consecutive days.
[b] Cure was defined as survival for more than 60 days after infection without showing a parasitemia relapse. MSD (mean survival days) was determined for mice with and without parasitemia relapse; infected but untreated control mice died between day 6 and day 10 postinfection. ND, not determined.

Treatment at 12.5 mg/kg on 10 consecutive days was tolerated and cured one/four mice. DB820 at 20 mg/kg i.p. on five consecutive days did not cure, but it extended the survival of the mice to >100 days. At an identical daily dose in the extended 10-day treatment, one/five mice was cured without any toxicity observed. DB829 was the first and is still the only diamidine that cured single mice at a dose of 20 mg/kg i.p. on five consecutive days, and it cured all infected mice when administered for 10 days at 20 mg/kg i.p. The high CNS activity of DB829 was unexpected and is still unique among diamidines.

In vivo STIB900 acute model results for metabolites. The monoamidoxime/monomethoxyamidine metabolites (M1s) (Fig. 2) of the dimethoxyamidine prodrugs DB289, DB844, and DB868 retain prodrug characteristics due to their monoamidoxime/monomethoxyamidine groups and were therefore administered p.o. in the mouse models. All M1s did show oral activity and cured at least some mice at 50 mg/kg p.o. on four consecutive days in the STIB900 acute mouse model (Table 5). DB775, the M1 of DB289, showed the least efficacy. The M1s of DB844, DB1284 and DB1058, retained excellent activities and cured all mice at 25 mg/kg p.o. on four consecutive days. Testing at the very low dose of 5 mg/kg p.o. on four consecutive days showed that DB1058 was even more active than DB1284. DB1679, the M1 of DB868, was also highly active and cured all mice at 25 mg/kg p.o. on four consecutive days. All diamidoxime metabolites (M2s) were considerably less active in vivo. None of them gave any cures in the STIB900 acute mouse model at the tested doses of 75 mg/kg (DB840) or 100 mg/kg p.o. on four consecutive days (DB290 and DB821).

In vivo GVR35 mouse CNS model results for M1s. The aza M1s were highly active in the acute mouse model and were therefore also studied for their CNS activity in the GVR35 mouse CNS model, at 100 mg/kg p.o. on five consecutive days (Table 6). Only DB775, the M1 of DB289, was not tested due to inferior STIB900 activity in vivo. Both M1s of DB844, DB1058 and DB1284, showed high CNS activities. DB1058 cured four/five mice and DB1284 cured all mice at 100 mg/kg p.o. on five consecutive days. DB1679, the M1 of DB868, also showed CNS potency (one/five mice cured at 100 mg/kg p.o. on five consecutive days), but its activity was clearly less than those of its prodrug DB868 and the M1s of DB844.

DISCUSSION

Treatment of second-stage HAT still depends on only two drugs, the organoarsenical melarsoprol and eflornithine. Melarsoprol is still the first-line drug for HAT in many countries. This arsenical compound is highly toxic and has severe adverse

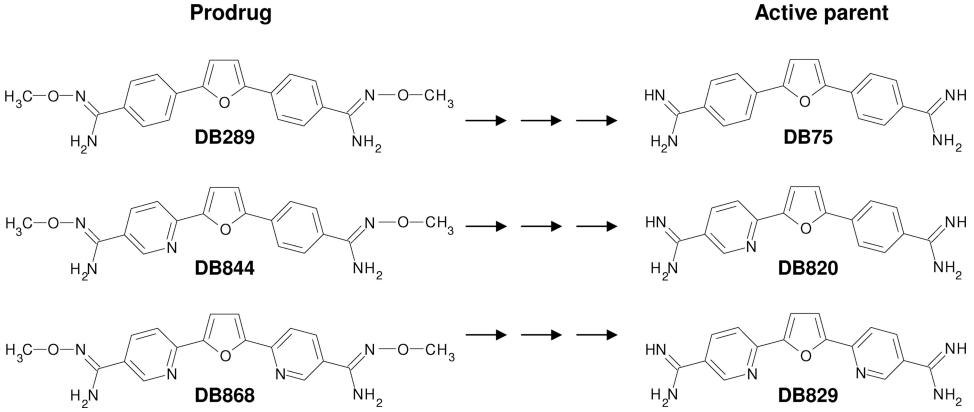

FIG. 1. Dimethoxyamidine prodrugs and their active parent diamidines.

TABLE 4. In vivo antitrypanosomal activity in the GVR35 CNS mouse model

Type of compound (method of administration)	Dose (mg/kg)/ no. of days administered	Result[a] for indicated compound					
		No. of mice cured	MSD or range	No. of mice cured	MSD	No. of mice cured	MSD
Parent (i.p.)		DB75		DB820		DB829	
	20/5	0/4[b]	92.25	0/4[b]	102.5	1/4[b]	>132.3
	20/10	Toxic[d]	NA	1/5	>128.2	4/4[b]	>180
	10/10	1/4[c]	>112[c]	ND		0/5	95.6
Prodrug (p.o.)		DB289		DB844		DB868	
	100/5	3/5	>167.8	5/5	>180	5/5	>180
	50/5	0/5	>153.6	1/5	>176.6	ND	
	25/5	0/5	75.4	0/5	117.6	0/4[b]	>95.8
	100/10	ND		ND		5/5	>180
	50/10	1/5	>172.2	3/5	>180	4/5	>153.4
	25/10	0/5	>146.6	1/5	>149.6	1/5	>132.4
	10/10	ND		0/5	75.25	0/5	70.0
Control (i.p.)		Melarsoprol or diminazene aceturate					
	15[e]/5	4/5	>175.4				
	10[e]/5	1/5	>148.6				
	5[e]/5	0/5	80.8				
	40[f]/1	0/5	47–83				

[a] Cure was defined as survival for more than 180 days after infection without showing a parasitemia relapse. MSD (mean survival days) was determined for mice with and without parasitemia relapse. ND, not determined. NA, not applicable.
[b] One mouse died during or directly after treatment (day 21 to day 28).
[c] DB75 was tested at 12.5 mg/kg i.p. for 10 consecutive days and cured one/four mice.
[d] DB75 tested at 25 mg/kg i.p. for 10 consecutive days was toxic.
[e] Melarsoprol.
[f] Diminazene aceturate. MSD of the diminazene aceturate-treated control group was 47 to 83 in different experiments.

effects which lead to fatalities in ≥5% of the patients treated (18). Additionally, there are alarming reports of treatment failures of up to 30% (7). Recent reports also indicate emerging resistance against eflornithine, the only alternative drug for second-stage HAT, with treatment failure rates already up to 16% (4). Nifurtimox, a drug against Chagas disease, is not very active against African trypanosomes as monotherapy, but in combination with melarsoprol and, especially, eflornithine, very promising results could be seen in clinical trials (9, 12, 26). The combination therapy may not work for isolates with some degree of resistance to melarsoprol or eflornithine. In a worst-case scenario, there could be no effective drug available for second-stage HAT in less than a decade. New safe and effective drugs are urgently needed for both disease stages to treat thousands of patients.

So far, no resistance has been reported in the field for pentamidine, although this drug has been in use for first-stage *T. b. gambiense* HAT for decades (23). This makes pentamidine an attractive molecule for analog-based drug discovery. To overcome the low oral bioavailability and the lack of CNS penetration, prodrugs were designed for this study.

In comparing the IC_{50}s of the aromatic diamidines DB75, DB820, and DB829, it became obvious that DB829 had higher IC_{50}s than DB75 and DB820 against all trypanosome strains

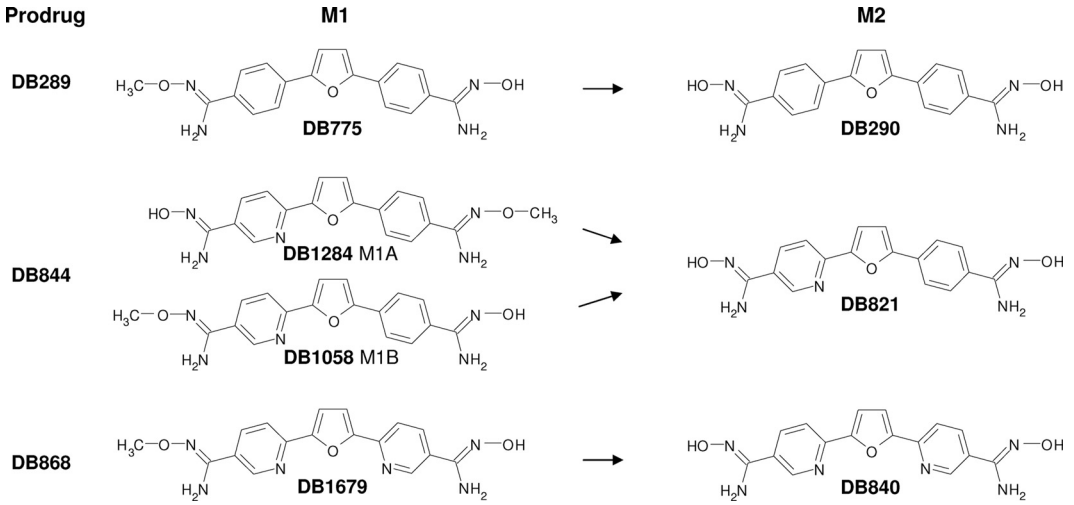

FIG. 2. Monoamidoxime/monomethoxyamidine metabolites (M1s) and diamidoxime metabolites (M2s).

TABLE 5. In vivo activity of intermediates in the STIB900 acute mouse model

Prodrug	Dose[a]	Result[b] for indicated drug intermediate					
		No. of mice cured	MSD	No. of mice cured	MSD	No. of mice cured	MSD
DB289		DB775				DB290	
	100	ND				0/4	50
	50	1/4	>56			ND	
	15	0/4	30.25			ND	
DB844		DB1284		DB1058		DB821	
	100	ND		4/4	>60	0/4	>54
	25	4/4	>60	4/4	>60	ND	
	5	1/4	>39.5	3/4	>52.75	ND	
DB868		DB1679				DB840	
	75	ND				0/4	18
	25	4/4	>60			ND	
	5	0/3[c]	29.7			ND	

[a] Dose (mg/kg) was administered p.o. on four consecutive days.
[b] Cure was defined as survival for more than 60 days after infection without showing a parasitemia relapse. MSD (mean survival days) was determined for mice with and without parasitemia relapse; infected but untreated control mice died between day 6 and 10 postinfection. ND, not determined.
[c] One mouse died due to p.o. application, with no toxicity observed.

tested. All three diamidines were less active against the *T. b. gambiense* isolates (~3- to 6-fold), the P2-transporter knockout of BS221 (~15-fold), and the laboratory-induced drug-resistant lines of STIB900 (~10- to 20-fold) (Table 2). The *T. b. gambiense* strain K03048 from South Sudan revealed a different sensitivity to pentamidine than the old drug-sensitive *T. b. gambiense* strain STIB930. Pentamidine resistance in the field has not been demonstrated; however, a reduced pentamidine susceptibility of K03048 was observed previously with a different in vitro method (hypoxanthine incorporation assay over 48 h) (20). K03048 was isolated from a patient in Ibba, Sudan, an area with high melarsoprol failure rates. This isolate, however, is melarsoprol sensitive in vitro and in the mouse model (20). The drug response of K03048 to the diamidines was comparable to those of the other two *T. b. gambiense* isolates. The two STIB900 lines selected for resistance to melarsoprol and pentamidine had 10- to 20-fold-increased IC_{50}s against the three diamidines. Molecular analysis revealed that the trypanosomes selected for melarsoprol resistance have lost the *TbAT1* gene that codes for the P2 transporter (23), while in the pentamidine-selected trypanosomes, the *TbAT1* gene was still present (8). Whether its P2 transporter is functionally expressed has not yet been investigated. Comparable resistance indices of the diphenylfuran diamidines for melarsoprol-resistant/wild type and AT1KO/wild type strains indicate that the moderate cross-resistance can probably be attributed to the loss of the P2 transporter only. The higher pentamidine resistance of the two resistant STIB900 lines indicates that there are additional alterations involved which cause loss of pentamidine sensitivity but not loss of sensitivity against the diphenylfuran diamidines. The P2 transporter has been identified as the primary uptake route for DB75 (19), but at least one other transporter participates in its uptake as well. In contrast, melarsoprol and pentamidine show only minor differences in activities in AT1KO and its wild type (at least two transporters involved in drug uptake). Bridges at al. have shown that the high-affinity pentamidine transporter (HAPT1) was absent from their high-level pentamidine-resistant and melarsoprol-resistant trypanosomes (11). If the high-level resistance of the melarsoprol- and pentamidine-selected STIB900 lines is similarly caused by a concomitant loss of TbAT1 and HAPT1, then the comparable loss of sensitivity of AT1KO indicates that HAPT1 is not involved or has only a minor impact on the uptake of furamidine and its aza analogs. The second major route of uptake has not yet been identified. Selective drug uptake can develop resistance, but on the other hand, it also facilitates selective uptake and drug accumulation by the parasite.

TABLE 6. In vivo activities of M1s versus those of dimethoxyamidine prodrugs in the GVR35 CNS model

Dose[a]	Result[b] for indicated compound:									
	DB844[c]		DB1058		DB1284		DB868		DB1679	
	No. of mice cured	MSD	No. of mice cured	MSD	No. of mice cured	MSD	No. of mice cured	MSD	No. of mice cured	MSD
100	5/5	>180	4/5	>180	5/5	>180	5/5	>180	1/5	>140.4
75	3/4, 1/5	>180, >172	1/5	>166	2/5	>164.8	ND		ND	
50	1/5	>176.6	ND		1/5	>157.2	ND		ND	

[a] Dose (mg/kg) was administered p.o. on five consecutive days.
[b] Cure was defined as survival for more than 180 days after infection without showing a parasitemia relapse. MSD (mean survival days) was determined for mice with and without parasitemia relapse. ND, not determined.
[c] DB844 has been tested twice at 75 mg/kg on five consecutive days; the 3/4 result is from a previous experiment, and the 1/5 result is from an experiment that included both M1s, DB1058 and DB1284.

DB820 and DB829 show in vivo activities superior to those of DB75 and pentamidine in both the acute and the mouse CNS model. Both aza parent compounds demonstrated comparable efficacies with no signs of overt toxicity after i.p. administration in the STIB900 acute mouse model. Both aza prodrugs, DB844 and DB868, were almost as efficacious as DB289 in the acute mouse model and were well tolerated at all doses tested. DB844 was more potent than DB868, although the parent compounds revealed similar efficacies. According to their efficacies in the acute model, both prodrugs could have the potential to serve as backup drugs to replace DB289 as the next oral drug to treat first-stage disease. However, the main focus and urgency is on finding a new treatment for second-stage HAT and an option for treatment after treatment failures with melarsoprol or eflornithine. The ideal solution would be one drug with the target product profile of a first-stage drug that could be used for both stages, thus rendering the painful lumbar puncture so far required for staging unnecessary.

DB868 was equally as potent as DB844 in the GVR35 mouse CNS model, despite its lower level of activity in the acute model. Both prodrugs have potential as oral drugs for second-stage sleeping sickness, according to their high CNS activity in the mouse model. However, safety studies of DB844 in the vervet monkey model for HAT demonstrated dose-dependent toxicity, especially, dose-limiting gastrointestinal toxicity, not previously observed with DB289 (John Thuita, personal communication). At 10 and 20 mg/kg p.o. for 10 days, it caused tissue damage in the gastrointestinal tract and liver, whereas at 5 mg/kg for 10 days, the clinical signs and hematological parameters were normal. But at 5 mg/kg, only three/eight vervet monkeys with CNS infection were cured (John Thuita, personal communication). The observed toxicity stopped further investigations of DB844. Recent toxicity studies of vervet monkeys have been completed for DB868. No signs of overt toxicity were observed in animals dosed for 10 days at 10 mg/kg or even 30 mg/kg p.o. (John Thuita, personal communication). DB868 does remain a promising preclinical candidate as it is substantially better tolerated than DB844 and DB289.

The high CNS activity of DB829 after i.p. administration was a surprise. This is the first parent diamidine that could cure all mice tested in the mouse CNS model. Passive diffusion across the BBB to reach sufficient concentrations in the CNS is unlikely for such a positively charged molecule. The transport is more likely to be mediated by specific transporters located in the BBB. Parenteral administration is an acceptable route of administration for second-stage HAT considering the fatal outcome without effective treatment.

The M1s of DB844 and DB868 were similarly active when administered orally in the acute mouse model and were almost as potent as their prodrugs. They could serve as orally active prodrug alternatives. DB1284 (metabolite of DB844) was slightly less active than the other metabolite, DB1058. The amidoxime metabolites of DB844 and DB868 lost the oral activity of the prodrugs. Previously, diamidoxime prodrugs have been shown to be less potent in the STIB900 acute model in several but not all cases (2, 16).

The M1s of DB844 and DB868 were also active in the mouse CNS model. Interestingly, DB1284, which was less active in the acute mouse model, did show a slightly higher efficacy in the mouse CNS model than DB1058 when tested at 75 mg/kg p.o. on five consecutive days. The bioactivation of the M1 to its active principle is abbreviated and therefore simplified in comparison to that of the dimethoxyamidine prodrug. It is conceivable to replace the prodrug with the M1 if other selection criteria, such as toxicity, simple pharmacokinetics, and cost of goods, are superior. DB1679, the M1 of DB868, is less CNS potent than DB868 and is therefore currently not considered an alternative candidate.

DB868, DB1058, and DB1284 are similarly CNS active in GVR35-infected mice and are candidates for an oral treatment for second-stage HAT. Their parent drugs showed comparable in vitro drug resistance and subspecies profiles. So far, DB868 has been the favored prodrug since its parent, DB829, is CNS active itself and its metabolism is simpler than that of its asymmetric analog (3). However, in several clinical trials with DB289, a highly variable pharmacokinetic profile was observed; it can be speculated that this may be due to the complicated metabolic prodrug activation (Christian Burri, personal communication). As parenterally administered DB829 penetrates the BBB, the pharmacokinetics will be much simplified compared to those of a prodrug treatment and predictions of optimized treatment regimes more reliable and therefore safer. Parenteral treatment for second-stage disease is acceptable, and DB829 may have potential to become the next new treatment option for second-stage HAT. To determine if it is indeed a leading preclinical candidate drug, extensive toxicity and efficacy studies for parenteral DB829 (CPD-0801) must be performed with vervet monkeys.

ACKNOWLEDGMENTS

We thank Guy Riccio and Christiane Braghiroli for technical assistance with the mouse experiments.

This work was supported by the Bill and Melinda Gates Foundation.

REFERENCES

1. **Anbazhagan, M., J. Y. Saulter, J. E. Hall, and D. W. Boykin.** 2003. Synthesis of metabolites of the prodrug 2,5-bis(4-O-methoxyamidinophenyl)furan. Heterocycles **60:**1133–1145.
2. **Ansede, J. H., M. Anbazhagan, R. Brun, J. D. Easterbrook, J. E. Hall, and D. W. Boykin.** 2004. O-Alkoxyamidine prodrugs of furamidine: in vitro transport and microsomal metabolism as indicators of in vivo efficacy in a mouse model of *Trypanosoma brucei rhodesiense* infection. J. Med. Chem. **47:**4335–4338.
3. **Ansede, J. H., R. D. Voyksner, M. A. Ismail, D. W. Boykin, R. R. Tidwell, and J. E. Hall.** 2005. In vitro metabolism of an orally active O-methyl amidoxime prodrug for the treatment of CNS trypanosomiasis. Xenobiotica **35:**211–226.
4. **Balasegaram, M., H. Young, F. Chappuis, G. Priotto, M.-E. Raguenaud, and F. Checchi.** 2009. Effectiveness of melarsoprol and eflornithine as first-line regimens for *gambiense* sleeping sickness in nine Médecins Sans Frontières programmes. Trans. R. Soc. Trop. Med. Hyg. **103:**280–290.
5. **Balmer, O., and A. Caccone.** 2008. Multiple-strain infections of *Trypanosoma brucei* across Africa. Acta Trop. **107:**275–279.
6. **Baltz, T., D. Baltz, C. Giroud, and J. Crockett.** 1985. Cultivation in a semi-defined medium of animal infective forms of *Trypanosoma brucei*, *T. equiperdum*, *T. evansi*, *T. rhodesiense* and *T. gambiense*. EMBO J. **4:**1273–1277.
7. **Barrett, M. P., D. W. Boykin, R. Brun, and R. R. Tidwell.** 2007. Human African trypanosomiasis: pharmacological re-engagement with a neglected disease. Br. J. Pharmacol. **152:**1155–1171.
8. **Bernhard, S. C., B. Nerima, P. Maser, and R. Brun.** 2007. Melarsoprol- and pentamidine-resistant *Trypanosoma brucei rhodesiense* populations and their cross-resistance. Int. J. Parasitol. **37:**1443–1448.
9. **Bisser, S., F.-X. N′Siesi, V. Lejon, P.-M. Preux, S. Van Nieuwenhove, C. Miaka Mia Bilenge, and P. Büscher.** 2007. Equivalence trial of melarsoprol and nifurtimox monotherapy and combination therapy for the treatment of second-stage *Trypanosoma brucei gambiense* sleeping sickness. J. Infect. Dis. **195:**322–329.
10. **Boykin, D. W., A. Kumar, J. E. Hall, B. C. Bender, and R. R. Tidwell.** 1996. Anti-pneumocystis activity of bis-amidoximes and bis-o-alkylamidoximes prodrugs. Bioorg. Med. Chem. Lett. **6:**3017–3020.

11. **Bridges, D. J., M. K. Gould, B. Nerima, P. Mäser, R. J. S. Burchmore, and H. P. de Koning.** 2007. Loss of the high-affinity pentamidine transporter is responsible for high levels of cross-resistance between arsenical and diamidine drugs in African trypanosomes. Mol. Pharmacol. **71:**1098–1108.
12. **Checchi, F., P. Piola, H. Ayikoru, F. Thomas, D. Legros, and G. Priotto.** 2007. Nifurtimox plus eflornithine for late-stage sleeping sickness in Uganda: a case series. PLoS Negl. Trop. Dis. **1:**e64.
13. **Dorlo, T. P. C., and P. A. Kager.** 2008. Pentamidine dosage: a base/salt confusion. PLoS Negl. Trop. Dis. **2:**e225.
14. **Felgner, P., U. Brinkmann, U. Zillmann, D. Mehlitz, and S. Abu-Ishira.** 1981. Epidemiological studies on the animal reservoir of *gambiense* sleeping sickness. Part II. Parasitological and immunodiagnostic examination of the human population. Tropenmed Parasitol. **32:**134–140.
15. **Ismail, M., and D. W. Boykin.** 2004. Synthesis of deuterium-labelled 6-[5-(-amidinophenyl)furan-2-yl]nicotinamidine and N-alkoxy-6-{5-[4-(N-alkoxyamidino) phenyl]-furan-2-yl}-nicotinamidines. J. Labelled Cpd. Radiopharm. **47:**233–242.
16. **Ismail, M. A., R. Brun, J. D. Easterbrook, F. A. Tanious, W. D. Wilson, and D. W. Boykin.** 2003. Synthesis and antiprotozoal activity of aza-analogues of furamidine. J. Med. Chem. **46:**4761–4769.
17. **Jennings, F. W., and G. D. Gray.** 1983. Relapsed parasitaemia following chemotherapy of chronic *T. brucei* infections in mice and its relation to cerebral trypanosomes. Contrib. Microbiol. Immunol. **7:**147–154.
18. **Kennedy, P. G. E.** 2008. The continuing problem of human African trypanosomiasis (sleeping sickness). Ann. Neurol. **64:**116–126.
19. **Lanteri, C. A., M. L. Stewart, J. M. Brock, V. P. Alibu, S. R. Meshnick, R. R. Tidwell, and M. P. Barrett.** 2006. Roles for the *Trypanosoma brucei* P2 transporter in DB75 uptake and resistance. Mol. Pharmacol. **70:**1585–1592.
20. **Maina, N., K. J. Maina, P. Mäser, and R. Brun.** 2007. Genotypic and phenotypic characterization of *Trypanosoma brucei gambiense* isolates from Ibba, South Sudan, an area of high melarsoprol treatment failure rate. Acta Trop. **104:**84–90.
21. **Mathis, A. M., A. S. Bridges, M. A. Ismail, A. Kumar, I. Francesconi, M. Anbazhagan, Q. Hu, F. A. Tanious, T. Wenzler, J. Saulter, W. D. Wilson, R. Brun, D. W. Boykin, R. R. Tidwell, and J. E. Hall.** 2007. Diphenyl furans and aza analogs: effects of structural modification on in vitro activity, DNA binding, and accumulation and distribution in trypanosomes. Antimicrob. Agents Chemother. **51:**2801–2810.
22. **Mathis, A. M., J. L. Holman, L. M. Sturk, M. A. Ismail, D. W. Boykin, R. R. Tidwell, and J. E. Hall.** 2006. Accumulation and intracellular distribution of antitrypanosomal diamidine compounds DB75 and DB820 in African trypanosomes. Antimicrob. Agents Chemother. **50:**2185–2191.
23. **Matovu, E., M. Stewart, F. Geiser, R. Brun, P. Mäser, L. J. Wallace, R. J. Burchmore, J. C. K. Enyaru, M. P. Barrett, R. Kaminsky, T. Seebeck, and H. de Koning.** 2003. Mechanisms of arsenical and diamidine uptake and resistance in *Trypanosoma brucei*. Eukaryot. Cell **2:**1003–1008.
24. **Mdachi, R. E., J. K. Thuita, J. M. Kagira, J. M. Ngotho, G. A. Murilla, J. M. Ndung'u, R. R. Tidwell, J. E. Hall, and R. Brun.** 2009. Efficacy of the novel diamidine compound 2,5-bis (4-amidinophenyl)-furan-bis-*O*-methlylamidoxime (pafuramidine, DB289) against *Trypanosoma brucei rhodesiense* infection in vervet monkeys after oral administration. Antimicrob. Agents Chemother. **53:**953–957.
25. **Pholig, G., S. Bernhard, J. Blum, C. Burri, A. Mpanya Kabeya, J.-P. Fina Lubaki, A. Mpoo Mpoto, B. Fungula Mununga, G. Kambau Manesa Deo, P. Nsele Mutantu, F. Mbo Kuikumbi, A. Fukinsia Mintwo, A. Kayeye Mununga, A. Dala, S. Macharia, C. Miaka Mia Bilenge, V. Kande Betu Ku Mesu, J. Ramon Franco, N. Dieyi Dituvanga, and C. Olson.** 2008. Phase 3 trial of pafuramidine maleate (DB289), a novel, oral drug, for treatment of first stage sleeping sickness: safety and efficacy, abstr. 542. 57th Meet. Am. Soc. Trop. Med. Hyg., New Orleans.
26. **Priotto, G., S. Kasparian, D. Ngouama, S. Ghorashian, U. Arnold, S. Ghabri, and U. Karunakara.** 2007. Nifurtimox-eflornithine combination therapy for second-stage *Trypanosoma brucei gambiense* sleeping sickness: a randomized clinical trial in Congo. Clin. Infect. Dis. **45:**1435–1442.
27. **Räz, B., M. Iten, Y. Grether-Bühler, R. Kaminsky, and R. Brun.** 1997. The Alamar Blue assay to determine drug sensitivity of African trypanosomes (*T.b. rhodesiense* and *T.b. gambiense*) in vitro. Acta Trop. **68:**139–147.
28. **Simarro, P. P., J. Jannin, and P. Cattand.** 2008. Eliminating human African trypanosomiasis: where do we stand and what comes next? PLoS Med. **5:**e55.
29. **Soeiro, M. N. C., E. M. De Souza, C. E. Stephens, and D. W. Boykin.** 2005. Aromatic diamidines as antiparasitic agents. Expert Opin. Investig. Drugs **14:**957–972.
30. **Stich, A., M. P. Barrett, and S. Krishna.** 2003. Waking up to sleeping sickness. Trends Parasitol. **19:**195–197.
31. **Thuita, J. K., S. M. Karanja, T. Wenzler, R. E. Mdachi, J. M. Ngotho, J. M. Kagira, R. R. Tidwell, and R. Brun.** 2008. Efficacy of the diamidine DB75 and its prodrug DB289, against murine models of human African trypanosomiasis. Acta Trop. **108:**6–10.
32. **Tidwell, R. R., and D. W. Boykin.** 2003. Dicationic DNA minor groove binders as antimicrobial agents, p. 414–460. *In* M. Demeunynck, C. Bailly, W. D. Wilson (ed.), DNA and RNA binders: from small molecules to drugs, vol. 2. Wiley-VCH, Weinheim, Germany.
33. **Trouiller, P., P. Olliaro, E. Torreele, J. Orbinski, R. Laing, and N. Ford.** 2002. Drug development for neglected diseases: a deficient market and a public-health policy failure. Lancet **359:**2188–2194.
34. **Wilson, W. D., F. A. Tanious, A. Mathis, D. Tevis, J. E. Hall, and D. W. Boykin.** 2008. Antiparasitic compounds that target DNA. Biochimie **90:**999–1014.
35. **World Health Organization.** 2006. Human African trypanosomiasis (sleeping sickness): epidemiological update. Wkly. Epidemiol. Rec. **81:**71–80.

Bioorganic & Medicinal Chemistry 21 (2013) 6732–6741

Contents lists available at ScienceDirect

Bioorganic & Medicinal Chemistry

journal homepage: www.elsevier.com/locate/bmc

Synthesis and antiprotozoal activity of dicationic 2,6-diphenylpyrazines and aza-analogues

Laixing Hu [a,b], Alpa Patel [a], Lavanya Bondada [a], Sihyung Yang [c], Michael Zhuo Wang [c], Manoj Munde [a], W. David Wilson [a], Tanja Wenzler [d,e], Reto Brun [d,e], David W. Boykin [a,*]

[a] Department of Chemistry, Georgia State University, Atlanta, GA 30303-3083, USA
[b] Institute of Medicinal Biotechnology, Chinese Academy of Medical Sciences and Peking Union Medical College, Beijing 100050, China
[c] Department of Pharmaceutical Chemistry, The University of Kansas, Lawrence, KS 66047, USA
[d] Swiss Tropical and Public Health Institute, Parasite Chemotherapy, Socinstrasse 57, Basel, CH-4002, Switzerland
[e] University of Basel, Basel, CH-4003, Switzerland

ARTICLE INFO

Article history:
Received 3 June 2013
Revised 28 July 2013
Accepted 4 August 2013
Available online 13 August 2013

Keywords:
Diamidines
Prodrugs
2,6-Diarylpyrazines
Antitrypanosomal agents
Antimalarial agents

ABSTRACT

Dicationic 2,6-diphenylpyrazines, aza-analogues and prodrugs were synthesized; evaluated for DNA affinity, activity against *Trypanosoma brucei rhodesiense* (*T. b. r.*) and *Plasmodium falciparum* (*P. f.*) in vitro, efficacy in *T. b. r.* STIB900 acute and *T. b. brucei* GVR35 CNS mouse models. Most diamidines gave poly(dA-dT)$_2$ ΔT_m values greater than pentamidine, IC_{50} values: *T. b. r.* (4.8–37 nM) and *P. f.* (10–52 nM). Most diamidines and prodrugs gave cures for STIB900 model (**11**, **19a** and **24b** 4/4 cures); **12** 3/4 cures for GVR35 model. Metabolic stability half-life values for *O*-methylamidoxime prodrugs did not correlate with STIB900 results.

1. Introduction

Tropical protozoan diseases, such as malaria and human African trypanosomiasis (HAT), affect millions of people in large parts of the world.[1] Malaria caused by *Plasmodium falciparum* (*P. f.*) leads to 665,000 deaths each year.[2] HAT (or sleeping sickness), another devastating disease, is caused by *Trypanosoma brucei rhodesience* (*T. b. r.*) and *Trypanosoma brucei gambiense* (*T. b. g.*), which is eventually fatal without treatment. There are below 10,000 reported cases and 30,000 estimated cases of HAT a year mostly in sub-Saharan Africa.[3,4] HAT has two stages: an early stage in which the parasites reside and proliferate in the hemolymphatic system and a second stage in which the parasites cross the blood–brain barrier (BBB) and infect the central nervous system (CNS).[5] The drugs currently in use against both malaria and HAT are far from satisfactory; most drugs suffer from poor oral bioavailability and severe side effects. For example, the second stage HAT drug melarsoprol causes a reactive encephalopathy which leads to death in 5% of treated patients.[6] Furthermore, for both diseases the cases of treatment failure because of drug resistance have increased in recent years. For second stage HAT, there are only two drugs melarsoprol and eflornithine available for monotherapy and NECT a combination therapy with niturtimox and eflornithine.[7] Therefore, there is an urgent need for development of more effective, orally available and less toxic drugs against these tropical protozoan diseases.

Although numerous DNA binding aromatic diamidines exhibit potent antiprotozoal activity against these tropical diseases, pentamidine **1** (Fig. 1) is the only one which has seen significant clinical use in humans.[8] Pentamidine has been used to treat first stage *T. b. g.* HAT, antimony-resistant leishmaniasis, and *Pneumocystis jiroveci* pneumonia. Because the amidine groups are protonated at physiological pH, pentamidine has low oral availability and requires parenteral administration, which makes its clinical use difficult in remote regions. Furamidine **2a** (Fig. 1), a diphenyl furan diamidine analogue, is the active metabolite of the di-*O*-methylamidoxime prodrug pafuramidine **2c** (Fig. 1) which reached phase III clinical trials against first-stage HAT and *P. jiroveci* pneumonia, and phase II clinical trials against malaria.[1,5,8,9] Due to hepatic and renal toxicity of pafuramidine in humans observed in an additional safety study paralleling the phase III trials, the further development of pafuramidine has been terminated. Introduction of a nitrogen atom into one or both of the terminal phenyl rings of furamidine resulted in aza-analogues of furamidine **3a** and **4a** (Fig. 1), which exhibited more potent in vivo activities against HAT than pentamidine and furamidine.[10,11] The *O*-methylamidoxime

* Corresponding author. Tel.: +1 404 413 5498; fax: +1 404 413 5505.
E-mail address: dboykin@gsu.edu (D.W. Boykin).

0968-0896/$ - see front matter © 2013 Elsevier Ltd. All rights reserved.
http://dx.doi.org/10.1016/j.bmc.2013.08.006

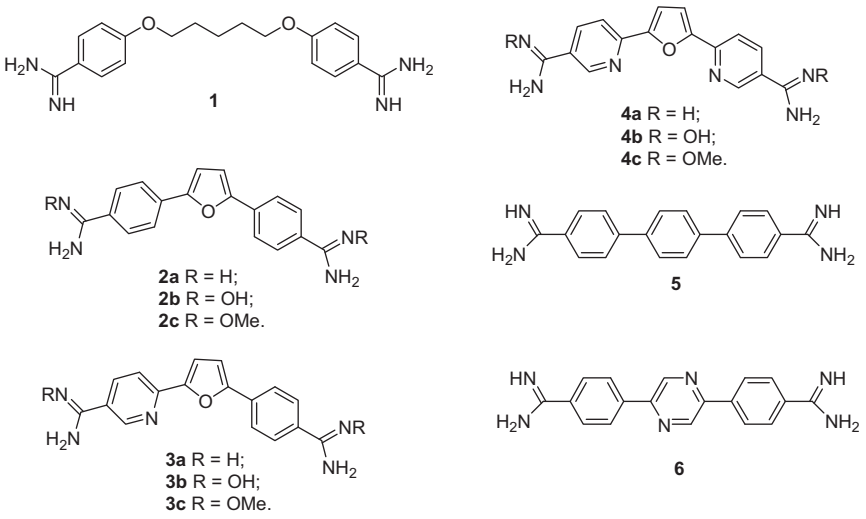

Figure 1. Aromatic diamidine antiprotozoal agents.

prodrugs of azafuramidines **3c** and **4c** (Fig. 1) were found to be quite effective in the second stage HAT GVR35 CNS mouse model[5] and **3c** was effective in a vervet monkey model of second stage HAT.[12] As yet, only very few compounds have shown good activity in the GVR35 CNS mouse model. Since the aza-analogue **4c** is better tolerated than **3c** in toxicity studies in vervet monkeys,[5] it is under further evaluation as a possible preclinical candidate for treatment of the second stage HAT. Unexpectedly, the parent diamidine **4a** also showed potent activity in the CNS mouse model on intraperitoneal injection; therefore, **4a** may have potential to become a treatment option for second stage HAT.[5]

Due to the promising results from the furamidine series, a large number of furamidine related diamidines have been synthesized.[8,13] Recently, we have described a series of linear terphenyl diamidine **5** (Fig. 1) and their aza-analogues (e.g. **6**), which showed significant DNA minor groove binding affinity and low nanomolar antiprotozoal activity against *T. b. r.* and *P. f.*[14,15] The in vivo efficacy for three of those aza-analogues in the *T. b. r.* STIB900 acute mouse model is much superior to that of furamidine, and comparable to the azafuramidines. Unfortunately, the di-amidoximes and di-*O*-methylamidoxime prodrugs of the terphenyl dicationic analogues showed poor bioconversion and were not effective on oral administration.[13]f In this study we have explored a series of novel curved dicationic 2,6-diarylpyrazines, their aza-analogues and their prodrugs which are isomeric with their linear 2,5-pyrazines.[14,15] Herein, we describe the synthesis, DNA binding affinity, in vitro activities against *T. b. r.* and *P. f.* and in vivo activities in the *T. b. r.* STIB900 acute mouse model and *T. b. brucei* GVR35 CNS mouse model for these curved 2,6-diarylpyrazines.

2. Chemistry

The synthesis of the parent dicationic 2,6-diphenylpyrazine **10** begins with Suzuki coupling of 2,6-dichloropyrazine (**7**) with 4-cyanophenylboronic acid (**8**) to yield the diphenylpyrazine dinitrile **9** (Scheme 1).[14–15] The di-nitrile **9** was converted to the diamidine **10** by the action of lithium trimethylsilylamide [LiN(TMS)$_2$] in THF. The di-amidoxime prodrug **11** was obtained by reaction of the di-nitrile **9** with hydroxylamine and followed by O-methylation with dimethylsulfate in the presences of lithium hydroxide to yield the corresponding di-*O*-methylamidoxime prodrug **12**.[10]

Employing the related Stille coupling process starting with 2,6-di(tri-*n*-butylstannyl)pyrazine the symmetrical di-nitriles **14a** and **14b** were made in one step (Scheme 2).[16] The di-nitriles **14a**–**b** were converted to the diamidines **15a**–**b** using LiN[TMS]$_2$ as previously mentioned.

The dissymmetric mono-aza analogues **19a**–**b** were made as outlined in Scheme 3. The pyridyl rings are introduced in the first step by performing Stille coupling between 2-chloro-6-(tri-*n*-butylstannyl)pyrazine and the appropriate bromocyanopyridines **16a**–**b**.[16] Subsequently, a Suzuki reaction between the 6-(pyridyl)-2-chloropyrazines **17a**–**b** and 4-cyanophenylboronic acid yields the dissymmetric di-nitriles **18a**–**b**. The di-nitriles were converted into the corresponding diamidines **19a**–**b**, the amidoxines **20a**,**b** and the *O*-methylamidoximes **21a**–**b** as discussed previously for Scheme 1.

The synthesis of the symmetrical di-aza analogues is presented in Scheme 4. It this case the needed di-nitriles **22a**–**b** are made directly by Stille coupling of the bromocyanopridines **16a**–**b** with 2,6-di(tri-*n*-butylstannyl)pyrazine. The di-nitriles were converted into the corresponding diamidines **23a**–**b**, the amidoxines **24a**–**b** and the *O*-methylamidoximes **25a**–**b** as discussed previously for Scheme 1.

3. Biology

The results for the evaluation of the dicationic 2,6-diarylpyrazine analogues and their prodrugs against *T. b. r.* and *P. f.* and their DNA binding affinities are shown in Table 1. For comparative purposes, the analogous data for pentamidine (**1**), furamidine (**2a**), azafuramidines **3a**, **4a** and 2,5-diphenyl pyrazine diamidine (**6**) are also included in Table 1.[10,15]

The interaction of diamidines with nuclear and kinetoplast DNA has been shown to be an important part of their mode of antiparasitic action.[8f] The ΔT_m values of these dicationic 2,6-diphenylpyrazines and their aza-analogues range from high values of 15.1 °C to low ones of 5.1 °C, as shown in Table 1. The parent diamidine **10** showed a ΔT_m value of 15.1 °C, which is lower than that of furamidine (**2a**) (ΔT_m = 25 °C) and higher than that of pentamidine (**1**) (ΔT_m = 12.6 °C). In comparison to **2a** the ΔT_m value of **10** is consistent with its increased hydrophilic property as a result of the additional two nitrogen atoms in the central pyrazine ring of **10**. This result may further suggest that the hydrophobic component is important for minor groove DNA binding. The ΔT_m value (15.1 °C) for **10** is higher than that of the linear 2,5-isomer **6** (ΔT_m = 8.0 °C). One possible explanation for this result may be that

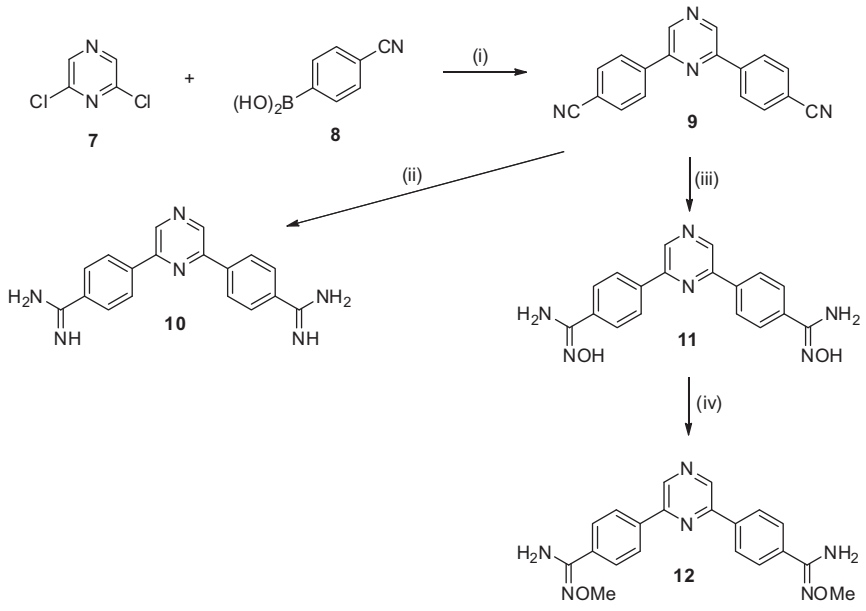

Scheme 1. Reagents and conditions: (i) $Pd(PPh_3)_4$, Na_2CO_3, toluene, 80 °C; (ii) (a) $LiN(TMS)_2$, THF; (b) HCl(gas), EtOH; (iii) NH_2OH–HCl, KO*t*-Bu, DMSO; (iv) LIOH, $(CH_3)_2SO_4$, DMF.

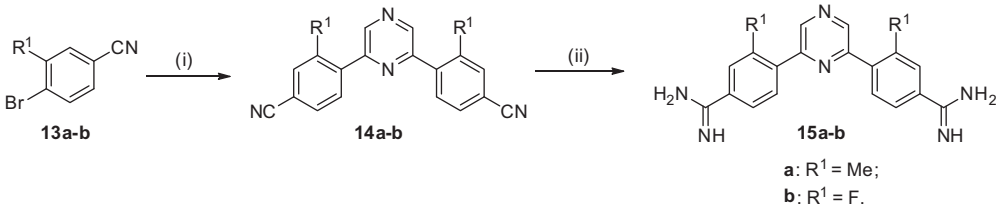

Scheme 2. Reagents and conditions: (i) 2,6-bis(tri-*n*-butylstannyl)pyrazine, $Pd(PPh_3)_4$, xylene, 120 °C; (iii) (a) $LiN(TMS)_2$, THF; (b) HCl(gas), EtOH.

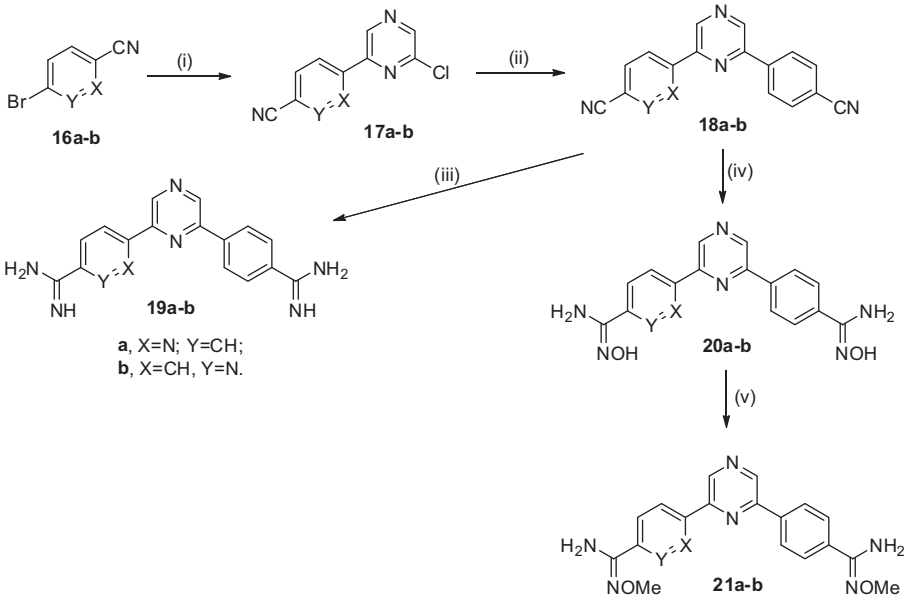

Scheme 3. Reagents and conditions: (i) 2-chloro-6-(tri-*n*-butylstannyl)pyrazine, $Pd(PPh_3)_4$, Na_2CO_3, toluene, 80 °C; (iii) (a) $LiN(TMS)_2$, THF; (b) HCl(gas), EtOH; (iv) NH_2OH–HCl, KO*t*-Bu, DMSO; (v) LiOH, $(CH_{32}SO_4)$, DMF.

compound **10** presents an approximately crescent shape which more closely fits the curvature of the DNA minor groove, similar to furamidine; and the linear isomer **6** needs incorporation of a water molecule in the complex to simulate the curved structure

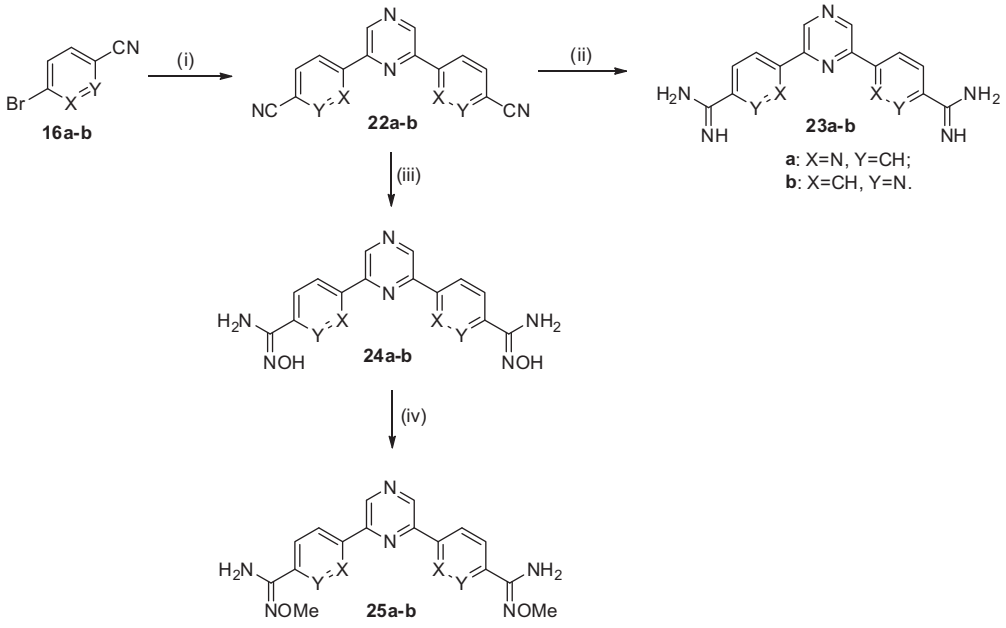

Scheme 4. Reagents and conditions: (i) 2,6-bis(tri-*n*-butylstannyl)pyrazine, $Pd(PPh_3)_4$, xylene, 120 °C; (ii) (a) $LiN(TMS)_2$, THF; (b) HCl(gas), EtOH; (iii) NH_2OH–HCl, KO*t*-Bu, DMSO; (iv) LiOH, $(CH_3)_2SO_4$, DMF.

Table 1
DNA affinities and antiprotozoan activity for 2,6-diarylpyrazine diamidines

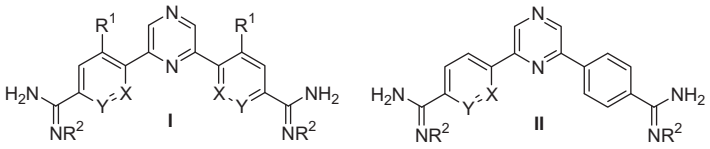

Code	Structure type	X	Y	R^1	R^2	ΔT_m [a] (°C)	*T. b. r.* IC_{50} [b] (nM)	*P. f.* IC_{50} [b] (nM)	Cytotoxicity IC_{50} [c] (nM)
1 pentamidne	/	/	/	/	/	12.6	2.2	46.4	2100
2a	/	/	/	/	/	25	4.5	15.5	6400
3a	/	/	/	/	/	19.3	6.5	6.5	77,900
4a	/	/	/	/	/	15.5	21	83	83,000
6	/	/	/	/	/	8.0	18	0.4	42,500
10	I	CH	CH	H	H	15.1	5.8	10	80,800
11	I	CH	CH	H	OH	/	7950	870	2900
12	I	CH	CH	H	OMe	/	18,900	410	58,700
15a	I	CH	CH	Me	H	5.1	462	323	117,000
15b	I	CH	CH	F	H	8.2	27	27	29,800
19a	II	N	CH	/	H	13.1	14	52	117,000
20a	II	N	CH	/	OH	/	7780	8400	24,600
21a	II	N	CH	/	OMe	/	25,300	5600	>180,000
19b	II	CH	N	/	H	15.1	6.0	10	34,100
20b	II	CH	N	/	OH	/	10,800	453	5000
21b	II	CH	N	/	OMe	/	194,000	453	>185,000
23a	I	N	CH	H	H	11.2	37	31	139,000
24a	I	N	CH	H	OH	/	90,600	7010	>196,000
25a	I	N	CH	H	OMe	/	119,600	7390	20,100
23b	I	CH	N	H	H	12.1	4.8	85	24,400
24b	I	CH	N	H	OH	/	95,400	785	>190,000
25b	I	CH	N	H	OMe	/	7870	328	>212,000

[a] Increase in thermal melting of poly(dA-dT)$_2$; see Refs. [24].
[b] The *T. b. r.* (*Trypanosoma brucei rhodesiense*) strain was STIB900, and the *P. f.* (*Plasmodium falciparum*) strain was K1. The IC_{50} values are the mean of two independent assays. Individual values differed by less than 50% of the mean see Ref. 17.
[c] Cytotoxicity was evaluated using cultured L6 rat myoblast cells; see Refs. [17].

of DNA minor groove.[18] The compounds **15a** and **15b**, methyl and fluorine substituted analogues, showed much lower ΔT_m values, which may be due to their twisted shape. Introduction of a nitrogen atom *meta* to the amidine group in one or both of the phenyl rings in the parent compound **10** leads to decreased DNA binding affinity: compound **19a** with one nitrogen resulted in a 2 °C

decrease in ΔT_m value and compound **23a** with two nitrogen atoms gave a ΔT_m value with a 3.9 °C decrease. However, their corresponding *ortho*-isomers **19b** and **23b** showed a smaller influence on the DNA binding affinity: compound **19b**, with one nitrogen atom, showed the same ΔT_m value as that of the parent compound **10** and compound **23b**, with two nitrogen atoms, showed a ΔT_m value reduced by 3.0 °C. These results are consistent with the effect of nitrogen substitution relationships found in the previous study of the aza-analogues of furamdine (**2a**).[10] It is also noteworthy that the compounds which exhibit the higher ΔT_m values showed the higher antitrypanosomal activity whereas weaker binding compounds show lower activity (see below) which is consistent with previous observations that while a threshold level of binding appears essential for activity a direct correlation between DNA affinity and in vitro activity is neither expected nor found.[8f] A similar trend was not found for the antiplasmodial activity.

These 2,6-diarylpyrazine diamidines exhibited significant in vitro antitrypanosomal and antiplasmodial activity at the low nanomolar level. The parent dicationic 2,6-diphenylpyrazine **10** showed an IC_{50} value of 6 nM against *T. b. r.*, comparable to that of pentamidine and furamidine. The antiplasmodial activity of **10** (IC_{50} = 10 nM) is approximately fivefold more active than pentamidine and slightly less active than furamidine. The antiprotozoal activity of **10** is similar to that of the azafuramidine **3a**. Compared to the isomer 2,5-dicationic diphenylpyrazine **6**, there are significant differences: the 2,6-isomer **10** was three times more active than 2,5-isomer **6** against *T. b. r.*; conversely, **10** was 25-fold less potent than **6** against *P. f.* The 2,6-isomer **10** lost the good selectivity for *P. f.* versus *T. b. r.* for which the 2,5-isomer **6** showed 45-fold selectivity for *P. f.*, compared to *T. b. r.* These differences may be due, in part, to the fact that the 2,6-diphenyl pyrazine diamidine **10** is an approximately crescent shaped molecule which more closely fits the curvature of the DNA minor groove, much similar to furamidine;[8,19] however, its dicationic isomer 2,5-diphenylpyrazine **6** is a linear molecule which presumably requires the incorporation of a water molecule into the recognition complex to simulate the curved structure of DNA minor groove.[18] The introduction of a methyl group or fluorine atom into the *meta*-position to the amidine group on both of the phenyl rings yielded compounds **15a** and **15b** which showed more than a sixty and fourfold loss of their antiprotozoal activities against *T. b. r.* and *P. f.*, respectively. Compound **19a** and **23a**, in which a nitrogen atom has been placed *meta* to the amidine group in one or both of the phenyl rings, showed a two and sixfold decrease in potency compared to the parent diamidine **10** against *T. b. r.* and a ten- and sixfold decreased potency against *P. f.* The two analogues 1**9b** and **23b**, in which the nitrogen atoms are *ortho* to the amidine, exhibited equivalent potency against *T. b. r.* and a similar or eightfold decrease in activity against *P. f.*, compared to the parent compound **10**. It is noted that the compounds **19b** and **23b** in which the nitrogen atoms are *ortho* to the amidine exhibited higher activity against *T. b. r.* than the corresponding *meta*-isomers **19a** and **23a**. However, a similar trend was not found for *P. f.* activity. Ten potential di-amidoxime and di-*O*-methylamidoxime prodrugs of the dicationic 2,6-diphenylpyrazine and aza-analogues were prepared. As expected, these amidoximes and *O*-methylamidoxime prodrugs showed low antiprotozoal activity when tested in vitro due to the absence of metabolizing enzymes.[10]

Given the promising in vitro *T. b. r.* activity of these new diamidines, except the methyl analogue **15a** which showed only moderate antitrypanosomial activity, we have evaluated them and their prodrugs in the stringent STIB900 acute mouse model for *T. b. r.* which mimics first stage disease.[5,9,17] Since the diamidines exhibit quite high pK_a values (10–11) and therefore unlikely to cross the intestinal barrier they were administered intraperitoneally; the prodrugs were designed to enhance oral bioavailability and hence were given orally. The results are shown in Table 2 (diamidines) and Table 3 (prodrugs).

Table 2
In vitro and in vivo anti-trypanosomal activity of 2,6-diarylpyrazine diamidines in the STIB900 mouse model[a]

Code	*T. b. r.* IC_{50} (nM)	Dosage[b] (ip, mg/kg)	Cures[c]	Survival[d] (days)
1	2.2	20	2/4	>57.5
		5	1/4	>38
2a	4.5	20	3/4	>57.75
		5	1/4	>46
3a	6.5	20	4/4	>60
		5	3/4	>54.5
4a	21	20	4/4	>60
		5	3/4	>49.5
6	18	5	0/4	36.5
10	5.8	5	3/4	>53.5
15a	462	/	/	/
15b	27	5	0/4	>41
19a	14	5	4/4	>60
19b	6	5	2/4	>60
23a	37	5	2/4	>53.75
23b	4.8	5	1/4	>36.5

[a] See Refs. 5 and 17 for details of STIB900 mouse model.
[b] Daily dosage was administered for 4 days; ip, intraperitoneal.
[c] Number of mice that survive and are parasite free for 60 days.
[d] Average days of survival; untreated control expires between day 7 and 9 post-infection.

Table 3
In vivo anti-trypanosomal activity of 2,6-diarylpyrazine diamidine prodrugs in the STIB900 mouse model[a]

Code[b]	Dosage[c] (po, mg/kg)	Cures[d]	Survival[e] (days)
2b(**2a**)	100	0/4	50
2c(**2a**)	25	4/4	>60
	10	4/4	>60
3c(**3a**)	25	4/4	>60
4c(**4a**)	25	2/4	>42
11(**10**)	25	4/4	>60
	10	0/4	22.5
12(**10**)	25	3/4	>53.5
	10	3/4	>56.5
20a(**19a**)	25	2/4	>45.75
21a(**19a**)	25	3/4	>57.5
	10	1/4	>49
20b(**19b**)	25	2/4	>50
21b(**19b**)	25	2/4	>50
24a(**23a**)	25	0/4	23.75
25a(**23a**)	25	2/4	>38.75
24b(**23b**)	25	4/4	>60
	10	1/4	>33.75
25b(23b)	25	1/4	>43.25

[a] See Refs. 5 and 17 for details of STIB900 mouse model.
[b] Code for parent of prodrug in parenthesis.
[c] Daily dosage was administered for 4 days.
[d] Number of mice that survive and are parasite free for 60 days.
[e] Average days of survival; untreated control expires between day 7 and 9 post-infection.

For comparative purposes Tables 2 and 3 also contain in vivo data for the dicationic analogues pentamidine (**1**), furamidine (**2a**), azafuramidines **3a** and **4a**, the dicationic 2,5-diphenylpyrazine **6** and the prodrugs **2b**, **2c**, **3c** and **4c** in the same mouse model.[10,15,22] On intraperitoneal dosing at 5 mg/kg all of the tested dications show a significant increase in survival time for the treated animals compared to untreated controls. The parent compound **10** gave 3/4 cures at a dose of 5 mg/kg, which is superior to that of pentamidine (**1**) and furamidine (**2a**) (1/4 cure), and is as effective as the azafuramidines **3a** and **4a** (3/4 cure). The linear 2,5-isomer **6** was less effective and gave no cure but did show an increase in mean survival time. The fluorine substituted analogue **15b** gave

Table 4
In vitro metabolic stability of 2,6-diarylpyrazine diamidine prodrugs

Code	Mouse $t_{1/2}$[b] (min)	Human $t_{1/2}$[b] (min)
2b	29 ± 10[a]	ND[c]
2c	150 ± 10[d]	6.8 ± 2[d]
11	1.9 ± 0.1[a]	ND
12	26 ± 6	8.6 ± 0.9
20a	30 ± 4[a]	ND
21a	210 ± 100	7.6 ± 0.3
20b	36 ± 5[a]	ND
21b	35 ± 6	6.5 ± 1.2
24a	20 ± 0.4[a]	ND
25a	200 ± 70	70 ± 23
24b	51 ± 1.4[a]	ND
25b	59 ± 10	14 ± 6

[a] Bis-amidoxime prodrugs were incubated with mouse liver S9 fraction, instead of liver microsomes.
[b] Mean ± standard deviations of triplicate determinations.
[c] ND, not determined.
[d] Substrate concentration for **2c** was 3 μM and its $t_{1/2}$ was shown as mean and range of duplicate determinations.

Table 5
In vivo anti-trypanosomal activity of 2,6-diarylpyrazine diamidine prodrugs in the GVR35 CNS mouse model[a]

Code[b]	Dosage (po, mg/kg)/no. of days administered	No. of mice cured[c]	MSD[d]
2c[e](**2a**)	100/5	3/5	>167.8
3c[e](**3a**)	100/5	5/5	>180
4c[e](**4a**)	100/5	5/5	>180
11(**10**)	100/5	0/5	69
12(**10**)	100/5	2/5	>173.8
	100/10	3/4	>180.0
24b(**23b**)	100/5	0/5	67.2
25a(**23a**)	100/5	0/5	95.2

[a] See Ref. 5 for details of GVR35 CNS mouse model.
[b] Code for parent of prodrug in parenthesis.
[c] Cure defined as survival for more than 180 days after infection without showing a parasitemia relapse.
[d] MSD (mean survival days) was determined for mice with and without parasitemia relapse.
[e] Data from Ref. 5.

also no cures in the in vivo model which is consistent with its lower in vitro activity against *T. b. r.* The four aza-analogues **19a**, **19b**, **23a** and **23b** exhibited identical or better results to that for furamidine at a dose of 5 mg/kg. The best result obtained was for compound **19a**, which showed 4/4 cures at a dose of 5 mg/kg. It is noteworthy that although compounds **19a** and **23a**, in which the nitrogen atom is *meta* to the amidine group, exhibited a significant loss of in vitro potency against *T. b. r.* compared to their isomeric compounds **19b** and **23b**, in which the nitrogen atom is *ortho* to the amidine, the in vivo efficacy of **19a** (4/4 cure) and **23a** (2/4 cure) was superior to the *ortho* isomers **19b** (2/4 cure) and **23b** (1/4 cure). This result may be due to pharmacokinetic differences between the *ortho* and *meta* isomers and/or the differential involvement of transporters. In general, the results for the aza-pyrazine analogues are consistent with those observed for the aza-furamidine system.[10]

Although previous studies of di-amidoxime and di-*O*-methylamidoxime prodrugs of the linear terphenyl diamidine analogues showed poor bioconversion and were not curative on oral administration,[13f] all the di-amidoxime and di-*O*-methylamidoxime prodrugs of the dicationic 2,6-diphenylpyrazine and aza-analogues showed activity when they were administered orally to the mice during this study. In vitro metabolic stability studies using mouse liver microsomes showed that di-*O*-methylamidoxime prodrugs were biotransformed at different rates, with **12**, **21b**, and **25b** showing shorter half-life than **21a** and **25a** (Table 4). However, this difference did not translate into activity in the STIB900 mouse model, as the latter generally gave more cures, with the exception of **12** (Table 3). This disconnect is likely due to a recent finding that intrahepatic binding and efflux of diamidines formed in the hepatocytes, rather than enzymatic biotransformation of prodrugs, determined the disposition of active diamidine metabolites.[20] It should also be noted that there was a marked interspecies difference in the metabolic stability of di-*O*-methylamidoxime prodrugs, as liver microsomes derived from humans metabolized the prodrugs much faster than those from mice (Table 4). This could be due to species differences in the enzyme activity and expression level of CYP4F/cyp4f enzymes, which were shown to be responsible for catalyzing the primary O-demethylation of the di-*O*-methylamidoxime pafuramidine in the human liver and intestinal microsomes.[21]

Very interestingly, treatment with the amidoxime produgs **11** and **24b** resulted in cures of all mice at the oral dose of 25 mg/kg, superior to the corresponding *O*-methylamidoxime prodrugs **12** (3/4 cure) and **25b** (1/4 cure) at the same dosage. Both of the amidoximes **11** and **24b** are more potent than the amidoxime prodrug **2b** of furamidine which gave no cure at an oral dose of 100 mg/kg (Table 3).[22] These results do not parallel those observed in the furamidine series, which showed that the *O*-methylamidoximes are more effective than the amidoximes.[10] The *O*-methylamidoxime prodrug **12** of the parent compound **10** gave 3/4 cures at the oral dose of 10 mg/kg. To evaluate the bioconversion of the di-amidoxime prodrugs, mouse liver S9 fractions were used as they contain cytochrome b_5 and cytochrome b_5 reductase, which are likely required to reduce amidoxime to amidine.[23] All di-amidoxime prodrugs examined in this study were efficiently metabolized (half-lives ranged from 2 to 51 min; Table 4), supporting their potential as prodrugs to generate active diamidine metabolites in vivo, but failed to explain the superiority of oral **24b** over other di-amidoximes (except **11**) in the STIB900 mouse model. As discussed above, this observation underscores the role of intrahepatic binding and efflux from hepatocytes, rather than bioconversion, in determining the disposition and activity of active diamidine metabolites in vivo.

Given the potent in vivo activity found in the *T. b. r.* STIB900 acute mouse model **11** and **12** were selected for study in the *T. b. brucei* GVR35 mouse model for second stage disease.[5] In sharp contrast to the results found in the STIB900 model, **11** was not effective at a dosage of 100 mg/kg for 5 days in the GVR35 model providing no cures and only a modest increase (69 days) in survival time (Table 5). This shows that compound **11** is only able to remove trypanosomes from the hemolymphatic compartment. However, at the same dosage **12** gave 2/5 cures. To achieve cures in the CNS mouse model drugs must cross the blood brain barrier and reach trypanocidal levels in the CSF and CNS. These additional barriers often result in CNS drug levels lower than that in blood. Hence, to attempt to compensate for this circumstance where possible we further test with increased doses. When the dosing of **12** was extended to 10 days 3/4 cures were noted showing that this compound is penetrating into the brain in sufficient concentration to cure CNS infection. The activity of **12** in the GVR35 CNS model, with 2/5 mice cured at dosage of 100 mg/kg for 5 days compares favorably with that for pafuramidine **2c** which showed 3/5 cured at the same dosage with the five day regimen. The efficacy of **12** is somewhat reduced from that of the *O*-methylamidoxime prodrug **4c** for treatment of second stage HAT which gave 5/5 cures at the same dosage (Table 5).[5] Nevertheless, prodrug **12** is one of only a very few compounds which have shown good activity in this CNS model. The compounds **24b** and **25a** were also selected for study in the *T. b. brucei* GVR35 CNS mouse model. Both compounds

were not curative at the oral dosage of 100 mg/kg for 5 days but they extended the survival time of mice similarly to control mice treated with diminazine (at 40 mg/kg ip single dose) which is a diamidine curing only first stage disease. The results for the amidoxime and *O*-methylamidoxime prodrugs of this series of dications provides stimulation for further evaluation of their efficacy and toxicity.

4. Conclusions

A series of dicationic 2,6-diphenylpyrazines and aza analogues have been prepared which exhibited DNA binding which is consistent with a role in their mode of action, showed potent in vitro activity against both *T. b. r.* and *P. f.*, and gave promising results on intraperitoneal administration in the stringent *T. b. r.* STIB900 mouse model. The diamidines **10** and **19a** exhibited in vivo efficacy (3/4 or 4/4 cures at 5 mg/kg dosage, ip) in the STIB900 model, superior to that of furamidine (**2a**), and comparable to or better than the azafuramidines **3a** and **4a**. Eight of the ten prodrugs of the dicatonic 2,6-diphenylpyrazine and aza-analogues showed good oral activity, giving cures in the STIB900 acute mouse model. The potent *O*-methylamidoxime prodrug **12** also showed good in vivo oral efficacy in the GVR35 second stage mouse model. This series of dicationic 2,6-diphenylpyrazine analogues and their prodrugs merit further evaluation for treatment of both stages of HAT.

5. Experimental section

5.1. Biology

5.1.1. Efficacy studies

The in vitro assays[17] with *T. b. r.* STIB 900 and *P. f.* K1 strain as well as the efficacy studies in an acute mouse model for *T. b. r.* STIB 900[5] were carried out as previously reported. The studies in the *T. b. brucei* GVR35 mouse model for second stage disease were performed as previously described.[5] All protocols and procedures for the mouse models used in the current study were reviewed and approved by the local veterinary authorities of Canton Basel-Stadt, Switzerland. The data was generated at the time the determination of survival was still accepted by the authorities.

5.1.2. T_m Measurements

Thermal melting experiments were conducted with a Cary 300 spectrophotometer. Cuvettes for the experiment were mounted in a thermal block and the solution temperatures monitored by a thermistor in the reference cuvette. Temperatures were maintained under computer control and increased at 0.5 °C/min. The experiments were conducted in 1 cm path length quartz curvettes in CAC 10 buffer (cacodylic acid 10 mM, EDTA 1 mM, NaCl 100 mM with NaOH added to give pH 7.0). The concentrations of DNA were determined by measuring its absorbance at 260 nm. A ratio of 0.3 mol compound per mole of DNA was used for the complex and DNA alone was used as a control. ΔT_m values were determined by the peak in first derivative curves (dA/dT).[24]

5.1.3. In vitro metabolic stability assays

The procedures used were similar to a reported method.[23a] Substrate stock solutions were prepared in DMSO. DMSO content was kept at 0.5% (v/v) in final incubations. Incubation mixtures (final volume 0.25 mL) consisted of 10 μM substrate and 0.5 mg/mL pooled liver microsomes from human or mouse (XenoTech, Lenexa, KS) for *O*-methylamidoxime prodrugs, or liver S9 fraction from mouse for amidoxime prodrugs. Reactions were carried out in 100 mM phosphate buffer (pH 7.4) containing 3.3 mM $MgCl_2$. Mouse liver S9 fractions were prepared from male Swiss Webster mice (25–30 g) as previously reported.[25] Briefly, four volumes of 0.25 M sucrose containing 0.1 M KCl and 1 mM EDTA was added to mouse liver and homogenized on ice with a sonic dismembrator (Fisher Scientific, Fair Lawn, NJ). The homogenate was centrifuged at 9000*g* for 20 min at 4 °C and then the supernatant fraction (S9 fraction) was collected and aliquoted before storing at −78 °C. After a 5-min pre-equilibration period at 37 °C, the metabolic stability reactions (in triplicate) were initiated by adding the cofactor (1 mM β-NADPH for microsomal incubations or a cocktail of 1 mM β-NADPH, 1 mM NADH, and 3.3 mM UDPGA for incubations with S9 fractions) and kept at 37 °C. Aliquots (100 μl) of the reaction mixtures were removed at 0, 15, 30, and 60 min and individually mixed with 100 μl of ice-cold acetonitrile. The mixtures were vortex-mixed, and precipitated protein was removed by centrifugation at 1400*g* for 15 min. The supernatant fractions were analyzed immediately by HPLC/UV.[21] In vitro half-lives were obtained using the one-phase exponential decay model with plateau set at zero (GraphPad Prism® 5.0, San Diego, CA).

5.2. Chemistry

5.2.1. General materials and methods

Melting points were determined on a Mel-Temp 3.0 melting point apparatus, and are uncorrected. TLC analysis was carried out on silica gel 60 F254 precoated aluminum sheets using UV light for detection. ^1H and ^{13}C NMR spectra were recorded on a Varian Unity Plus 300 MHz or Bruker 400 MHz spectrometer using indicated solvents. Mass spectra was obtained from the Georgia State University Mass Spectrometry Laboratory, Atlanta, GA. Elemental analysis were performed by Atlantic Microlab Inc., Norcross, GA, and are within ±0.4 of the theoretical values. The compounds reported as salts frequently analyzed correctly for fractional moles of water and/or other solvents; in each case ^1H NMR spectra was consistent with the analysis. All chemicals and solvents were purchased from Aldrich Chemical Co., VWR International, or Combi-Blocks, Inc.

*2,6-Di-(4′-cyanophenyl)pyrazine (**9**).* To a stirred solution of 2,6-dichloropyrazine (**7**, 2.0 g, 13.4 mmol) in toluene (56 mL) under nitrogen atmosphere at 80 °C was added 27 mL of 2 M aqueous solution of Na_2CO_3 followed by 4-cyanophenylboronic acid **8** (4.34 g, 29.5 mmol) in 30 mL of methanol. After 30 min, tetrakis(triphenylphosphine) palladium (1.34 g, 1.16 mmol) was added to the reaction mixture. The reaction mixture was stirred overnight at 80 °C. After cooling to room temperature, water was added to the mixture. The solution was filtered, and the precipitate was washed with water and MeOH. The crude product was purified by recrystallization to afford the title compound **9** (2.92 g, 77% yield); mp 298.5–299 °C. ^1H NMR (DMSO-d_6): δ 8.04 (d, J = 8.1 Hz, 4H), 8.47 (d, J = 8.1 Hz, 4H), 9.41 (s, 2H). ^{13}C NMR (DMSO-d_6): δ 148.8, 142.1, 139.9, 133.0, 127.7, 118.6, 112.6. MS: m/z 282 (M^+). Anal. Calcd for $C_{18}H_{10}N_4$: C, 76.58; H, 3.57; N, 19.85. Found: C, 76.33; H, 3.55; N, 19.76.

*2,6-Di-(4′-amidinophenyl)pyrazine hydrochloride (**10**).* The above dinitrile **9** (0.14 g, 0.48 mmol), suspended in freshly distilled THF (4 mL), was treated with lithium trimethylsilylamide (1 M solution in THF, 2.5 mL, 2.5 mmol), and the reaction was allowed to stir overnight. The reaction mixture was then cooled to 0 °C and to which was added HCl saturated ethanol (3 mL), whereupon a precipitate started forming. The mixture was allowed to stir overnight, after which it was diluted with ether, and the precipitate was filtered. The diamidine was purified by neutralization with 1 N NaOH followed by filtration of the resultant solid and washing with water. Finally, the free base was stirred with ethanolic HCl over-

night and diluted with ether, and the solid formed was filtered and dried to give the diamidine salt **10** (0.14 g, 76% yield); mp >300 °C. ^{1}H NMR (DMSO-d_6): δ 8.05 (d, J = 7.6 Hz, 4H), 8.53 (d, J = 7.6 Hz, 4H), 9.31 (s, 4H), 9.48 (s, 2H), 9.57 (s, 4H). ^{13}C NMR (DMSO-d_6): δ 165.1, 149.1, 141.6, 140.5, 129.0, 128.9, 127.2. Anal. Calcd for $C_{18}H_{16}N_6$-2.0HCl-2.3H_2O: C, 50.19; H, 5.29; N, 19.51. Found: C, 50.31; H, 4.92; N, 19.18.

*2,6-Di-(4′-N-hydroxyamidinophenyl)pyrazine hydrochloride (**11**).* A mixture of hydroxylamine hydrochloride (4.9 g, 70.8 mmol) in anhydrous DMSO (60 mL) was cooled to 5 °C under nitrogen. Potassium *tert*-butoxide (7.95 g, 70.8 mmol) was added in portions and the mixture was stirred for 30 min. To this mixture was added the above dinitrile **9** (1.0 g, 3.54 mmol) and the mixture was stirred overnight. The reaction mixture was poured slowly into a beaker with ice water and stirred for 15 min. The white precipitate was filtered and washed with water to afford the free base of **11**. The free base was stirred with ethanolic HCl overnight and diluted with ether, and the precipitate which formed was collected by filtration to give the title compound HCl salt **11** in 87% yield; mp >300 °C. ^{1}H NMR (DMSO-d_6): δ 3.86 (s, 6H), 4.64 (s, 2H), 7.96 (d, J = 8.4 Hz, 4H), 8.51 (d, J = 8.4 Hz, 4H), 9.25 (s, 4H), 9.43 (s, 2H), 11.42 (s, 2H), 13.13 (s, 2H). ^{13}C NMR (DMSO-d_6): δ 158.8, 149.1, 141.8, 140.0, 128.9, 127.3, 126.7. Anal. Calcd for $C_{18}H_{16}N_6O_2$-2.2HCl-2.0H_2O: C, 46.53; H, 4.82; N, 18.09. Found: C, 46.59; H, 4.45; N, 17.80.

*2,6-Di-(4′-N-methoxyamidinophenyl)pyrazine hydrochloride (**12**).* A solution of lithium hydroxide monohydrate (0.24 g, 5.74 mmol) in water (4 mL) was added dropwise to the mixture of the free base of the above di-amidoxime **11** (0.43 g, 1.44 mmol) in DMF (26 mL) at room temperature. The reaction mixture was stirred for 30 min at room temperature. Dimethylsulfate (0.45 g, 3.59 mmol) was added to the reaction mixture and the mixture was stirred at room temperature overnight. The reaction mixture was poured slowly into a beaker with ice water and stirred for 15 min. The precipitate was filtered and washed with water to afford the free base of **12**. The free base was stirred with ethanolic HCl overnight and diluted with ether, and the precipitate which formed was collected by filtration to give the title compound **12** in 58% yield; mp 244–246 °C. ^{1}H NMR (DMSO-d_6): δ 3.49 (s, 8H), 3.83 (s, 6H), 7.90 (d, J = 8.4 Hz, 4H), 8.38 (d, J = 8.4 Hz, 4H), 9.33 (s, 2H). ^{13}C NMR (DMSO-d_6): δ 156.7, 149.2, 141.6, 139.3, 128.5, 128.2, 127.1, 63.1. Anal. Calcd for $C_{20}H_{20}N_6O_2$-2.0HCl-1.5H_2O: C, 50.43; H, 5.29; N, 17.64. Found: C, 50.28; H, 5.17; N, 17.46.

*2,6-Di-(4′-amidino-2′-methylphenyl)pyrazine hydrochloride (**15a**).* A solution of 2,6-di(tri-*n*-butylstannyl)pyrazine (77% purity)[16] (4.04 g, 4.68 mmol), 4-bromo-3-methylbenzonitrile **13a** (2.02 g, 10.30 mmol), tetrakis(triphenylphosphine) palladium (0.56 g, 0.56 mmol) in degassed xylene (80 mL) was heated at 120 °C under nitrogen atmosphere for 24 h. After cooling to room temperature, the mixture was filtered and the precipitate was washed with xylene and ether. The crude product was purified by recrystallization (DMF) to afford compound **14a** in 62% yield [mp 239–141 °C (dec). ^{1}H NMR (DMSO-d_6): δ 2.43 (s, 6H), 7.74 (d, J = 8.1 Hz, 2H), 7.83 (d, J = 8.1 Hz, 2H), 7.89 (s, 2H), 8.95 (s, 2H). ^{13}C NMR (DMSO-d_6): δ 151.8, 143.5, 140.8, 137.8, 134.4, 131.0, 129.9, 118.5, 111.8, 19.8] and it was used directly in the next step without further characterization.

The same procedure described for the preparation of **10** was used starting with the above dinitrile **14a**; 52% yield; mp 250–252 °C (dec). ^{1}H NMR (DMSO-d_6): δ 2.46 (s, 6H), 7.80 (d, J = 8.1 Hz, 2H), 7.84 (d, J = 8.1 Hz, 2H), 7.89 (s, 2H), 8.98 (s, 2H), 9.32 (s, 4H), 9.52 (s, 4H). ^{13}C NMR (DMSO-d_6): δ 165.2, 152.1, 143.4, 141.2, 137.1, 130.6, 130.6, 128.6, 125.9, 20.2. Anal. Calcd for $C_{20}H_{20}N_6$-2.5HCl-1.0H_2O: C, 52.96; H, 5.44; N, 18.53. Found: C, 52.96; H, 5.31; N, 18.26.

*2,6-Di-(4′-amidino-2′-fluorophenyl)pyrazine hydrochloride (**15b**).* The same procedure described above for the preparation of **14a** was used starting with 4-bromo-3-fluorobenzonitrile **13b**; to give **14b** 62% yield [mp >300 °C. ^{1}H NMR (DMSO-d_6): δ 8.12–8.16 (m, 2H), 8.37 (d, J = 8.4 Hz, 2H), 8.49 (d, J = 10.4 Hz, 2H), 9.48 (s, 2H). HRMS: m/z 319.0800 (M+1) (calculated for $C_{18}H_9N_4F_2$, 319.0795)] and it was used directly in the next step without further characterization.

The same procedure described for the preparation of **10** was used starting with the above dinitrile **14b**; 60% yield; mp >300 °C. ^{1}H NMR (DMSO-d_6): δ 7.89–7.92 (m, 2H), 8.37 (d, J = 8.4 Hz, 2H), 8.44 (d, J = 12.4 Hz, 2H), 9.46 (s, 4H), 9.49 (s, 2H), 9.63 (s, 4H). ^{13}C NMR (DMSO-d_6): δ 161.9, 159.2 (d, J = 248.2 Hz), 147.9 (d, J = 2.3 Hz), 142.0, 141.6 (d, J = 8.6 Hz), 130.7, 122.8 (d, J = 2.9 Hz), 118.3 (d, J = 13.7 Hz), 114.4 (d, J = 23.5 Hz). HRMS: m/z 353.1311 (M+1) (calculated for $C_{18}H_{15}N_6F_2$, 353.1326). Anal. Calcd for $C_{18}H_{14}F_2N_6$-2.0HCl-1.3H_2O: C, 48.18; H, 4.18; N, 18.73. Found: C, 48.37; H, 4.11; N, 18.67.

*2-Chloro-6-(5′-cyanopyridin-2′-yl)pyrazine (**17a**).* A solution of 2-chloro-6-(tri-*n*-butylstannyl)pyrazine[16] (3.62 g, 9.0 mmol), 2-bromo-5-cyanopyridine **16a** (1.67 g, 9.0 mmol), tetrakis(triphenylphosphine) palladium (0.52 g, 0.45 mmol) in degassed xylene (20 mL) was heated at 120 °C under nitrogen atmosphere overnight. After cooling to room temperature, the mixture was filtered. Most of the solvent was removed under reduced pressure; the precipitate which formed was filtered and washed with xylene and ether. The crude product was purified by column chromatography on silica gel (eluent hexane/ethyl acetate (5/1)) to give the title compound **17a** in 67% yield; mp 148–150 °C. ^{1}H NMR (DMSO-d_6): δ 8.41 (d, J = 8.4 Hz, 1H), 8.51 (dd, J = 2.0, 8.4 Hz, 1H), 8.97 (s, 1H), 9.20 (d, J = 2.0 Hz, 1H), 9.51 (s, 1H). ^{13}C NMR (DMSO-d_6): δ 154.9, 152.6, 148.5, 147.9, 145.7, 141.7, 141.0, 121.2, 116.7, 110.1. Anal. Calcd for $C_{10}H_5ClN_4$: C, 55.44; H, 2.33; N, 25.86. Found: C, 55.55; H, 2.28; N, 25.83.

*2-(4′-Cyanophenyl)-6-(5′-cyanopyridin-2′-yl)pyrazine (**18a**).* The same procedure described for 2,6-di-(4′-cyanophenyl)pyrazine **9** was used by employing 2-chloro-6-(5′-cyanopyridin-2′-yl)pyrazine **17a** and 4-cyanophenylboronic acid **8** to furnish the compound **18a** in 71% yield; mp 293–295 °C. ^{1}H NMR (DMSO-d_6): δ 8.04 (d, J = 8.4 Hz, 2H), 8.50 (d, J = 8.4 Hz, 2H), 8.53 (dd, J = 2.0, 8.4 Hz, 1H), 8.71 (d, J = 8.4 Hz, 1H), 9.19 (d, J = 2.0 Hz, 1H), 9.48 (s, 1H), 9.57 (s, 1H). HRMS: m/z 284.0930 (M+1) (calculated for $C_{17}H_{10}N_5$, 284.0936). Anal. Calcd for $C_{17}H_9N_5$: C, 72.08; H, 3.20; N, 24.75. Found: C, 71.85; H, 3.17; N, 24.64.

*2-(4′-Amidinophenyl)-6-(5′-amidinopyridin-2′-yl)pyrazine hydrochloride (**19a**).* The same procedure described for the preparation of **10** was used starting with the above dinitrile **18a**; 90% yield; mp 296–298 °C (dec). ^{1}H NMR (DMSO-d_6): δ 8.05 (d, J = 8.4 Hz, 2H), 8.46 (dd, J = 2.0, 8.4 Hz, 1H), 8.58 (d, J = 8.4 Hz, 2H), 8.77 (d, J = 8.4 Hz, 1H), 9.17 (d, J = 2.0 Hz, 1H), 9.27 (s, 2H), 9.40 (s, 2H), 9.56 (s, 2H), 9.56 (s, 1H), 9.62 (s, 1H), 9.73 (s, 2H). ^{13}C NMR (DMSO-d_6): δ 165.1, 163.7, 157.2, 149.0, 148.9, 148.2, 143.5, 142.1, 140.1, 137.9, 129.2, 128.9, 127.4, 125.2, 120.9. Anal. Calcd for $C_{17}H_{15}N_7$-3.0HCl-1.7H_2O: C, 44.64; H, 4.72; N, 21.44. Found: C, 44.67; H, 4.52; N, 21.44.

*2-(4′-N-Hydroxyamidinophenyl)-6-(5′-N-hydroxyamidinopyridin-2′-yl)pyrazine hydrochloride (**20a**).* The same procedure described for the preparation of **11** was used starting with the above dinitrile **18a**; yield 89%; mp 283–285 °C (dec). ^{1}H NMR (DMSO-d_6): δ 3.43 (s, 8H), 7.95 (d, J = 8.4 Hz, 2H), 8.36 (dd, J = 2.0, 8.4 Hz, 1H), 8.52 (d, J = 8.4 Hz, 2H), 8.68 (d, J = 8.4 Hz, 1H), 9.08 (d, J = 2.0 Hz, 1H), 9.47 (s, 1H), 9.57 (s, 1H). ^{13}C NMR (DMSO-d_6): δ 158.8, 156.9, 156.8, 149.0, 148.7, 148.2, 143.4, 142.0, 139.8, 137.9, 128.9, 127.5, 126.8, 122.9, 121.1. Anal. Calcd for $C_{17}H_{15}N_7O_2$-3.0HCl-0.8H_2O: C, 43.16; H, 4.18; N, 20.72. Found: C, 43.15; H, 4.22; N, 20.62.

*2-(4′-N-Methoxyamidinophenyl)-6-(5′-N-methoxyamidinopyridin-2′-yl)pyrazine hydrochloride (**21a**).* The same procedure

described for the preparation of **12** was used starting with the above compound **20a**; 29% yield; mp 213–215 °C (dec). ^{1}H NMR (DMSO-d_6): δ 3.43 (s, 8H), 3.83 (s, 3H), 3.85 (s, 3H), 7.92 (d, J = 8.4 Hz, 2H), 8.29 (dd, J = 2.0, 8.4 Hz, 1H), 8.39 (d, J = 8.4 Hz, 2H), 8.57 (d, J = 8.4 Hz, 1H), 9.03 (d, J = 2.0 Hz, 1H), 9.38 (s, 1H), 9.52 (s, 1H). ^{13}C NMR (DMSO-d_6): δ 157.5, 155.1, 152.7, 149.0, 148.4, 147.7, 143.0, 141.8, 139.5, 136.6, 128.7, 127.4, 127.3, 126.1, 121.0, 63.4, 62.3. Anal. Calcd for $C_{19}H_{19}N_7O_2$-3.0HCl-0.7H_2O: C, 45.70; H, 4.72; N, 19.63. Found: C, 45.91; H, 4.67; N, 19.29.

*2-Chloro-6-(2′-cyanopyridin-5′-yl)pyrazine (**17b**).* The same procedure described for 2-chloro-6-(5′-cyanopyridin-2′-yl)pyrazine **17a** was used by employing 2-chloro-6-(tri-*n*-butylstannyl)pyrazine[16] and 2-bromo-5-cyanopyridine **16b** to furnish the title compound **17b** in 52% yield; mp 149–151 °C. ^{1}H NMR (DMSO-d_6): δ 8.24 (d, J = 8.4 Hz, 1H), 8.71 (dd, J = 2.0, 8.4 Hz, 1H), 8.91 (s, 1H), 9.45 (d, J = 2.0 Hz, 1H), 9.46 (s, 1H). ^{13}C NMR (DMSO-d_6): δ 149.4, 148.1, 147.7, 144.7, 141.3, 136.0, 133.5, 133.4, 129.2, 117.3. Anal. Calcd for $C_{10}H_5ClN_4$: C, 55.44; H, 2.33; N, 25.86. Found: C, 55.67; H, 2.30; N, 25.60.

*2-(4′-Amidinophenyl)-6-(2′-amidinopyridin-5′-yl)pyrazine hydrochloride (**19b**).* The same procedure described for 2,6-di-(4′-cyanophenyl)pyrazine **9** was used by employing 2-chloro-6-(2′-cyanopyridin-5′-yl)pyrazine **17b** and 4-cyanophenylboronic acid **8** to furnish the compound **18b** in 88% yield [mp 271–273 °C. ^{1}H NMR (DMSO-d_6): δ 8.06 (d, J = 8.4 Hz, 2H), 8.26 (d, J = 8.4 Hz, 1H), 8.51 (d, J = 8.4 Hz, 2H), 8.90 (dd, J = 2.0, 8.4 Hz, 1H), 9.48 (s, 1H), 9.50 (s, 1H), 9.63 (d, J = 2.0 Hz, 1H). ^{13}C NMR (DMSO-d_6): δ 149.5, 149.0, 147.0, 142.6, 142.4, 139.6, 135.9, 134.6, 133.3, 133.0, 129.2, 127.8, 118.6, 117.4, 112.7] and it was used directly in the next step without further characterization.

The same procedure described for the preparation of **10** was used starting with the above dinitrile **18b**; yield 87%; mp >300 °C. ^{1}H NMR (DMSO-d_6): δ 8.04 (d, J = 8.8 Hz, 2H), 8.52 (d, J = 8.4 Hz, 1H), 8.55 (d, J = 8.8 Hz, 2H), 9.02 (dd, J = 2.0, 8.4 Hz, 1H), 9.21 (s, 2H), 9.46 (s, 2H), 9.51 (s, 2H), 9.51 (s, 1H), 9.54 (s, 1H), 9.65 (d, J = 2.0 Hz, 1H), 9.70 (s, 2H). ^{13}C NMR (DMSO-d_6): δ 165.1, 161.6, 149.3, 148.1, 147.2, 144.7, 142.6, 142.4, 140.2, 136.4, 135.3, 129.3, 128.9, 127.4, 123.6. Anal. Calcd for $C_{17}H_{15}N_7$-2.0HCl-1.55H_2O: C, 48.83; H, 4.84; N, 23.44. Found: C, 49.15; H, 4.78; N, 23.07.

*2-(4′-N-Hydroxyamidinophenyl)-6-(2′-N-hydroxyamidinopyridin-5′-yl)pyrazine hydrochloride (**20b**).* The same procedure described for the preparation of **11** was used starting with the above dinitrile **18b**; yield 87%; mp 291–293 °C (dec). ^{1}H NMR (DMSO-d_6): δ 3.44 (s, 4H), 7.95 (d, J = 8.4 Hz, 2H), 8.24 (d, J = 8.4 Hz, 1H), 8.53 (d, J = 8.8 Hz, 2H), 8.87 (dd, J = 2.0, 8.4 Hz, 1H), 9.21 (s, 2H), 9.45 (s, 1H), 9.49 (s, 1H), 9.56 (d, J = 2.0 Hz, 1H), 11.01 (s, 1H), 11.20 (s, 1H). ^{13}C NMR (DMSO-d_6): δ 158.7, 154.7, 149.2, 147.9, 147.4, 145.0, 142.3, 142.1, 139.7, 136.0, 134.4, 128.9, 127.4, 126.8, 123.0. Anal. Calcd for $C_{17}H_{15}N_7O_2$-2.0HCl-1.4H_2O: C, 45.63; H, 4.46; N, 21.91. Found: C, 45.99; H, 4.40; N, 21.56.

*2-(4′-N-Methoxyamidinophenyl)-6-(2′-N-methoxyamidinopyridin-5′-yl)pyrazine hydrochloride (**21b**).* The same procedure described for the preparation of **12** was used starting with the above compound **20b**; yield 37%; mp 160–162 °C (dec). ^{1}H NMR (DMSO-d_6): δ 3.86 (s, 3H), 3.88 (s, 3H), 3.89 (s, 8H), 7.96 (d, J = 8.0 Hz, 2H), 8.10 (d, J = 8.4 Hz, 1H), 8.46 (d, J = 8.0 Hz, 2H), 8.87 (dd, J = 2.0, 8.4 Hz, 1H), 9.41 (s, 1H), 9.43 (s, 1H), 9.47 (d, J = 2.0 Hz, 1H). ^{13}C NMR (DMSO-d_6): δ 157.3, 150.7, 149.3, 148.3, 147.9, 147.2, 141.8, 141.7, 139.5, 135.5, 132.8, 128.7, 127.6, 127.2, 121.1, 63.4, 62.0. Anal. Calcd for $C_{19}H_{19}N_7O_2$-2.0HCl-2.0H_2O: C, 46.92; H, 5.18; N, 20.16. Found: C, 46.98; H, 5.09; N, 19.93.

*2,6-Di-(5′-cyanopyridin-2′-yl)pyrazine (**22a**).* The same procedure described for 2,6-di-(4′-cyano-2′-methylphenyl)pyrazine **14a** was used by employing 2,6-di(tri-*n*-butylstannyl)pyrazine and 2-bromo-5-cyanopyridine **16a** to furnish the title compound **22a** in 58% yield; mp 264–266 °C (dec).^{1}H NMR (DMSO-d_6): δ 8.69 (dd, J = 2.1, 8.4 Hz, 2H), 8.80 (d, J = 8.4 Hz, 2H), 9.23 (s, 2H), 9.67 (d, J = 2.1 Hz, 2H). ^{13}C NMR (DMSO-d_6): δ 155.9, 152.6, 147.8, 143.8, 141.6, 121.4, 116.9, 110.0. Anal. Calcd for $C_{16}H_8N_6$: C, 67.60; H, 2.84; N, 29.56. Found: C, 67.41; H, 2.73; N, 29.31.

*2,6-Di-(5′-amidinopyridin-2′-yl)pyrazine hydrochloride (**23a**).* The same procedure described for the preparation of **10** was used starting with the above dinitrile **22a**; 50% yield; mp 277–279 °C (dec). ^{1}H NMR (DMSO-d_6): δ 8.48 (dd, J = 2.4, 8.4 Hz, 2H), 8.86 (d, J = 8.1 Hz, 2H), 9.18 (d, J = 2.4 Hz, 2H), 9.41 (s, 4H), 9.72 (s, 2H), 9.74 (s, 4H). ^{13}C NMR (DMSO-d_6): δ 163.7, 156.9, 149.0, 148.1, 143.6, 138.0, 125.2, 121.1. Anal. Calcd for $C_{16}H_{14}N_8$-2.0HCl-2.5H_2O: C, 44.05; H, 4.85; N, 25.68. Found: C, 44.08; H, 4.67; N, 25.39.

*2,6-Di-(5′-N-hydroxyamidinopyridin-2′-yl)pyrazine hydrochloride (**24a**).* The same procedure described for the preparation of **11** was used starting with the above dinitrile **22a** in 97% yield; mp 274–276 °C (dec).^{1}H NMR (DMSO-d_6-D_2O): δ 3.52 (s, 6H), 8.32 (dd, J = 2.0, 8.4 Hz, 2H), 8.74 (d, J = 8.4 Hz, 2H), 9.03 (d, J = 2.0 Hz, 2H), 9.65 (s, 2H), 11.08 (s, 2H). ^{13}C NMR (DMSO-d_6): δ 156.4, 156.2, 148.6, 148.1, 143.4, 137.6, 123.5, 121.2. Anal. Calcd for $C_{16}H_{14}N_8O_2$-2.0HCl-2.1H_2O: C, 41.68; H, 4.42; N, 24.30. Found: C, 41.71; H, 4.30; N, 24.30.

*2,6-Di-(5′-N-methoxyamidinopyridin-2′-yl)pyrazine hydrochloride (**25a**).* The same procedure described for the preparation of **12** was used starting with the above compound **24a**; yield 58%; mp 216–218 °C (dec). ^{1}H NMR (DMSO-d_6): δ 3.82 (s, 6H), 4.00 (s, 6H), 6.70 (s, 2H), 8.27 (dd, J = 1.8, 8.4 Hz, 2H), 8.64 (d, J = 8.4 Hz, 2H), 9.04 (d, J = 1.8 Hz, 2H), 9.61 (s, 2H). ^{13}C NMR (DMSO-d_6): δ 154.5, 151.4, 148.4, 147.4, 142.8, 135.9, 127.2, 121.1, 61.9. Anal. Calcd for $C_{18}H_{18}N_8O_2$-3.0HCl-2.3H_2O: C, 40.85; H, 4.88; N, 21.17. Found: C, 41.01; H, 4.89; N, 21.07.

*2,6-Di-(2′-cyanopyridin-5′-yl)pyrazine (**22b**).* The same procedure described for 2,6-di-(4′-cyano-2′-methylphenyl)pyrazine **14a** was used by employing 2,6-di(tri-*n*-butylstannyl)pyrazine and 5-bromo-2-cyanopyridine **16b** to furnish the title compound **22b**; 70% yield; mp >300 °C. ^{1}H NMR (DMSO-d_6): δ 8.27 (d, J = 8.0 Hz, 2H), 8.94 (dd, J = 2.0, 8.0 Hz, 2H), 9.54 (s, 2H), 9.66 (d, J = 2.0 Hz, 2H). ^{13}C NMR (DMSO-d_6): δ149.6, 147.2, 143.0, 136.1, 134.4, 133.4, 129.2, 117.4. Anal. Calcd for $C_{16}H_8N_6$: C, 67.60; H, 2.84; N, 29.56. Found: C, 67.34; H, 2.73; N, 29.28.

*2,6-Di-(2′-amidinopyridin-5′-yl)pyrazine hydrochloride (**23b**).* The same procedure described for the preparation of **10** was used starting with the above dinitrile **22b**; 83% yield; mp 249–251 °C (dec). ^{1}H NMR (DMSO-d_6): δ 8.58 (d, J = 8.1 Hz, 2H), 9.06 (dd, J = 1.2, 8.1 Hz, 2H), 9.59 (s, 4H), 9.61 (s, 2H), 9.68 (d, J = 1.2 Hz, 2H), 9.78 (s, 4H). ^{13}C NMR (DMSO-d_6): δ 151.3, 147.9, 147.6, 147.3, 142.0, 135.6, 133.0, 121.5. Anal. Calcd for $C_{16}H_{14}N_8$-2.0HCl-1.4H_2O: C, 46.14; H, 4.55; N, 26.91. Found: C, 46.42; H, 4.52; N, 26.52.

*2,6-Di-(2′-N-hydroxyamidinopyridin-5′-yl)pyrazine hydrochloride (**24b**).* The same procedure described for the preparation of **11** was used starting with the above dinitrile **22b**; 69% yield; mp 280–282 °C (dec). ^{1}H NMR (DMSO-d_6): δ 8.40 (dd, J = 2.1, 8.4 Hz, 2H), 8.80 (d, J = 8.4 Hz, 2H), 8.82 (s, 2H), 9.10 (d, J = 2.1 Hz, 2H), 9.68 (s, 2H), 11.28 (s, 2H). ^{13}C NMR (DMSO-d_6): δ 155.0, 148.0, 147.6, 144.8, 142.7, 136.2, 134.4, 123.2. Anal. Calcd for $C_{16}H_{14}N_8O_2$-3.0HCl-0.75H_2O: C, 40.61; H, 3.94; N, 23.68. Found: C, 40.81; H, 4.18; N, 23.35.

*2,6-Di-(2′-N-methoxyamidinopyridin-5′-yl)pyrazine hydrochloride (**25b**).* The same procedure described for the preparation of **12** was used starting with the above compound **24b**; 50% yield; mp 89–91 °C. ^{1}H NMR (DMSO-d_6): δ 3.85 (s, 6H), 8.07 (d, J = 8.4 Hz, 2H), 8.72 (dd, J = 2.4, 8.4 Hz, 2H), 9.43 (s, 2H), 9.46 (d, J = 2.4 Hz, 2H). ^{13}C NMR (DMSO-d_6): δ 150.1, 149.0, 148.3, 146.9, 141.5, 135.0,

131.8, 119.9, 61.2. Anal. Calcd for $C_{18}H_{18}N_8O_2$-2.0HCl-0.7H_2O: C, 46.60; H, 4.65; N, 24.15. Found: C, 46.80; H, 4.79; N, 23.95.

Acknowledgments

This work was supported by The Bill and Melinda Gates Foundation through a subcontract with the Consortium of Parasitic Drug Development (CPDD) (R.B., W.D.W., D.W.B.) and by NIH Grant AI064200 (W.D.W., D.W.B.).

References and notes

1. Brun, R.; Blum, J.; Chappuis, F.; Burri, C. *Lancet* **2010**, *375*, 148.
2. World Health Organisation 2012. WHO7|Malaria. Fact sheet No 94. http://www.who.int/mediacentre/factsheets/fs094/en/.
3. Simarro, P. P.; Jannin, J.; Cattand, P. *Plos Med.* **2008**, *68*, e55.
4. World Health Organisation. 2012. WHO | African trypanosomiasis (sleeping sickness). Fact sheet N°259. http://www.who.int/mediacentre/factsheets/fs259/en/.
5. Wenzler, T.; Boykin, D. W.; Ismail, M. A.; Hall, J. E.; Tidwell, R. R.; Brun, R. *Antimicrob. Agents Chemother.* **2009**, *53*, 4185.
6. Kennedy, P. G. E. *Ann. Neurol.* **2008**, *64*, 116.
7. (a) Priotto, G.; Kasparian, S.; Mutombo, W.; Ngouama, D.; Ghorashian, S.; Arnold, U.; Ghabri, S.; Baudin, E.; Buard, V.; Kazadi-Kyanza, S.; Ilunga, M.; Mutangala, W.; Pohlig, G.; Schmid, C.; Karunakara, U.; Torreele, E.; Kande, V. *Lancet* **2009**, *374*, 56; (b) Simarro, P. P.; Franco, J.; Diarra, A.; Postigo, J. A. R.; Jannin, J. *Parasitology* **2012**, *139*, 842.
8. (a) Tidwell, R. R.; Boykin, D. W. Dicationic DNA Minor Groove Binders as Antimicrobial agents In *Small Molecule DNA and RNA Binders: From Synthesis to Nucleic Acid Complexes*; Demeunynck, M., Bailly, C., Wilson, W. D., Eds.; Wiley-VCH: New York, 2003; Vol. 2, pp 414–460; (b) Wilson, W. D.; Nguyen, B.; Tanious, F. A.; Mathis, A.; Hall, J. E.; Stephens, C. E.; Boykin, D. W. *Curr. Med. Chem.-Anti-Cancer Agents* **2005**, *5*, 389; (c) Soeiro, M. N. C.; de Souza, E. M.; Stephens, C. E.; Boykin, D. W. *Expert Opin. Invest. Drugs* **2005**, *14*, 957; (d) Dardonville, C. *Expert Ther. Pat.* **2005**, *15*, 1241; (e) Werbovetz, K. A. *Curr. Opin. Invest. Drugs* **2006**, *7*, 147; (f) Wilson, W. D.; Tanious, F. A.; Mathis, A.; Tevis, D.; Hall, J. E.; Boykin, D. W. *Biochimie* **2008**, *90*, 999.
9. Thuita, J. K.; Karanja, S. M.; Wenzler, T.; Mdachi, R. E.; Ngotho, J. M.; Kagira, J. M.; Tidwell, R.; Brun, R. *Acta Trop.* **2008**, *108*, 6.
10. Ismail, M. A.; Brun, R.; Easterbrook, J. D.; Tanious, F. A.; Wilson, W. D.; Boykin, D. W. *J. Med. Chem.* **2003**, *46*, 4761.
11. Ansede, J. H.; Voyksner, R. D.; Ismail, M. A.; Boykin, D. W.; Tidwell, R. R.; Hall, J. E. *Xenobiotica* **2005**, *35*, 211.
12. Thuita, J. K.; Wang, M. Z.; Kagira, J. M.; Denton, C. L.; Paine, M. F.; Mdachi, R. E.; Murilla, G. A.; Ching, S.; Boykin, D. W.; Tidwell, R. R.; Hall, J. E.; Brun, R. *PLoS Negl. Trop. Dis.* **2012**, *6*, e1734. http://dx.doi.org/10.1371/journal.pntd.0001734.
13. (a) Berger, O.; Kanti, A.; van Ba, C. T.; Vial, H.; Ward, S. A.; Biagini, G. A.; Gray, P. G.; O'Neill, P. M. *ChemMedChem* **2011**, *6*, 2094; (b) Chackal-Catoen, S.; Miao, Y.; Wilson, W. D.; Wenzler, T.; Brun, R.; Boykin, D. W. *Bioorg. Med. Chem.* **2006**, *14*, 7434; (c) Patrick, D. A.; Bakunov, S. A.; Bakunova, S. M.; Kumar, E. V. K. S.; Lombardy, R. J.; Jones, S. K.; Bridge, S. A.; Zhirnov, O.; Hall, J. E.; Wenzler, T.; Brun, R.; Tidwell, R. R. *J. Med. Chem.* **2007**, *50*, 2468; (d) Ismail, M. A.; Arafa, R. K.; Wenzler, T.; Brun, R.; Tanious, F. A.; Wilson, W. D.; Boykin, D. W. *Bioorg. Med. Chem.* **2008**, *16*, 683; (e) Bakunov, S. A.; Bakunova, S. M.; Wenzler, T.; Ghebru, M.; Werbovetz, K. A.; Brun, R.; Tidwell, R. R. *J. Med. Chem.* **2010**, *53*, 254; (f) Ismail, M. A.; Arafa, R. K.; Brun, R.; Wenzler, T.; Miao, Y.; Wilson, D. W.; Generaux, C.; Bridges, A.; Hall, J. E.; Boykin, D. W. *J. Med. Chem.* **2006**, *49*, 5324.
14. Hu, L.; Arafa, R. K.; Ismail, M. A.; Wenzler, T.; Brun, R.; Munde, M.; Wilson, W. D.; Nzimiro, S.; Samyesudhas, S.; Werbovetz, K. A.; Boykin, D. W. *Bioorg. Med. Chem. Lett.* **2008**, *18*, 247.
15. Hu, L.; Arafa, R. K.; Ismail, M. A.; Patel, A.; Munde, M.; Wilson, W. D.; Wenzler, T.; Brun, R.; Boykin, D. W. *Bioorg. Med. Chem.* **2009**, *17*, 6651.
16. Darabantu, M.; Boully, L.; Turck, A.; Ple, N. *Tetrahedron* **2005**, *61*, 2897.
17. Bakunova, S. M.; Bakunov, S. A.; Patrick, D. A.; Kumar, E. V. K. S.; Ohemeng, K. A.; Bridges, A. S.; Wenzler, T.; Barszcz, T.; Kilgore Jones, S.; Werbovetz, K. A.; Brun, R.; Tidwell, R. R. *J. Med. Chem.* **2009**, *52*, 2016.
18. (a) Nguyen, B.; Lee, M. P.; Hamelberg, D.; Bailly, C.; Brun, R.; Neidle, S.; Wilson, W. D. *J. Am. Chem. Soc.* **2002**, *124*, 13680; (b) Nguyen, B.; Hamelberg, D.; Bailly, C.; Colson, J.; Stenek, J.; Brun, R.; Neidle, S.; Wilson, W. D. *Biophys. J.* **2004**, *86*, 1028; (c) Miao, Y.; Lee, M. P. H.; Parkinson, G. N.; Batista-Parra, A.; Ismail, M. A.; Neidle, S.; Boykin, D. W.; Wilson, D. W. *Biochemistry* **2005**, *44*, 14701.
19. Boykin, D. W.; Kumar, A.; Xiao, G.; Wilson, W. D.; Bender, B. C.; McCurdy, D. R.; Hall, J. E.; Tidwell, R. R. *J. Med. Chem.* **1998**, *41*, 124.
20. Yan, G. Z.; Brouwer, K. L. M.; Pollack, G. M.; Wang, M. Z.; Tidwell, R. R.; Hall, J. E.; Paine, M. F. *J. Pharmacol. Exp. Ther.* **2011**, *337*, 503.
21. (a) Wang, M. Z.; Saulter, J. Y.; Usuki, E.; Cheung, Y.-L.; Hall, M.; Bridges, A. S.; Loewen, G.; Parkinson, O. T.; Stephens, C. E.; Allen, J. L.; Zeldin, D. C.; Boykin, D. W.; Tidwell, R. R.; Parkinson, A.; Paine, M. F.; Hall, J. E. *Drug Metab. Dispos.* **2006**, *34*, 1985; (b) Wang, M. Z.; Wu, J. Q.; Bridges, A. S.; Zeldin, D. C.; Kornbluth, S.; Tidwell, R. R.; Hall, J. E.; Paine, M. F. *Drug Metab. Dispos.* **2007**, *35*, 2067.
22. Ansede, J. H.; Anbazhagan, M.; Brun, R.; Easterbrook, J. D.; Hall, J. E.; Boykin, D. W. *J. Med. Chem.* **2004**, *47*, 4335.
23. Saulter, J. Y.; Kurian, J. R.; Trepanier, L. A.; Tidwell, R. R.; Bridges, A. S.; Boykin, D. W.; Stephens, C. E.; Anbazhagan, M.; Hall, J. E. *Drug Metab. Dispos.* **2005**, *33*, 1886.
24. Wilson, W. D.; Tanious, F. A.; Fernandez-Saiz, M.; Rigl, C. T. *Methods Mol. Biol. Drug–DNA Interaction Protocols* **1997**, *90*, 219.
25. Prochaska, H. J.; Talalay, P.; Sies, H. *J. Biol. Chem.* **1987**, *262*, 1931.

OPEN ACCESS Freely available online

PLOS | NEGLECTED TROPICAL DISEASES

Aquaporin 2 Mutations in *Trypanosoma brucei gambiense* Field Isolates Correlate with Decreased Susceptibility to Pentamidine and Melarsoprol

Fabrice E. Graf[1,2], Philipp Ludin[1,2], Tanja Wenzler[1,2], Marcel Kaiser[1,2], Reto Brun[1,2], Patient Pati Pyana[3,4], Philippe Büscher[4], Harry P. de Koning[5], David Horn[6], Pascal Mäser[1,2]*

1 Swiss Tropical and Public Health Institute, Basel, Switzerland, **2** University of Basel, Basel, Switzerland, **3** Institut National de Recherche Biomédicale, Kinshasa-Gombe, Democratic Republic of the Congo, **4** Department of Biomedical Sciences, Institute of Tropical Medicine, Antwerp, Belgium, **5** Institute of Infection, Immunity and Inflammation, College of Medical, Veterinary and Life Sciences, University of Glasgow, Glasgow, United Kingdom, **6** Biological Chemistry and Drug Discovery, College of Life Sciences, University of Dundee, Dundee, United Kingdom

Abstract

The predominant mechanism of drug resistance in African trypanosomes is decreased drug uptake due to loss-of-function mutations in the genes for the transporters that mediate drug import. The role of transporters as determinants of drug susceptibility is well documented from laboratory-selected *Trypanosoma brucei* mutants. But clinical isolates, especially of *T. b. gambiense*, are less amenable to experimental investigation since they do not readily grow in culture without prior adaptation. Here we analyze a selected panel of 16 *T. brucei* ssp. field isolates that (i) have been adapted to axenic *in vitro* cultivation and (ii) mostly stem from treatment-refractory cases. For each isolate, we quantify the sensitivity to melarsoprol, pentamidine, and diminazene, and sequence the genomic loci of the transporter genes *TbAT1* and *TbAQP2*. The former encodes the well-characterized aminopurine permease P2 which transports several trypanocides including melarsoprol, pentamidine, and diminazene. We find that diminazene-resistant field isolates of *T. b. brucei* and *T. b. rhodesiense* carry the same set of point mutations in *TbAT1* that was previously described from lab mutants. Aquaglyceroporin 2 has only recently been identified as a second transporter involved in melarsoprol/pentamidine cross-resistance. Here we describe two different kinds of *TbAQP2* mutations found in *T. b. gambiense* field isolates: simple loss of *TbAQP2*, or loss of wild-type *TbAQP2* allele combined with the formation of a novel type of *TbAQP2/3* chimera. The identified mutant *T. b. gambiense* are 40- to 50-fold less sensitive to pentamidine and 3- to 5-times less sensitive to melarsoprol than the reference isolates. We thus demonstrate for the first time that rearrangements of the *TbAQP2/TbAQP3* locus accompanied by *TbAQP2* gene loss also occur in the field, and that the *T. b. gambiense* carrying such mutations correlate with a significantly reduced susceptibility to pentamidine and melarsoprol.

Citation: Graf FE, Ludin P, Wenzler T, Kaiser M, Brun R, et al. (2013) Aquaporin 2 Mutations in *Trypanosoma brucei gambiense* Field Isolates Correlate with Decreased Susceptibility to Pentamidine and Melarsoprol. PLoS Negl Trop Dis 7(10): e2475. doi:10.1371/journal.pntd.0002475

Editor: Enock Matovu, Makerere University, Uganda

Received June 28, 2013; **Accepted** August 28, 2013; **Published** October 10, 2013

Funding: This work was supported by the Swiss National Science Foundation (31003A_135746). PPP received a PhD grant from the Institute of Tropical Medicine; PL received fellowships from the Emilia Guggenheim-Schnurr Foundation, the Mathieu-Stiftung, and the Freiwillige Akademische Gesellschaft Basel; DH is funded by a Wellcome Trust Senior Investigator Award (100320/Z/12/Z). The funders had no role in study design, data collection and analysis, decision to publish, or preparation of the manuscript.

Competing Interests: The authors have declared that no competing interests exist.

* E-mail: pascal.maeser@unibas.ch

Introduction

The chemotherapy of human African trypanosomiasis (HAT, also known as sleeping sickness) currently relies on suramin or pentamidine for the first, haemolymphatic stage and on melarsoprol or eflornithine/nifurtimox combination therapy (NECT) for the second stage, when the trypanosomes have invaded the central nervous system (CNS) [1]. All five drugs have unfavorable pharmacokinetics and adverse effects. Melarsoprol is particularly toxic, causing severe encephalopathies in over 5% of the treated patients [2]. And yet, melarsoprol is the only treatment for late-stage *T. b. rhodesiense* infections. New and safer drugs are at various stages of (pre)clinical development, thanks largely to the Drugs for Neglected Diseases initiative (www.dndi.org). Two molecules that have successfully passed clinical Phase I trials are now being tested in patients: the nitroimidazole fexinidazole [3,4] and the benzoxaborole SCYX-7158 [5,6]. Both are orally available and cure 2nd stage *T. b. brucei* infections in a mouse model [7]. However, until new drugs for HAT are on the market, the current ones – problematic as they are – need to be used in a sustainable way. This requires an understanding of the mechanisms of drug resistance.

The mechanisms of drug resistance in African trypanosomes have been studied in the lab for over 100 years [8]. Two observations were made recurrently, namely (i) reduced drug uptake by drug resistant trypanosomes [9–14] and (ii) cross-resistance between melarsoprol and pentamidine [15,16]. Both phenomena were attributed to the fact that melarsoprol and pentamidine are taken up by trypanosomes via the same transporters, which appeared to be lacking in drug-resistant mutants. The first transporter identified was called P2 since it was one of two purine nucleoside transporters identified [17,18]. It is

Author Summary

Human African Trypanosomiasis, or sleeping sickness, is a fatal disease restricted to sub-Saharan Africa, caused by *Trypanosoma brucei gambiense* and *T. b. rhodesiense*. The treatment relies on chemotherapy exclusively. Drug resistance in *T. brucei* was investigated mainly in laboratory-selected lines and found to be linked to mutations in transporters. The adenosine transporter TbAT1 and the aquaglyceroporin TbAQP2 have been implicated in sensitivity to melarsoprol and pentamidine. Mutations in these transporters rendered trypanosomes less susceptible to either drug. Here we analyze *T. brucei* isolates from the field, focusing on isolates from patients where melarsoprol treatment has failed. We genotype those isolates to test for mutations in *TbAQP2* or *TbAT1*, and phenotype for sensitivity to pentamidine and melarsoprol. Six *T. b. gambiense* isolates were found to carry mutations in *TbAQP2*. These isolates stemmed from relapse patients and exhibited significantly reduced sensitivity to pentamidine and melarsoprol as determined in cell culture. These findings indicate that mutations in *TbAQP2* are present in the field, correlate with loss of sensitivity to pentamidine and melarsoprol, and might be responsible for melarsoprol treatment failures.

encoded by the gene *TbAT1* for adenine/adenosine transporter 1 [19]. Homozygous genetic deletion of *TbAT1* in bloodstream-form *T. b. brucei* resulted in pentamidine and melarsoprol cross-resistance, albeit only by a factor of about 2.5 [20]. This weak phenotype, together with the fact that the $TbAT1^{-/-}$ mutants still exhibited saturable drug import [21], indicated that further transporters are involved in melarsoprol-pentamidine cross-resistance [16,21,22]. One such transporter was recently identified, the aquaglyceroporin TbAQP2 [23,24]. Aquaporins and aquaglyceroporins belong to the major intrinsic protein (MIP) family and form channels that facilitate transmembrane transport of water and small non-ionic solutes such as glycerol and urea [25]. The three aquaporins of *T. brucei* (TbAQP1-3) are thought to physiologically function as osmoregulators and are involved in glycerol transport [26]. Aquaporins were described to mediate uptake of arsenite in mammalian cells [27] and in *Leishmania*, and loss of aquaporin function was implicated in heavy metal resistance [28]. Homozygous genetic deletion of *TbAQP2* in bloodstream-form *T. b. brucei* increased the IC_{50} towards melarsoprol and pentamidine by about 2- and 15- fold, respectively [24]. Moreover, a *T. b. brucei* lab mutant selected for high-level pentamidine resistance [21] carried a chimeric *TbAQP2* gene, where 272 nucleotides had been replaced by the corresponding sequence from a neighboring, very similar gene *TbAQP3* [24]. Differences in the *TbAQP2/TbAQP3* tandem locus on chromosome 10 were also observed between the reference genome sequences of *T. b. gambiense* DAL972 [29] and *T. b. brucei* TREU927 [23,30]. They possess identical versions of *TbAQP2* but differ in *TbAQP3* [31]. More recent field isolates of *T. brucei* ssp. have so far not been genotyped regarding their *TbAQP2/TbAQP3* locus.

The genotypic status of *TbAT1*, located proximal to a telomere on chromosome 5 [32], has been more intensely investigated. Point mutations in *TbAT1* were described, both in selected lab strains and in clinical *T. brucei* ssp. isolates, which rendered the gene non-functional when expressed in yeast [19]. The occurrence of these mutations correlated to a certain degree with melarsoprol treatment failure in 2nd stage *T. b. gambiense* HAT patients [33–36]. However, the relationship between polymorphisms in *TbAT1*, drug susceptibility, and treatment failure in patients is not fully resolved as the *TbAT1* mutant *T. b. gambiense* were not analyzed phenotypically. Such investigations are notoriously difficult since clinical *T. b. gambiense* isolates are hard to obtain (given the inaccessibility of HAT foci and the poor success rate of isolation and adaptation in rodents) and cannot readily be propagated in axenic culture. Here we concentrate on clinical *T. brucei* ssp. isolates from drug refractory cases that have been adapted to axenic *in vitro* cultivation, aiming to investigate whether mutations at the known melarsoprol and pentamidine transporter loci also occur in the field – and if so, whether such mutations are accompanied by loss of drug susceptibility.

Materials and Methods

Trypanosoma brucei ssp. isolates

The 16 analyzed isolates are described in Table 1 (origin) and Table 2 (clinical outcome). For more details on the recent isolates from the DRC please refer to Table S4 of Pyana et al (2011) [37]. All have previously been adapted to axenic cultivation. *T. b. brucei* and *T. b. rhodesiense* isolates were cultured in minimum essential medium (MEM) with Earle's salts with the addition of 0.2 mM 2-mercaptoethanol, 1 mM Na-pyruvate, 0.5 mM hypoxanthine, and 15% heat-inactivated horse serum as described by Baltz et al (1985) [38]. *T. b. gambiense* strains were cultured in IMDM medium supplemented according to Hirumi and Hirumi (1989) [39], plus 0.2 mM 2-mercaptoethanol, 15% heat-inactivated fetal calf serum and 5% human serum. The cultures were maintained under a humidified 5% CO_2 atmosphere at 37°C and were subpassaged 3 times a week to ensure growth in the exponential (log) phase.

Phenotyping

Drug sensitivity was determined with the Alamar blue assay as described by Räz et al (1997) [40], using the redox-sensitive dye resazurin as an indicator of cell number and viability. The trypanosomes were cultivated in 96-well microtiter plates in serial dilutions of drugs for 70 h. 10 ul of resazurin (125 ug/ml (Sigma) dissolved in PBS pH 7.2) was added to each well. The plates were further incubated for 2–4 hours for *T. b. rhodesiense* and *T. b. brucei*, and 6–8 hours for *T. b. gambiense*, before being read with a SpectraMax Gemini XS microplate fluorescence scanner (Molecular Devices) at an excitation wavelength of 536 nm and an emission wavelength of 588 nm. IC_{50} values were calculated by non-linear regression to a sigmoidal inhibition curve using SoftMax Pro software (V. 5.2). The IC_{50} values given in Table 2 are averages ± standard deviation of at least 3 independent assays (n = 3–12), each determined in duplicate. Melarsoprol (Sanofi-Aventis) was obtained from WHO. Pentamidine isothionate and diminazene aceturate were purchased from Sigma.

Genotyping

Genomic DNA was isolated from 10 ml dense trypanosome cultures. The cells were spun down and the pellets resuspended in 300 µl 10 mM TrisHCl pH 8, 1 mM EDTA and 3 µl 10% SDS was added before incubating for 10–15 min at 55°C. After 5 min incubation 3 µl of pronase mix (20 mg/ml, Sigma) was added to increase the stability of the extracted DNA. 90 µl of ice cold 5 M potassium acetate was added and the mixture was incubated for 5 min on ice. After spinning down for 5 minutes at max speed in a microfuge, the supernatant was transferred to a new tube and DNA was precipitated in 2–2.5 volumes of absolute ethanol, washed in 70% ethanol and dissolved in 20 µl ddH_2O. PCR was performed with Taq polymerase (Solis BioDyne, Estonia); the primers and annealing temperatures are summarized in Table S1.

Table 1. Origin of the analyzed *T. brucei* isolates.

Isolate	Species	Origin	Reference
STIB 930	*Tbg*	Republic of Côte d'Ivoire, 1978	[49]
ITMAP 141267	*Tbg*	Democratic Republic of the Congo, 1960	[50]
STIB 756	*Tbg*	Liberia, 1981	[51]
STIB 891	*Tbg*	Uganda, 1995	[33]
DAL 870R	*Tbg*	Republic of Côte d'Ivoire, 1985	[52]
DAL 898R	*Tbg*	Republic of Côte d'Ivoire, 1985	[52]
K03048	*Tbg*	South Sudan, 2003	[53]
45 BT (MHOM/CD/INRB/2006/1)	*Tbg*	Democratic Republic of the Congo, 2006	[37]
130 BT (MHOM/CD/STI/2006/02)	*Tbg*	Democratic Republic of the Congo, 2006	[37]
349 BT (MHOM/CD/INRB/2006/16)	*Tbg*	Democratic Republic of the Congo, 2006	[37]
349 AT (MHOM/CD/INRB/2006/19)	*Tbg*	Democratic Republic of the Congo, 2006	[37]
40 AT (MHOM/CD/INRB/2006/07)	*Tbg*	Democratic Republic of the Congo, 2006	[37]
STIB 900	*Tbr*	Tanzania, 1982	[52]
STIB 871	*Tbr*	Uganda, 1994	[54]
STIB 940	*Tbb*	Somalia, 1985	[42,55]
STIB 950	*Tbb*	Somalia, 1985	[41]

doi:10.1371/journal.pntd.0002475.t001

PCR products were run on a 0.8% agarose gel and purified on a silica membrane column (Nucleospin gel and PCR clean up, Macherey Nagel, Germany). The purified PCR products were directly sequenced (Microsynth, Switzerland or GATC, Germany) with the same primers as used for PCR amplification. Only the *TbAQP2/TbAQP3* locus of *T. b. gambiense* K03048 produced two PCR products, which were cloned in pCR2.1-TOPO (Invitrogen). The assembled sequences were submitted to GenBank; accession numbers are listed in Table S2.

Results

A panel of *Trypanosoma brucei* ssp. field isolates

To be able to compare – and possibly correlate – genotype and phenotype of *T. brucei* ssp., we assembled a set of 16 isolates that had been adapted to axenic *in vitro* cultivation as blood-stream forms. These included 5 recent *T. b. gambiense* isolates from the Democratic Republic of the Congo (DRC), 2 older isolates from the Republic of Côte d'Ivoire and one isolate from South Sudan,

Table 2. Drug sensitivity ($IC_{50} \pm$ SD in nM), genotypic status of *TbAT1* and *TbAQP2*, and clinical outcome of melarsoprol treatment of the patients.

Isolate	MelB	Pentamidine	Diminazene	*TbAT1*	*TbAQP2*	Clinics
STIB 930	9.6±4.5	1.9±0.7	21.0±8.5	Ref	Ref	Cure
ITMAP 141267	15.0±8.1	8.3±3.4	9.9±4.4	WT	WT	Cure
STIB 756	6.2±1.1	1.3±0.7	24.7±7.9	WT	WT	Unknown
STIB 891	5.3±0.9	1.7±1.4	23.3±2.7	WT	WT	Unknown
DAL 870R	4.4±1.7	1.1±1.0	5.3±2.2	WT	WT	Relapse
DAL 898R	8.9±5.9	1.7±1.2	22.7±16.8	WT	WT	Relapse
K03048	24.8±9.2	81.2±21.9	58.0±33.6	WT	deletion/chimeric	Relapse
45 BT	25.9±8.6	91.8±29.7	37.5±10.8	WT	chimeric	Relapse
130 BT	42.3±17.6	76.9±22.3	12.3±4.5	WT	chimeric	Probable relapse
349 BT	26.2±11.3	71.9±12.4	20.0±3.2	WT	chimeric	Relapse
349 AT	25.6±11.8	81.9±31.8	15.4±1.0	WT	chimeric	Relapse
40 AT	22.0±8.0	72.2±21.1	39.9±16.7	WT	chimeric	Relapse
STIB 900	4.6±2.6	3.2±0.9	3.8±1.5	Ref	Ref	Cure
STIB 871	4.4±1.3	2.5±1.0	201±163	R allele	WT	Cure
STIB 940	13.6±7.0	3.4±2.0	340±218	R allele	WT	n.a.
STIB 950	27.6±9.4	1.8±0.4	102±53.6	R allele	WT	n.a.

WT = identical to reference (Ref) strain, being STIB 930 for *T. b. gambiense* isolates and STIB 900 for *T. b. brucei* and *T. b. rhodesiense* strains.

doi:10.1371/journal.pntd.0002475.t002

which were all isolated from patients who had relapsed after melarsoprol chemotherapy. Other *T. b. gambiense* isolates from the DRC, northwestern Uganda, and Liberia were from patients who were successfully treated with melarsoprol or the treatment outcome is unknown. *T. b. gambiense* STIB 930 is a fully drug-susceptible lab strain that was used as a reference strain. We further included the field isolates *T. b. brucei* STIB 940, *T. b. brucei* STIB 950 and *T. b. rhodesiense* STIB 871, which are multidrug-resistant to isometamidium, diminazene and tubercidin. The fully drug-susceptible reference strain *T. b. rhodesiense* STIB 900 was included as a reference. The different isolates and their origin are summarized in Table 1. All isolates were genotyped regarding *TbAQP2* and *TbAT1*.

Naturally occurring mutations in *TbAQP2*

When the *TbAQP2/TbAQP3* genomic locus was amplified by PCR from the 16 *T. brucei* ssp. isolates, all the recent *T. b. gambiense* isolates from the DRC (40 AT, 45 BT, 130 BT, 349 BT and 349 AT) exhibited a smaller band than expected for the wild-type locus. Direct sequencing of the PCR product in each of the five isolates revealed only one gene at the locus: a chimeric version of *TbAQP2* and *TbAQP3*. The first 813 bp of the open reading frame perfectly matched *TbAQP2* while the remaining 126 bp derived from *TbAQP3* (Figure 1C). These 126 bp perfectly matched to *TbAQP3* of *T. b. rhodesiense* STIB 900 but this exact sequence is not found in the published genome of *T. b. gambiense* DAL 972. Note that the present *TbAQP2-TbAQP3* chimeric gene (Figure 1C) differs from the one described by Baker et al. from a pentamidine-selected *T. b. brucei* lab mutant (Figure 1B; [24]). *T. b. gambiense* K03048 from the South Sudan also gave rise to an abnormal pattern upon PCR amplification of the *TbAQP2/TbAQP3* locus from genomic DNA: a distinctly smaller double band instead of the expected product, indicative of heterozygosity. The smaller band contained the upstream region of *TbAQP2* followed by the open reading frame of *TbAQP3* while the *TbAQP2* open reading frame was missing (Figure 1D). The larger band contained a *TbAQP2/3* chimera similar to that encountered in the *T. b. gambiense* isolates of the DRC (Figure 1C). Point mutations in *TbAQP2* were encountered in the multidrug-resistant field isolates *T. b. brucei* STIB 940, *T. b. brucei* STIB 950 and *T. b. rhodesiense* STIB 871, all of which had the same 4 SNPs in *TbAQP2* compared to the *T. b. brucei* 927 reference gene (Tb927.10.14170), leading to the amino acid change threonine^{159} to alanine (Figure 1E). However, the same 4 SNPs also occurred in our drug-susceptible reference strain *T. b. rhodesiense* STIB 900, so they are not likely to be involved in the *mdr* phenotype [41,42] of these isolates. All other isolates analyzed had a wild-type copy of *TbAQP2*. The identified sequence polymorphisms are summarized in Table 2, GenBank accession numbers are in Table S2.

Naturally occurring mutations in *TbAT1*

All of the 12 analyzed *T. b. gambiense* isolates were identical in *TbAT1* sequence to the reference STIB 930 as well as to the genome strain DAL972. The previously described $TbAT1^R$ allele [19,33] was found in the 3 *mdr* lines *T. b. brucei* STIB 940, *T. b. brucei* STIB 950 and *T. b. rhodesiense* STIB 871. $TbAT1^R$ carries 5 coding and 4 silent mutations and a codon deletion as compared to the reference sequence (STIB 900), and the resultant protein appeared to be non-functional when expressed in *Saccharomyces cerevisiae* [19] or re-expressed in a *tbat1* null *T. b. brucei* (De Koning, unpublished results). The remainder of the isolates did not possess mutations in *TbAT1* when compared to the respective reference isolate. The GenBank accession numbers of all the sequences are in Table S2.

Correlating *TbAQP2* and *TbAT1* genotype to drug susceptibility

Drug sensitivities of the bloodstream-forms of all isolates were determined *in vitro* regarding melarsoprol, pentamidine, and diminazene. The five *T. b. gambiense* that possessed the chimeric *TbAQP2/3* gene (45 BT, 130 BT, 349 BT, 349 AT, 40 AT), as well as K03048 which carries a deletion of *TbAQP2* in one allele, in addition to one chimeric *TbAQP2/3* allele, all showed a similar drug sensitivity profile with markedly increased IC_{50} values towards pentamidine and, to a lesser extent, also melarsoprol (Figure 2). IC_{50} values were in the range of 70–92 nM for pentamidine and 22–42 nM for melarsoprol (Table 2); compared to the median of the four drug sensitive *T. b. gambiense* lines STIB 930, STIB 891, STIB 756 and ITMAP 141267, this corresponds to a 40- to 52-fold decrease in susceptibility to pentamidine and a 2.8- to 5.3-fold decrease for melarsoprol. The higher IC_{50} values of

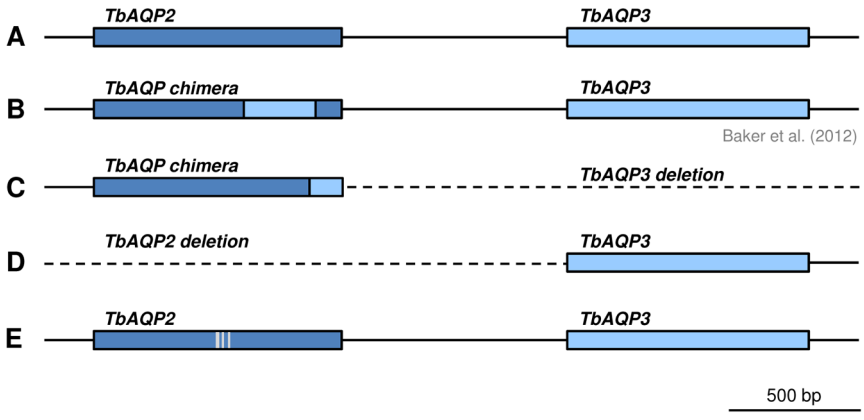

Figure 1. Schematic view of the *TbAQP2/TbAQP3* locus on chromosome 10. A) Reference locus of *T. b. brucei* TREU927, *T. b. gambiense* STIB 930 and *T. b. gambiense* DAL972 (minor differences in *TbAQP3* are not highlighted). B) Chimera of *TbAQP2* and *TbAQP3* as described by Baker et al. (2012) [24] for the *in vitro* selected, pentamidine-resistant *T. b. brucei* line B48. C) Chimera of *TbAQP2* and *TbAQP3* plus loss of *TbAQP3* in *T. b. gambiense* 40 AT, 45 BT, 130 BT, 349 BT, and 349 AT, and in one K03048 allele. D) Deletion of the *TbAQP2* ORF in the other *T. b. gambiense* K03048 allele. E) *TbAQP2* polymorphisms (C474A, G475A, C477T, T480C) in several *T. b. rhodesiense* and *T. b. brucei* isolates from East Africa (STIB 900, STIB 950, STIB 940, and STIB 871).
doi:10.1371/journal.pntd.0002475.g001

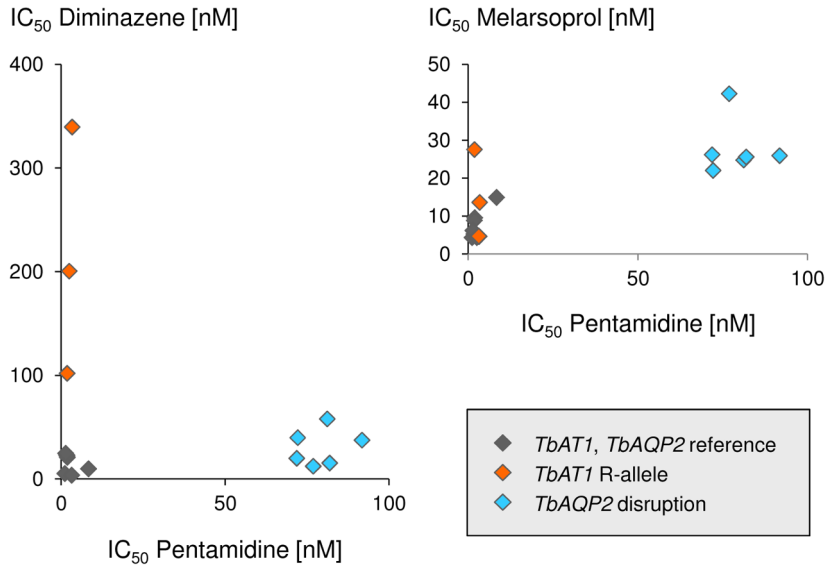

Figure 2. *In vitro* drug sensitivities. 50% inhibitory concentrations (IC_{50}) as determined with the Alamar blue assay. Susceptibility to pentamidine correlates with that to melarsoprol but not diminazene. *TbAT1* and *TbAQP2* genotypes are indicated.
doi:10.1371/journal.pntd.0002475.g002

the isolates that carried a mutation in *TbAQP2* (n = 6) compared to the remainder (n = 10) were statistically significant both with respect to pentamidine (p = 0.0002, two-tailed Mann-Whitney test) and melarsoprol (p = 0.0047); no association was observed regarding *TbAQP2* status and sensitivity to diminazene. However, the isolates that carried the known resistance allele $TbAT1^R$ (i.e. STIB 940, STIB 950 and STIB 871) exhibited strongly increased IC_{50} values to diminazene (p = 0.01, two-tailed Mann-Whitney test) but not to pentamidine (Figure 2, Table 2). *T. b. brucei* STIB 950 also had an elevated IC_{50} against melarsoprol (Figure 2), but over all three $TbAT1^R$ isolates there was no significant effect on melarsoprol susceptibility.

Across all 16 *T. brucei* isolates, pentamidine sensitivity positively correlated with that to melarsoprol (Spearman's rank correlation coefficient of 0.67, p = 0.005) while there was no correlation between the two structurally related diamidines, pentamidine and diminazene (Figure 2).

Discussion

It is an intriguing phenomenon with African trypanosomes that drug resistance is predominantly linked to reduced drug import, typically arising from loss of function mutation of a non-essential transporter [12,19,24]. Here we investigated the aminopurine transporter TbAT1 and the aquaglyceroporin TbAQP2, two proteins known to be involved in uptake of – and susceptibility to – melarsoprol and diamidines in bloodstream-form *T. brucei*. While there is evidence for a link between *TbAT1* mutations and melarsoprol treatment failure in the field [33–36], the more recently identified gene *TbAQP2* has so far not been analyzed in a clinical setting. *TbAQP2* is dispensable for growth in culture [24] and partial gene replacement of *TbAQP2* with *TbAQP3* was observed in a pentamidine-selected *T. b. brucei* lab mutant [24] that displayed reduced infectivity to rodents [21]. However, it was unknown whether similar mutations also occur in the field, as they might bear a fitness cost in patients or during transmission by the tsetse fly. Concentrating on a panel of clinical *T. brucei* ssp. isolates that (i) derived from treatment-refractory cases and (ii) had been adapted to axenic *in vitro* culture, we have genotyped their *TbAT1* and *TbAQP2* loci, and phenotyped their *in vitro* sensitivity towards melarsoprol, pentamidine and diminazene. Our aim was to explore whether *TbAQP2* mutations occur in the field and if so, whether mutant isolates exhibit reduced drug susceptibility.

Five of the analyzed *T. b. gambiense* isolates, all from melarsoprol relapse patients of Dipumba Hospital in Mbuji-Mayi, DRC, carried only one gene at the *TbAQP2/TbAQP3* tandem locus, an unprecedented *TbAQP2/3* chimera. The high degree of sequence similarity between *TbAPQ2* and *TbAQP3* allows for homologous recombination between the two genes, leading to chimerization and gene loss. TbAQP2 has a unique selectivity filter with unusual NSA/NPS motifs instead of the characteristic NPA/NPA that occur in the vast majority of MIP family members [43] including TbAQP1 and TbAQP3 [24]. The published, pentamidine-resistant *T. b. brucei* lab mutant possessed a TbAQP2/3 chimera whose C-terminal filter triplet was from TbAQP3, suggesting that the unusual NPS triplet may be involved in pentamidine transport. However, the presently described pentamidine-resistant *T. b. gambiense* isolates carry a *TbAQP2/3* chimera encoding a predicted protein with both selectivity filter triplets from TbAQP2. We hypothesize that the TbAQP2/3 chimera observed in the *T. b. gambiense* isolates fails to contribute to pentamidine and melarsoprol susceptibility despite having the proposed selectivity filter residues of TbAQP2. Functional expression of the chimeric gene in *tbaqp2* null cells will be necessary to test this hypothesis.

The occurrence of rearrangements at the *TbAQP2/TbAQP3* locus correlated with reduced susceptibility to pentamidine and, to a lesser extent, melarsoprol. Thus field isolates also exhibit the well known cross-resistance between melarsoprol and pentamidine [15,16,31], while no cross-resistance was observed to diminazene aceturate. This is in agreement with *TbAT1* being the primary uptake route for diminazene [44,45] and consistent with results obtained using $TbAQP2^{-/-}$ cells, which showed no resistance to the rigid diamidines diminazene or DB75 [24], as opposed to pentamidine which has a highly flexible structure. It is also noteworthy that *T. b. rhodesiense* STIB 871 and *T. b. brucei* STIB 940 are susceptible to melarsoprol and pentamidine *in vitro* although both carry the $TbAT1^r$ allele. Loss of TbAT1 function has been described without mutations in the open reading frame of

the gene [32]. However, since in the present study all isolates with a 'wild-type' *TbAT1* ORF were fully susceptible to diminazene, we conclude that they possess a functional TbAT1 (i.e. P2) transporter. *Trypanosoma congolense* and *T. vivax* appear to lack an AT1 orthologue [46], therefore diminazene transport and resistance must have a different mechanism in these livestock parasites.

The plasma levels of pentamidine in treated patients peak about 1 hour after injection and vary extensively from 0.42 µM to 13 µM, while the mean elimination half-life after multiple applications is approximately 12 days [47]. Thus, since pentamidine is very potent, even a 50-fold increase in IC_{50} of pentamidine as observed here for the *T. b. gambiense* isolates with mutations in *TbAQP2*, is unlikely to jeopardize the success of treatment. With melarsoprol, however, the obtainable drug levels are more critical. Only 1–2% of the maximal plasma levels are seen in the CSF [48], and a 5-fold reduced sensitivity to melarsoprol might allow trypanosomes to survive in the CSF during melarsoprol therapy. Thus mutations in *TbAQP2* might indeed be responsible for melarsoprol treatment failures with *T. b. gambiense*. However, two of the *T. b. gambiense* isolates from relapse patients (DAL 870R and DAL 898 R) were sensitive to melarsoprol and pentamidine, and they possessed wild-type copies of *TbAT1* and *TbAQP2*, indicating that factors other than drug resistance can contribute to treatment failures. Larger sample sizes will be required to test the significance of *TbAQP2* for successful treatment. We show here for the first time that a *TbAQP2/3* chimera as well as loss of *TbAQP2* occurs in *T. b. gambiense* clinical isolates, and that the presence of such rearrangements at the *TbAQP2/TbAQP3* locus is accompanied by a 40- to 50-fold loss in pentamidine sensitivity and a 3- to 5-fold loss in melarsoprol sensitivity. We recommend genotyping of the *TbAQP2/TbAQP3* locus to be integrated into larger field trials such as clinical studies with drug candidates.

Supporting Information

Table S1 Primers used for PCR, their target gene, annealing temperature and sequence (5′ to 3′).
(PDF)

Table S2 GenBank accession numbers of the sequenced genes.
(PDF)

Acknowledgments

We are grateful to Christina Kunz, Monica Cal and Eva Greganova for help in the lab, Simon Hänni for the quick DNA isolation protocol, and Christian Burri for comments on the manuscript.

Author Contributions

Conceived and designed the experiments: FEG PM. Performed the experiments: FEG TW MK. Analyzed the data: FEG PL. Contributed reagents/materials/analysis tools: PPP PB HPdK DH. Wrote the paper: FEG RB PB HPdK DH PM.

References

1. Brun R, Blum J, Chappuis F, Burri C (2010) Human African trypanosomiasis. Lancet 375: 148–159. doi:10.1016/S0140-6736(09)60829-1.
2. Kennedy PGE (2008) The continuing problem of human African trypanosomiasis (sleeping sickness). Ann Neurol 64: 116–126. doi:10.1002/ana.21429.
3. Torreele E, Bourdin Trunz B, Tweats D, Kaiser M, Brun R, et al. (2010) Fexinidazole–a new oral nitroimidazole drug candidate entering clinical development for the treatment of sleeping sickness. PLoS Negl Trop Dis 4: e923. doi:10.1371/journal.pntd.0000923.
4. Kaiser M, Bray MA, Cal M, Bourdin Trunz B, Torreele E, et al. (2011) Antitrypanosomal activity of fexinidazole, a new oral nitroimidazole drug candidate for treatment of sleeping sickness. Antimicrob Agents Chemother 55: 5602–5608. doi:10.1128/AAC.00246-11.
5. Nare B, Wring S, Bacchi C, Beaudet B, Bowling T, et al. (2010) Discovery of novel orally bioavailable oxaborole 6-carboxamides that demonstrate cure in a murine model of late-stage central nervous system african trypanosomiasis. Antimicrob Agents Chemother 54: 4379–4388. doi:10.1128/AAC.00498-10.
6. Jacobs RT, Nare B, Wring SA, Orr MD, Chen D, et al. (2011) SCYX-7158, an orally-active benzoxaborole for the treatment of stage 2 human African trypanosomiasis. PLoS Negl Trop Dis 5: e1151. doi:10.1371/journal.pntd.0001151.
7. Mäser P, Wittlin S, Rottmann M, Wenzler T, Kaiser M, et al. (2012) Antiparasitic agents: new drugs on the horizon. Curr Opin Pharmacol 12: 562–566. doi:10.1016/j.coph.2012.05.001.
8. Ehrlich P (1907) Chemotherapeutische trypanosomen-studien. Berl Klin Wochenzeitschrift 44.
9. Hawking F (1937) Studies on Chemotherapeutic Action I. the Absorption of Arsenical Compounds and Tartar Emetic by Normal and Resistant Trypanosomes and Its Relation to Drugresistance. J Pharmacol Exp Ther 59: 123–156.
10. Frommel TO, Balber AE (1987) Flow cytofluorimetric analysis of drug accumulation by multidrug-resistant Trypanosoma brucei brucei and T. b. rhodesiense. Mol Biochem Parasitol 26: 183–191.
11. Mäser P, Lüscher A, Kaminsky R (2003) Drug transport and drug resistance in African trypanosomes. Drug Resist Updat Rev Comment Antimicrob Anticancer Chemother 6: 281–290.
12. Vincent IM, Creek D, Watson DG, Kamleh MA, Woods DJ, et al. (2010) A molecular mechanism for eflornithine resistance in African trypanosomes. PLoS Pathog 6: e1001204. doi:10.1371/journal.ppat.1001204.
13. Baker N, Alsford S, Horn D (2011) Genome-wide RNAi screens in African trypanosomes identify the nifurtimox activator NTR and the eflornithine transporter AAT6. Mol Biochem Parasitol 176: 55–57. doi:10.1016/j.molbiopara.2010.11.010.
14. Schumann Burkard G, Jutzi P, Roditi I (2011) Genome-wide RNAi screens in bloodstream form trypanosomes identify drug transporters. Mol Biochem Parasitol 175: 91–94. doi:10.1016/j.molbiopara.2010.09.002.
15. ROLLO IM, WILLIAMSON J (1951) Acquired resistance to "Melarsen", tryparsamide and amidines in pathogenic trypanosomes after treatment with "Melarsen" alone. Nature 167: 147–148.
16. De Koning HP (2008) Ever-increasing complexities of diamidine and arsenical crossresistance in African trypanosomes. Trends Parasitol 24: 345–349. doi:10.1016/j.pt.2008.04.006.
17. Carter NS, Fairlamb AH (1993) Arsenical-resistant trypanosomes lack an unusual adenosine transporter. Nature 361: 173–176. doi:10.1038/361173a0.
18. Carter NS, Berger BJ, Fairlamb AH (1995) Uptake of diamidine drugs by the P2 nucleoside transporter in melarsen-sensitive and -resistant Trypanosoma brucei brucei. J Biol Chem 270: 28153–28157.
19. Mäser P, Sütterlin C, Kralli A, Kaminsky R (1999) A nucleoside transporter from Trypanosoma brucei involved in drug resistance. Science 285: 242–244.
20. Matovu E, Stewart ML, Geiser F, Brun R, Mäser P, et al. (2003) Mechanisms of arsenical and diamidine uptake and resistance in Trypanosoma brucei. Eukaryot Cell 2: 1003–1008.
21. Bridges DJ, Gould MK, Nerima B, Mäser P, Burchmore RJS, et al. (2007) Loss of the high-affinity pentamidine transporter is responsible for high levels of cross-resistance between arsenical and diamidine drugs in African trypanosomes. Mol Pharmacol 71: 1098–1108. doi:10.1124/mol.106.031351.
22. De Koning HP (2001) Uptake of pentamidine in Trypanosoma brucei brucei is mediated by three distinct transporters: implications for cross-resistance with arsenicals. Mol Pharmacol 59: 586–592.
23. Alsford S, Eckert S, Baker N, Glover L, Sanchez-Flores A, et al. (2012) High-throughput decoding of antitrypanosomal drug efficacy and resistance. Nature 482: 232–236. doi:10.1038/nature10771.
24. Baker N, Glover L, Munday JC, Aguinaga Andrés D, Barrett MP, et al. (2012) Aquaglyceroporin 2 controls susceptibility to melarsoprol and pentamidine in African trypanosomes. Proc Natl Acad Sci U S A 109: 10996–11001. doi:10.1073/pnas.1202885109.
25. Uzcategui NL, Szallies A, Pavlovic-Djuranovic S, Palmada M, Figarella K, et al. (2004) Cloning, heterologous expression, and characterization of three aquaglyceroporins from Trypanosoma brucei. J Biol Chem 279: 42669–42676. doi:10.1074/jbc.M404518200.
26. Bassarak B, Uzcátegui NL, Schönfeld C, Duszenko M (2011) Functional characterization of three aquaglyceroporins from Trypanosoma brucei in osmoregulation and glycerol transport. Cell Physiol Biochem Int J Exp Cell Physiol Biochem Pharmacol 27: 411–420. doi:10.1159/000327968.
27. Liu Z, Shen J, Carbrey JM, Mukhopadhyay R, Agre P, et al. (2002) Arsenite transport by mammalian aquaglyceroporins AQP7 and AQP9. Proc Natl Acad Sci U S A 99: 6053–6058. doi:10.1073/pnas.092131899.
28. Gourbal B, Sonuc N, Bhattacharjee H, Legare D, Sundar S, et al. (2004) Drug uptake and modulation of drug resistance in Leishmania by an aquaglyceroporin. J Biol Chem 279: 31010–31017. doi:10.1074/jbc.M403959200.
29. Jackson AP, Sanders M, Berry A, McQuillan J, Aslett MA, et al. (2010) The genome sequence of Trypanosoma brucei gambiense, causative agent of chronic

human african trypanosomiasis. PLoS Negl Trop Dis 4: e658. doi:10.1371/journal.pntd.0000658.
30. Berriman M, Ghedin E, Hertz-Fowler C, Blandin G, Renauld H, et al. (2005) The genome of the African trypanosome Trypanosoma brucei. Science 309: 416–422. doi:10.1126/science.1112642.
31. Baker N, de Koning HP, Mäser P, Horn D (2013) Drug resistance in African trypanosomiasis: the melarsoprol and pentamidine story. Trends Parasitol 29: 110–118. doi:10.1016/j.pt.2012.12.005.
32. Stewart ML, Burchmore RJS, Clucas C, Hertz-Fowler C, Brooks K, et al. (2010) Multiple genetic mechanisms lead to loss of functional TbAT1 expression in drug-resistant trypanosomes. Eukaryot Cell 9: 336–343. doi:10.1128/EC.00200-09.
33. Matovu E, Geiser F, Schneider V, Mäser P, Enyaru JC, et al. (2001) Genetic variants of the TbAT1 adenosine transporter from African trypanosomes in relapse infections following melarsoprol therapy. Mol Biochem Parasitol 117: 73–81.
34. Nerima B, Matovu E, Lubega GW, Enyaru JCK (2007) Detection of mutant P2 adenosine transporter (TbAT1) gene in Trypanosoma brucei gambiense isolates from northwest Uganda using allele-specific polymerase chain reaction. Trop Med Int Heal TM IH 12: 1361–1368. doi:10.1111/j.1365-3156.2007.01918.x.
35. Maina N, Maina KJ, Mäser P, Brun R (2007) Genotypic and phenotypic characterization of Trypanosoma brucei gambiense isolates from Ibba, South Sudan, an area of high melarsoprol treatment failure rate. Acta Trop 104: 84–90. doi:10.1016/j.actatropica.2007.07.007.
36. Kazibwe AJN, Nerima B, de Koning HP, Mäser P, Barrett MP, et al. (2009) Genotypic status of the TbAT1/P2 adenosine transporter of Trypanosoma brucei gambiense isolates from Northwestern Uganda following melarsoprol withdrawal. PLoS Negl Trop Dis 3: e523. doi:10.1371/journal.pntd.0000523.
37. Pyana PP, Ngay Lukusa I, Mumba Ngoyi D, Van Reet N, Kaiser M, et al. (2011) Isolation of Trypanosoma brucei gambiense from cured and relapsed sleeping sickness patients and adaptation to laboratory mice. PLoS Negl Trop Dis 5: e1025. doi:10.1371/journal.pntd.0001025.
38. Baltz T, Baltz D, Giroud C, Crockett J (1985) Cultivation in a semi-defined medium of animal infective forms of Trypanosoma brucei, T. equiperdum, T. evansi, T. rhodesiense and T. gambiense. EMBO J 4: 1273–1277.
39. Hirumi H, Hirumi K (1989) Continuous cultivation of Trypanosoma brucei blood stream forms in a medium containing a low concentration of serum protein without feeder cell layers. J Parasitol 75: 985–989.
40. Räz B, Iten M, Grether-Bühler Y, Kaminsky R, Brun R (1997) The Alamar Blue assay to determine drug sensitivity of African trypanosomes (T.b. rhodesiense and T.b. gambiense) in vitro. Acta Trop 68: 139–147.
41. Kaminsky R, Chuma F, Zweygarth E (1989) Trypanosoma brucei brucei: expression of drug resistance in vitro. Exp Parasitol 69: 281–289.
42. Zweygarth E, Röttcher D (1989) Efficacy of experimental trypanocidal compounds against a multiple drug-resistant Trypanosoma brucei brucei stock in mice. Parasitol Res 75: 178–182.
43. Gupta AB, Verma RK, Agarwal V, Vajpai M, Bansal V, et al. (2012) MIPModDB: a central resource for the superfamily of major intrinsic proteins. Nucleic Acids Res 40: D362–369. doi:10.1093/nar/gkr914.
44. De Koning HP, Anderson LF, Stewart M, Burchmore RJS, Wallace LJM, et al. (2004) The trypanocide diminazene aceturate is accumulated predominantly through the TbAT1 purine transporter: additional insights on diamidine resistance in african trypanosomes. Antimicrob Agents Chemother 48: 1515–1519.
45. Teka IA, Kazibwe AJN, El-Sabbagh N, Al-Salabi MI, Ward CP, et al. (2011) The diamidine diminazene aceturate is a substrate for the high-affinity pentamidine transporter: implications for the development of high resistance levels in trypanosomes. Mol Pharmacol 80: 110–116. doi:10.1124/mol.111.071555.
46. Munday JC, Rojas López KE, Eze AA, Delespaux V, Van Den Abbeele J, et al. (2013) Functional expression of TcoAT1 reveals it to be a P1-type nucleoside transporter with no capacity for diminazene uptake. Int J Parasitol Drugs Drug Resist 3: 69–76. doi:10.1016/j.ijpddr.2013.01.004.
47. Burri C, Stich A, Brun R (2004) Chemotherapy of Human African Trypanosomiasis. In: Maudlin I, Holmes PH, Miles MA, editors. The Trypanosomiasis. Wallingford, UK; Cambridge, MA, USA: CABI Pub. pp. 403–419.
48. Burri C, Baltz T, Giroud C, Doua F, Welker HA, et al. (1993) Pharmacokinetic properties of the trypanocidal drug melarsoprol. Chemotherapy 39: 225–234.
49. Felgner P, Brinkmann U, Zillmann U, Mehlitz D, Abu-Ishira S (1981) Epidemiological studies on the animal reservoir of gambiense sleeping sickness. Part II. Parasitological and immunodiagnostic examination of the human population. Tropenmed Parasitol 32: 134–140.
50. Likeufack ACL, Brun R, Fomena A, Truc P (2006) Comparison of the in vitro drug sensitivity of Trypanosoma brucei gambiense strains from West and Central Africa isolated in the periods 1960–1995 and 1999–2004. Acta Trop 100: 11–16. doi:10.1016/j.actatropica.2006.09.003.
51. Richner D, Brun R, Jenni L (1988) Production of metacyclic forms by cyclical transmission of west African Trypanosoma (T.) brucei isolates from man and animals. Acta Trop 45: 309–319.
52. Brun R, Schumacher R, Schmid C, Kunz C, Burri C (2001) The phenomenon of treatment failures in Human African Trypanosomiasis. Trop Med Int Heal TM IH 6: 906–914.
53. Maina NWN, Oberle M, Otieno C, Kunz C, Maeser P, et al. (2007) Isolation and propagation of Trypanosoma brucei gambiense from sleeping sickness patients in south Sudan. Trans R Soc Trop Med Hyg 101: 540–546. doi:10.1016/j.trstmh.2006.11.008.
54. Matovu E, Iten M, Enyaru JC, Schmid C, Lubega GW, et al. (1997) Susceptibility of Ugandan Trypanosoma brucei rhodesiense isolated from man and animal reservoirs to diminazene, isometamidium and melarsoprol. Trop Med Int Heal TM IH 2: 13–18.
55. Kaminsky R, Zweygarth E (1989) Effect of in vitro cultivation on the stability of resistance of Trypanosoma brucei brucei to diminazene, isometamidium, quinapyramine, and Mel B. J Parasitol 75: 42–45.

OPEN ACCESS Freely available online

PLoS NEGLECTED TROPICAL DISEASES

Isothermal Microcalorimetry, a New Tool to Monitor Drug Action against *Trypanosoma brucei* and *Plasmodium falciparum*

Tanja Wenzler[1,2]*, Andrea Steinhuber[3], Sergio Wittlin[1,2], Christian Scheurer[1,2], Reto Brun[1,2], Andrej Trampuz[3¤]

1 Medical Parasitology and Infection Biology, Swiss Tropical and Public Health Institute, Basel, Switzerland, **2** University of Basel, Basel, Switzerland, **3** Infectious Diseases Research Laboratory, Department of Biomedicine, University Hospital Basel, Basel, Switzerland

Abstract

Isothermal microcalorimetry is an established tool to measure heat flow of physical, chemical or biological processes. The metabolism of viable cells produces heat, and if sufficient cells are present, their heat production can be assessed by this method. In this study, we investigated the heat flow of two medically important protozoans, *Trypanosoma brucei rhodesiense* and *Plasmodium falciparum*. Heat flow signals obtained for these pathogens allowed us to monitor parasite growth on a real-time basis as the signals correlated with the number of viable cells. To showcase the potential of microcalorimetry for measuring drug action on pathogenic organisms, we tested the method with three antitrypanosomal drugs, melarsoprol, suramin and pentamidine and three antiplasmodial drugs, chloroquine, artemether and dihydroartemisinin, each at two concentrations on the respective parasite. With the real time measurement, inhibition was observed immediately by a reduced heat flow compared to that in untreated control samples. The onset of drug action, the degree of inhibition and the time to death of the parasite culture could conveniently be monitored over several days. Microcalorimetry is a valuable element to be added to the toolbox for drug discovery for protozoal diseases such as human African trypanosomiasis and malaria. The method could probably be adapted to other protozoan parasites, especially those growing extracellularly.

Citation: Wenzler T, Steinhuber A, Wittlin S, Scheurer C, Brun R, et al. (2012) Isothermal Microcalorimetry, a New Tool to Monitor Drug Action against *Trypanosoma brucei* and *Plasmodium falciparum*. PLoS Negl Trop Dis 6(6): e1668. doi:10.1371/journal.pntd.0001668

Editor: Philippe Büscher, Institute of Tropical Medicine, Belgium

Received January 6, 2012; **Accepted** April 18, 2012; **Published** June 5, 2012

Funding: This project was supported by the Consortium for Parasitic Drug Development (CPDD), Swiss Tropical and Public Health Institute, Stanley Thomas Johnson Foundation and Gebert Rüf Stiftung. The funders had no role in study design, data collection and analysis, decision to publish, or preparation of the manuscript.

Competing Interests: The authors have declared that no competing interests exist.

* E-mail: tanja.wenzler@unibas.ch

¤ Current address: Infectious Diseases Service, Department of Internal Medicine, University Hospital Lausanne (CHUV), Lausanne, Switzerland

Introduction

Human African trypanosomiasis (HAT), also known as African sleeping sickness, and malaria are important tropical diseases caused by protozoan parasites. HAT threatens millions of people living in sub-Saharan Africa [1]. In recent years, the number of cases dropped due to improved control measures such as trapping of tsetse flies, active surveillance and appropriate treatment of patients, and is currently estimated at 30,000 cases annually [2]. However, the disease may reemerge, if control is neglected. African sleeping sickness is fatal without treatment, so the availability of effective drugs is vital. Malaria has a higher public health impact with 225 million infections and almost 800'000 deaths annually [3]. The most affected populations are children and pregnant women in Africa. Effective drugs are available for prophylaxis and treatment, but drug resistant parasites represent a major challenge. Therefore, new drugs for both diseases are needed on a continuous basis particularly since no effective vaccine is yet available for either of these diseases, so drug development is of crucial importance.

Drug discovery and development requires rapid methods for screening large number of compounds. For both trypanosomes and malaria parasites, in vitro drug activity tests are available. These are routinely performed in 96-well microtiter plates with a drug exposure time of 72 hours. For *Trypanosoma brucei* spp. bloodstream forms are cultivated axenically. Parasite inhibition is determined in a simple and cost-effective way using the viability marker Alamar blue (resazurin) [4]. *P. falciparum* is cultured as asexual erythrocytic stages, and parasite growth inhibition is classically assessed by measuring the uptake of tritium-labelled hypoxanthine [5]. Using these assays, the antiprotozoal activity of added compounds, expressed as 50% inhibitory concentration (IC_{50}) can be determined. These methods can also be used to determine the time of onset of drug action and the time to kill, which are of great importance for subsequent in vivo studies. However, following changes over time using these currently available in vitro tests is not very accurate and is particularly labor intensive.

An alternative method of estimating growth inhibition is isothermal microcalorimetry. This nonspecific technique allows direct measurement of heat generated by biological processes in living cells. Growth of microorganisms results in an increase of heat flow over time which is documented by a continuous real-

Author Summary

Microcalorimetry is a technology developed to record minute changes in temperature as a result of physical, chemical or biological reactions over time. The method has been applied to bacterial and eukaryotic cells and it was found that the metabolic activity of living cells in a culture medium produces enough heat flow to be measured. Protozoan parasites, some of which cause tropical diseases such as African sleeping sickness or malaria, are larger cells than bacteria and are metabolically very active. We explored the applicability of heat flow measurement to follow the growth of a parasite population and to study the effect of drugs. We first established optimal parameters for obtaining heat flow curves of a growing parasite culture. Then we added antiparasitic drugs at two concentrations and followed the heat flow curves over several days. Thus we could determine the time of onset of drug action and the time until all parasites stopped producing heat (time to kill). The microcalorimeter measurements once per second allowed a continuous monitoring of changes in the parasite population. This novel tool is accurate and simple to use, and will certainly prove to be of great value for the discovery and development of new drugs for protozoan parasites.

time electronic signal. The method has already been used to study heat production of bacteria, mammalian cells and worms [6–10]. For example, bacteria produce on average 1–3 pW heat per viable cell [6,11]. The detection time depends on the sensitivity of the instrument as well as the initial number of living cells, their growth rate and the amount of heat produced per cell [12,7]. To our knowledge, this technique has not been applied yet to any pathogenic protozoa.

In the present study, we established microcalorimetry as a new tool for a rapid determination of effects of drugs on *Trypanosoma brucei rhodesiense* and *Plasmodium falciparum*. We used the real-time measurements of metabolic heat flow produced by these protozoan parasites, to measure the time of the onset of action at different drug concentrations and also the time to death of the parasite population.

Materials and Methods

Culture of *T. b. rhodesiense* and preparation of calorimetry ampoules

Bloodstream forms of the *T. b. rhodesiense* strain STIB900 were cultivated in Minimum Essential Medium with Earle's salts, supplemented according to Baltz et al. [13] with the following modifications: 0.2 mM 2-mercaptoethanol, 1 mM sodium pyruvate, 0.5 mM hypoxanthine and 15% heat-inactivated horse serum. For calorimetry, trypanosomes were washed and diluted with fresh culture medium to give the desired initial cell density then transferred to 4 ml sterile glass ampoules which were hermetically sealed with a rubber septum.

For the determination of a suitable cell density to use to obtain growth curves, ampoules were filled with 3 ml trypanosome culture containing 10^4, 10^5 and 10^6 cells/ml initial densities, each in triplicate. Culture medium without trypanosomes served as negative control. Continuous heat measurements (1/sec) were conducted over a period of up to 6 days. For determination of parasite densities at different time points, small aliquots (≈50 µl) were collected through the rubber septum of the hermetically closed ampoules using a 1 ml syringe. Cell counting of motile trypanosomes was performed microscopically using a Neubauer chamber.

The influence of the sample volume was evaluated using an initial density of 10^5 cells/ml, and 1 ml, 2 ml and 3 ml of culture medium each in triplicate.

The standard drugs suramin, pentamidine and melarsoprol were selected to monitor drug action. Eflornithine was excluded because of its weak in vitro activity against African trypanosomes. We used a multiple of the IC_{50} value of each drug since time to kill can not be determined with an IC_{50} (determined over 72 hrs) or lower concentrations. For the investigation of drug activity, trypanosome cultures were diluted with fresh culture medium to a density of 10^5 cells/ml. Each ampoule was filled with 3 ml cell suspension and supplemented with suramin, pentamidine or melarsoprol at concentrations corresponding to 5× IC_{50} or 25× IC_{50} (for actual concentrations in ng/ml see table 1). Each measurement was performed in triplicate. The IC_{50} values were determined prior the experiment as previously described [14].

Culture of *P. falciparum* and preparation of calorimetry ampoules

The *P. falciparum* strain NF54 was cultivated as previously described [15,16]. An aliquot of 0.5 ml of unsynchronized *P. falciparum* culture with 10% parasitemia and 5% hematocrit was mixed with fresh human erythrocytes and culture medium to give the desired initial parasitemia and 5% hematocrit.

Samples with an initial parasitemia of 1.0, 0.5, 0.25 and 0.125% were tested to find the optimal initial parasitemia for the evaluation of fast-acting drugs. In addition, the influence of the volume on the thermal profile was evaluated using 4 ml-ampoules filled with 0.5, 1.0, 2.0 or 3.0 ml of unsynchronized culture with an initial parasitemia of 0.5% and 5% hematocrit. This was done

Table 1. Heat flow parameters of *T. b. rhodesiense* culture exposed to pentamidine, melarsoprol or suramin at two concentrations.

Drugs	Concentration	Onset of action (hours)	Time to peak (hours)	Peak heat flow (µW)	Time to base level (hours)
Drug-free control	-	-	30	8.0	120
Pentamidine	5× IC_{50} (8.5 ng/ml)	≤3	3	2.2	28
Pentamidine	25× IC_{50} (42.5 ng/ml)	≤3	3	2.0	22
Melarsoprol	5× IC_{50} (11.0 ng/ml)	6	9	4.1	>120
Melarsoprol	25× IC_{50} (55.0 ng/ml)	≤3	3	1.7	12
Suramin	5× IC_{50} (833 ng/ml)	5	9	4.3	42
Suramin	25× IC_{50} (4165 ng/ml)	5	9	4.0	32

doi:10.1371/journal.pntd.0001668.t001

because erythrocytes settle rapidly, so different volumes of culture medium in a 4 ml ampoule might influence parasite development owing to differences in oxygen supply and availability of nutrients. Ampoules filled with non-infected erythrocytes (5% hematocrit) were used in triplicate as negative controls. Continuous heat measurements were conducted over a period of 5 days. Parasitemia was assessed by microscopic counting of Giemsa-stained smears prepared from samples aspirated at defined time points with a syringe through the rubber septum of the closed ampoules.

For the drug test, aliquots of stock solutions of the drugs were mixed with fresh *P. falciparum* culture to give the desired concentration and then distributed into sterile calorimetry ampoules. The antiplasmodial drugs chloroquine, artemether and dihydroartemisinin were tested at concentrations corresponding to 3× and 10× the published IC_{50} values [17]. Dilutions of the 10 mg/ml stock solutions were freshly prepared in culture medium, immediately before the start of the experiment.

Calorimetric equipment and measurements

An isothermal calorimetry instrument (Thermal Activity Monitor, Model 3102 TAM III, TA Instruments, New Castle, DE, USA) equipped with 48 channels was used to measure heat flow continuously at 37°C. The temperature of the instrument was maintained within 0.00001°C. The calorimetric sensitivity according to the manufacturer is ±0.2 µW. The calorimeter continuously measured heat generated or absorbed by test or control samples in air-tight 4 ml glass ampoules sealed with a rubber septum. The gas phase was ambient air. For each series of measurements, ampoules were introduced into the calorimeter and remained at least 15 minutes in the thermal equilibration position at 37°C before they were lowered into the measurement position. Due to short-term thermal disturbance after introduction of the samples into the measuring position of the calorimeter the heat signal of the first 1 hour was considered unspecific. For the study of the relationship between heat flow events and the number of parasites in the sample, ampoules were removed at defined time points and aliquots of the samples were aspirated with a 1 ml syringe through the rubber septum, and the parasites counted.

Analysis of calorimetric data

Thermal changes in each ampoule were recorded as a continuous electronic signal (in Watts), which is proportional to the heat production rate. After measurement, data were reduced from 1 second to 1 minute intervals and exported. Data reduction is optional and can be set individually to any degree after each experiment. Data analysis was accomplished using the manufacturer's software (TAM Assistant, TA Instruments, New Castle, DE, USA) and Origin 7.5 (Microcal, Northampton, MA, USA). For the analysis of time points one hour of incubation time was added to the time of the calorimetric measurement. This time was needed for preparation of the ampoules, their transfer from the bench to the calorimeter and for equilibration in the calorimeter prior the measurement.

Results

Influence of initial density of *T. b. rhodesiense* cultures on heat flow

We plotted heat flow (in µW) over time in all present experiments as the heat flow data can be used as a proxy for the number of viable trypanosome cells.

Figure 1 shows the heat flow over time from 3 ml samples in closed 4 ml glass ampoules of *T. b. rhodesiense* containing three

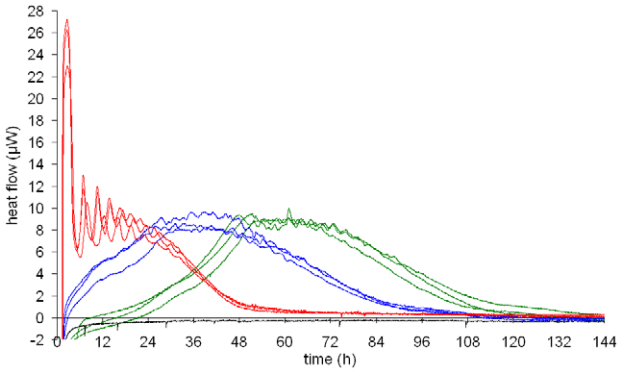

Figure 1. Calorimetric measurements of *T. b. rhodesiense* at different initial densities. Heat flow curves of *T. b. rhodesiense* at initial densities of 10^6 cells/ml (red), 10^5 cells/ml (blue) and 10^4 cells/ml (green) in medium without the addition of drugs. All curves are means of triplicate measurements. The curves with the same initial trypanosome densities were measured in three independent experiments performed on different days.
doi:10.1371/journal.pntd.0001668.g001

different initial trypanosome densities of 10^4, 10^5 and 10^6 cells/ml. With an initial trypanosome density of 10^4 cells/ml, a lag phase was observed before the exponential growth phase started. A stationary phase was reached after 48 hours. After 72 hours, the culture overgrew, which led to a decline of the heat flow. With an initial trypanosome density of 10^5 cells/ml, the exponential phase started immediately, and the stationary phase as well as the dying off phase was observed one day earlier than with 10^4 cells/ml. The maximum trypanosome density in the ampoules containing the cells was reached at maximum heat flow of around 8 µW.

At the lower initial trypanosome densities of 10^4/ml and 10^5/ml, the heat flow increased continuously and only minor amplitude oscillations occurred when the maximum heat flow was reached (above 8 µW). With 10^6 cells/ml initial trypanosome density, unexpected heat flow oscillations were noted during the first 24 hours. A first peak of up to 26 µW was observed 2.5 hours after the start of the experiment (Figure 1). Then, the heat flow dropped and an oscillating heat flow started with continuously decreasing amplitudes during the first 24 hours. After 48 hours, the culture overgrew and the heat flow was close to the base level.

Parallel determinations of cell counts showed that the increase in heat production was consistent with the increase in cell numbers and the heat flow curves were similar to the growth curves obtained by cell counting (data not shown). The following decrease in heat production is due to decreasing numbers of viable cells combined with decreasing metabolic activity of the cells over time. The intra- and inter-experimental reproducibility was evaluated by running three independent measurements. Each was performed on different days, in triplicates and with trypanosome cultures freshly diluted to the desired densities. As expected, the reproducibility was higher within one experiment than between experiments. However, reproducibility was good also between different experiments, as illustrated in Figure 1, which shows the mean heat flow curves of triplicates of each experiment.

In the subsequent experiments for monitoring drug action, a trypanosome density of 10^5 cells/ml was chosen to avoid the lag phase observed with 10^4 cells/ml and to avoid the strong oscillations originating from samples with 10^6 cells/ml initial density. A further disadvantage of using 10^6 cells/ml is that only a very limited growth is possible, since the maximum trypanosome density under ideal culture conditions is $\sim 2\times10^6$ cells/ml.

The time-courses for heat flow using 0.5 ml, 1 ml, 2 ml and 3 ml of cell culture at an initial density of 10^5 cells/ml were all in a similar range (data not shown). As the largest volume contained the highest total number of cells and therefore produced the highest heat flow peak, a volume of 3 ml was chosen for the following experiments.

Influence of antitrypanosomal drugs on the heat flow of *T. b. rhodesiense*

The standard drugs suramin, pentamidine and melarsoprol were selected to monitor drug action.

The heat flow of cultures containing melarsoprol (Figure 2B), pentamidine (Figure 2C) and suramin (Figure 2D) in concentrations corresponding to 5× IC_{50} and 25× IC_{50} was measured in parallel to that of control cultures containing no drug. Whereas the heat signal of the control cultures increased continuously to a peak value of 8 µW after 24–36 hours, curves for all drug containing samples reached markedly lower peaks, at earlier time points (Figure 2A and Table 1). Inhibition depended on the drug used, and its concentration. During the first 3 hours of measurement, the heat production of all samples increased in a similar way. The onset of action of the drugs was marked by a divergence in the continuously increasing heat flow curves of the drug containing specimens from the curves for the control specimens (blue curves). For all three drugs, the onset of action was within the first 6 hours of drug incubation (Figure 2A and Table 1). Then after the peak the heat flow continuously declined over a few hours until the heat production was reduced to the level of the sterile medium control (base level). The time required to reach this point, when the parasite culture was completely inactivated, was the time to kill. The fastest antitrypanosomal effect was observed with melarsoprol at 25× IC_{50}, with a decline in heat production starting within the first 3 hours and reaching base line after 12 hours of incubation. The slowest acting drug among those tested was suramin. The heat production of suramin-treated trypanosomes started to decline after 9 hours of drug incubation. The heat flow was reduced to the base level after 32 hours at 25× IC_{50} and after 42 hours at 5× IC_{50} concentrations.

Influence of different culture volumes of *P. falciparum* on heat flow

Blood stages of *Plasmodium falciparum* were cultured using human erythrocytes in culture medium [15,16]. In our samples, erythrocytes settled and accumulated at the bottom of the vial within a few hours. This could tend to reduce the availability of both oxygen and nutrients, and produce an accumulation of metabolites. Both these effects might lead to decreased viability of the cells. The cultures used to evaluate the influence of different sample volumes in the 4 ml closed glass ampoules all had the same concentration of cells and the same initial parasitemia. The largest volume tested contained the highest overall number of cells and thus produced the highest amount of heat. The course of the heat flow curves was more or less similar for the different sample volumes tested (data not shown). However, with 3 ml or 2 ml

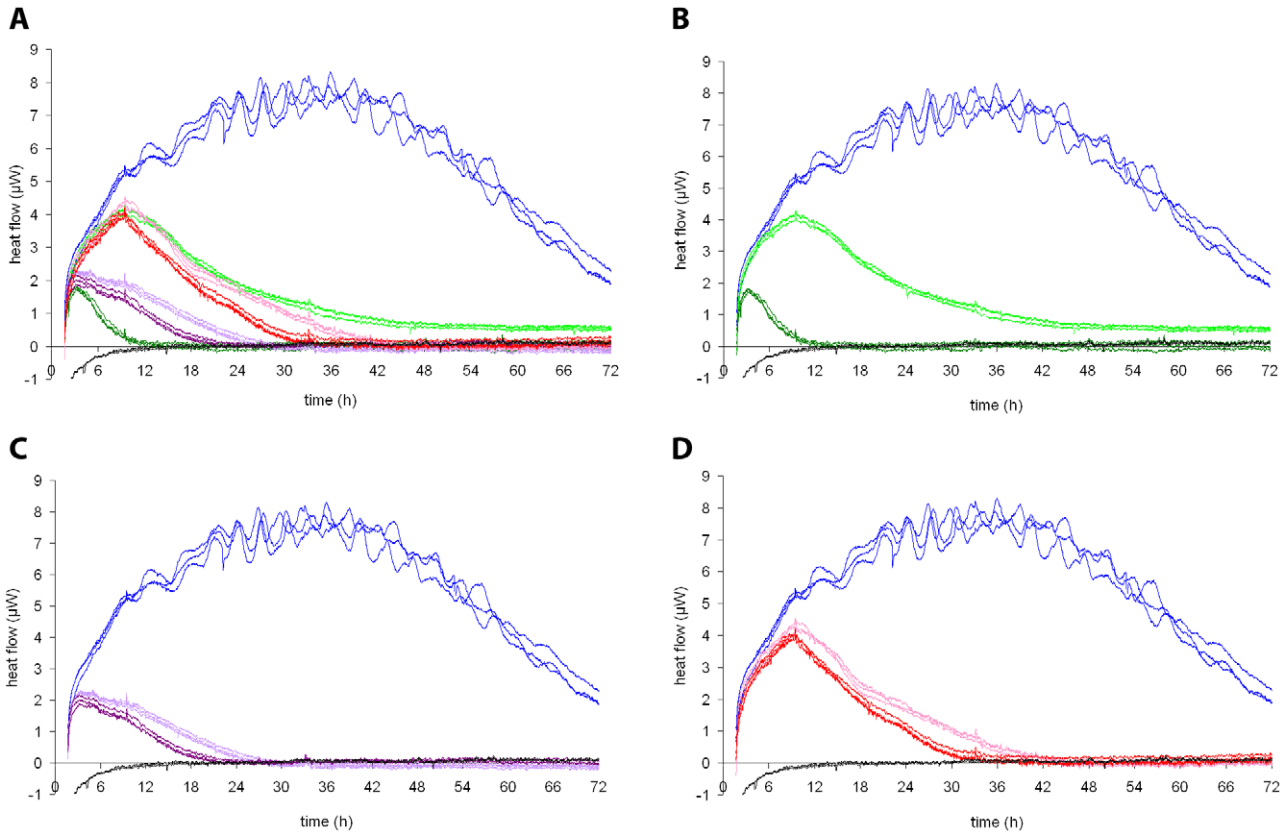

Figure 2. Calorimetric measurements of *T. b. rhodesiense* exposed to different drugs. Heat flow curves of *T. b. rhodesiense* at initial densities of 10^5 cells/ml in medium without drugs (blue) or with drugs at two different concentrations, and a medium control without trypanosomes (black). All measurements were performed in triplicate. A: summary, all three compounds at 5× IC_{50} and 25× IC_{50}; B: Melarsoprol at 5× IC_{50} (light green) and 25× IC_{50} (dark green); C: Pentamidine at 5× IC_{50} (light violet) and 25× IC_{50} (dark violet); D: Suramin at 5× IC_{50} (magenta) and 25× IC_{50} (red).
doi:10.1371/journal.pntd.0001668.g002

samples, there was an initial pre-peak at 3–4 hours followed by a sharp drop at 7 hours before the heat flow increased again to reach the main peak, whereas with the 1 ml samples the heat flow signal increased steadily from the start of measurement until the main peak at ~10 μW, and the heat flow curves of samples containing infected erythrocytes could easily be distinguished from those for uninfected erythrocytes (controls) immediately after the start of the measurement. This was not the case for the samples with 0.5 ml, the lowest volume tested. We therefore chose a volume of 1 ml at 5% hematocrit for the following experiments.

Influence of initial density of *P. falciparum* on heat flow

The heat production of 1 ml specimens containing erythrocytes (5% hematocrit) infected with *P. falciparum* at initial levels of parasitemia varying between 0.125%–1.0% increased, reached a peak and declined afterwards at all densities. The average time to peak was dependent on the initial parasitemia with the shortest time to peak being measured in the specimens with the highest initial parasitemia (1.0%: 43 h, 0.5%: 57 h, 0.25%: 72 h, 0.125%: 81 h) (Figure 3). Microscopic observation of the culture by Giemsa staining confirmed that the decreasing heat flow after the peak was due to dying of the parasites (data not shown). For the subsequent experiments we chose an initial parasitemia of 0.5%. With this concentration the heat flow reached a maximum peak value (9 μW) among the initial parasitemia levels tested. The time to reach the peak was approximately 57 hours.

Influence of antimalarial drugs on the heat flow of *P. falciparum*

The influence of three standard drugs was measured using 1 ml of a non-synchronous *P. falciparum* culture with 0.5% initial parasitemia. The previously determined IC_{50} values of 5.1 (±0.8) ng/ml for chloroquine, 1.2 (±0.1) ng/ml for artemether [17] and 0.76 (±0.04) ng/ml for dihydroartemisinin were taken as a reference. Figure 4 shows the heat flow curves of a typical measurement in triplicate containing drugs at 3× and 10× the IC_{50}. At 10× IC_{50} all drugs reduced the heat flow compared to the increasing heat flow observed in the drug free control (Figure 4A). The curves were highly reproducible. The most effective drug tested was dihydroartemisinin at 10× IC_{50} (Figure 4B), where the heat flow curves blended with those of the negative controls,

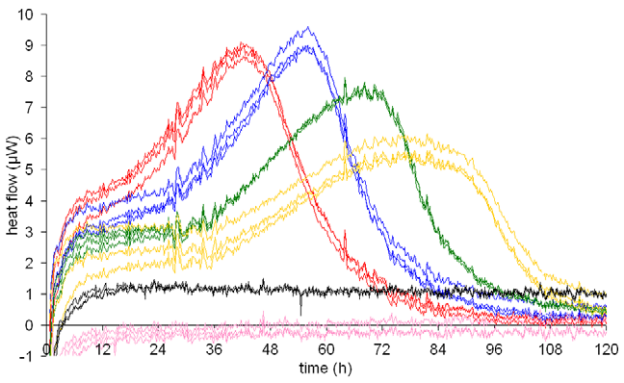

Figure 3. Calorimetric measurements of *P. falciparum* at different initial parasitemia. Heat flow curves of *P. falciparum* in 1 ml culture samples with 5% hematocrit and initial parasitemia of 1% (red), 0.5% (blue), 0.25% (green) or 0.125% (yellow). Control measurements were performed with samples containing uninfected erythrocytes only (black) and culture medium without any cells (pink). All measurements were performed in triplicate.
doi:10.1371/journal.pntd.0001668.g003

containing uninfected erythrocytes. Chloroquine at 10× IC_{50} started to repress the parasite-specific heat production around 6 hours after measurement started. Afterwards the heat signal decreased continuously and matched the signal from uninfected erythrocytes from 48 hours onwards (Figure 4C). At 10× IC_{50}, artemether appeared to be the least effective antiplasmodial drug of the ones tested. During 30 hours of measurement the heat flow signal was comparable with that of the samples with chloroquine at 10× IC_{50}. However, plasmodial activity could be observed afterwards by an increasing heat flow leading to a low peak of 4.5 μW at 85 hours (Figure 4D). At the lower concentrations (3× IC_{50}), dihydroartemisinin was again more effective than chloroquine and artemether, which both led to similar heat flow curves comparable to those for the drug-free control.

Discussion

The calorimetric approach described here, offers the possibility of obtaining real-time measurements in up to 48 samples in parallel. This is not possible with conventional drug activity assays, where inhibition is measured at a single time point. Estimation of the time of drug action requires several assays with different drug exposure times, making such analysis highly labour-intensive. Isothermal microcalorimetry allows a more accurate determination of the onset of action and the time to kill based on the continuous measurement of the heat flow (1×/sec). Calorimetry is an unspecific tool, which cannot discriminate between metabolically inactive cells and dead cells, but it does allow the continuous monitoring of metabolic changes in a parasite population with little effort. It can be used to gain additional information when combined with established drug sensitivity assays.

In our study, we have plotted heat flow over time as the heat flow is proportional to microbial activity [6]. We considered that the heat flow correlates also with the number of viable (i.e., metabolically active) cells because metabolic activity of each trypanosome cell is expected to be more or less constant until it reaches the dying off phase with the decrease of metabolic activity per cell. A similar effect was observed with CHO 320 cells by Kemp et al [10]. An integration of the heat flow leads to a heat over time curve. Heat is proportional to total biomass produced or the quantity of a metabolic product released [6]. As we were interested in viable cells only, we used heat flow data (and not heat data) for our analysis.

In our microcalorimetric experiments, we found that the time to maximum heat flow varied according to the initial parasite density and the sample volume used. Optimization of these parameters led us to use a volume of 3 ml for *T. b. rhodesiense* with an initial trypanosome density of 10^5 cells/ml and of 1 ml for *P. falciparum* with an initial hematocrit of 5% and a parasitemia of 0.5%. At these conditions, the heat flow signals were in the μW range which is well above the detection limit, which was specified by the manufacturer as 200 nW.

A limitation of this new methodology is the airtight sealing of the ampoules which is required for a proper measurement but could potentially affect the action of drugs, since no exchange of the gas phase or the culture medium is possible. Metabolic production of CO_2 can lead to an acidification of the culture medium, as oxygen supply is limited. After a prolonged time of growth the conditions are likely to become non-physiological, therefore the period of accurate measurement is limited. After this, thermal effects might be misinterpreted. The samples were filled into the ampoules at normal laboratory conditions. Therefore the gas phase in each ampoule was normal ambient air rather than the special gas mixtures used for parasite cultures. An improvement of

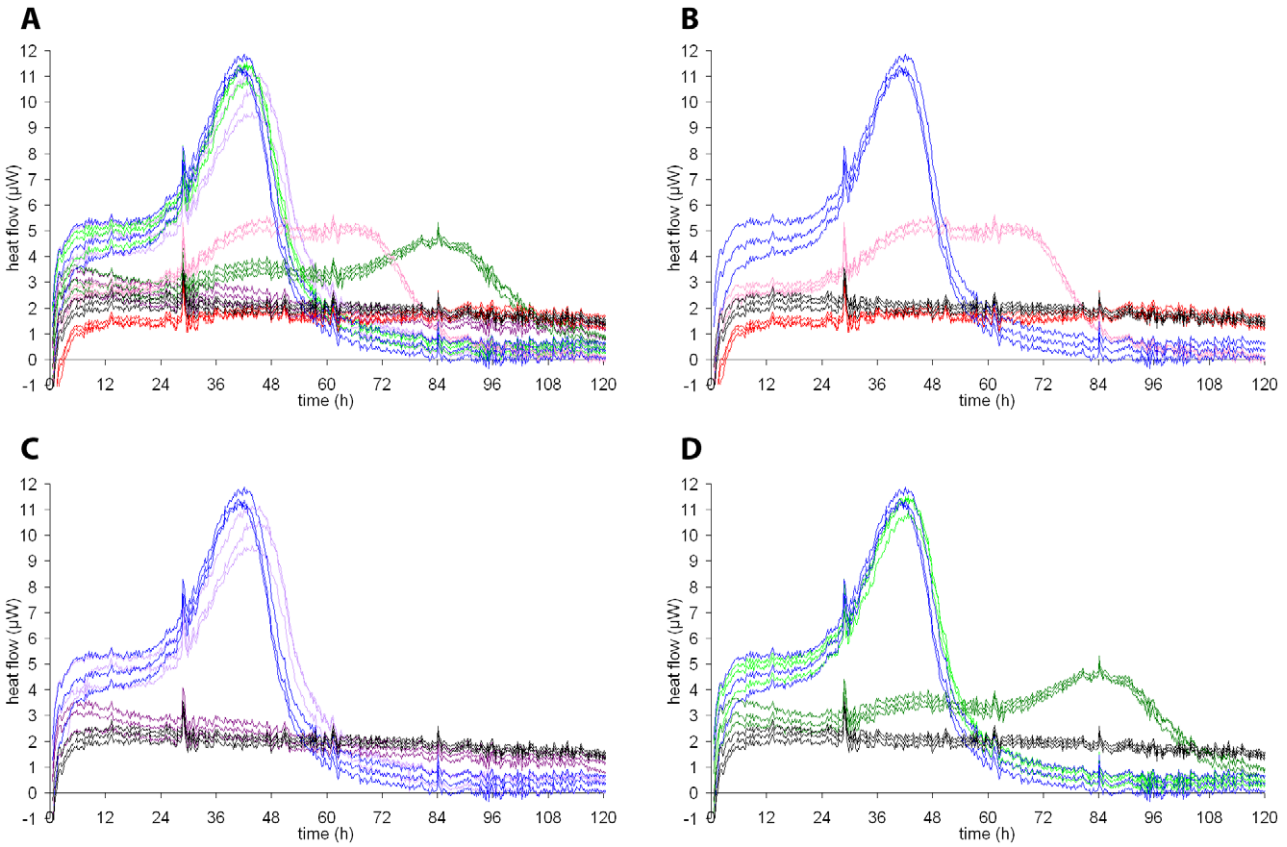

Figure 4. Calorimetric measurements of *P. falciparum* exposed to different drugs. Heat flow curves of *P. falciparum* in culture with 5% hematocrit and an initial parasitemia of 0.5% without drugs (blue) or with drugs at two different concentrations. Control measurements were performed with samples containing uninfected erythrocytes only (black). All measurements were performed in triplicate. A: summary, all three compounds at 3× IC_{50} and 10× IC_{50}; B: Dihydroartemisinin at 3× IC_{50} (magenta) and 10× IC_{50} (red). C: Chloroquine at 3× IC_{50} (light violet) and 10× IC_{50} (dark violet); D: Artemether at 3× IC_{50} (light green) and 10× IC_{50} (dark green).
doi:10.1371/journal.pntd.0001668.g004

the culture conditions in the ampoules could be achieved by replacing the air in the ampoules by the gas used for trypanosome culture (5% CO_2 in ambient air) or the special mixture used for malaria parasite cultures (4% CO_2, 3% O_2, 93% N_2). However, no considerable deleterious effect of ambient air could be observed in our experiments over the maximum measurement period of 5 days. If further optimization of gas exchange is necessary for other experiments, a modified cap for the ampoules with a porous silicon rubber membrane could be used to allow gas exchange but no water evaporation [18].

The parasites used in our study are cultured under different conditions. African trypanosomes, as extracellular parasites, offer the advantage of axenic cultivation. There was therefore no background due to other cells to interfere with the heat flow signal, which allowed direct interpretation. *P. falciparum*, on the other hand, is an intracellular parasite. Non-infected erythrocytes produced a background heat level. They gave a rather constant heat flow between 1 and 2 µW. However, this background did not interfere with the interpretation of the heat flow curves produced by the parasite-infected erythrocytes (Figure 3). Another difference between the two parasites is the multiplication rate. Trypanosomes are mobile and replicate by binary fission, while *P. falciparum* after infecting the erythrocyte undergoes multiple replications and destroys the host cell. Erythrocytes tended to settle rapidly at the bottom of the ampoule, which may explain why smaller volumes (1 ml) of *P. falciparum* cultures in the calorimetric ampoules gave better signals.

When dense cultures of *T. b. rhodesiense* (10^6 cells/ml) were used, they exhibited synchronized oscillations in heat production with a period of about 4 hours (Figure 1). These oscillations were highly reproducible even though the cultures themselves had not been synchronized prior to the experiments. Oscillations were also induced in samples with low initial trypanosome density when aliquots were taken for parasite counting or when the cell suspensions were mixed once they had reached a high trypanosome density. The oscillations were not dependent on the cell cycle as the generation time of *T. b. rhodesiense* is 8 to 9 hours. The oscillations may reflect underlying metabolic changes; glycolytic oscillations have been observed before in microcalorimetric studies by Lamprecht [19] in systems far from equilibrium. The author detected correlations of heat flow oscillations with NAD/NADH+ absorption in *S. cerevisiae* [19]. Analysis of the cause of heat flow oscillations in trypanosome cultures would be of interest but is beyond the scope of the current study. To avoid interference with drug inhibition by these oscillations, lower trypanosome densities were used for all experiments studying drug action.

Using the optimal conditions described, three antitrypanosomal and three antiplasmodial drugs were used to demonstrate that microcalorimetry is a helpful tool to monitor drug action against the two pathogenic protozoans on a real time basis. With only two concentrations per drug, we could observe the rate of action of each of the drugs tested and also the differences between them. Among the antitrypanosomal drugs, melarsoprol was found to be

the fastest acting, followed by pentamidine and then by suramin. This ranking is in agreement with data obtained by the standard drug assays with different drug exposure times where the difference of IC_{50} values at 24 and 48 hours was smallest for melarsoprol (unpublished data). Similar studies have been performed with the antiplasmodial drugs. For *P. falciparum*, the microcalorimetric results are in agreement with data employing the standard [3H]hypoxanthine incorporation assay [20]. In our studies chloroquine and artemether showed pronounced parasite growth inhibition ($\geq$94%) after incubations of 6 hours or longer at concentrations of 10× the IC_{50}.

The method can be used with more than two different drug concentrations, which would enable the inhibition kinetics of a compound to be fully described, with an accuracy far greater than that of standard drug assays.

Another method which allows the determination of the time for a drug to exert its activity is real-time high content imaging. With this method, a higher throughput and more information can be obtained than with microcalorimetry. However, this results in a huge amount of data as pictures are taken instead of measuring a single value at each time point. Transmission light microscopy might not be sufficient to measure viability of trypanosomes, which are small and highly motile, or of plasmodia, which are intracellular, without any markers. Isothermal microcalorimetry has the further advantage that it is a label-free technique, therefore no interventions with the samples such as fixation, staining, or insertion of reporter genes in the parasites are required. Heat flow measurements can give information beyond viability and density such as indications of metabolic state [6,19].

In spite of its many advantages, it is not likely that microcalorimetry will replace the routine screening assays which are currently used to determine antiprotozoal activities of new compounds. With conventional standard assays a higher throughput can be generated, using 96 well or even 384 well formats. However, microcalorimetry is a promising tool for gathering information about selected compounds beyond the IC_{50}, such as the time until onset of action. Measuring this can be a challenge for fast acting compounds that begin to affect growth within the first 3 to 4 hours. In our studies with trypanosomes we found that the time for the preparation of the specimens, their transfer, and the equilibration time in the calorimeter could overlap with the time of onset of action. This problem could be reduced by using an injection system which allows equilibration in the calorimeter prior to the injection of the compounds (personal communication Matthias Rottmann).

The new approach to studying the effect of drugs, as described for the two model organisms *T. b. rhodesiense* and *P. falciparum*, may be applicable also for other protozoan parasites. Resistance or sensitivity analysis of different parasite isolates or screening for resistance development may be an additional interesting field for the use of microcalorimetry. Real-time drug inhibition data can be used in combination with pharmacokinetic and pharmacodynamic data as a helpful tool to predict the outcome of in vivo experiments in the field of drug discovery.

Acknowledgments

We thank Christoph Hatz for establishing the link between the University Hospital Basel and Swiss Tropical and Public Health Institute and for his useful comments and suggestions, and Jennifer Jenkins for critical reading of the manuscript. We acknowledge the pioneering work of A.U. Dan Daniels on the microcalorimetric evaluation of mammalian cells and microorganisms.

Author Contributions

Conceived and designed the experiments: TW AS CS SW RB AT. Performed the experiments: TW AS CS. Analyzed the data: TW AS CS SW RB AT. Contributed reagents/materials/analysis tools: TW AS CS SW RB AT. Wrote the paper: TW AS SW RB CS AT.

References

1. Brun R, Blum J, Chappuis F, Burri C (2010) Human African trypanosomiasis. Lancet 375: 148–159.
2. World Health Organization (2011) African trypanosomiasis (sleeping sickness). Fact sheet N°259. Available: http://www.who.int/mediacentre/factsheets/fs259/en/#. Accessed 2012 Jan 3.
3. World Health Organization (2011) Malaria. Fact sheet N°94. Available: http://www.who.int/mediacentre/factsheets/fs094/en/index.html. Accessed 2011 Nov 27.
4. Räz B, Iten M, Grether-Bühler Y, Kaminsky R, Brun R (1997) The Alamar Blue assay to determine drug sensitivity of African trypanosomes (*T.b. rhodesiense* and *T.b. gambiense*) in vitro. Acta Trop 68: 139–147.
5. Desjardins RE, Canfield CJ, Haynes JD, Chulay JD (1979) Quantitative assessment of antimalarial activity in vitro by a semiautomated microdilution technique. Antimicrob Agents Chemother 16: 710–718.
6. Braissant O, Wirz D, Göpfert B, Daniels AU (2010) Use of isothermal microcalorimetry to monitor microbial activities. FEMS Microbiol Lett 303: 1–8.
7. von Ah U, Wirz D, Daniels A (2009) Isothermal micro calorimetry - a new method for MIC determinations: results for 12 antibiotics and reference strains of E. coli and S. aureus RID B-8154-2008. BMC Microbiol 9: doi:10.1186/1471-2180-9-106.
8. Bermudez J, Bäckman P, Schön A (1992) Microcalorimetric evaluation of the effects of methotrexate and 6-thioguanine on sensitive T-lymphoma cells and on a methotrexate-resistant subline. Cell Biophys 20: 111–123.
9. Manneck T, Braissant O, Haggenmüller Y, Keiser J (2011) Isothermal microcalorimetry to study drugs against *Schistosoma mansoni*. J Clin Microbiol 49: 1217–1225.
10. Kemp RB, Guan YH (1999) Chapter 11 Microcalorimetric studies of animal tissues and their isolated cells. From Macromolecules to Man. Elsevier Science B.V., Vol. Volume 4. pp 557–656.
11. James AM (1987) Thermal and energetic studies of cellular biological systems. Bristol, UK: Wright. 4 p.
12. Trampuz A, Steinhuber A, Wittwer M, Leib SL (2007) Rapid diagnosis of experimental meningitis by bacterial heat production in cerebrospinal fluid. BMC Infect Dis 7: 116.
13. Baltz T, Baltz D, Giroud C, Crockett J (1985) Cultivation in a semi-defined medium of animal infective forms of *Trypanosoma brucei*, *T. equiperdum*, *T. evansi*, *T. rhodesiense* and *T. gambiense*. EMBO J 4: 1273–1277.
14. Bakunov SA, Bakunova SM, Wenzler T, Ghebru M, Werbovetz KA, et al. (2010) Synthesis and antiprotozoal activity of cationic 1,4-diphenyl-1H-1,2,3-triazoles. J Med Chem 53: 254–272.
15. Snyder C, Chollet J, Santo-Tomas J, Scheurer C, Wittlin S (2007) In vitro and in vivo interaction of synthetic peroxide RBx11160 (OZ277) with piperaquine in *Plasmodium* models. Exp Parasitol 115: 296–300.
16. Trager W, Jensen JB (1976) Human malaria parasites in continuous culture. Science 193: 673–675.
17. Vennerstrom JL, Arbe-Barnes S, Brun R, Charman SA, Chiu FCK, et al. (2004) Identification of an antimalarial synthetic trioxolane drug development candidate. Nature 430: 900–904.
18. Ljungholm K, Norén B, Wadsö I (1979) Microcalorimetric Observations of Microbial Activity in Normal and Acidified Soils. Oikos 33: 24–30.
19. Lamprecht I (2003) Calorimetry and thermodynamics of living systems. Thermochim Acta 405: 1–13.
20. Maerki S, Brun R, Charman SA, Dorn A, Matile H, et al. (2006) In vitro assessment of the pharmacodynamic properties and the partitioning of OZ277/RBx-11160 in cultures of *Plasmodium falciparum*. J Antimicrob Chemother 58: 52–58.

AAC
Journals.ASM.org

Pharmacokinetics, *Trypanosoma brucei gambiense* Efficacy, and Time of Drug Action of DB829, a Preclinical Candidate for Treatment of Second-Stage Human African Trypanosomiasis

Tanja Wenzler,[a,b] Sihyung Yang,[c] Olivier Braissant,[d,e] David W. Boykin,[f] Reto Brun,[a,b] Michael Zhuo Wang[c]

Medical Parasitology & Infection Biology, Swiss Tropical and Public Health Institute, Basel, Switzerland[a]; University of Basel, Basel, Switzerland[b]; Department of Pharmaceutical Chemistry, School of Pharmacy, The University of Kansas, Lawrence, Kansas, USA[c]; Laboratory of Biomechanics and Biocalorimetry (LOB2), Faculty of Medicine, University of Basel, Basel, Switzerland[d]; Department of Urology, University Hospital Basel, Basel, Switzerland[e]; Department of Chemistry, Georgia State University, Atlanta, Georgia, USA[f]

Human African trypanosomiasis (HAT, also called sleeping sickness), a neglected tropical disease endemic to sub-Saharan Africa, is caused by the parasites *Trypanosoma brucei gambiense* and *T. brucei rhodesiense*. Current drugs against this disease have significant limitations, including toxicity, increasing resistance, and/or a complicated parenteral treatment regimen. DB829 is a novel aza-diamidine that demonstrated excellent efficacy in mice infected with *T. b. rhodesiense* or *T. b. brucei* parasites. The current study examined the pharmacokinetics, *in vitro* and *in vivo* activity against *T. b. gambiense*, and time of drug action of DB829 in comparison to pentamidine. DB829 showed outstanding *in vivo* efficacy in mice infected with parasites of *T. b. gambiense* strains, despite having higher *in vitro* 50% inhibitory concentrations (IC_{50}s) than against *T. b. rhodesiense* strain STIB900. A single dose of DB829 administered intraperitoneally (5 mg/kg of body weight) cured all mice infected with different *T. b. gambiense* strains. No cross-resistance was observed between DB829 and pentamidine in *T. b. gambiense* strains isolated from melarsoprol-refractory patients. Compared to pentamidine, DB829 showed a greater systemic exposure when administered intraperitoneally, partially contributing to its improved efficacy. Isothermal microcalorimetry and *in vivo* time-to-kill studies revealed that DB829 is a slower-acting trypanocidal compound than pentamidine. A single dose of DB829 (20 mg/kg) administered intraperitoneally clears parasites from mouse blood within 2 to 5 days. In summary, DB829 is a promising preclinical candidate for the treatment of first- and second-stage HAT caused by both *Trypanosoma brucei* subspecies.

Human African trypanosomiasis (HAT), also known as sleeping sickness, is a neglected tropical disease threatening the health of millions of people in the poorest regions of sub-Saharan Africa (1). HAT is fatal if left untreated. The disease is caused by two subspecies of the unicellular parasite *Trypanosoma brucei*, *T. b. gambiense* and *T. b. rhodesiense*, and is transmitted through the bite of an infected tsetse fly. Two clinical stages are defined. In the first stage, the parasites reside in the blood and lymph system, whereas in the second stage, the parasites cross the blood-brain barrier (BBB) and infect the central nervous system (CNS). The disease was almost eliminated around 1960, but it reemerged as a result of political instability and lack of an adequate health care and control system (2). The most recent epidemic occurred in the 1990s, when the number of estimated cases in 1998 was alarmingly high, with about 300,000 cases per year (3). Since the turn of the millennium, the number of infections has declined due to interventions to control the disease, such as trapping tsetse flies, surveillance, and appropriate treatment of patients (2, 4). The number of actual cases in 2009 was estimated at 30,000 annually by the World Health Organization. Control measures have to be maintained by all means, otherwise the disease will reemerge, as history has shown (2, 4).

The availability of effective drugs is crucial for HAT control and elimination, as chemotherapy is the only option for cure. Vaccines are not available for HAT and are unlikely to be developed, mainly because of the antigenic variation of the surface glycoproteins of the parasites (5–7). There are four drugs available as monotherapies (two for the first stage and two for the second stage) to treat the disease, and all require parenteral administration, which is a significant problem in the remote rural areas of Africa, where HAT primarily occurs. Moreover, drugs used to treat second-stage HAT (i.e., melarsoprol and eflornithine) are unsatisfactory due to severe adverse reactions, increasing treatment failures, and/or complicated treatment schedules requiring frequent infusion. Hence, new or improved chemotherapies are needed, especially for second-stage HAT.

One of the compounds used to treat first-stage HAT is the aromatic diamidine drug pentamidine (Fig. 1). It was discovered in 1941 and has been used against *T. b. gambiense* infections for 7 decades. It is still highly efficacious, as shown by the fact that no increase in treatment failures has been reported (6). The diamidine structure of pentamidine seems to be essential for its antiparasitic activity, which is primarily based on binding to the parasite DNA (8). The exact mechanism of action, however, is still unknown. During the last 4 decades, our research has focused on the identification of novel diamidines with improved efficacy, oral bioavailability, and BBB penetration. One of the first lead com-

Received 25 February 2013 Returned for modification 8 June 2013
Accepted 8 August 2013
Published ahead of print 19 August 2013
Address correspondence to Michael Zhuo Wang, michael.wang@ku.edu.
Supplemental material for this article may be found at http://dx.doi.org/10.1128/AAC.00398-13.

doi:10.1128/AAC.00398-13

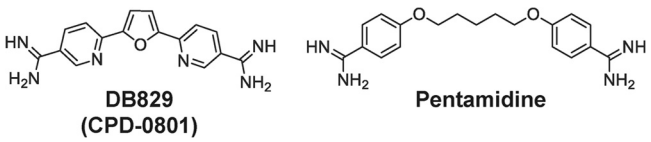

FIG 1 Chemical structures of DB829 and pentamidine.

pounds was furamidine (DB75), which is highly active *in vitro* as well as *in vivo* but has poor oral bioavailability. Its methamidoxime prodrug, pafuramidine (DB289 maleate), has good oral bioavailability (9) and good oral efficacy in *T. b. rhodesiense*-infected mice (10). Pafuramidine was selected by the Consortium for Parasitic Drug Development (CPDD) in 2000 to enter clinical trials as the first oral drug to be tested for first-stage HAT. During a phase III clinical trial, this compound was as effective as pentamidine and its safety profile was inconspicuous (11). However, during a phase I clinical trial for safety with an extended treatment regimen, reversible hepatotoxicity and delayed-onset renal insufficiency were observed, which led to the discontinuation of pafuramidine development (12).

Further screening of novel diamidines and prodrugs has continued in order to identify compounds that are safer, offer the possibility of oral administration, and are in particular active in the CNS for second-stage HAT (10, 13, 14). The prodrug approach was originally employed to improve oral absorption by masking the positive charge of amidine moieties but also had potential to improve drug delivery across the BBB, a prerequisite to cure patients with second-stage infections. Several diamidine prodrugs have been tested in the GVR35 CNS mouse model, in which DB844 and DB868 administered orally cured CNS infections in mice (10). DB844 and DB868 have been further tested in the vervet monkey model of second-stage HAT, and results have been reported recently (15, 16). DB868 was significantly better tolerated in vervet monkeys than was DB844 and could be a promising oral drug candidate, especially for first-stage disease (17).

The active metabolite of the prodrug DB868 is DB829 (or CPD-0801 [Fig. 1]). It is a cationic aza-diamidine, potent *in vitro* against *T. b. rhodesiense* STIB900 parasites (50% inhibitory concentration [IC_{50}], 20 nM). DB829 is of special interest, because when administered intraperitoneally it cured mice with second-stage infections (with *T. b. brucei*) (10). This indicated that it was able to cross the BBB. DB829 therefore represents a new class of cationic diamidines that are CNS active and holds promise for the direct use of active diamidines to treat second-stage HAT. This potentially avoids any detrimental effects of the prodrug strategy, such as variable prodrug activation between different patients, which would simplify pharmacokinetic predictions and dosage selection.

The aim of this study was to characterize the pharmacokinetics, *in vitro* and *in vivo* activity against *T. b. gambiense*, and time of drug action of the CNS-active diamidine DB829. Since more than 98% of HAT cases are due to *T. b. gambiense* infections currently (18), it is imperative to determine the effectiveness of DB829 against *T. b. gambiense* parasites. Isothermal microcalorimetry (19) was employed to monitor *in vitro* parasite killing rate (time of drug action) of DB829 on a real-time basis. Lastly, the *in vivo* parasite clearance time and pharmacokinetics of DB829 in mice were determined. These results are important factors to be considered for further development of DB829 and related compounds to treat African sleeping sickness.

MATERIALS AND METHODS

Materials. Pentamidine isethionate was purchased from Sigma-Aldrich (St. Louis, MO). Synthesis of DB829 (or CPD-0801; hydrochloride salt form) and deuterium-labeled DB75 (DB75-d8; deuterated phenyl rings; internal standard) has been previously reported (20, 21). CPD-0801 and CPD-0802 are both synonyms for DB829. The different codes indicate their different salt forms. CPD-0801 is the hydrochloride salt form, and CPD-0802 is the diacetate salt form of DB829. Only the hydrochloride salt form of DB829 was used in this study.

Animals for pharmacokinetic studies. Protocols for the animal studies were approved by the Institutional Animal Care and Use Committee of the University of Kansas. Male Swiss Webster mice (weighing 20 to 25 g) were purchased from the Charles River Laboratories (O'Fallon, MO). Mice were housed in a clean room under filtered, pathogen-free air, in a 12-h light/dark cycle, and with food pellets and water available *ad libitum*.

Pharmacokinetics of DB829 and pentamidine after i.v. and i.p. administration in mice. DB829 and pentamidine were first dissolved in sterile water and further diluted with saline (1:1, vol/vol) to the desired concentrations. This prevented the precipitation that occurred if the compounds were added directly to saline. The dose level for intravenous (i.v.) administration was 7.5 μmol/kg body weight (approximately 2.3 mg/kg for DB829 and 2.6 mg/kg for pentamidine), which was well tolerated in a preliminary overt toxicity study in mice. The dose level for intraperitoneal (i.p.) administration was 20 mg/kg (approximately 65 μmol/kg for DB829 and 59 μmol/kg for pentamidine), which was the higher of two doses used in the following efficacy study and was selected to directly evaluate if pharmacokinetics played a role in determining *in vivo* efficacy of the two compounds. The dose volume was 5 ml/kg. Blood samples were collected via submandibular bleeding (~0.04 ml per bleed) for serial sampling or cardiac puncture (~0.8 ml of blood) for terminal sampling. To accurately determine the concentration-time curve near and shortly after the time to maximum concentration of drug in plasma (T_{max}) and terminal elimination half-life ($t_{1/2}$), the time points for blood sampling included 0.0167, 0.0833 (two additional time points for i.v. administration), 0.25, 0.5, 1, 2, 4, 6, 8, 12, 24, 48, and 72 h following drug administration, and three mice were used for blood sampling at each time point. Plasma was separated by centrifugation in lithium heparin-coated Microvet tubes (Sarstedt Inc., Newton, NC) or Microtainer tubes (BD Biosciences, Franklin Lakes, NJ). Plasma samples were stored at −20°C until ultraperformance liquid chromatography-tandem mass spectrometry (UPLC-MS/MS) analysis.

Unbound fraction in mouse plasma. The unbound fraction of DB829 and pentamidine in mouse plasma was determined using rapid equilibrium dialysis devices (Thermo Scientific Pierce, Rockford, IL) as previously described (22). Blank mouse plasma was spiked with DB829 or pentamidine to give a final concentration of 1 μM, below which they spent the majority of time after a single i.v. or i.p. administration of the tested doses. Spiked plasma (in triplicate) was incubated for 6 h at 37°C to allow equilibration with a phosphate-buffered saline (100 mM, pH 7.4) and then analyzed for total and unbound concentrations by UPLC-MS/MS.

UPLC-MS/MS analysis. (i) Sample preparation. Plasma samples (2 μl) were mixed with 200 μl of 7:1 (vol/vol) methanol-water containing 0.1% trifluoroacetic acid and internal standard (1 nM DB75-d8) and then vortex mixed for 30 s, followed by centrifugation (2,800 × *g*) to pellet proteins. The supernatant was transferred to a new tube and dried using a 96-well microplate evaporator (Apricot Designs Inc., Covina, CA) under N_2 at 50°C and reconstituted with 100 μl of 15% methanol containing 0.1% trifluoroacetic acid.

(ii) Determination of drug concentration. The reconstituted samples (5-μl injection volume) were analyzed for drug concentration using a Waters Xevo TQ-S mass spectrometer (Foster City, CA) coupled with a Waters Acquity UPLC I-Class system. Compounds were separated on a Waters UPLC BEH C_{18} column (2.1 by 50 mm, 1.7 μm) equilibrated at

TABLE 1 *T. b. gambiense* isolates

Trypanosome strain[a]	Yr of isolation	Origin
STIB930/STIB754	1978	Cote d'Ivoire
ITMAP141267	1960	DRC
130R	2005	DRC
40R	2005	DRC
45R	2005	DRC
349R	2006	DRC
DAL898R	1985	Cote d'Ivoire
K03048	2003	South Sudan

[a] Strains labeled with an "R" were isolated from patients after a relapse with a melarsoprol treatment.

50°C. UPLC mobile phases consisted of water containing 0.1% formic acid (A) and methanol containing 0.1% formic acid (B). After a 0.15-min initial holding period at 5% B, the mobile phase composition started with 5% B and was increased to 60% B over 2.2 min with a flow rate of 0.4 ml/min. Then, the column was washed with 90% B for 0.5 min and was reequilibrated with 5% B for 1.1 min before the next sample was injected. The characteristic single-reaction monitoring (SRM) transitions for DB829, pentamidine, and DB75-d8 were *m/z* 307.1→273.1, 341.4→120.1, and 313.2→296.3, respectively, under positive electrospray ionization mode. The calibration curves for DB829 and pentamidine ranged from 0.5 nM to 50 μM and 2.5 nM to 50 μM, respectively, for plasma samples. The interday coefficient of variation (CV) and accuracy were determined by measuring the same preparation of three standards three times on different days. At concentrations of 5, 500, and 10,000 nM, the intraday CV and average accuracy of DB829 quantification were 8.4% and 91%, 9.4% and 104%, and 3.6% and 99%, respectively. The interday CV and average accuracy of pentamidine quantification were 7.4% and 108% (at 5 nM), 4.7% and 93% (at 500 nM), and 8.1% and 97% at (at 10,000 nM), respectively.

(iii) Pharmacokinetic analysis. The area under the plasma concentration-time curve (AUC), terminal elimination half-life ($t_{1/2}$), maximum concentration of drug in plasma (C_{max}), and time to reach C_{max} (T_{max}) were calculated using the trapezoidal rule-extrapolation method and noncompartmental analysis (WinNonlin Version 5.0; Pharsight, Mountain View, CA).

Antitrypanosomal activity of DB829 and pentamidine *in vitro*. (i) Preparation of compounds. Compounds were dissolved in 100% dimethyl sulfoxide (DMSO) and finally diluted in culture medium prior to the *in vitro* assay. The DMSO concentration never exceeded 1% in the *in vitro* alamarBlue assays at the highest drug concentration. For microcalorimetry assays, the DMSO concentration was kept at 0.1% in all samples to avoid any DMSO effect on the membrane permeability of the trypanosomes. Melarsoprol was diluted in water instead of DMSO. For *in vivo* experiments, the compounds were dissolved in DMSO and further diluted with distilled water to a final DMSO concentration of 10% prior to administration to the animals.

(ii) Parasites. The *T. b. rhodesiense* strain STIB900 is a derivative of strain STIB704 (23), which was isolated from a patient in Ifakara, Tanzania, in 1982. STIB900 was used for routine *in vitro* screening and for the standard acute mouse model, which mimics the first stage of HAT. Strain STIB799, also known as KETRI 243, is a *T. b. rhodesiense* strain isolated from a patient from Busoga in Uganda in 1961 after four treatment failures with melarsoprol (24).

The *T. b. gambiense* strains used within this study were STIB930, ITMAP141267, 130R, 45R, 349R, DAL898R, K03048, and 40R (Table 1). We included more isolates from the Democratic Republic of the Congo (DRC) in our panel of different strains, as most of the *T. b. gambiense* infections occur in this central African country (25, 26). The strains labeled with an "R" were isolated from patients after a melarsoprol treatment failure. STIB930 (also named STIB754) is a derivative of the strain TH1/78E(031),which was isolated from a patient in Cote d'Ivoire in 1978 (27). ITMAP141267, was isolated from a patient in DRC in 1960 (28). Strain 130R was isolated from a patient in DRC in 2005 after two treatment failures with melarsoprol. The first relapse was detected 8 months after a 3-day melarsoprol treatment, and the second relapse was detected 1 year after a melarsoprol-nifurtimox combination therapy (29). Strain 45R was isolated from a patient in DRC in 2005 after two treatment failures with melarsoprol. The first relapse was detected 1 year after a 3-day melarsoprol treatment, and the second relapse was detected 8 months after a melarsoprol-nifurtimox combination therapy (29). Strain 40R was also isolated from a patient in DRC in 2005, 6 months after failure of the 10-day melarsoprol treatment (29). The strain 349R was isolated from a patient in DRC in 2006 after a treatment failure with a 10-day melarsoprol treatment (29). DAL898R was isolated from a patient in Cote d'Ivoire in 1985 after melarsoprol treatment failure (23). DAL898R was the only strain that had previously shown an increased IC_{50} for melarsoprol among the panel of tested DAL (Daloa in Cote d'Ivoire) isolates (23). Strain K03048 was isolated from a patient in South Sudan in 2003 (30).

(iii) *In vitro* growth inhibition assays using *T. brucei* subspecies. The 50% inhibitory concentrations were determined using the alamarBlue assay as described by Raz et al. (31), with minor modifications. Assays were carried out at least three times independently, set up on different days and each time in duplicate. Coefficients of variation of these assays were less than 50%. Different culture and assay media were used for *T. b. gambiense* and for *T. b. rhodesiense*. For *T. b. rhodesiense*, the compounds were tested in minimum essential medium with Earle's salts, supplemented according to the protocol of Baltz et al. (32) with the following modifications: 0.2 mM 2-mercaptoethanol, 1 mM Na-pyruvate, 0.5 mM hypoxanthine, and 15% heat-inactivated horse serum. For *T. b. gambiense*, a modified protocol of Hirumi and Hirumi (33) was used: Iscove's modified Dulbecco's medium (IMDM) was supplemented with 0.2 mM 2-mercaptoethanol, 1 mM Na-pyruvate, 0.5 mM hypoxanthine, 0.05 mM bathocuproindisulfate, 1.5 mM L-cysteine-HCl, 2 mM L-glutamine, and 5% heat-inactivated human serum plus 15% heat-inactivated fetal calf serum.

Serial drug dilutions were prepared in 96-well microtiter plates, and each well was inoculated with 2,000 bloodstream forms for the *T. b. rhodesiense* isolates and with 2,500 bloodstream forms for the *T. b. gambiense* isolates. Drug treatment was carried out for 70 h for *T. b. rhodesiense* and 68 h for *T. b. gambiense*. Ten microliters of the viability marker alamarBlue (12.5 mg resazurin dissolved in 100 ml phosphate-buffered saline) was then added to each well, and the plates were incubated for an additional 2 to 6 h until the signal/background fluorescence ratio was about 10 for *T. b. rhodesiense* isolates or about 5 for *T. b. gambiense* isolates. The plates were read in a SpectraMax Gemini XS microplate fluorescence scanner (Molecular Devices, Sunnyvale, CA) using an excitation wavelength of 536 nm and an emission wavelength of 588 nm. The IC_{50}s were calculated from the sigmoidal inhibition curves using SoftmaxPro software.

(iv) Microcalorimetry studies using *T. brucei* subspecies. *In vitro* time of drug action was monitored using isothermal microcalorimetry. Previous experiments have shown that heat flow data can be used as a proxy for the number of viable cells (34), defined as trypanosomes still moving under the microscope. With this method, the time to the onset of drug action and the time to kill the parasite population can be determined on a real-time basis (19). The same culture media were used for the *T. b. rhodesiense* strain and for the *T. b. gambiense* strains as for the *in vitro* growth inhibition assays. Strain STIB900 was used as a representative for *T. b. rhodesiense* and STIB930 (and sometimes ITMAP141267) for *T. b. gambiense*.

For experiments with permanent drug exposure, bloodstream trypanosomes (2 ml at 5×10^4 organisms/ml per ampoule) were placed in 4-ml ampoules and spiked with DB829 or pentamidine at different concentrations with a final DMSO concentration of 0.1% (vol/vol). The trypanocidal drug melarsoprol was dissolved in water and included as a nondiamidine control for the first experiments with STIB900. Trypano-

some-free negative controls contained only culture medium. After the ampoules had been inserted into the isothermal microcalorimetry instrument (Thermal Activity Monitor, model 249 TAM III; TA Instruments, New Castle, DE), heat flow was continuously measured (1 reading/second) at 37°C. Each experiment with permanent drug exposure was set up in triplicate and repeated 3 times.

(v) Inoculum studies. For studies of drug effects on different parasite densities in the inoculum, the parasite density was reduced to 1×10^4/ml bloodstream trypanosomes and supplemented with DB829 or pentamidine at the desired concentrations. Inhibition of growth and viability was compared with the samples containing the standard inoculum of 5×10^4/ml bloodstream trypanosomes and the same drug concentrations. Inoculum experiments with higher parasite densities were omitted, as the heat flow oscillations, which appear at high initial densities, interfere with drug action (19).

(vi) Drug washout experiments. For the 24-h exposure experiment, trypanosomes (*T. b. rhodesiense* strain STIB900 and *T. b. gambiense* strain STIB930) were incubated with DB829 for 24 h at 37°C and then washed twice at 1,850 × *g* for 10 min to remove the compound. Subsequently, the washed trypanosomes were resuspended in drug-free culture medium and transferred to ampoules and inserted into the isothermal microcalorimetry instrument. The drug dilution factor after two washing steps was estimated to be >1,800-fold. The drug-free control samples (drug free, washed) were washed identically to the drug-containing samples. Each 24-h exposure experiment was set up in triplicate for each assay and repeated 2 times.

(vii) Analysis of microcalorimetry heat flow data. The metabolic heat production rate in each ampoule was recorded continuously. The electric signal was calibrated to obtain a reading in watts. To facilitate data handling, the recorded data were resampled to obtain an effective sampling frequency of 1 data point per 90 s, using the manufacturer's software (TAM assistant version v1.2.4.0), and exported to Microsoft Excel. A time correction was needed for the preparation of the ampoules and the transfer from the bench to the calorimeter prior to equilibration in the calorimeter and the measurement. The correction was achieved by adding 45 min to the time recorded by the microcalorimeter. Resulting data were plotted as heat flow (in μW) over time. Each single curve for heat flow (in W) over time was analyzed using software R (The R Foundation for Statistical Computing, Vienna, Austria). Due to metabolic oscillations clearly visible in the heat flow curves, a cubic spline was applied to smooth the data prior to parameter determination (i.e., onset of drug action, time to peak, and time to kill). The time to onset of drug action was determined as the time at which a divergence between the heat flow rate of the drug-free controls and the drug-containing specimens could be observed (19). The time to peak was determined as the time point at which the maximum heat flow was observed for each sample. The reversal shows the time after which a decrease of the parasite density is expected. The time to kill the parasite population was defined as the time point at which the heat production was reduced to the level of the sterile medium control (base level). At this time, the metabolic heat production of the culture was below the detection limit, suggesting that most of the parasites were inactivated. Typically, a heat flow of 8 μW was recorded at the maximum density of 1×10^6 to 1.5×10^6 trypanosomes/ml, and the microcalorimeter had a detection limit around 100 to 200 nW. The surviving population at the detection limit was about 1.25% to 2.5% of the maximum density, representing a density of $<4 \times 10^4$ trypanosomes/ml.

Finally, the growth rate (μ) of each culture was calculated using the data of heat over time (i.e., the integrated heat flow data over time). For this calculation, the Gompertz growth model (35) was fitted over the whole curve using software R and the Grofit package (36) as described previously (37, 38). Although both heat and heat flow data can be used for the determination of the growth rate, the long thermal equilibration period and the metabolic oscillations observed previously (19) can interfere with the curve-fitting process when using the heat flow data. Therefore, in our case, the calculated growth rate is more precisely determined when using the heat data. The growth rates calculated by this approach cannot be directly compared to the growth rate of exponential phase determined by a conventional approach, because processes such as lysis or chemical processes due to the nature of the medium might also contribute to the overall heat signal. The growth rate calculated based on the heat released by the metabolic activity in the culture should be considered a proxy for the conventional growth rate (34).

***In vivo* assays. (i) Measurement of efficacy and time to kill.** Adult female NMRI mice were obtained from Janvier, France. They weighed between 20 and 25 g at the beginning of the study and were housed under standard conditions with food pellets and water *ad libitum*. All protocols and procedures used in the current study were reviewed and approved by the local veterinary authorities of the Canton Basel-Stadt, Switzerland.

(ii) Mouse model to measure drug efficacy against *T. b. rhodesiense* STIB900. Experiments were performed as previously reported (10) with minor modifications. Briefly, 72 h prior to drug administration, female NMRI mice ($n = 4$ per group) were infected i.p. with 5×10^3 STIB900 bloodstream forms. Drug administration (i.p.) began on day 3 postinfection and continued for four consecutive days (for a total of 4 doses) for a standard treatment regimen. Since a full dose-response curve had been previously determined for DB829 (10), only an effective dose (4×5 mg/kg i.p.) was tested here for DB829. An additional, higher dose (4×20 mg/kg i.p.) was tested for pentamidine due to its inferior *in vivo* efficacy. For single-dose treatment, drug administration took place on day 3 only. A control group was infected but remained untreated. Since the minimum curative dose of DB829 was 4×5 to 10 mg/kg i.p. (10), we chose 20 mg/kg i.p. for the single-dose study, expecting that this dose would give a decent activity without eliciting any toxicity. An additional, lower dose at 5 mg/kg was also tested to probe the minimal curative single dose. The same dose regimen was used for pentamidine. All mice were monitored for parasitemia by microscopic examination of tail blood until 60 days after infection when surviving, and aparasitemic mice were considered cured. Mice with a parasitemia relapse prior to 60 days were not considered cured, and the time to parasite relapse was recorded to calculate the mean relapse time (MRD) in days postinfection.

(iii) Mouse model to measure drug efficacy against *T. b. gambiense*. Female NMRI mice ($n = 4$ per group) were immunosuppressed with 200 mg/kg cyclophosphamide (Endoxan; Baxter, Deerfield, IL) 2 days prior to infection with 10^5 bloodstream forms with one of the four *T. b. gambiense* strains (i.e., ITMAP141267, STIB930, 130R, or 45R) (Table 1). Immunosuppression with cyclophosphamide followed once a week until the end of the experiment. Drug administration (i.p.) began on day 3 postinfection and continued for four consecutive days (for a total of 4 doses) for a standard treatment regimen. For single-dose treatment, drug administration took place on day 3 only. A control group was infected but remained untreated. The same dose regimens as those for *T. b. rhodesiense* STIB900 infections were evaluated for acute *T. b. gambiense* infections. Surviving and aparasitemic mice at day 90 postinfection were considered cured, and the time to parasite relapse was recorded to calculate MRD in days postinfection.

(iv) *In vivo* time to kill. Trypanosome infection and immunosuppression (for *T. b. gambiense*-infected mice) were carried out as described above for the efficacy experiments. The parasite load varied between the different mouse models, which was also observed in the efficacy experiments. The parasitemia was higher in STIB900-infected and STIB930-infected mice than in ITMAP141267-infected mice due to better adaptation of the parasites in mice. Mice were treated with a single dose of 20 mg/kg i.p. 3 days postinfection, the same dose as that used in the pharmacokinetic studies. At this dose, DB829 cured all acute *T. b. rhodesiense* and *gambiense* infections in mice, whereas pentamidine initially cleared parasites, but 2/4 mice infected with *T. b. rhodesiense* STIB900 later relapsed. The first microscopic parasitemia examination was 24 h after treatment (as DB829 is a slow-acting compound) and was followed by two examinations per day until all parasites had disappeared. When parasite detection by microscopy was not sensitive enough to detect any parasites, a

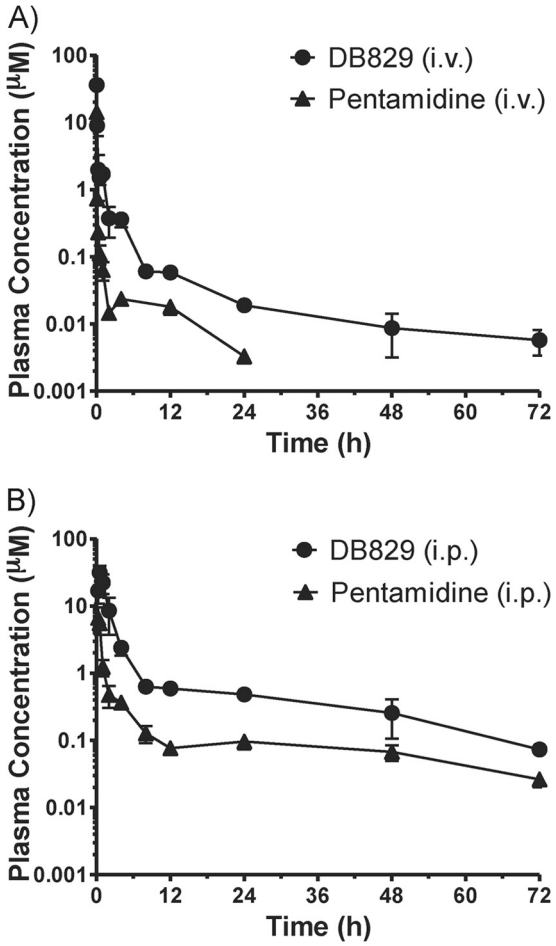

FIG 2 Concentration-time profiles of DB829 (circles) and pentamidine (triangles) in plasma following intravenous (A) or intraperitoneal (B) administration to uninfected mice. A single dose of DB829 (or pentamidine) was administered at 7.5 μmol/kg i.v. or 20 mg/kg i.p. Symbols and error bars represent means and standard errors (SEs), respectively, of triplicate determinations.

hematocrit buffy coat examination was performed. The first time point at which no trypanosomes were detected on the microscopic slide or in the buffy coat was considered the clearance time (or time to kill) in mice. The detection limit by buffy coat examination was $<10^2$ trypanosomes/ml of blood. Mice were kept and further observed by tail blood examination until the end of the experiment to verify whether the administered dose was curative in the infected mice.

RESULTS

Pharmacokinetics of DB829 and pentamidine after i.p. and i.v. administration in mice. The mean concentration in plasma over time profiles of DB829 and pentamidine after a single i.p. or i.v. dose were determined to compare the systemic exposure and other pharmacokinetic properties of the two compounds (Fig. 2 and Table 2). The profiles exhibited a biphasic decline with an initial distribution phase and a terminal elimination phase. About 1 min after i.v. administration at 7.5 μmol/kg (or approximately 2.3 mg/kg for DB829 and 2.6 mg/kg for pentamidine), concentration in plasma reached 36.1 and 14.3 μM and then declined to below 0.1 μM within 4 to 8 h for DB829 and 0.5 to 1 h for pentamidine. DB829 and pentamidine stayed above their IC_{50}s of 20 and 3 nM (against *T. b. rhodesiense* strain STIB900) for at least 12 h (60 nM for DB829 and 18 nM for pentamidine at 12 h) before decreasing slightly below the IC_{50}s by 24 h (19 and 2 nM at 24 h, respectively). The total body clearance of DB829 was considerably smaller (by 84%) than that of pentamidine. Both compounds appeared to be extensively tissue bound, as indicated by large volumes of distribution (Table 2). The observed terminal plasma half-lives were 18.1 h for DB829 and 6.8 h for pentamidine, and the systemic exposure (as determined by AUC) of DB829 was 6.4-fold greater than that of pentamidine. Furthermore, the unbound fraction of DB829 in mouse plasma was 4.8-fold greater than that of pentamidine (Table 2).

After i.p. administration at 20 mg/kg, DB829 and pentamidine were absorbed into the systemic circulation. DB829 reached a C_{max} of 31.6 μM at 0.5 h and pentamidine a C_{max} of 6.7 μM at 0.25 h postdosing (Table 2). Although both compounds stayed above their IC_{50}s against strain STIB900 for the entire 72-h experimental period and had similar terminal half-lives, DB829 achieved significantly greater exposure; AUC was 6.2-fold greater and C_{max} 4.7-fold greater than for pentamidine.

***In vitro* activity of DB829 and pentamidine against different trypanosome isolates.** *In vitro* activity was originally determined against bloodstream trypanosomes of *T. b. rhodesiense* reference strain STIB900 using the alamarBlue assay and a 72-h drug exposure time (10). As most sleeping sickness cases are due to *T. b. gambiense* infections, here we tested DB829 and pentamidine against a panel of different *T. b. gambiense* isolates. Among them were isolates from different regions, older and more recent isolates, and isolates from relapse patients after melarsoprol treatment (Table 1). DB829 was less potent against *T. b. gambiense* isolates (IC_{50} in the range of 69 to 314 nM) than against the *T. b. rhodesiense* reference strain STIB900 (IC_{50}, 20 nM) (Table 3 and Fig. 3), as well as *T. b. rhodesiense* strain STIB799 (IC_{50}, 27 nM) (unpublished data) and *T. b. brucei* strain BS221 (IC_{50},14 nM) (10). This indicates a reduced *in vitro* potency of DB829 against the *T. b. gambiense* subspecies. Among the *T. b. gambiense* isolates,

TABLE 2 Pharmacokinetics of DB829 and pentamidine in uninfected mice

Route	Parameter,[a] unit	DB829	Pentamidine
i.v.	Dose, μmol/kg (mg/kg)	7.5 (2.3)	7.5 (2.6)
	C_{max}, μM	36.1	14.3
	AUC_{last}, μmol/liter · h	7.5	1.2
	$AUC_{0-\infty}$, μmol/liter · h	7.6	1.2
	$t_{1/2}$, h	18	6.8
	CL, liter/h/kg	0.99	6.3
	V_z, liter/kg	26	66
	MRT, h	7.0	3.7
i.p.	Dose, μmol/kg (mg/kg)	65 (20)	58 (20)
	C_{max}, μM	31.6	6.66
	T_{max}, h	0.5	0.25
	AUC_{last}, μmol/liter · h	72	11
	$AUC_{0-\infty}$, μmol/liter · h	74	12
	$t_{1/2}$, h	21	34
	$f_{u,\,P}$, %	40 ± 8.2	8.4 ± 1.2

[a] Abbreviations: C_{max}, maximum concentration; T_{max}, time to reach C_{max}; AUC_{last}, area under the curve from time zero to the last measurable concentration; $AUC_{0-\infty}$, area under the curve from time zero to infinite time; $t_{1/2}$, terminal elimination half-life; CL, total body clearance; V_z, volume of distribution; MRT, mean residence time; $f_{u,\,P}$, unbound fraction in mouse plasma (mean ± standard deviation).

TABLE 3 *In vitro* and *in vivo* antitrypanosomal activity of DB829 and pentamidine against different *T. brucei* strains

Organism and drug regimen (no. of doses × mg/kg i.p.)	DB829		Pentamidine	
	Mean IC_{50} ± SD (nM)	No. cured/no. infected (MRD[a])	Mean IC_{50} ± SD (nM)	No. cured/no. infected (MRD)
T. b. rhodesiense STIB900[b]	20 ± 4		3 ± 0.8	
1 × 5		2/4 (53.5)		ND[d]
1 × 20		4/4		2/4 (22.5)
4 × 5		4/4		1/4 (23)
4 × 20		ND		2/4 (28.5)
T. b. gambiense ITMAP141267	69 ± 17		6 ± 1.2	
1 × 5		3/3[c]		3/4[c] (48)
1 × 20		4/4		4/4
4 × 5		4/4		4/4
4 × 20		ND		ND
T. b. gambiense STIB930	304 ± 87		2 ± 1.1	
1 × 5		4/4		3/4 (59)
1 × 20		4/4		4/4
4 × 5		4/4		4/4
4 × 20		ND		ND
T. b. gambiense 130R	99 ± 23		53 ± 28	
1 × 5		ND		ND
1 × 20		4/4		4/4
4 × 5		4/4		2/3 (60)
4 × 20		ND		4/4
T. b. gambiense 45R	302 ± 113		81 ± 8	
1 × 5		ND		ND
1 × 20		4/4		4/4
4 × 5		4/4		3/3
4 × 20		ND		ND

[a] MRD, mean relapse time in days.
[b] DB829 also cured 3/4 mice at 4 × 50 mg/kg administered orally, 4/4 mice at 1 × 10 mg/kg i.p. or 1 × 10 mg/kg i.v., and 1/4 mice at 4 × 5 mg/kg i.v. for STIB900-infected animals.
[c] The experiment was terminated on day 60 postinfection, instead of day 90 for other experiments with *T. b. gambiense*.
[d] ND, not done.

there was no clear relationship between melarsoprol treatment failure (strains marked with "R") and reduced potency of DB829, whereas pentamidine appeared to be less active against recently isolated strains (Table 3 and Fig. 3). For example, DB829 was more potent against three "R" strains (130R, 349R, and DAL898R) than the reference melarsoprol-sensitive strain STIB930. Furthermore, pentamidine exhibited reduced trypanocidal activity (IC_{50}, >40 nM) against strains recently isolated (after the year 2000), i.e., 40R, 45R, 130R, 349R, and K03048. ITMAP141267 was the oldest strain (isolated in 1960 in DRC) tested in this study, and it was the strain most sensitive to DB829 and among those most sensitive to pentamidine. However, no correlation in reduced trypanocidal activity among *T. b. gambiense* strains was observed between DB829 and pentamidine (Pearson $r^2 = 0.14$, $P = 0.37$; Fig. 3), suggesting lack of cross-resistance.

***In vivo* efficacy in *T. b. gambiense*-infected mice.** To investigate whether potency against *T. b. gambiense* was lower than against *T. b. rhodesiense in vivo* as well as *in vitro*, we tested DB829 and pentamidine in mice infected with four different *T. b. gambiense* isolates and compared their activities with those obtained in the *T. b. rhodesiense* STIB900 mouse model. Both compounds were more efficacious in mice infected with *T. b. gambiense* strains than with *T. b. rhodesiense* strain STIB900 (Table 3). In contrast to the trend observed *in vitro*, DB829 cured *T. b. gambiense*-infected mice at lower doses than it cured *T. b. rhodesiense* STIB900-infected mice. DB829 was curative (3/3 or 4/4 mice) at 1 × 5 mg/kg i.p. in the *T. b. gambiense*-infected mice (ITMAP141267 or STIB930), whereas the same dose was not sufficient to cure all (only 2/4) *T. b. rhodesiense* STIB900-infected mice. Similarly, pentamidine was curative (4/4 mice) at 1 × 20 mg/kg i.p. in all mice infected with any of the four *T. b. gambiense* strains, whereas this dose cured only 2/4 mice infected with *T. b. rhodesiense* STIB900. Both compounds were efficacious in mice infected with *T. b. gambiense* strains associated with melarsoprol treatment failure (i.e., 130R and 45R; Table 3), suggesting lack of cross-resistance with melarsoprol *in vivo*.

Comparison of the two drugs showed that despite being less potent *in vitro*, DB829 was more active than pentamidine *in vivo*. The lowest curative dose of DB829 in STIB900-infected mice was 4 × 5 mg/kg i.p. or 1 × 20 mg/kg i.p., but pentamidine was only partially curative (2/4 mice) at 4 × 20 mg/kg i.p. (Table 3). For *T. b. gambiense*-infected mice, DB829 was completely curative at all doses tested, even with a single dose of 5 mg/kg i.p. In contrast, it took a higher dose of 1 × 20 mg/kg i.p. for pentamidine to achieve a complete cure. These *in vivo* experiments highlight the high *in vivo* potency of DB829, especially against *T. b. gambiense* infections.

In addition to testing i.p. administration, we also evaluated the efficacy of DB829 via i.v. or oral (p.o.) administration based on the observed pharmacokinetics of the compound. The maximum concentration of DB829 in plasma following an i.v. dose of 7.5 μmol/kg (or 2.3 mg/kg) was similar (36.1 versus 31.6 μM) to that after an i.p. dose of 65 μmol/kg (or 20 mg/kg) (Table 2). Previous experiments had demonstrated that DB829 could be absorbed after oral administration, reaching a C_{max} of 83 nM following a single dose of 100 μmol/kg (or 31 mg/kg) (14). Hence, we tested

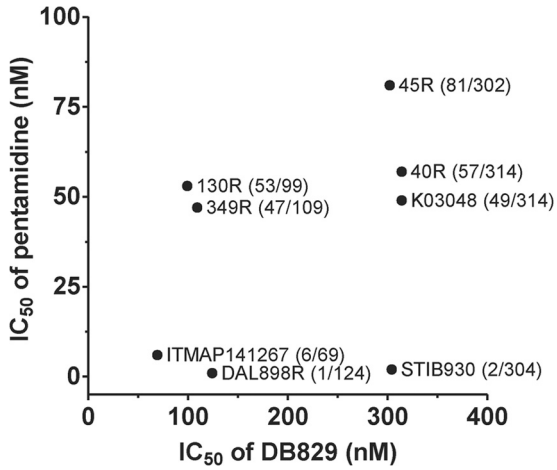

FIG 3 *In vitro* activities of DB829 and pentamidine against different *T. b. gambiense* strains. Symbols represent the average IC_{50}s of three independent determinations. The first number in parentheses represents IC_{50} for pentamidine, and the second number is the IC_{50} for DB829. No significant correlation between pentamidine and DB829 activities was observed (Pearson $r^2 = 0.14$; $P = 0.37$).

DB829 efficacy in the standard mouse model with *T. b. rhodesiense* STIB900 using an i.v. dose of 4 × 5 mg/kg and an oral dose of 4 × 50 mg/kg. DB829 cured 1/4 mice after i.v. administration, so it was less active than with i.p. administration using the same dose regimen (Table 3). However, to our surprise, oral DB829 cured 3/4 mice. This was the first time that a cationic diamidine was shown to have oral efficacy in this first-stage HAT model.

In addition to being less active, DB829 administered i.v. also showed a narrower therapeutic window, as signs of acute toxicity (lethal hypotension) were observed above 20 mg/kg of DB829 in a single dose. In contrast, i.p. administration was much better tolerated up to >50 mg/kg. The slow release by the i.p. route seems to improve tolerability without any loss of efficacy. Pentamidine exhibited a similar tolerability pattern in relation to the site of administration, but in general, DB829 was more efficacious than pentamidine.

Time of drug action *in vitro*. (i) Parameters to describe time of drug action. The time of drug action of DB829 and that of pentamidine *in vitro* against *T. b. rhodesiense* strain STIB900 and *T. b. gambiense* strains ITMAP141267 and STIB930 were recorded and analyzed using isothermal microcalorimetry analysis. We originally proposed to use three parameters (i.e., onset of drug action, time to peak, and time to kill) to describe time of drug action (19). Here, another parameter, the growth rate (μ), was added to describe how fast the culture grows (if any growth is observed) and hence the level of growth rate inhibition, i.e., $1 - (\mu_{drug}/\mu_{drug\ free})$.

(ii) Time of drug action against *T. b. rhodesiense* strain STIB900. The onset of drug action on *T. b. rhodesiense* strain STIB900 ranged from 5 to 19 h for DB829 and from <4 to 14 h for pentamidine, depending on effective drug concentrations (≥0.5× IC_{50}). The onset of drug action of melarsoprol was more concentration dependent than that of DB829 and pentamidine (Table 4). At 200 nM (~50× IC_{50}), melarsoprol instantly inhibited parasite growth, resulting in a heat flow curve comparable to that of trypanosome-free control samples (Fig. 4). The time to peak did not vary much for DB829 (17 to 32 h) at different concentrations (20 to 20,000 nM). For melarsoprol and pentamidine, the time to peak was considerably shorter, and at the high drug concentration of 200 nM (50× to 80× IC_{50}) it could not be calculated because of complete or almost-complete inhibition. The time to kill the parasite population ranged from approximately 3 to 4 days for DB829, showing little variation with drug concentrations (ranging from 20 to 20,000 nM). In contrast, for pentamidine the time to kill decreased over 6-fold (89 h versus 14 h) as the drug concentration increased. Melarsoprol (at 200 nM) killed all parasites in so short a time that time to kill could not be measured (Table 4 and Fig. 4). The inhibition of growth rate (μ) by DB829 was dependent on drug concentration up to 2,000 nM and did not reach more than 72% even at the highest drug concentration tested (20,000 nM, ~1,000× IC_{50}) (Table 4). However, pentamidine and melarsoprol nearly completely inhibited parasite growth at 200 nM. From visual inspection, the overall shapes of the isothermal curves of DB829 and pentamidine were similar, but the shape was different for melarsoprol, especially at 20 nM (Fig. 4C), presumably as a result of distinct modes of action for cationic diamidines and organoarsenicals.

(iii) Time of drug action against *T. b. gambiense* strains. In drug-free control cultures, the growth rate of the two *T. b. gambiense* strains was lower than that of the *T. b. rhodesiense* reference strain STIB900 at identical starting trypanosome densities (5×10^4 trypanosomes/ml) (Fig. 5 and Table 4). The time to peak was 53 to 58 h versus 36 h for STIB900, the growth rate (μ) was 0.024 to 0.018 h^{-1} versus 0.029 h^{-1} for STIB900, and the time to death by overgrowth was also longer, 139 to 170 h compared to 119 h for STIB900. In cultures treated with drugs, the onset of drug action, the time to peak, and the time to kill of DB829 and pentamidine were generally longer for the two *T. b. gambiense* strains (except pentamidine against STIB930) than for the *T. b. rhodesiense* reference strain STIB900 (Table 4). In particular, the time to kill the two *T. b. gambiense* strains with DB829 ranged from 97 to 124 h (or 4 to 5 days) at effective concentrations of 20,000 to 200 nM. This is considerably longer than the standard 72 h observed in the *in vitro* growth inhibition assay. The slow trypanocidal action could be one reason for the greatly increased *in vitro* IC_{50}s of DB829 observed in the growth inhibition assays with the *T. b. gambiense* strains (Table 3 and Fig. 3). However, pentamidine appeared to be faster acting, with a time to kill of <2 days at 20 nM or higher concentrations (Table 4).

(iv) Effects of drug washout on parasites. To determine whether continuous drug exposure for several days is required for DB829 to kill the trypanosomes, experiments were carried out in which the drug was washed out after 24 h of drug incubation, and heat flow was compared with that for parasites exposed to the drug throughout (permanent) the isothermal microcalorimetry assay. These measurements were compared for two strains (STIB900 and STIB930). The time to peak of the heat flow over time for the washed, drug-free samples was delayed by 11 to 22 h compared to that for the drug-free samples that were not washed (subjected to permanent exposure) (Fig. 6 and Table 5). As both samples were set up and run simultaneously, we attribute this delay to the loss of some trypanosomes during the washing steps. Trypanosomes were still viable, as seen by heat production right after the 24-h DB829 exposure at 200 or 2,000 nM, but they died later on when cultured in the drug-free medium (Fig. 6). The times to kill after drug washout were longer than with permanent drug exposure (96 versus 72 h for the *T. b. rhodesiense* reference strain STIB900 at 200 nM and 130 versus 89 h for *T. b. gambiense* strain STIB930 at 2,000 nM) (Table 5). A 24-h exposure with DB829 at 200 nM was finally sufficient to kill the *T. b. rhodesiense* strain STIB900 and at 2,000 nM to kill the *T. b. gambiense* strain STIB930. A revival of the parasite strain STIB930 occurred in a single experiment at 200 nM. These results suggest that the trypanosomes took up lethal concentrations of DB829 at 200 nM (STIB900) or 2,000 nM (STIB930) in the first 24 h, and this was sufficient to kill them at a later time.

(v) Effects of inoculum on time of drug action. Inhibition of trypanosome growth by DB829 was dependent on the initial parasite density (inoculum effect). With an inoculum of 5×10^4/ml, the growth rate of *T. b. rhodesiense* strain STIB900 was inhibited by 15% and 52% with DB829 concentrations of 20 nM and 200 nM, respectively. Considerably stronger inhibition, 72% with 20 nM drug and 90% with 200 nM drug, was observed with an initial inoculum of 1×10^4/ml (Table 5). However, the two parameters, onset of action and time to peak of the heat flow curves, remained similar at different inocula (Table 5 and Fig. 7). We also examined inoculum effects with *T. b. gambiense* strain STIB930. At a drug concentration of 200 nM DB829, parasite growth rate was inhibited by 4% and with 2,000 nM by 52% with an initial inoculum of 5×10^4/ml. Significantly stronger inhibition was observed (42%

TABLE 4 Drug action analysis of antitrypanosomal compounds by isothermal microcalorimetry

T. brucei strain[b] and drug regimen and concn (nM)	Mean (SD)				
	Onset of action (h)	Time to peak (h)	Time to kill (h)	Growth rate (μ) (h^{-1}/1,000)	Inhibition[e] (%)
STIB900					
Drug free		36 (4)	119 (13)	29 (2)	
DB829					
2[c]	19 (8)[c]	35 (4)	115 (10)	28 (1)	5
20	19 (4)	32 (3)	98 (5)	25 (1)	15
200	11 (2)	26 (2)	77 (13)	16 (4)	46
2,000	7 (2)	17 (4)	58 (17)	10 (3)	66
20,000	5 (1)	21 (3)	67 (10)	8 (3)	72
Pentamidine					
0.2[c]	23 (3)[c]	39 (6)	138 (10)	25 (4)	12
2	14 (4)	31 (3)	89 (14)	19 (4)	34
20	<4	9 (2)	25 (2)	<1	~98
200[d]	<4	NM	14 (0)	<1	~98
Melarsoprol					
2[c]	NM[a]	40 (5)	135 (14)	27 (2)	3
20	7 (3)	25 (11)	107 (56)	7 (4)	74
200[d]	NM	NM	NM	NM	~100
STIB930					
Drug free		53 (2)	139 (3)	24 (2)	
DB829					
20[c]	NM	51 (4)	136 (19)	25 (2)	~0
200	26 (7)	52 (2)	124 (4)	23 (1)	2
2,000	17 (7)	41 (5)	99 (11)	16 (3)	33
20,000	10 (2)	41 (2)	97 (8)	14 (2)	43
Pentamidine					
0.2[c]	NM	53 (2)	140 (3)	23 (2)	4
2	8 (1)	30 (2)	75 (8)	11 (2)	54
20[b]	<4	12 (1)	22 (2)	<1	~96
200[b]	<4	NM	NM	<1	~96
ITMAP141267					
Drug free		58 (4)	170 (12)	18 (3)	
DB829					
20[c]	NM	57 (5)	167 (4)	17 (3)	6
200	28 (9)	50 (3)	124 (7)	17 (4)	5
2,000	14 (5)	33 (12)	100 (13)	12 (2)	33
20,000	12 (5)	34 (14)	113 (10)	10 (2)	42
Pentamidine					
2[c]	28 (7)	57 (2)	159 (3)	18 (3)	~0
20	6 (1)	10 (1)	41 (8)	3.5 (0.7)	80
200	4 (1)	8 (2)	23 (9)	1.2 (0.4)	94

[a] NM, not measurable.
[b] Initial inoculum density was 5×10^4 trypanosomes/ml.
[c] Inhibition was too small to accurately recover parameters from every experiment performed.
[d] Inhibition was too strong to accurately recover parameters from every experiment performed.
[e] Inhibition is measured by the formula $[1 - (\mu_{drug}/\mu_{drugfree})] \times 100$.

at 200 nM and 91% at 2,000 nM) when the initial inoculum was 1×10^4/ml (Table 5). As with STIB900, the other two parameters of the heat flow curves remained similar at different inocula (Table 5 and Fig. 7). The same inoculum effects were also observed for pentamidine (Table 5 and Fig. 7).

(vi) Time of drug action *in vivo*. The *in vivo* time of drug action of DB829 and that of pentamidine were determined, following a single i.p. dose of 20 mg/kg to mice infected with *T. b. rhodesiense* strain STIB900 or *T. b. gambiense* strains ITMAP141267 and STIB930, to compare the time of drug action *in vitro* with that *in vivo*. For mice infected with *T. b. rhodesiense* strain STIB900, the *in vivo* onset of drug action of DB829 was less than 24 h, which is in accordance with the *in vitro* time of the onset of action (5 to 19 h at DB829 concentrations of 20 to 20,000 nM) (Table 4). The *in vivo* time to kill (parasite clearance time) was on average 78 h (i.e., the first mouse was parasite free 72 h after drug administration and the last mouse after 80 h) (Table 6). This is in the range of the *in vitro* time to kill (58 to 98 h; Table 4) at the different DB829 concentrations (20 to 20,000 nM). The time to kill in mice infected with *T. b. gambiense* strain ITMAP141267 was on average 102 h (96 to 120 h), and in STIB930-infected mice, it was

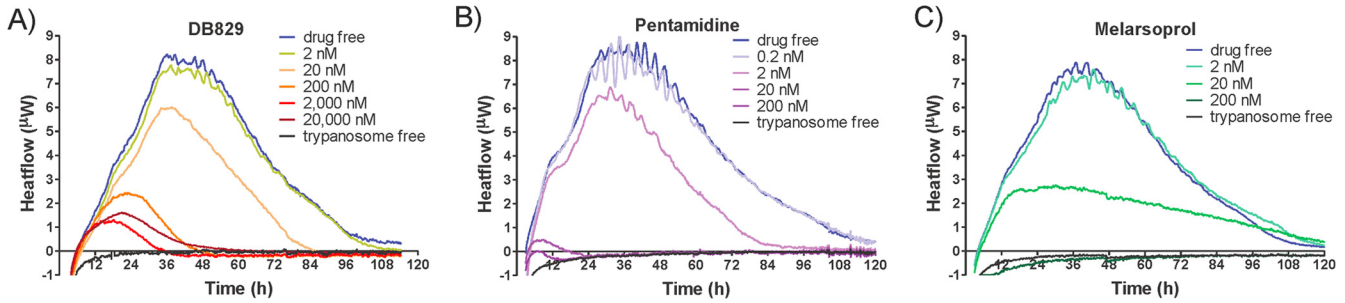

FIG 4 Microcalorimetry growth profiles of *T. b. rhodesiense* strain STIB900 in the presence of various concentrations of DB829 (A), pentamidine (B), and melarsoprol (C). The drug-free experiment included parasites (5×10^4/ml inoculum) without drug treatment, and the trypanosome-free experiment did not include parasites or drug treatment. Each curve represents the mean of three incubations.

62 h (56 to 80 h) (Table 6). This is similar to or slightly faster than the *in vitro* time to kill for these two parasite strains (100 to 124 h and 99 h, respectively, at approximately 10× IC_{50}) (Table 4).

In addition, the *in vivo* times to kill of pentamidine were shorter than those of DB829 in all experiments, although some mice infected with the *T. b. rhodesiense* strain STIB900 relapsed later (Table 3). The *in vivo* times to kill of pentamidine were on average 26 h, 30 h, and 48 h for mice infected with *T. b. rhodesiense* strain STIB900 and *T. b. gambiense* strains ITMAP141267 and STIB930, respectively. These results are similar to the *in vitro* time to kill at relevant drug concentrations (around 20 nM) (Table 4). The parasite load in STIB930-infected mice was higher than in mice with ITMAP141267 infections due to better adaptation of STIB930 in mice.

DISCUSSION

Recent efforts to enhance the CNS activity of antiparasitic diamidines led to the discovery of aza analogues of furamidine. One of these, DB829, cured all mice in the second-stage HAT model using *T. b. brucei* strain GVR35 when administered intraperitoneally (10), in spite of the dogma that cationic diamidines cannot traverse cellular membranes via passive diffusion. This liability limits their oral bioavailability and brain penetration, so that they are generally considered to be effective only against first-stage HAT and only through parenteral administration. Our discovery of

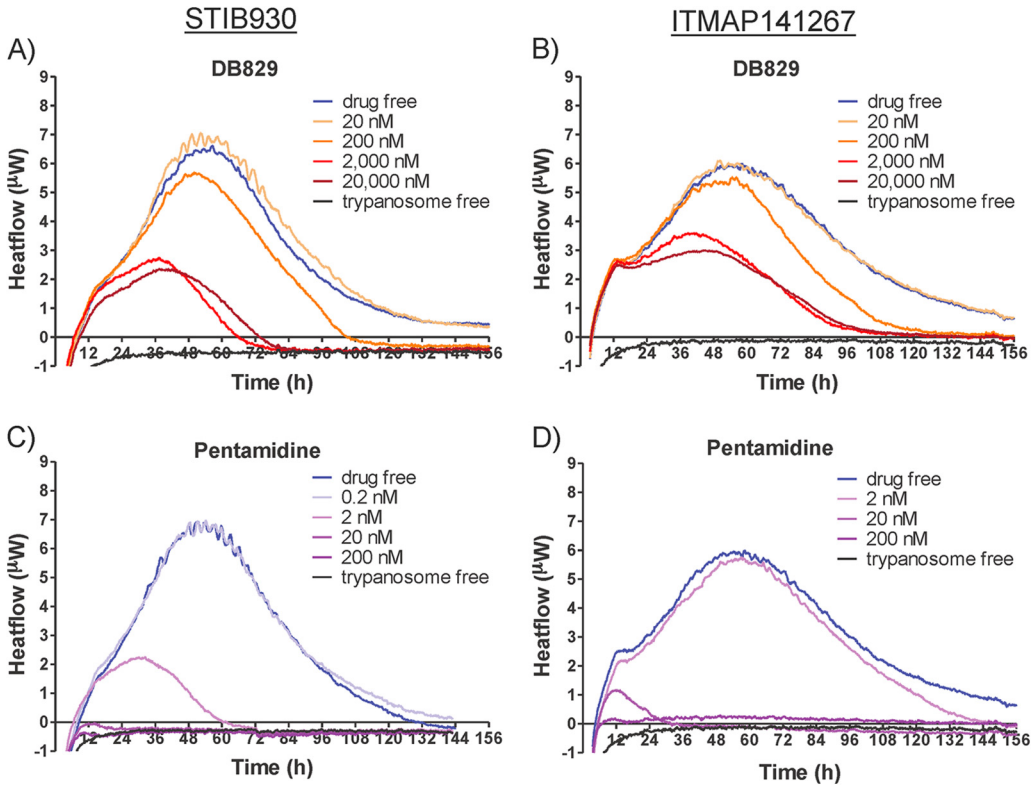

FIG 5 Microcalorimetry growth profiles of *T. b. gambiense* strains STIB930 (A and C) and ITMAP141267 (B and D) in the presence of various concentrations of DB829 (A and B) and pentamidine (C and D). The drug-free experiment included parasites (5×10^4/ml inoculum) without drug treatment and the trypanosome-free experiment did not include parasites or drug treatment. Each curve represents the mean of three incubations.

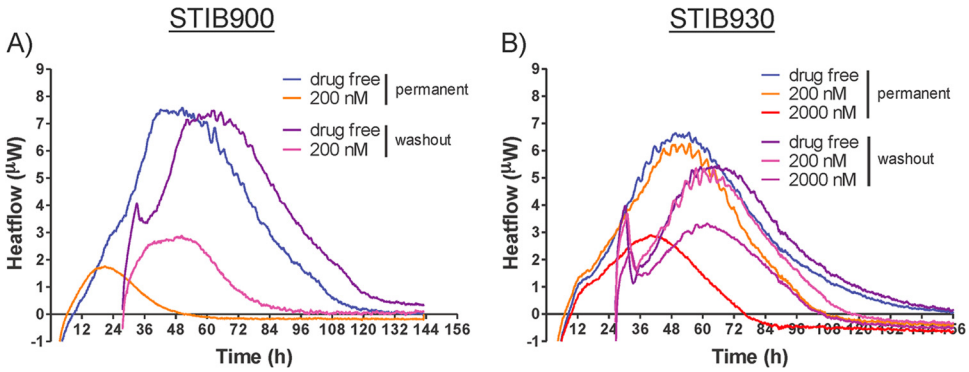

FIG 6 Effects of drug washout on microcalorimetry growth profiles of *T. b. rhodesiense* strain STIB900 (A) and *T. b. gambiense* strain STIB930 (B) in the presence of DB829. Drug washout was performed after a 24-h exposure to DB829. The drug-free experiment included parasites (5×10^4/ml inoculum) without drug treatment. Each curve represents the mean of three incubations.

aza-diamidines led to the further testing of DB829 in a second-stage HAT monkey model (results will be published in due course) and in the present study to the comprehensive pharmacological characterization of DB829 and the comparator drug pentamidine with two human-infective *T. brucei* subspecies. Effectiveness against *T. b. gambiense* is of special interest since most HAT patients are infected with this trypanosome subspecies.

In comparison to the activity against the reference strain *T. b. rhodesiense* STIB900, the potency of DB829 *in vitro* against *T. b. gambiense* strains was reduced, ranging from 3.5- to 15-fold

TABLE 5 Effects of inoculum and drug washout on drug action of DB829 and pentamidine by isothermal microcalorimetry

T. brucei strain and inoculum	Compound	Drug concn (nM)	Mean (SD)				Inhibition[f] (%)
			Onset of action (h)	Time to peak (h)	Time to kill (h)	Growth rate (µ) ($\times$1,000 h^{-1})	
STIB900		0 (drug free)		37 (4)	123 (12)	28 (3)	
5×10^4/ml	DB829	20	22 (5)	34 (2)	98 (4)	22 (4)	15
		200	10 (2)	24 (3)	72 (8)	13 (2)	52
	Pentamidine	0.2	20 (1)	36 (4)	134 (11)	27 (2)	4
		2	12 (2)	30 (2)	84 (14)	19 (5)	35
		20[b]	3 (1)	9 (2)	21 (9)	<1	~98
1×10^4/ml		0 (drug free)		52 (5)	135 (13)	27 (1)	
	DB829	20	17 (4)	33 (2)	69 (7)	8 (3)	72
		200[b]	14 (2)	16 (4)	36 (12)	2 (2)	>90
	Pentamidine	0.2[a,c]	20 (1)	42 (3)	152 (9)	28 (1)	3
		2[b]	12 (3)	20 (4)	40 (5)	<1	~97
		20[b]	NM[e]	NM	NM	<1	~99
5×10^4/ml	Washout	0 (drug free)		59 (5)	132 (5)	26 (2)	
	DB829	200[c]	<27	46 (6)	96 (6)	9 (0.4)	64
STIB930		0 (drug free)		52 (2)	151 (9)	25 (2)	
5×10^4/ml	DB829	200	27 (6)	51 (1)	121 (4)	24 (1)	4
		2,000[c]	16 (5)	39 (1)	89 (2)	12 (1)	52
	Pentamidine	0.2[d]	<4	53 (1)	163 (19)	23 (1)	8
		2	6 (1)	29 (7)	66 (12)	8 (3)	67
1×10^4/ml		0 (drug free)		69 (2)	159 (11)	24 (2)	
	DB829	200	34 (10)	56 (4)	111 (10)	14 (3)	42
		2,000[b,c]	15 (5)	37 (4)	66 (3)	2 (0.3)	91
	Pentamidine	0.2[d]	<6	74 (2)	161 (5)	22 (4)	12
		2[b]	<6	NM	NM	NM	~100
5×10^4/ml	Washout	0 (drug free)		63 (5)	154 (11)	21 (1)	
	DB829	200[c]	<27	60 (2)	128 (9)	21 (0.5)	~0
		2,000[d]	<27	58 (2)	130 (12)	15 (2)	28

[a] Inhibition was too small to accurately recover parameters from every experiment performed.
[b] Inhibition was too strong to accurately recover parameters from every experiment performed.
[c] Two independent experiments were performed (each in triplicate).
[d] One independent experiment was performed (in triplicate).
[e] NM, not measurable.
[f] Inhibition is measured by the formula $[1 - (\mu_{drug}/\mu_{drugfree})] \times 100$.

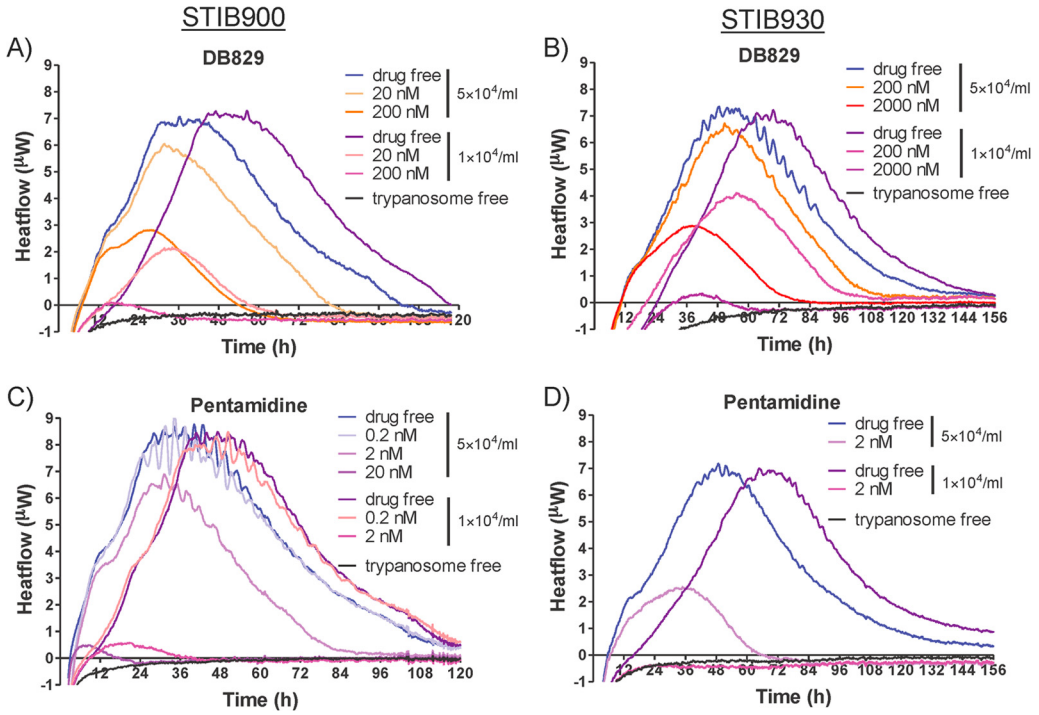

FIG 7 Inoculum effect on microcalorimetry growth profiles of *T. b. rhodesiense* strain STIB900 (A and C) and *T. b. gambiense* strain STIB930 (B and D) in the presence of various concentrations of DB829 (A and B) and pentamidine (C and D). Two initial trypanosome densities were tested: standard inoculum at 5×10^4/ml and low inoculum at 1×10^4/ml. The drug-free experiment included parasites without drug treatment, and the trypanosome-free experiment did not include parasites or drug treatment. Each curve represents the mean of three incubations.

(Table 3). Pentamidine also displayed a reduction in potency (2- to 27-fold) against most *T. b. gambiense* strains, except for STIB930 and DAL898R strains (Fig. 3). No cross-resistance between DB829 and pentamidine was observed in this study, which included isolates from relapsed patients, in contrast to the cross-resistance previously reported for pentamidine and melarsoprol (39, 40). Transporters are known to be an important determinant for developing resistance in trypanosomes to pentamidine and melarsoprol (41–44). The P2 aminopurine transporter plays a predominant role in the uptake of aza analogues of furamidine into *T. b. brucei* s427 trypanosomes (45). The limited cross-resistance of DB829 to pentamidine is presumably because different transporters (41, 46)—in addition to P2—are involved in drug uptake of both pentamidine and melarsoprol but do not transport DB829. The existence of less efficient transporters in the *T. b. gambiense* strains may also explain the observed lower *in vitro* potency of DB829 against these parasite strains.

Despite being less active against *T. b. gambiense* strains *in vitro*, DB829 was surprisingly more efficacious *in vivo*, curing all mice infected with different *T. b. gambiense* isolates at all dose regimens tested (Table 3). In particular, a single dose of DB829 administered intraperitoneally was highly effective, curing all *T. b. gambiense*-infected animals at a dose as low as 5 mg/kg of body weight, whereas the same dose of DB829 cured only 2/4 mice infected with *T. b. rhodesiense* strain STIB900. The high efficacy of the lowest DB829 doses used in our present study meant that the minimal curative dose of DB829 for *T. b. gambiense*-infected mice has not yet been established. In comparison, pentamidine was less efficacious than DB829 in *T. b. gambiense*-infected mice (3/4 cures at 5 mg/kg, single dose, compared with 4/4 or 3/3 cures with DB829) and in *T. b. rhodesiense*-infected mice (1/4 cures compared to 4/4 cures at 4 × 5 mg/kg or 2/4 versus 4/4 cures at 20 mg/kg, single dose, respectively).

TABLE 6 *In vivo* time to kill (parasite clearance time) in infected mice administered DB829 or pentamidine[a]

T. brucei strains	Mean (range) time to kill (h)	
	DB829	Pentamidine
STIB900	78 (72–80)	26 (24–32)
ITMAP141267	102 (96–120)	30 (24–48)
STIB930	62 (56–80)	48 (48)

[a] Mean data for four mice per group; range, time elapsed between the first mouse and the last mouse becoming aparasitemic. For each drug, a single dose of 20 mg/kg was administered i.p. on day 3 postinfection.

Two factors may have contributed to the observed difference in the activity of DB829 against *T. b. gambiense in vitro* and *in vivo*. First, downregulation of diamidine uptake transporter(s) (e.g., P2 aminopurine transporter) under the *in vitro* culturing conditions could have reduced the susceptibility of the *T. b. gambiense* isolates to DB829, whereas *in vivo* bloodstream trypanosomes in infected mice maintain a normal expression and function of diamidine uptake transporter(s) and hence would be more susceptible to DB829 than trypanosomes in *in vitro* culture. A striking decrease (from 100% to 4.2%) in the functional activity of the P2 aminopurine transporter in *T. b. brucei* s427 cells over a 24-h culture period after fresh isolation from an infected rat was observed by Ward et al. (45). However, it is yet to be demonstrated that such downregulation of the P2 aminopurine transporter also occurred in the *T. b. gambiense* isolates tested *in vitro* in our study. The

observed decrease in *in vitro* potency (IC_{50}) of the *T. b. gambiense* isolates did not seem to have a major effect on the time to kill. At approximately 10× IC_{50} the *in vitro* and *in vivo* times to kill were similar (Tables 4 and 6), which indicates that the drug uptake *in vitro* was high enough to kill the parasites in a period similar to that *in vivo*.

A second reason for the greater potency of DB829 against *T. b. gambiense* isolates *in vivo* compared with *T. b. rhodesiense* could have been the levels of parasitemia. Mice infected with *T. b. gambiense* strains generally have a lower parasitemia ($<10^7$ trypanosomes/ml of blood) than those infected with *T. b. rhodesiense* strain STIB900 ($\geq 10^8$ trypanosomes/ml of blood) (47). An inoculum effect (i.e., initial parasite density-dependent growth inhibition) could result in a better-than-expected *in vivo* activity due to lower parasitemia in mice infected with *T. b. gambiense* strains. We assessed inoculum effects on time of drug action by DB829 and pentamidine *in vitro* using isothermal microcalorimetry and confirmed that inhibition of trypanosome growth rate by DB829 and pentamidine depended on the initial inoculum: the lower the density of parasites, the stronger the inhibition of growth of either *T. b. rhodesiense* or *gambiense* strains (Fig. 7 and Table 5). Although the causes of the inoculum effect are still unclear to us (see additional discussion in the supplemental material), the observed inoculum effect is not expected to have any untoward effect on efficacy in HAT patients treated with pentamidine (or potentially DB829), since parasitemia in human patients, especially those with *T. b. gambiense* infections, is very low ($<10^5$ trypanosomes/ml).

Using isothermal microcalorimetry, we were able to make a real-time comparison of the effects of different drugs on different parasite strains. It provided us with a convenient tool to monitor parasite growth and to visualize and quantify the level of growth rate inhibition by antiparasitic drugs on a real-time basis. Wenzler et al. (19) first described the use of this technology to characterize the parasite growth and effects of drug treatments for *T. brucei* and *Plasmodium falciparum*. Here we used mathematical models and included an additional parameter, growth rate (μ). The new four-parameter model (onset of drug action, time to peak, time to kill, and growth rate) describes time of drug action in more detail.

The inoculum effect was revealed by using the same drug concentration but different initial inocula (Table 5). The effect on the inhibition of growth rate is discussed above. In contrast, inoculum effects were not as clearly apparent on onset of drug action or time to peak. This indicates that the drug action starts almost simultaneously at identical drug concentrations for DB829 and pentamidine at the different inocula. Inhibition is considerably stronger in the samples with lower trypanosome densities, when their drug-free control samples are still in the exponential growth phase. On the other hand, at higher parasite densities inhibition may be less observable because the onset of drug action and/or time to peak is already close to the stationary phase, when growth of the drug-free control samples is reduced as well—not by drug inhibition but due to overgrowth of the parasite culture. Growth inhibition by slow-acting drugs was less visible at higher inocula since a decreased metabolic activity may coincide with the overgrowing culture.

The time of onset of drug action is a pharmacodynamic parameter that is important when considering potential use for treatment. A main feature of isothermal microcalorimetry is real-time monitoring of organism growth, which can be used to readily calculate *in vitro* time of drug action. Traditionally, time of drug action was obtained through laborious multiple single time point antiparasitic inhibition assays with variable drug exposure times. Onset of action, time to peak, and time to kill could only be estimated, and the level of inhibition was calculated at the few tested time points (19). Microcalorimetry offers a more reliable and less laborious method. However, as the microcalorimeter typically requires a few hours to fully equilibrate 4-ml ampoules containing 2 ml of culture medium, the analysis of onset of drug action is still difficult, especially for fast-acting compounds. Further technical improvements (e.g., adding an injection system) will be desirable to allow preequilibration of ampoules prior to injecting compound solutions, thus reducing the equilibration time following drug addition (48).

DB829 was shown to be a slow-acting trypanocidal compound. It was possible to obtain reliable results for the *in vitro* time to kill at a range of concentrations. This ranged from 3 to 4 days for *T. b. rhodesiense* strain STIB900 and from 4 to 5 days for the *T. b. gambiense* strains, depending on effective ($\geq 0.5\times$ IC_{50}) drug concentrations (Table 4). In comparison, pentamidine is faster acting, reducing parasites to below the detection limit within 1 day after drug addition at 200 nM concentration for all three strains and at 20 nM for STIB900 and ITMAP141267. This is probably due to differences in the parasite uptake kinetics of the two compounds, which have been previously characterized using *T. b. brucei* strain s427 (45, 49). It is noteworthy that parasites of *T. b. rhodesiense* strain STIB900 grew faster than those of the two *T. b. gambiense* strains in the absence of drug treatment, resulting in a shorter time to death of the parasite culture (approximately 5 days versus 6 to 7 days, respectively) as a result of overgrowing. Since our standard *in vitro* growth inhibition assays utilize a 72-h of incubation period, we believe that the slow trypanocidal action of DB829 contributed, in part, to the increases in measured IC_{50}s against the *T. b. gambiense* strains.

Activity of DB829 *in vitro* was not increased with drug concentrations higher than 2,000 nM (Fig. 4A and 5A and B). This is most likely due to the saturation of the P2 transporter, which is the main route of DB829 uptake (45). In a P2 transporter-mediated uptake assay, the Michaelis-Menten constant, K_m, of DB829 is 1.1 μM, indicating that saturation (maximum uptake rate, V_{max}) is almost reached after 2 μM and therefore no significant higher inhibition can be expected with this compound at higher drug concentrations.

Parasite clearance time *in vivo*, following a single intraperitoneal injection of DB829 at a dose of 20 mg/kg of body weight, ranged from 3 to 3.3 days for mice infected with *T. b. rhodesiense* strain STIB900 and from 2.3 to 5 days for mice infected with the different *T. b. gambiense* strains (Table 6). These times were in good agreement with the *in vitro* times to kill, given the high concentration in plasma of DB829 (C_{max} = 31.6 μM) reached at this dose level (Table 2). As predicted based on *in vitro* time to kill, pentamidine is also faster acting *in vivo* than DB829, clearing parasites from the bloodstream within 1 to 1.3 days for mice infected with *T. b. rhodesiense* strain STIB900 and 1 to 2 days for mice infected with the *T. b. gambiense* strains. In summary, it generally takes more time for DB829 to clear *T. brucei* parasites than for pentamidine.

An interesting feature of the action of DB829 is that despite being slow acting, it was able to kill parasites *in vitro* after a short (24-h) drug exposure, as demonstrated by drug washout experi-

ments (Fig. 6 and Table 5). This is consistent with the observation that a single dose of DB829 could effectively cure infected mice (Table 3), which was partially due to desirable pharmacokinetics, with a high maximum drug concentration in plasma, relatively long terminal elimination half-life at the dose tested, and relatively low plasma protein binding (Table 2).

Based on the outstanding efficacy of DB829 in the mouse models with acute infections and its desirable pharmacokinetic properties, it is of interest to consider the potential value of this compound in the treatment of HAT. A single dose of DB829 administered intramuscularly could be suggested as a new short treatment for first-stage HAT. An even more important property of DB829 is that it was shown to be efficacious in mice with second-stage infection when administered intraperitoneally (10). This has prompted further testing of parenteral DB829 (as well as its methamidoxime oral prodrug, DB868) in the vervet monkey model for second-stage HAT with promising results (16).

New, safe, and effective drugs are urgently needed for treatment of both stages of HAT. It is also desirable that they be easy to administer, with a simple dosing regimen. With improved drugs, it should be possible to control HAT effectively and perhaps even eliminate the disease. DB829 is a promising candidate for further development. It is CNS active (by itself, without bioconversion), so it could be used against second-stage HAT. In mouse models, it showed outstanding efficacy against both first and second stages of infection. Furthermore, it cured both *T. b. gambiense* and *T. b. rhodesiense* infections at low and well-tolerated doses. Parenteral DB829 with a short dosing regimen such as 5 days or less for the second stage and a single dose for the first stage should be seriously considered for further development as a new treatment for sleeping sickness.

ACKNOWLEDGMENTS

We thank Pati Pyana and Anne Clarisse Lekane Likeufack for isolating *T. b. gambiense* strains from patients in the Democratic Republic of the Congo, Jennifer Jenkins for critical reading and inputs to the manuscript, Guy Riccio and Christiane Braghiroli for carrying out experiments on *in vivo* efficacy and time to kill in mice, and Kirsten Gillingwater for time-to-kill experiments in mice.

This work was supported by the Bill and Melinda Gates Foundation through the Consortium for Parasitic Drug Development (CPDD).

REFERENCES

1. **Simarro PP, Cecchi G, Franco JR, Paone M, Fevre EM, Diarra A, Postigo JA, Mattioli RC, Jannin JG.** 2011. Risk for human African trypanosomiasis, Central Africa, 2000–2009. Emerg. Infect. Dis. **17:**2322–2324.
2. **Simarro PP, Jannin J, Cattand P.** 2008. Eliminating human African trypanosomiasis: where do we stand and what comes next? PLoS Med. **5:**e55. doi:10.1371/journal.pmed.0050055.
3. **WHO.** 1998. Control and surveillance of African trypanosomiasis. Report of a WHO Expert Committee. World Health Organ. Tech. Rep. Ser. **881**(I–VI):1–114.
4. **Barrett MP.** 2006. The rise and fall of sleeping sickness. Lancet **367:**1377–1378.
5. **Barrett MP, Gilbert IH.** 2006. Targeting of toxic compounds to the trypanosome's interior. Adv. Parasitol. **63:**125–183.
6. **Brun R, Blum J, Chappuis F, Burri C.** 2010. Human African trypanosomiasis. Lancet **375:**148–159.
7. **McCulloch R.** 2004. Antigenic variation in African trypanosomes: monitoring progress. Trends Parasitol. **20:**117–121.
8. **Wilson WD, Nguyen B, Tanious FA, Mathis A, Hall JE, Stephens CE, Boykin DW.** 2005. Dications that target the DNA minor groove: compound design and preparation, DNA interactions, cellular distribution and biological activity. Curr. Med. Chem. Anticancer Agents **5:**389–408.
9. **Midgley I, Fitzpatrick K, Taylor LM, Houchen TL, Henderson SJ, Wright SJ, Cybulski ZR, John BA, McBurney A, Boykin DW, Trendler KL.** 2007. Pharmacokinetics and metabolism of the prodrug DB289 (2,5-bis[4-(N-methoxyamidino)phenyl]furan monomaleate) in rat and monkey and its conversion to the antiprotozoal/antifungal drug DB75 (2,5-bis(4-guanylphenyl)furan dihydrochloride). Drug Metab. Dispos. **35:**955–967.
10. **Wenzler T, Boykin DW, Ismail MA, Hall JE, Tidwell RR, Brun R.** 2009. New treatment option for second-stage African sleeping sickness: in vitro and in vivo efficacy of aza analogs of DB289. Antimicrob. Agents Chemother. **53:**4185–4192.
11. **Burri C.** 2010. Chemotherapy against human African trypanosomiasis: is there a road to success? Parasitology **137:**1987–1994.
12. **Paine MF, Wang MZ, Generaux CN, Boykin DW, Wilson WD, De Koning HP, Olson CA, Pohlig G, Burri C, Brun R, Murilla GA, Thuita JK, Barrett MP, Tidwell RR.** 2010. Diamidines for human African trypanosomiasis. Curr. Opin. Investig. Drugs **11:**876–883.
13. **Maser P, Wittlin S, Rottmann M, Wenzler T, Kaiser M, Brun R.** 2012. Antiparasitic agents: new drugs on the horizon. Curr. Opin. Pharmacol. **12:**562–566.
14. **Brun R, Don R, Jacobs RT, Wang MZ, Barrett MP.** 2011. Development of novel drugs for human African trypanosomiasis. Future Microbiol. **6:**677–691.
15. **Thuita JK, Wang MZ, Kagira JM, Denton CL, Paine MF, Mdachi RE, Murilla GA, Ching S, Boykin DW, Tidwell RR, Hall JE, Brun R.** 2012. Pharmacology of DB844, an orally active aza analogue of pafuramidine, in a monkey model of second stage human African trypanosomiasis. PLoS Negl. Trop. Dis. **6:**e1734. doi:10.1371/journal.pntd.0001734.
16. **Thuita JK.** 2012. Biological and pharmacological investigations of novel diamidines in animal models of human African trypanosomiasis. Ph.D. thesis. University of Basel, Basel, Switzerland.
17. **Thuita JK, Wolf KK, Murilla GA, Liu Q, Mutuku JN, Chen Y, Bridges AS, Mdachi RE, Ismail MA, Ching S, Boykin DW, Hall JE, Tidwell RR, Paine MF, Brun R, Wang MZ.** 2013. Safety, pharmacokinetic, and efficacy studies of oral DB868 in a first stage vervet monkey model of human African trypanosomiasis. PLoS Negl. Trop. Dis. **7**(6):e2230. doi:10.1371/journal.pntd.0002230.
18. **WHO.** Updated June 2013. Media Centre, fact sheet N°259. Trypanosomiasis, human African (sleeping sickness). http://www.who.int/mediacentre/factsheets/fs259/en/. Accessed 25 July 2013.
19. **Wenzler T, Steinhuber A, Wittlin S, Scheurer C, Brun R, Trampuz A.** 2012. Isothermal microcalorimetry, a new tool to monitor drug action against Trypanosoma brucei and Plasmodium falciparum. PLoS Negl. Trop. Dis. **6:**e1668. doi:10.1371/journal.pntd.0001668.
20. **Das BP, Boykin DW.** 1977. Synthesis and antiprotozoal activity of 2,5-bis(4-guanylphenyl)furans. J. Med. Chem. **20:**531–536.
21. **Ismail MA, Brun R, Easterbrook JD, Tanious FA, Wilson WD, Boykin DW.** 2003. Synthesis and antiprotozoal activity of aza-analogues of furamidine. J. Med. Chem. **46:**4761–4769.
22. **Yan GZ, Brouwer KL, Pollack GM, Wang MZ, Tidwell RR, Hall JE, Paine MF.** 2011. Mechanisms underlying differences in systemic exposure of structurally similar active metabolites: comparison of two preclinical hepatic models. J. Pharmacol. Exp. Ther. **337:**503–512.
23. **Brun R, Schumacher R, Schmid C, Kunz C, Burri C.** 2001. The phenomenon of treatment failures in Human African Trypanosomiasis. Trop. Med. Int. Health **6:**906–914.
24. **Bacchi CJ, Nathan HC, Livingston T, Valladares G, Saric M, Sayer PD, Njogu AR, Clarkson AB, Jr.** 1990. Differential susceptibility to DL-alpha-difluoromethylornithine in clinical isolates of Trypanosoma brucei rhodesiense. Antimicrob. Agents Chemother. **34:**1183–1188.
25. **Simarro PP, Cecchi G, Paone M, Franco JR, Diarra A, Ruiz JA, Fevre EM, Courtin F, Mattioli RC, Jannin JG.** 2010. The atlas of human African trypanosomiasis: a contribution to global mapping of neglected tropical diseases. Int. J. Health Geogr. **9:**57. doi:10.1186/1476-072X-9-57.
26. **Simarro PP, Diarra A, Ruiz Postigo JA, Franco JR, Jannin JG.** 2011. The human African trypanosomiasis control and surveillance programme of the World Health Organization 2000–2009: the way forward. PLoS Negl. Trop. Dis. **5:**e1007. doi:10.1371/journal.pntd.0001007.
27. **Felgner P, Brinkmann U, Zillmann U, Mehlitz D, Abu-Ishira S.** 1981. Epidemiological studies on the animal reservoir of gambiense sleeping sickness. Part II. Parasitological and immunodiagnostic examination of the human population. Tropenmed. Parasitol. **32:**134–140.
28. **Likeufack AC, Brun R, Fomena A, Truc P.** 2006. Comparison of the in

vitro drug sensitivity of Trypanosoma brucei gambiense strains from West and Central Africa isolated in the periods 1960–1995 and 1999–2004. Acta Trop. **100:**11–16.
29. **Pyana PP, Ngay Lukusa I, Mumba Ngoyi D, Van Reet N, Kaiser M, Karhemere Bin Shamamba S, Buscher P.** 2011. Isolation of Trypanosoma brucei gambiense from cured and relapsed sleeping sickness patients and adaptation to laboratory mice. PLoS Negl. Trop. Dis. **5:**e1025. doi:10.1371/journal.pntd.0001025.
30. **Maina N, Maina KJ, Maser P, Brun R.** 2007. Genotypic and phenotypic characterization of Trypanosoma brucei gambiense isolates from Ibba, South Sudan, an area of high melarsoprol treatment failure rate. Acta Trop. **104:**84–90.
31. **Raz B, Iten M, Grether-Buhler Y, Kaminsky R, Brun R.** 1997. The Alamar Blue assay to determine drug sensitivity of African trypanosomes (T.b. rhodesiense and T.b. gambiense) in vitro. Acta Trop. **68:**139–147.
32. **Baltz T, Baltz D, Giroud C, Crockett J.** 1985. Cultivation in a semi-defined medium of animal infective forms of Trypanosoma brucei, T. equiperdum, T. evansi, T. rhodesiense and T. gambiense. EMBO J. **4:**1273–1277.
33. **Hirumi H, Hirumi K.** 1989. Continuous cultivation of Trypanosoma brucei blood stream forms in a medium containing a low concentration of serum protein without feeder cell layers. J. Parasitol. **75:**985–989.
34. **Braissant O, Wirz D, Gopfert B, Daniels AU.** 2010. Use of isothermal microcalorimetry to monitor microbial activities. FEMS Microbiol. Lett. **303:**1–8.
35. **Zwietering MH, Jongenburger I, Rombouts FM, van't Riet K.** 1990. Modeling of the bacterial growth curve. Appl. Environ. Microbiol. **56:**1875–1881.
36. **Kahm M, Hasenbrink G, Lichtenberg-Frate H, Ludwig J, Kschischo M.** 2010. Grofit: fitting biological growth curves with R. J. Statistical Software **33:**1–21.
37. **Astasov-Frauenhoffer M, Braissant O, Hauser-Gerspach I, Daniels AU, Wirz D, Weiger R, Waltimo T.** 2011. Quantification of vital adherent Streptococcus sanguinis cells on protein-coated titanium after disinfectant treatment. J. Mater. Sci. Mater. Med. **22:**2045–2051.
38. **Braissant O, Bonkat G, Wirz D, Bachmann A.** 2013. Microbial growth and isothermal microcalorimetry: growth models and their application to microcalorimetric data. Thermochimica Acta **555:**64–71.
39. **Bernhard SC, Nerima B, Maser P, Brun R.** 2007. Melarsoprol- and pentamidine-resistant Trypanosoma brucei rhodesiense populations and their cross-resistance. Int. J. Parasitol. **37:**1443–1448.
40. **Williamson J, Rollo IM.** 1959. Drug resistance in trepanosomes: cross-resistance analyses. Br. J. Pharmacol. Chemother. **14:**423–430.
41. **Baker N, Glover L, Munday JC, Aguinaga Andres D, Barrett MP, de Koning HP, Horn D.** 2012. Aquaglyceroporin 2 controls susceptibility to melarsoprol and pentamidine in African trypanosomes. Proc. Natl. Acad. Sci. U. S. A. **109:**10996–11001.
42. **De Koning HP.** 2001. Uptake of pentamidine in Trypanosoma brucei brucei is mediated by three distinct transporters: implications for cross-resistance with arsenicals. Mol. Pharmacol. **59:**586–592.
43. **Maser P, Sutterlin C, Kralli A, Kaminsky R.** 1999. A nucleoside transporter from Trypanosoma brucei involved in drug resistance. Science **285:**242–244.
44. **Matovu E, Stewart ML, Geiser F, Brun R, Maser P, Wallace LJ, Burchmore RJ, Enyaru JC, Barrett MP, Kaminsky R, Seebeck T, de Koning HP.** 2003. Mechanisms of arsenical and diamidine uptake and resistance in Trypanosoma brucei. Eukaryot. Cell **2:**1003–1008.
45. **Ward CP, Wong PE, Burchmore RJ, de Koning HP, Barrett MP.** 2011. Trypanocidal furamidine analogues: influence of pyridine nitrogens on trypanocidal activity, transport kinetics, and resistance patterns. Antimicrob. Agents Chemother. **55:**2352–2361.
46. **Teka IA, Kazibwe AJ, El-Sabbagh N, Al-Salabi MI, Ward CP, Eze AA, Munday JC, Maser P, Matovu E, Barrett MP, de Koning HP.** 2011. The diamidine diminazene aceturate is a substrate for the high-affinity pentamidine transporter: implications for the development of high resistance levels in trypanosomes. Mol. Pharmacol. **80:**110–116.
47. **Maina NW, Oberle M, Otieno C, Kunz C, Maeser P, Ndung'u JM, Brun R.** 2007. Isolation and propagation of Trypanosoma brucei gambiense from sleeping sickness patients in south Sudan. Trans. R. Soc. Trop. Med. Hyg. **101:**540–546.
48. **Manneck T, Braissant O, Haggenmuller Y, Keiser J.** 2011. Isothermal microcalorimetry to study drugs against Schistosoma mansoni. J. Clin. Microbiol. **49:**1217–1225.
49. **Mathis AM, Bridges AS, Ismail MA, Kumar A, Francesconi I, Anbazhagan M, Hu Q, Tanious FA, Wenzler T, Saulter J, Wilson WD, Brun R, Boykin DW, Tidwell RR, Hall JE.** 2007. Diphenyl furans and aza analogs: effects of structural modification on in vitro activity, DNA binding, and accumulation and distribution in trypanosomes. Antimicrob. Agents Chemother. **51:**2801–2810.

Journal of Medicinal Chemistry

Article

pubs.acs.org/jmc

Synthesis and Antiprotozoal Activity of Dicationic *m*-Terphenyl and 1,3-Dipyridylbenzene Derivatives

Donald A. Patrick,[†] Mohamed A. Ismail,[‡,§] Reem K. Arafa,[‡,∥] Tanja Wenzler,[⊥,#] Xiaohua Zhu,[∞] Trupti Pandharkar,[∞] Susan Kilgore Jones,[†] Karl A. Werbovetz,[∞] Reto Brun,[⊥,#] David W. Boykin,[‡] and Richard R. Tidwell*[,†]

[†]Department of Pathology and Laboratory Medicine, School of Medicine, University of North Carolina, Chapel Hill, North Carolina 27599-7525, United States

[‡]Department of Chemistry and Center for Biotechnology and Drug Design, Georgia State University, Atlanta, Georgia 30303-3083, United States

[§]Department of Chemistry, College of Science, King Faisal University, Hofuf 31982, Saudi Arabia

[∥]Department of Medicinal and Pharmaceutical Chemistry, Faculty of Pharmacy, Cairo University, Cairo, Egypt

[⊥]Department of Medical Parasitology and Infection Biology, Swiss Tropical and Public Health Institute, Basel, Switzerland

[#]University of Basel, Basel, Switzerland

[∞]Division of Medicinal Chemistry and Pharmacognosy, College of Pharmacy, The Ohio State University, Columbus, Ohio 43210, United States

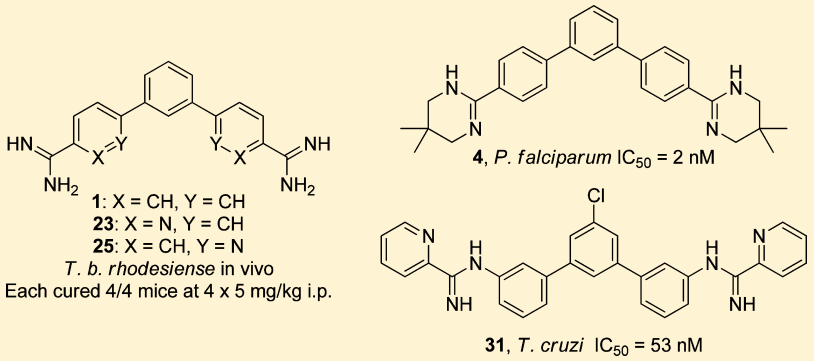

ABSTRACT: 4,4″-Diamidino-*m*-terphenyl (**1**) and 36 analogues were prepared and assayed in vitro against T*rypanosoma brucei rhodesiense*, *Trypanosoma cruzi*, *Plasmodium falciparum*, and *Leishmania amazonensis*. Twenty-three compounds were highly active against *T. b. rhodesiense* or *P. falciparum*. Most noteworthy were amidines **1**, **10**, and **11** with IC_{50} of 4 nM against *T. b. rhodesiense*, and dimethyltetrahydropyrimidinyl analogues **4** and **9** with IC_{50} values of ≤ 3 nM against *P. falciparum*. Bis-pyridylimidamide derivative **31** was 25 times more potent than benznidazole against *T. cruzi* and slightly more potent than amphotericin B against *L. amazonensis*. Terphenyldiamidine **1** and dipyridylbenzene analogues **23** and **25** each cured 4/4 mice infected with *T. b. rhodesiense* STIB900 with four daily 5 mg/kg intraperitoneal doses, as well as with single doses of ≤10 mg/kg. Derivatives **5** and **28** (prodrugs of **1** and **25**) each cured 3/4 mice with four daily 25 mg/kg oral doses.

INTRODUCTION

The vector borne protozoal diseases trypanosomiasis, malaria, and leishmaniasis continue to affect some of the poorest areas of the world.[1−5] Human African trypanosomiasis (HAT), which occurs in over 20 sub-Saharan African countries, was largely controlled by the 1960s but has since re-emerged. After continued control efforts, fewer than 10 000 new cases were reported in 2009 for the first time in 50 years, and the World Health Organization (WHO) estimates that 30 000 actual cases currently exist (vs 300 000 cases in 1988).[1,6] The disease progresses from an early hemolymphatic stage to a late central nervous system (CNS) stage and has a 100% mortality rate if not treated.[7] Two forms of HAT exist. A chronic infection due to *Trypanosoma brucei gambiense*, prevalent in western and central Africa, accounts for about 95% of reported cases. The remaining cases arise from an acute infection of *T. brucei rhodesiense*, prevalent in eastern and southern Africa.[8]

American trypanosomiasis, or Chagas disease, is caused by *Trypanosoma cruzi*. An estimated 10 million people were infected in 2010, and an estimated 10 000 died in 2008 because of the disease. Originally endemic to Latin America, the disease has now spread to other continents. It progresses from an acute phase lasting about 2 months after infection, in which the

Received: April 8, 2013
Published: June 24, 2013

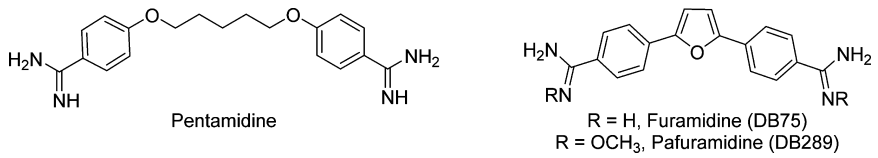

Figure 1. Structures of 1,5-bis(4-amidinophenoxy)pentane (pentamidine), 2,5-bis(4-amidinophenyl)furan (furamidine), and 2,5-bis(4-*N*′-methoxyamidinophenyl)furan (pafuramidine).

parasites are concentrated in the blood, to a chronic phase, in which the parasites are hidden in the heart and digestive muscle. Myocardial damage can lead to death.[4]

Malaria is concentrated in sub-Saharan Africa but is also endemic to other continents, affecting approximately 100 countries. The WHO has estimated 216 million cases of malaria in 2010 and 655 000 deaths.[2] Most of the deaths occur in Africa, primarily among young children. Four *Plasmodium* species are recognized as human pathogens. Among these, *P. falciparum* causes the most deadly infection.[2,7]

Infections due to various species of *Leishmania* affect nearly 12 million people in 88 countries. The diseases range in severity from a spontaneously healing cutaneous form due to *L. mexicana* to a life-threatening visceral form, 90% of which occurs in Bangladesh, India, Nepal, and Sudan (due to *L. donovani*) or in Brazil (due to *L. chagasi*).[5,8] Cases of patients infected with both visceral leishmaniasis (VL) and human immunodeficiency virus (HIV) continue to be reported.[9−16]

The need for safe, orally active, and economical drugs against HAT persists. Available therapies are scarce, antiquated, toxic, prone to resistance, and require parenteral (usually intravenous) administration.[1,6,7,17−19] Suramin, a polysulfonated naphthylurea, and pentamidine (Figure 1), an aromatic diamidine, are the two drugs used to treat early stage HAT. Late-stage therapies are generally more problematic. The organoarsenical melarsoprol is associated with an encephalopathy leading to death in about 5% of the cases.[7,20] Eflornithine is the only new anti-HAT drug introduced in the past 60 years. Although better tolerated than melarsoprol, eflornithine is ineffective against *T. b. rhodesiense*, and high doses must be given intravenously four times daily over long periods.[6] A combination of eflornithine and nifurtimox (nifurtimox−eflornithine combination therapy, NECT) was licensed in 2009.[1] It is easier to administer and has a shorter treatment duration than the eflornithine monotherapy and is currently the best choice to treat late stage patients with *T. b. gambiense* infections.

Drugs of choice against Chagas disease are benznidazole and nifurtimox, both of which are given orally. Both drugs are highly effective in curing the disease if treatments begins at the onset of the acute stage, but the efficacy of each diminishes with delayed initiation of treatment.[4,7] Severe side effects have also been reported for both drugs.[21] No drugs are currently approved for the chronic phase of the disease, but at least two drug candidates are currently in clinical trials.[4,7]

Although a number of economical orally active antimalarial drugs are available, drug resistance is a growing problem.[22] Resistance to chloroquine, observed in Thailand in the 1960s, has been followed by resistance in other locations and to other drugs, including sulfadoxine−pyrimethamine and mefloquine. Resistance to artemisinin led to the development of artemisinin-based combination therapy, but resistance to at least one combination, artesunate−mefloquine, has also been reported.[7]

Pentavalent antimonial compounds, including sodium stibogluconate and meglumine antimoniate, introduced in the 1940s, continue to be the drugs of choice against VL in most endemic countries despite their toxicity. High rates of treatment failures have been reported in Bihar, India, since the 1980s.[23] Antimony resistant VL was treated with pentamidine in the past, but the efficacy of pentamidine against VL has decreased,[24] and the use of pentamidine against leishmaniasis is now restricted to some forms of cutaneous disease that occur in South America.[25] Amphotericin B is an effective option in the treatment of VL,[26] but the less toxic liposomal formulations of the drug are limited by their expense. The aminoglycoside paromomycin has shown high efficacy in India and low toxicity, but a 3-week course of daily injections is required.[27] Miltefosine is orally active but is teratogenic, nephrotoxic, and hepatotoxic.[28] Various miltefosine combination therapies have been under recent investigations.[8,23,28]

Furamidine[29] (DB75, Figure 1) is a conformationally restricted analogue of pentamidine. These positively charged molecules have poor oral bioavailability; however, their *N*′-hydroxy and *N*′-methoxy derivatives with lower pK_a values have shown potential as orally active prodrugs.[30] Pafuramidine (DB289, Figure 1),[31] the methamidoxime prodrug of furamidine, advanced to phase III clinical trials against early stage HAT and phase II trials against malaria.[32,33] The compound exhibited nephro- and hepatotoxicity in a recent expanded phase I trial,[34] resulting in a suspension of phase III trials.[35]

Numerous analogues of pentamidine and furamidine, including those with modifications of both the central and outer rings, have been prepared and assayed against various organisms,[36−56] with the intent of finding comparably efficacious but less toxic drug candidates. A number of arylimidamides (AIAs), or "reversed" amidines, have been prepared and tested primarily against *T. cruzi* or *Leishmania* species.[57−60] A few diamidine derivatives of *o*-, *m*-, and *p*-terphenyl were originally prepared as serine protease inhibitors.[61] More recently, a larger number of dicationic *p*-terphenyls and their aza-analogues have been prepared as antiprotozoals.[62−64] Dicationic *m*-terphenyl derivatives have remained virtually unexplored, with respect to both the number of molecules synthesized and their potential antiprotozoal activities. While the *p*-terphenyls are linear in shape, the *m*-terphenyls are more conformationally similar to furamidine. The present work describes the synthesis of a rather diverse group of dicationic *m*-terphenyl derivatives and their biological evaluation against four parasites.

CHEMISTRY

A total of 37 cationically substituted *m*-terphenyl analogues were prepared (Table 1). This group consists of 29 diamidine derivatives (**1**−**29**), six bis-arylimidamides (bis-AIAs, **30**−**35**), and two mono-AIAs (**36** and **37**). The amidine group includes 16 simple amidines (**1**, **7**−**8**, **10**−**13**, **19**−**26**, and **29**), seven *N*-

Table 1. Structures of Cationic *m*-Terphenyl and 1,3-Dipyridylbenzene Derivatives 1−37[a]

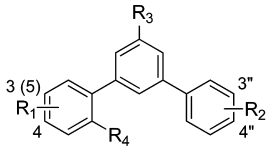

1-22, 30-37

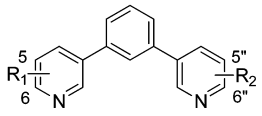

23-24

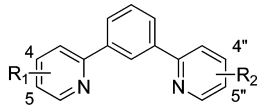

25-29

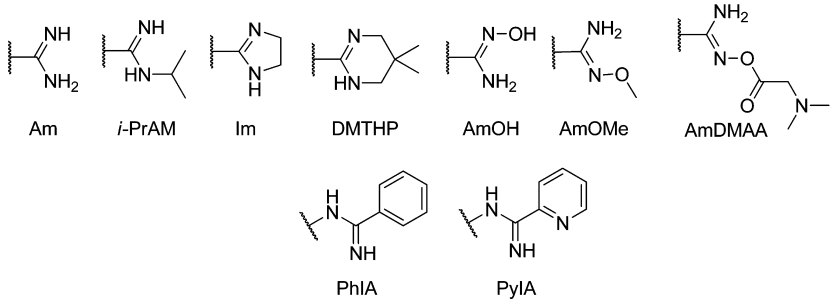

compd	R_1	R_2	R_3	R_4
1	4-Am	4″-Am	H	H
2	4-*i*-PrAm	4″-*i*-PrAm	H	H
3	4-Im	4″-Im	H	H
4	4-DMTHP	4″-DMTHP	H	H
5	4-AmOH	4″-AmOH	H	H
6	4-AmOMe	4″-AmOMe	H	H
7	4-Am	4″-Am	Cl	H
8	4-Am	4″-Am	NO_2	H
9	4-DMTHP	4″-DMTHP	NO_2	H
10	4-Am	4″-Am	NH_2	H
11	4-Am	4″-Am	OH	H
12	4-Am	4″-Am	OMe	H
13	3-Am	3″-Am	H	H
14	3-*i*-PrAm	3″-*i*-PrAm	H	H
15	3-Im	3″-Im	H	H
16	3-DMTHP	3″-DMTHP	H	H
17	3-AmOH	3″-AmOH	H	H
18	3-AmOMe	3″-AmOMe	H	H
19	3-Am	3″-Am	Cl	H
20	3-Am	3″-Am	OMe	H
21	3-Am	4″-Am	H	H
22	3-Am	4″-Am	Cl	H
23	6-Am	6″-Am		
24	5-Am	5″-Am		
25	5-Am	5″-Am		
26	5-Am	5″-Am		
27	5-AmOMe	5″-AmOMe		
28	5-AmDMAA	5″-AmDMAA		
29	4-Am	4″-Am		
30	3-PhIA	3″-PhIA	Cl	H
31	3-PyIA	3″-PyIA	Cl	H
32	3-PhIA	4″-PhIA	H	H
33	3-PyIA	4″-PyIA	H	H
34	3-PhIA	4″-PhIA	Cl	H
35	3-PyIA	4″-PyIA	Cl	H
36	4-PyIA	H	Cl	O-*i*-Pr
37	5-PyIA	H	Cl	O-*i*-Pr

[a]All compounds were isolated as hydrochloride salts except **26** (acetate salt) and **28** (free base).

alkyl and *N*,*N*′-alkylene derivatives (**2**−**4**, **9**, and **14**−**16**), and six prodrugs (**5**, **6**, **17**, **18**, **27**, and **28**). Structural variations include the orientation of the cationic groups, substituents on the amidine nitrogen atoms and/or on the central aromatic ring, and the insertion of nitrogen atoms in the outer aromatic rings. Compounds **1**−**22** and **30**−**37** have *m*-terphenyl nuclei,

Scheme 1. Synthesis of Symmetric *m*-Terphenylamidine Derivatives and Prodrugs[a]

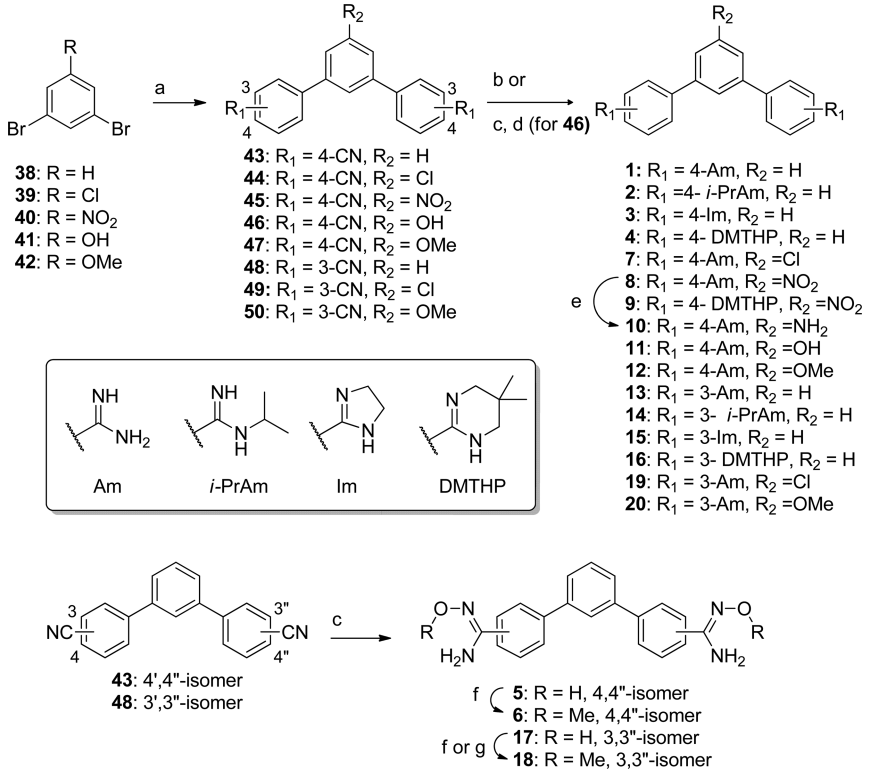

[a]Reagents and conditions: (a) 3- or 4-cyanophenylboronic acid, $Pd(PPh_3)_4$, aq Na_2CO_3, DME, reflux (52−81%); (b) EtOH, HCl, 1,4-dioxane, and then NH_3 or amine, EtOH; (c) $NH_2OH{\cdot}HCl$, *t*-BuOK, DMF; (d) Ac_2O, AcOH, and then H_2, 10% Pd/C, EtOH, AcOH; (e) H_2, 10% Pd/C, EtOH; (f) CH_3I, *t*-BuOK, DMSO; (g) $(CH_3)_2SO_4$, aq NaOH, dioxane.

Scheme 2. Synthesis of Asymmetric *m*-Terphenyldiamidines[a]

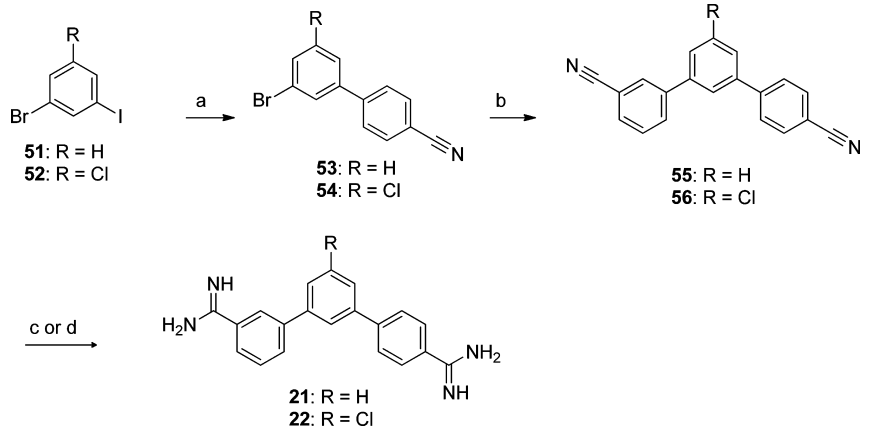

[a]Reagents and conditions: (a) 4-cyanophenylboronic acid, $Pd(PPh_3)_4$, aq Na_2CO_3, DME; (b) (3-cyanophenyl)boronic acid, $Pd(PPh_3)_4$, aq Na_2CO_3, DME; (c) EtOH, HCl, 1,4-dioxane and then NH_3, EtOH; (d) $LiN(TMS)_2$, THF.

while analogues **23**−**24** and **25**−**29** have 1,3-bis(pyridin-3-yl)benzene and 1,3-bis(pyridin-2-yl)benzene scaffolds, respectively. All 37 compounds are novel except **13**, which was previously reported but as a different salt.[61] The activities of analogues **7**, **19**, **23**, and **24** against *T. cruzi* have been reported,[65,66] although details of their syntheses have yet to be reported. All target compounds were isolated as their hydrochloride salts except acetate salt **26** (an alternative salt form of **25**) and free base **28**.

The syntheses of the symmetric *m*-terphenylamidines and prodrugs **1**−**20** are depicted in Scheme 1. Dibromobenzene starting materials **38**, **39**, and **41** were commercially available. Nitro analogue **40**[67] was prepared by deamination of 2,6-dibromo-4-nitroaniline. Methoxy derivative **42** was prepared by bromination[68]−deamination[67] of *p*-anisidine. Double Suzuki couplings involving dibromobenzenes **38**−**42** and 2−2.5 equiv of 3- or (4-cyanophenyl)boronic acid catalyzed by tetrakis(triphenylphosphine)palladium(0) readily gave terphenyldinitriles **43**−**50** in yields of 52−81%. The nitriles (except **46**) were then subjected to modified Pinner reaction conditions (ethanol, HCl gas, dioxane cosolvent)[50,51] to generate the corresponding imidate esters, which were then reacted immediately with

Scheme 3. Synthesis of 1,3-Dipyridylbenzeneamidines and Prodrugs[a]

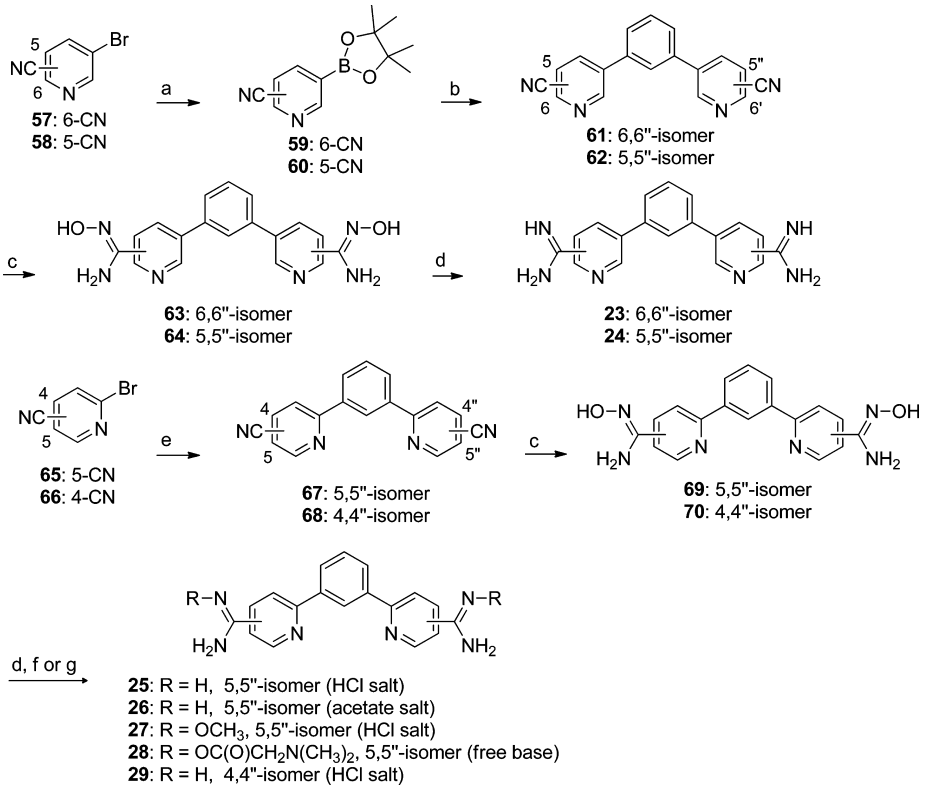

[a]Reagents and conditions: (a) bis(pinacolato)diboron, $PdCl_2$(dppf), KOAc, DMSO; (b) 1,3-diiodobenzene, $Pd(PPh_3)_4$, Ag_2CO_3, THF; (c) NH_2OH·HCl, *t*-BuOK, DMSO; (d) Ac_2O, AcOH, and then H_2, 10% Pd/C; (e) 1,3-benzenediboronic acid, $Pd(PPh_3)_4$, Ag_2CO_3, THF; (f) Me_2SO_4, LiOH·H_2O, DMF; (g) dimethylaminoacetyl chloride·HCl, K_2CO_3, DMF.

ammonia (for simple amidines **1**, **7**, **8**, **12**, **13**, **19**, and **20**), isopropylamine (for *N*-isopropylamidines **2** and **14**), ethylenediamine (for imidazolines **3** and **15**), or 2,2-dimethylpropane-1,3-diamine (for 5,5-dimethyl-1,4,5,6-tetrahydropyrimidin-2-yl (DMTHP) derivatives **4**, **9**, and **16**). Catalytic hydrogenation of nitro-substituted diamidine **8** gave the amino analogue **10**. Conversion of nitrile **46** to its amidoxime derivative using excess hydroxylamine in DMSO,[69] followed by O-acylation and catalytic hydrogenation,[50] gave 5′-hydroxydiamidine **11**. Amidoxime prodrugs **5** and **17** were prepared by similar treatment of nitriles **43** and **48** with hydroxylamine.[69] The amidoxime bases were converted to their hydrochloride salts for biological testing or underwent O-methylation to methamidoxime derivatives **6** and **18**, which were also converted to their hydrochloride salts.

Syntheses of asymmetric *m*-terphenyldiamidines **21** and **22** (Scheme 2) were similar to those of their symmetric counterparts, but their dinitrile precursors were prepared by successive single Suzuki couplings. High selectivity for single over double coupling has resulted from the use of bromoiodobenzene rather than dibromobenzene starting materials.[70] The coupling between bromoiodobenzene **51** and (4-cyanophenyl)boronic acid gave biphenyl **53** in 71% isolated yield. An analogous Suzuki coupling involving bromoiodide **52** (prepared by iodination−deamination of 4-bromo-2-chloroaniline)[71,72] gave biphenyl **54** in 59% yield. Successive couplings of bromobiphenyls **53** and **54** with (3-cyanophenyl)boronic acid gave the desired asymmetric terphenyldinitriles **55** and **56** (83% and 74% yields). A Pinner synthesis employing dinitrile **55** gave asymmetric diamidine **21**. Similar strategy using chloro analogue **56** failed, presumably because of the extremely low solubility of the nitrile in the reaction medium. Diamidine **22** was successfully prepared from dinitrile **56** using lithium bis(trimethylsilyl)amide in THF.[64]

The preparation of dipyridylbenzene derivatives **23**−**29** is shown in Scheme 3. 3-Bromopyridyl starting materials **57** (also commercially available) and **58** were prepared by treatment of 5-bromo-*N*-(*tert*-butyl)picolinamide[73] or 5- bromonicotinamide with phosphorus oxychloride.[73] The reactions of compounds **57** and **58** with bis(pinacolato)diboron and catalytic $PdCl_2$(dppf)[74] gave boronate esters **59** and **60**, which underwent Suzuki coupling with 1,3-diiodobenzene under anhydrous conditions ($Pd(PPh_3)_4$, Ag_2CO_3, THF)[75] to give 1,3-di(pyridin-3-yl)benzenedinitriles **61** and **62** (60% and 69% yields). Attempted Pinner syntheses of amidines **23** and **24** from dipyridylbenzenenitriles **61** and **62** were unsuccessful. The nitriles were treated with excess hydroxylamine in DMSO to give amidoxime intermediates **63** and **64**. The amidoximes were treated with acetic anhydride in acetic acid to generate the *N*′-acetoxy derivatives in situ, which were hydrogenated at 60 psi over 10% Pd/C in acetic acid.[69] The use of neat acetic acid in place of acetic acid−ethanol[69] proved to be necessary for selective cleavage of the oxygen−nitrogen bond (amidine deprotection) over the oxygen−carbon bond (reversion to the amidoxime).

Similar strategy was employed for the syntheses of the di(pyridin-2-yl)benzene analogues except for the reversal of functional groups for the Suzuki couplings. 2-Bromopyridylnitriles **65** and **66** were prepared by dechlorobromination of 6-chloronicotinonitrile[76] or 2-chloro-4-cyanopyridine using phos-

Scheme 4. Synthesis of *m*-Terphenyl-bis-arylimidamides (Bis-AIAs)[a]

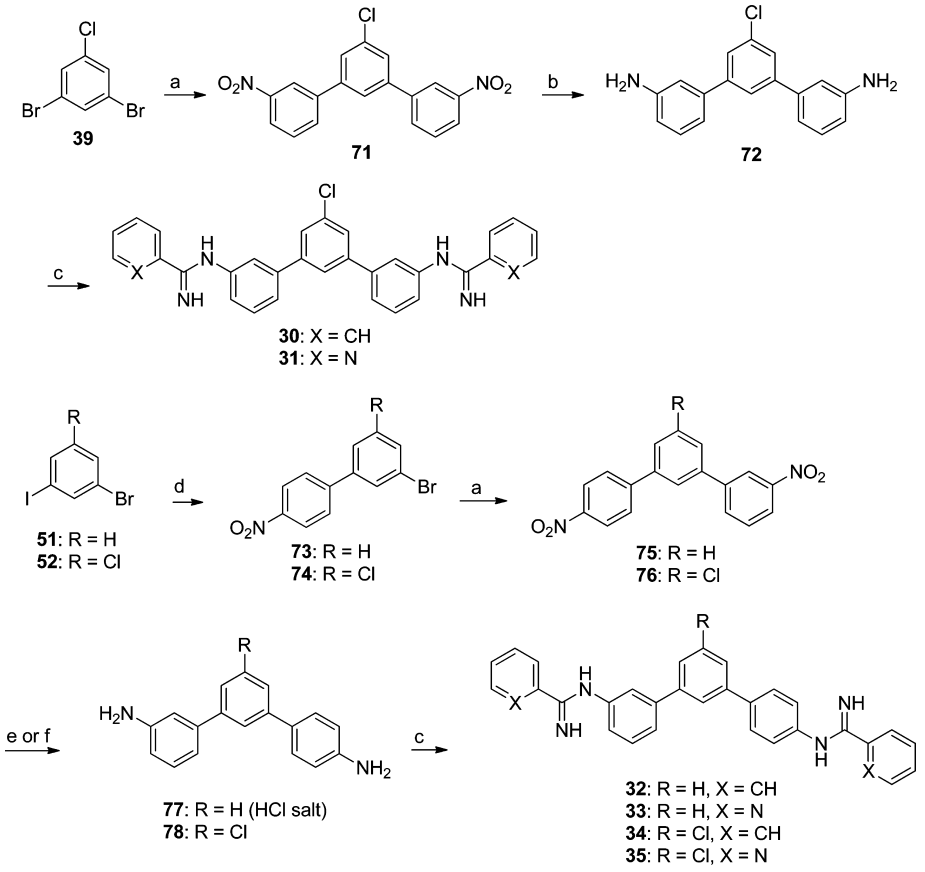

[a]Reagents and conditions: (a) 3-nitrophenylboronic acid, $Pd(PPh_3)_4$, aq Na_2CO_3, DME, reflux; (b) $SnCl_2{\cdot}2H_2O$, EtOH; (c) Et_3N (for **77** only), benzonitrile or 2-cyanopyridine, $NaN(TMS)_2$, THF; (d) 4-nitrophenylboronic acid pinacol ester, $Pd(PPh_3)_4$, aq Na_2CO_3, DME; (e) H_2, 60 psi, 10% Pd/C, EtOH; (f) Fe, NH_4Cl, aq EtOH.

Scheme 5. Synthesis of *m*-Terphenyl Monoarylimidamides (Mono-AIAs)[a]

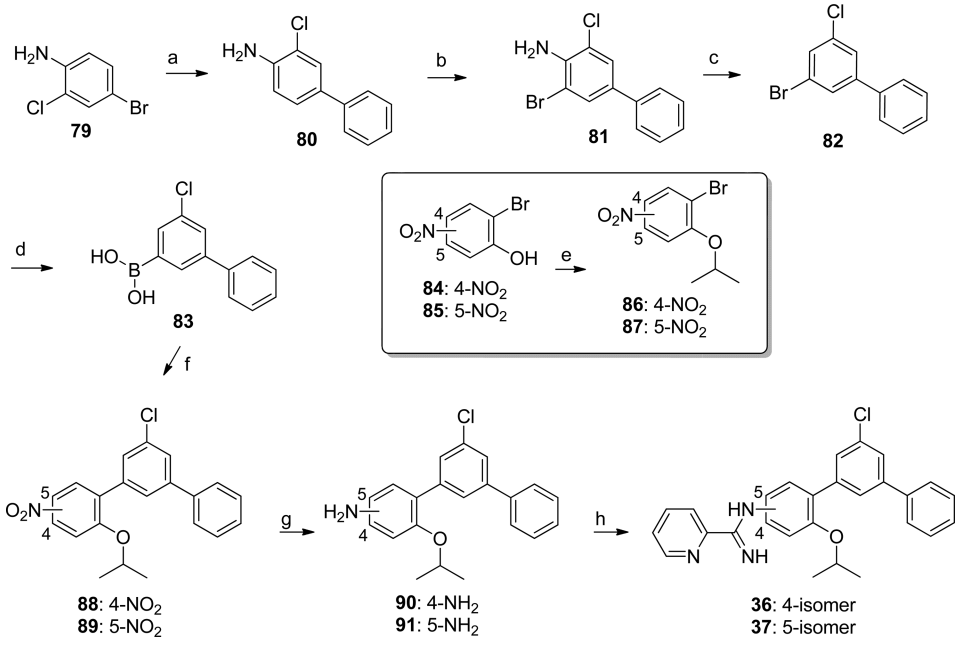

[a]Reagents and conditions: (a) phenylboronic acid, $Pd(PPh_3)_4$, aq Na_2CO_3, DME; (b) NBS, THF; (c) $NaNO_2$, H_2SO_4, EtOH; (d) BuLi, THF and then triisopropyl borate; (e) $(CH_3)_2CHI$, Cs_2CO_3, K_2CO_3, DMF; (f) **86** or **87**, $Pd(PPh_3)_4$, aq Na_2CO_3, DME; (g) $SnCl_2{\cdot}2H_2O$, EtOH; (h) benzonitrile or 2-cyanopyridine, $NaN(TMS)_2$, THF.

Table 2. Antiprotozoal Activities, Cytotoxicities, and Selectivity Indices of Compounds 1−37 in Vitro

	T. b. rhodesiense[a]		*T. cruzi*[b]		*P. falciparum*[c]		*L. amazonensis*[d]		
compd	IC_{50} (μM)[f]	SI_{Tb}[g]	IC_{50} (μM)[f]	SI_{Tc}[h]	IC_{50} (μM)[f]	SI_{P}[i]	IC_{50} (μM)[j]	SI_{L}[k]	cytotox[e] IC_{50} (μM)[f]
1	0.004	8494	71.6	<1	0.024	1279			31.2
2	0.047	2157	>150	<1	0.016	6583			102
3	0.068	37	18.9	<1	0.073	35			2.55
4	0.140	871	151	<1	0.002	49347			122
5	10.9	>14	>150	ND[l]	>10	ND[l]			>150
6	4.44	4	92.6	<1	>10	<2			19.2
7	0.031	700	65.5	<1	0.039	561			21.9
8	0.020	>7481	57.2	>2	0.018	>8376			>150
9	0.692	>217	>150	ND[l]	0.003	>46781			>150
10	0.004	>39791	149	>1	0.136	>1103			>150
11	0.004	>37500	>150	<1	0.038	>3947			>150
12	0.005	7266	59.1	<1	0.048	693			33.0
13	0.055	2268	35.0	4	0.038	3319			125
14	0.617	>243	141	>1	0.031	>4194			>150
15	1.60	20	20.4	2	0.619	51			31.7
16	0.809	70	45.4	1	0.006	9498			56.6
17	2.55	2	11.2	<1	8.23	<1			5.60
18	11.3	2	24.1	<1	9.31	2			20.3
19	0.044	709	50.2	<1	0.033	944			30.9
20	0.029	4695	55.9	2	0.028	4964			137
21	0.052	544	27.1	1	0.015	1947			28.5
22	0.097	130	46.6	<1	0.010	1248			12.7
23	0.006	3720	43.4	<1	0.015	1485			22.3
24	0.527	>285	>150	ND[l]	0.058	>2577			>150
25	0.017	>8824	>150	ND[l]	0.040	>3763			>150
26	0.022	>6856	>150	ND[l]	0.045	>3339			>150
27	26.3	>6	117	>1	3.56	>42			>150
28	9.84	6	72.3	<1	0.486	129			62.9
29	1.17	>128	>150	ND[l]	0.077	>1939			>150
30	0.533	8	2.09	2	0.071	58	2.43	2	4.10
31	0.019	133	0.053	47	0.006	450	0.095	26	2.50
32	0.635	4	2.14	1	0.038	66	0.907	3	2.52
33	1.94	1	0.388	7	0.208	13	0.123	22	2.72
34	0.178	13	2.04	1	0.039	58	1.02	2	2.27
35	0.109	24	1.54	2	0.219	12	0.211	13	2.64
36	32.4	<1	4.18	2	>10	<1	0.933	10	9.69
37	12.3	<1	2.98	1	3.075	1	1.88	2	3.77
PMD[m]	0.003	11436			0.046	1004			46.6
FMD[n]	0.003	2000	23.3	<1	0.014	464			6.40
MSP[o]	0.004	1275							5.12
BNZ[p]			1.30	115					>150
CQ[q]					0.125	612			76.5
ATM[r]					0.004	34884			150
AMB[s]							0.124		
PPT[t]									0.017

[a] *Trypanosoma brucei rhodesiense* (STIB900).[83] [b] *Trypanosoma cruzi* Tulahuen C2C4 Lac Z.[83] [c] *Plasmodium falciparum* (K1, chloroquine resistant).[83] [d] *Leishmania amazonensis* infected CD-1 mouse intracellular amastigotes.[82] [e] Cytotoxicity to L6 rat myoblast cells.[83] [f] The IC_{50} values are the mean of two independent assays. Individual values differed by less than 50% of the mean value. [g] Selectivity index for *T. b. rhodesiense* expressed as the ratio IC_{50}(L6 cells)/IC_{50}(*T. b. rhodesiense*). [h] Selectivity index for *T. cruzi* expressed as the ratio IC_{50}(L6 cells)/IC_{50}(*T. b. cruzi*). [i] Selectivity index for *P. falciparum* expressed as the ratio IC_{50}(L6 cells)/IC_{50}(*P. falciparum*). [j] The IC_{50} values are the mean of three independent assays. The standard deviations varied from the mean values by 8−64%. [k] Selectivity index for *L. amazonensis* expressed as the ratio IC_{50}(L6 cells)/IC_{50}(*L. amazonensis*). [l] Value not determinable. [m] Pentamidine. [n] Furamidine. [o] Melarsoprol. [p] Benznidazole. [q] Chloroquine. [r] Artemisinin. [s] Amphotericin-B. [t] Podophyllotoxin.

phorus tribromide.[77] Various attempts at preparing boronic acids or esters from **65**, **66**, or their 2-chloro precursors were unsuccessful. Suzuki couplings of 2-bromopyridines **65** and **66** with 1,3-phenyldiboronic acid under anhydrous conditions ($Pd(PPh_3)_4$, Ag_2CO_3, THF)[75] gave 1,3-di(pyridin-2-yl)-benzenedinitriles **67** and **68** (63% and 87% yields). Compound **67** was also prepared in 91% yield by the coupling of 6-chloronicotinonitrile[76] and the diboronic acid in toluene/2 M aqueous Na_2CO_3.[47] Nitriles **67** and **68** were reacted with excess hydroxylamine in DMSO to give amidoxime intermediates **69**

and **70**, which underwent O-acetylation followed by catalytic hydrogenation to give amidine hydrochlorides **25** and **29**. The former compound was also isolated as acetate salt **26**. Amidine **25** was also prepared directly from nitrile **67** using lithium bis(trimethylsilyl)amide in THF.[64] The prodrugs, methamidoxime **27** (hydrochloride salt) and dimethylaminoacetoxyamidine **28** (free base), were prepared by O-methylation or O-acylation of amidoxime **69**. Compound **27** was also prepared as the hydrochloride salt (59% yield) directly from nitrile **67** using methoxylamine hydrochloride in the presence of triethylamine and thioglycolic acid.[78]

The syntheses of bis-AIAs **30**−**35** are depicted in Scheme 4. A double Suzuki coupling between dibromobenzene **39** and 3-nitrophenylboronic acid gave the symmetric dinitroterphenyl **71** in 76% isolated yield. Reduction of **71** with tin(II) chloride dihydrate in ethanol gave the diamine **72**, which was reacted with benzonitrile or 2-cyanopyridine in the presence of sodium bis(trimethylsilyl)amide in THF[79] to give symmetric bis-phenylimidamide **30** and the corresponding di(pyridin-2-yl) derivative **31**. Similar strategy was employed for the asymmetric analogues **32**−**35** except for the requirement of successive single Suzuki couplings. Bromoiodobenzenes **51** and **52**[71,72] were coupled with 4-nitrophenylboronic acid pinacol ester to give bromobiphenyls **73** and **74**, which in turn were coupled with 3-nitrophenylboronic acid to give terphenyls **75** and **76** (52% and 55% yields overall). Hydrogenation of dinitroterphenyl **75** over 10% Pd in ethanol gave diamine **77** (72% yield as the HCl salt). The chloro-substituted dinitro analogue **76** was reduced to diamine **78** (69% yield) using iron powder and ammonium chloride in aqueous ethanol. Diamines **77** and **78** were reacted with benzonitrile or 2-cyanopyridine in the presence of sodium bis(trimethylsilyl)amide in THF[79] to give bis-AIAs **32**−**35** (34−64% yields).

The syntheses of mono-AIAs **36** and **37** (Scheme 5) began with the Suzuki coupling of bromoaniline **79** and phenylboronic acid to give biphenylamine **80** (70%). This intermediate underwent bromination to **81** (*N*-bromosuccinimide in THF, 83%), followed by deamination to bromobiphenyl **82** (sodium nitrite and sulfuric acid in ethanol, 86%). The latter underwent lithiation followed by quenching with triisopropyl borate to give crude boronic acid **83**. This intermediate underwent Suzuki couplings with bromoisopropoxynitrobenzenes **86**[80] and **87**[81] (prepared by Williamson ether syntheses from the corresponding phenols **84** and **85**[81]) to give nitroterphenyls **88** (82%) and **89** (91%). The nitro compounds were reduced to the corresponding amines **90** (83%) and **91** (94%) using tin(II) chloride dihydrate in ethanol. The amines were reacted with 2-cyanopyridine in the presence of sodium bis(trimethylsilyl)amide in THF to give mono-AIAs **36** (41%) and **37** (50%) as their HCl salts.

IN VITRO ANTIPROTOZOAL ACTIVITIES, SELECTIVITIES, AND STRUCTURE−ACTIVITY RELATIONSHIPS

In vitro activities of target compounds against *T. b. rhodesiense* strain STIB900, the intracellular amastigote form of the *T. cruzi* Tulahuen strain C2C4, the chloroquine resistant *P. falciparum* strain K1, and *L. amazonensis* intracellular amastigotes were measured following established protocols,[82,83] and the results are shown in Table 2. Cytotoxicities against L6 rat myoblast cells[83] were determined to calculate the selectivity indices (the ratios of cytotoxic IC_{50} values to antiprotozoal IC_{50} values) of each compound for each of the four parasites. Standard drugs include pentamidine and furamidine (against *T. b. rhodesiense* and *P. falciparum*), melarsoprol (against *T. b. rhodesiense*), benznidazole (against *T. cruzi*), chloroquine and artemisinin (against *P. falciparum*), amphotericin B (against *L. amazonensis*), and podophyllotoxin (against L6 cells).

T. b. rhodesiense. A total of 17 compounds were highly active with IC_{50} values below 100 nM, and 11 of these analogues had selectivity indices above 2000 (more selective than furamidine and melarsoprol). Five congeners exhibited IC_{50} values below 10 nM (comparable in potency to the three standard drugs). The most potent were lead compound **1** and derivatives **10** and **11**, all exhibiting IC_{50} values of 4 nM and selectivity indices above 8000, followed by analogues **12** (IC_{50} = 5 nM, SI = 7270) and **23** (IC_{50} = 6 nM, SI = 3720). Eight congeners (**2**, **7**, **8**, **19**, **20**, **25**, **26**, and **31**) exhibited IC_{50} values between 10 and 50 nM, of which analogues **8**, **25**, and **26** had selectivity indices above 6000 and derivatives **2** and **20** had selectivity indices above 2000. Four derivatives (**3**, **13**, **21**, and **22**) showed IC_{50} values between 50 and 100 nM, of which congener **13** had a selectivity index greater than 2000. Another nine compounds (**4**, **9**, **14**, **16**, **24**, **30**, **32**, **34**, and **35**) exhibited IC_{50} values between 100 nM and 1.0 μM.

The group of 17 most highly active compounds with IC_{50} values below 100 nM included 14 simple diamidines, *N*-isopropylamidine **2**, imidazoline **3**, and AIA derivative **31**. The diamidines included all 11 of the terphenyldiamidines (**1**, **7**, **8**, **10**−**13**, and **19**−**22**) and three of the five dipyridyl diamidines **23**, **25**, and **26**.

Among the terphenylamidine derivatives **1**−**22**, optimal potency and selectivity were observed when both cationic groups were oriented para to the central ring. Lead compound **1** (IC_{50} = 4 nM, SI ≈ 8500), was over 10 times more potent and over 4 times more selective than its regioisomer **13** (IC_{50} = 55 nM), with both amidine functions situated meta to the central ring. The asymmetric 3,4″-diamidine **21** was similar in potency (IC_{50} = 52 nM) to **13** but about 4 times less selective.

The introduction of substituents on the amidine nitrogen atoms resulted in diminished activity. The *N*-isopropylamidines **2** and **14** were more than 10 times less potent than the corresponding simple amidines **1** and **13**. The corresponding imidazoline derivatives **3** and **15** showed a further 2-fold decrease in potency. The DMTHP derivatives **4**, **9**, and **16** showed varied degrees of decreased potencies relative to the corresponding amidines **1**, **8**, and **13**. The prodrugs **5**, **6**, **17**, and **18** were inactive in vitro, as expected.[30,33]

The introduction of substituents on the central ring had varied effects upon activity, depending upon the orientation of the cationic groups. The potency of lead compound **1** was retained in its amino and hydroxy derivatives **10** and **11**, and these two analogues also had the highest selectivity indices (above 37 500). The methoxy derivative **12** was similar in both potency and selectivity to parent molecule **1**, while methoxy analogue **20** was slightly more potent and selective than its parent molecule **13**. None of the chloro analogues **7**, **19**, and **22** showed advantages of both potency and selectivity compared to parent molecules **1**, **13**, and **21**, respectively. The nitro analogue **8** was quite potent (IC_{50} = 20 nM), albeit 5 times less potent than parent amidine **1**, and showed at least comparable selectivity.

The orientation of both amidine functions para to the central ring was also required for optimal potency among the regioisomeric dipyridylbenzenediamidines **23**−**25** and **29**. The points of attachment of the pyridine rings proved to be

less crucial. Analogues **23** (IC_{50} = 6 μM, SI ≈ 3700) and **25** (IC_{50} = 17 μM, SI > 8800), with both cationic groups positioned para to the central ring, were highly potent and highly selective for the parasite, and their potencies varied by less than 3-fold. Their regioisomers with both amidine moieties situated meta to the central ring were over 50 times less potent (**23** vs **24**, **25** vs **29**). The hydrochloride salt **25** and acetate salt **26** (different salts of the same diamidine base) gave similar results in the in vitro assays.

The AIA derivatives **30**−**37** were, as a whole, less potent and less selective compared to the amidine derivatives **1**−**29**. Even though the bis-pyridylimidamide **31** was the sixth most potent overall (IC_{50} = 19 nM), it was the least selective (SI = 133) of the 13 compounds with IC_{50} values below 50 nM. None of the other AIA derivatives had IC_{50} values below 100 nM.

T. cruzi. The bis-pyridylimidamides **31**, **33**, and **35** were most potent against the intracellular amastigote form of the *T. cruzi* Tulahuen strain. The order of decreasing potencies continued with the bis-phenylimidamide, monopyridylimidamide, and diamidine derivatives. The pyridylimidamide **31** (IC_{50} = 53, SI = 47) showed the most promising results, being about 25 times more potent than benznidazole (IC_{50} = 1.30 μM, SI = 115). The other pyridyl analogues **33** (IC_{50} = 388 nM) and **35** (IC_{50} = 1.54 μM) showed potencies greater than or comparable to benznidazole but selectivity indices below 10. Compound **31** merits further investigation, as selectivity indices above 10 are a common cutoff value for in vivo testing against *T. cruzi*. None of the other compounds exhibited IC_{50} values below 2 μM.

P. falciparum. Twenty-one compounds exhibited IC_{50} values below 50 nM (compared to IC_{50} = 46 nM for pentamidine) against the chloroquine resistant *P. falciparum* strain K1. The two most potent derivatives **4** and **9**, with IC_{50} values of 2 and 3 nM, respectively, and each having a selectivity index above 45 000, were more potent and selective for the parasite than artemisinin (IC_{50} = 4 nM, SI = 34 900). Analogues **16** and **31** each had IC_{50} values of 6 nM, while congener **22** had an IC_{50} value of 10 nM and a selectivity index of 1250. Only analogue **16** had a selectivity index below 1000. Four derivatives (**2**, **8**, **21**, and **23**) exhibited IC_{50} values between 10 and 20 nM. All had selectivity indices above 1000, with those of **2** and **8** being above 5000. Twelve compounds (**1**, **7**, **11**−**14**, **19**, **20**, **25**, **26**, **32**, and **34**) had IC_{50} values between 20 and 50 nM, of which seven analogues (**1**, **11**, **13**, **14**, **20**, **25**, and **26**) had selectivity indices above 1000. Four derivatives (**3**, **24**, **29**, and **30**) were less potent, with IC_{50} values between 50 and 100 nM. Overall, 15 compounds (**1**, **2**, **4**, **8**, **9**, **11**, **13**, **14**, **16**, **20**−**23**, **25**, and **26**) exhibited IC_{50} values below 50 nM and selectivity indices above 1000.

The group of 21 compounds with IC_{50} values below 50 nM includes 13 simple amidines (10 terphenyl and three dipyridylbenzene derivatives), five *N*-alkylamidines, and three AIA analogues. In contrast to the structural requirements for antitrypanosomal activity, antiplasmodial potency was less dependent on the positions of the cationic groups and was enhanced by alkylation of the amidine nitrogen atoms. The regioisomeric diamidines **1**, **13**, and **21** lacking central ring substituents showed rather small differences in potency (IC_{50} values of 24, 38, and 15 nM, respectively) but with activity favored by at least one cation in the para position. The chloro analogue **22** (a derivative of **21**) was the most potent of the terphenyl simple diamidines (IC_{50} = 10 nM).

The DMTHP derivatives **4**, **9**, and **16** (IC_{50} values of 2, 3, and 6 nM, respectively, and SI > 45 000 for **4** and **9**) were the most potent terphenyl *N*-alkyldiamidines, accounting for three of the four most potent and the three most highly selective analogues overall. They were also highly specific for this parasite, being 70−230 times more potent against *P. falciparum* compared to *T. b. rhodesiense*. The *N*-isopropylamidines **2** and **14** (IC_{50} of 16 and 31 nM, respectively, and SI > 4000 for each) also exhibited enhanced potencies and selectivities relative to corresponding amidines **1** and **13** and were the eighth and twelfth most potent overall. The imidazoline derivatives **3** and **15** (IC_{50} of 73 and 620 nM, respectively) were both less potent and less selective than the corresponding amidines **1** and **13**. Thus, diamidine **1** and its N-substituted derivatives **2**−**4** were all more potent than the corresponding 3,3″-isomers **13**−**16**.

The introduction of substituents on the central ring had varied effects upon activity, depending on the nature of the substituent and the position of the cationic groups. Both the potency and selectivity of the 4,4″-diamidine **1** were diminished by the presence of chloro, amino, and methoxy substituents on the central ring (derivatives **7**, **10**, and **12**). The nitro analogue **8** was slightly more potent than **1** with significantly enhanced selectivity. The potency of 3′3″-diamidine **13** was enhanced by a chloro or methoxy group on the central ring (analogues **19** and **20**), but selectivity was enhanced only in the latter instance. The potency of asymmetric diamidine **21** was enhanced, but its selectivity was diminished, by a chlorine atom on the central ring (derivative **22**).

The order of potencies of the four dipyridylbenzene diamidines was the same as that against *T. b. rhodesiense*. Analogues **23** (IC_{50} = 15 nM) and **25** (IC_{50} = 40 nM), each having both amidine groups positioned para to the central ring, were more potent than their respective counterparts **24** (IC_{50} = 58 nM) and **29** (IC_{50} = 77 nM) having two meta-amidine functions. Selectivity indices ranged from around 1500 for **23** to greater than 3500 for **25**. Acetate salt **26**, an alternative salt form of **25**, gave results similar to those of hydrochloride salt **25**. The difference in IC_{50} values between the most potent (**23**) and the least potent (**29**) analogues was just over 5-fold, compared to a nearly 200-fold differences in their IC_{50} values against *T. b. rhodesiense*.

The AIA derivatives, as a whole, were less potent and less selective compared to the amidine derivatives. The symmetric bis-pyridylimidamide **31** (IC_{50} = 6 nM, SI = 450) was the most potent AIA derivative and most selective for this parasite, followed by the asymmetric bis-phenylimidamides **32** and **34**, with IC_{50} values around 40 nM but selectivity indices below 100. These three compounds had the three lowest selectivity indices among the 21 compounds with IC_{50} values below 50 nM, despite the fact that analogue **31** was the third most potent overall. Congener **30** was the only other AIA derivative with an IC_{50} value below 100 nM.

L. amazonensis. Given that other AIAs have shown outstanding in vitro and promising in vivo antileishmanial activity in past work,[57,59,60,84] compounds **30**−**37** were assayed against *L. amazonensis* in the intracellular amastigote model.[82] The bis-pyridylamidamides **31**, **33**, and **35** were the three most potent compounds (in descending order). Analogue **31** (IC_{50} = 95 nM) was slightly more potent than amphotericin B (IC_{50} = 124 nM), while congener **33** (IC_{50} = 123 nM) showed comparable potency and derivative **35** (IC_{50} = 211 nM) showed lower potency. The IC_{50} values for the five mono- and bis-phenylimidamides ranged between 907 nM and 2.43 μM for

bis-AIAs **32** and **30**, respectively. Thus, pyridylimidamide **31** and the corresponding phenyl analogue **30** were the most and least potent. For the relatively small number of compounds tested, the antileishmanial data are somewhat similar to anti-*T. cruzi* data. Bis-pyridylimidamides **31**, **33**, and **35** were the three most potent compounds (in descending order) against both parasites. However, the orders of activity of the phenylimidamides differed, without the clear distinction of potencies between mono- and bis-phenylimidamides, as observed against *T. cruzi*.

IN VIVO ACTIVITIES AND STRUCTURE–ACTIVITY RELATIONSHIPS

T. b. rhodesiense. Twenty compounds (including six prodrugs) were tested in mice infected with the *T. b. rhodesiense* strain STIB900 (Table 3).[85] The amidines and *N*-alkylamidines were given intraperitoneally (four daily doses of 5 mg/kg), while the prodrugs were given orally (four daily doses of 25 mg/kg). Mice that survived for 60 days after infection without showing a parasitemia relapse were considered as cured. This model is highly stringent, mimicking the acute stage of HAT, and the low doses applied allowed for the distinction of activities among the highly trypanocidal compounds. Pentamidine and furamidine attained 1/4 cures at 4 × 5 mg/kg ip, and any compound attaining a higher cure rate is considered to have enhanced activity in vivo.

Table 3. In Vivo Antiprotozoal Activity of Select *m*-Terphenyl and Dipyridylbenzene Derivatives[a]

compd	dose (mg/kg)[b]	route[c]	cured/infected[d]	MSD (days)[e]
1	4 × 5	ip	4/4	>60
	1 × 10	ip	4/4	>60
2	4 × 5	ip	0/4	13.5
3	4 × 5	ip	0/4	9.25
5	4 × 25	po	3/4	>51.25
6	4 × 25	po	1/4	>34.25
7	4 × 5	ip	0/4	15.25
8	4 × 5	ip	0/4	20
10	4 × 5	ip	0/4	>35
11	4 × 5	ip	1/4	>41.25
12	4 × 5	ip	2/4	>38
13	4 × 5	ip	0/4	18.5
17	4 × 25	po	0/4	7.25
18	4 × 25	po	0/4	17.75
20	4 × 5	ip	0/4	10
21	4 × 5	ip	0/4	34.75
23	4 × 5	ip	4/4	>60
	1 × 5	ip	4/4	>60
25	4 × 5	ip	4/4	>60
	1 × 10	ip	4/4	>60
26	4 × 5	ip	4/4	>60
27	4 × 25	po	2/4	>53.75
28	4 × 25	po	3/4	>52
MLSP[f]	4 × 5	ip	4/4	>60
FMD[g]	4 × 5	ip	1/4	>46
PMD[h]	4 × 5	ip	1/4	>38

[a]Female NMRI mice infected with *Trypanosoma brucei rhodesiense* (STIB900).[85] [b]Administration was once per day on 4 consecutive days for all compounds, and single doses for select compounds. [c]Route of administration: intraperitoneal (ip) or oral (po). [d]Mice that survived for 60 days after infection without showing a parasitemia relapse were considered as cured. [e]Mean survival days after infection. All mice were used to calculate the MSD (the relapsed mice and the cured mice, where MSD > 60 days). [f]Melarsoprol. [g]Furamidine. [h]Pentamidine.

Three diamidines, lead compound **1** and dipyridyl analogues **23** and **25**, each cured 4/4 infected mice at the 4 × 5 mg/kg ip regimen, exhibiting excellent cure rates comparable to that of melarsoprol. These three compounds also attained 4/4 cures in single doses of 10 mg/kg for diamidines **1** and **25** and 5 mg/kg for analogue **23**. Acetate salt **26**, a different salt form of **25**, also effected 4/4 cures at the 4 × 5 mg/kg regimen. Diamidines **12** and **11** cured 2/4 and 1/4 infected mice, respectively. Prodrugs of diamidines **1** and **25** demonstrated efficacy with the 4 × 25 mg/kg oral regimen. Compound **5**, the amidoxime derivative of **1**, cured 3/4 mice, while methamidoxime derivative **6** attained 1/4 cures. Compound **28**, the dimethylaminoacetoxy derivative of dipyridyl analogue **25**, cured 3/4 mice, and the methamidoxime derivative **27** attained 2/4 cures. Mean survival rates exceeded 50 days for prodrugs **5**, **27**, and **28**..

Two simple amidine moieties oriented para to the central ring, regardless of the presence or position of nitrogen atoms in the outer rings, were required for maximum efficacy in vivo (compounds **1**, **23**, and **25**). Among the terphenyl analogues, the introduction of alkyl substituents on the amidine nitrogen (**1** vs **2**, **1** vs **3**) or meta orientations of one or both amidine groups (**1** vs **13**, **1** vs **21**, **12** vs **20**) resulted in loss of efficacy. In these respects, a high correlation exists between potencies in vitro and efficacies in vivo. All analogues of diamidine **1** with substituents on the central ring were less effective in vivo. Derivatives **10**–**12** had potencies in vitro similar to that of the parent molecule, but the methoxy (**12**), hydroxy (**11**), and amino (**10**) analogues attained 2/4, 1/4, and 0/4 cures, respectively, but all with significantly prolonged mean survival times (exceeding 35 days) compared to untreated mice (10 days or less). The chloro and nitro derivatives **7** and **8**, which were less potent in vivo, cured no mice but with less prolonged survival times. In cases where prodrugs exist, the prodrugs reflected the efficacies of the parent amidines. Prodrugs of the highly effective amidines **1** and **25** demonstrated oral efficacy, as stated above. Neither amidine **13** nor its prodrugs (**17** and **18**) were effective in vivo.

L. donovani. On the basis of their in vitro antileishmanial efficacy and selectivity, compounds **31**, **33**, and **35** were selected for in vivo evaluation. These molecules were first tested in groups of two uninfected BALB/c mice at five daily doses of 30 mg/kg intraperitoneally to ensure that they were well tolerated in the animals prior to evaluation of in vivo antileishmanial efficacy in larger groups. Compounds **31** and **33** were toxic at this dose, with the animals displaying tremors and hyperactivity after the second and first doses, respectively. Mice were euthanized after these adverse effects were observed, and compounds **31** and **33** were not tested further in vivo. After no overt signs of toxicity were observed when compound **35** was given at 5 × 30 mg/kg ip, an in vivo antileishmanial efficacy test[82] was carried out with this compound. Unfortunately, only 23 ± 11% inhibition of liver parasitemia (mean ± standard deviation, n = 4) was observed when *L. donovani*-infected BALB/c mice were given compound **35** at 5 × 30 mg/kg ip. In the same experiment, miltefosine treatment of infected BALB/c mice at 5 × 10 mg/kg orally resulted in 96 ± 2% inhibition of liver parasitemia (n = 4).

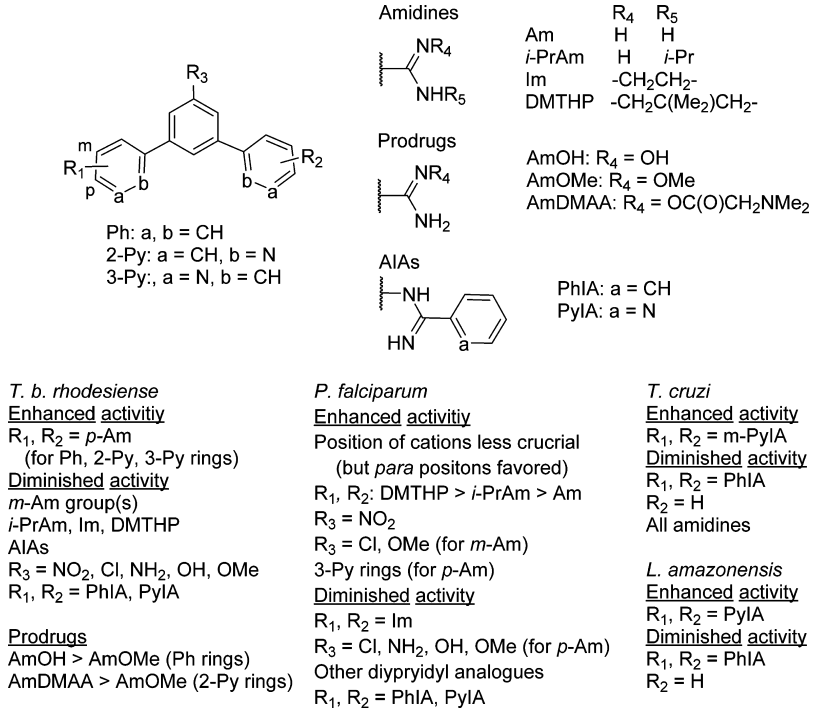

Figure 2. Summary of antiprotozoal SARs of *m*-terphenyl derivatives.

DISCUSSION

The *m*-terphenyl derivatives exhibited complementary SAR profiles against the four parasites, as summarized in Figure 2. In general, the amidine derivatives were more active against *T. b. rhodesiense* and *P. falciparum*, while the AIAs showed more promising results against the other parasites. The orientation of both amidine moieties para to the central ring, regardless of the presence or position of nitrogen atoms in the outer rings, was required for optimal activity against *T. b. rhodesiense*. Altered positions of the amidine groups, alkylation of the amidine nitrogen atoms, and substituents on the central ring all resulted in diminished activity either in vitro or in vivo. A general trend of diminished activities of *N*-alkyl analogues has been observed,[37,38,40,41,50,51,86,87] but the effects of substituents on the central or outer rings have varied from one class of compounds to another.[29,38,51] The insertion of nitrogen atoms into phenyl rings has resulted in retained or enhanced activity in the diphenylfuran and *p*-terphenyl analogues.[46,62,64,85] The replacement of a central furan ring with 1,3-phenylene was clearly beneficial with respect to the diamidine analogues but not for the prodrugs. Compound **1** attained 4/4 cures in the STIB900 acute model, compared to 1/4 cures for furamidine. Its similarly efficacious dipyridyl analogues **23** and **25** were also more active in vivo than the corresponding dipyridyl derivatives of furamidine.[46,85] Pafuramidine was more efficacious than the corresponding amidoxime[88] and has been one of few prodrugs to attain 4/4 cures in the STIB900 model at four daily 25 mg/kg oral doses.[85] By contrast, methamidoxime **6** (a prodrug of **1**) cured 1/4 mice under the same conditions, while the corresponding amidoxime **5** attained 3/4 cures. Methamidoxime **27** (a prodrug of **25**) and the di(pyridin-2-yl) analogue of pafuramidine[85] each cured 2/4 mice. Another prodrug of **25**, dimethylaminoacetoxy derivative **28**, attained 3/4 cures.

Antiplasmodial activity was less dependent upon the position of the cationic groups (although still favored by at least one para cation) and was enhanced by alkylation of the amidine nitrogen atoms, especially in the DMTHP derivatives and to a lesser extent in the *N*-isopropyl analogues. The imidazoline derivatives, however, were less potent than the corresponding amidines. In other examples from this lab, the effect of N-alkylation has varied from one class of compounds to another.[36−38,50,51] The effects of substituents on the central ring varied with the nature of the substituents and the orientation of the cationic groups. Only one dipyridyl analogue, the bis(6-amidinopyridin-3-yl) derivative **23**, was more potent than the corresponding terphenyldiamidine.

The bis-pyridylimidamide **31** was unique in demonstrating activity against all four parasites in vitro. Despite its high potencies against *T. b. rhodesiense* and *P. falciparum*, it was much less selective for these parasites over mammalian cells compared to the amidine derivatives. This compound, having both cations in the meta position and a chlorine atom attached to the central ring, was also the most active against *T. cruzi* and *L. amazonensis*. The SAR of these compounds against *T. cruzi* was rather clearly defined: the bis-pyridylimidamides were the most potent, followed by the bis-phenylamidamides, the mono-AIAs, and the amidine derivatives. The bis-pyridylimidamides were also the most active against *L. amazonensis*; however, the IC_{50} values of the less potent bis-phenylamidamides and mono-AIAs overlapped, and the amidine derivatives were not tested in this model.

A large number of mechanisms of antimicrobial activity have been proposed for the diamidine class of molecules.[89−101] These positively charged molecules bind to many negatively charged surfaces and receptors and accordingly have numerous potential sites of action. The antimicrobial action of these compounds probably occurs at multiple sites, and the primary site of action may vary from organism to organism. This is a huge problem with regard to drug design but is advantageous with regard to the potential development of drug resistance. It has been suggested that the highly selective toxicity of many of the compounds in this class toward pathogenic organisms over

mammalian cells is due to active transport mechanisms. For example, trypanosomes have a number of active transport systems that allow cationic molecules to be concentrated in the parasites at levels over 1000 times higher than in mammalian cells.[97] Thus, the only way to optimize these compounds for specific targets is via focused parallel synthesis and in vitro testing or focusing on the active transport systems. Unfortunately, not enough is known with regard to the specificities of the transporters to aid in the drug design process.

Because of the propensity of dications to bind to numerous sites, the toxicity of these molecules is always a concern with regard to drug design.[85,102−108] The nature of the toxicity does not appear class related but may vary from compound to compound. For instance, hypoglycemia is the major concern with regard to pentamidine,[104,106] while nephrotoxicity resulted in the cancellation of human clinical trials with pafuramine.[85] An obvious approach to decreasing host toxicity is to produce more potent compounds against the targeted organisms. However, even the most potent diamidine compounds must be subjected to a battery of toxicity tests.

A number of the *m*-terphenyl analogues, as well as diamidine derivatives of other classes of compounds,[36−41,50,51] have shown high potencies against *P. falciparum* in vitro. However, the lack of a reliable animal model has been a major obstacle in their further development against malaria. Standard rodent models, which must use *Plasmodium* species that are nonpathogenic to humans due to the high specificity of *P. falciparum* for human erythrocytes, do not necessarily predict the efficacy of a given drug in human malaria,[109] and their relevance to human malaria has been questioned.[110,111] For example, pafuramidine, which is known to be effective in human malaria,[33] was inactive in a commonly used *P. berghei* mouse model,[112] as were pentamidine and other analogues of furamidine.[29,56,112] Murine *P. falciparum* models employing immunodeficent mice engrafted with human erythrocytes or hepatocytes (humanized mice)[110,112−114] should more accurately predict the efficacies of new therapies in human malaria, although they are generally more costly and more difficult to handle than standard rodent models.[114] These models may be useful in determining which standard rodent model offers better correlation with *P. falciparum* for given compounds; for example, one study suggested that *P. vinckei* may be a better surrogate than *P. berghei* for diamidines.[112] These findings may provide at least a starting point in the further evaluation of other diamidines.

CONCLUSIONS

This communication describes several novel diamidine derivatives that show excellent in vitro potency against *T. b. rhodesiense*, are curative in a mouse model of early stage HAT, and have the potential for reduced toxicity when compared to the prototype molecule furamidine. Most outstanding were diamidines **1**, **23**, and **25**, which attained 4/4 cures not only in four daily intraperitoneal doses of 5 mg/kg but also in single doses of 10 mg/kg or lower. Prodrugs of compounds **1** and **25** (derivatives **5** and **28**) also attained 3/4 cure rates in this model with four daily 25 mg/kg oral doses. Further evaluations of these compounds against other *T. brucei* strains and a mouse model of late stage HAT are in progress. A number of compounds, most significantly the DMTHP derivatives **4**, **9**, and **16**, showed promising antiplasmodial potencies in vitro and merit in vivo evaluation, contingent upon the selection of appropriate animal models. Although these compounds, as a class, did not show promising results against *T. cruzi*, AIA derivative **31** proved to be 25 times more potent than the clinical standard benznidazole and thus warrants further evaluation against this parasite.

EXPERIMENTAL SECTION

General Experimental Methods. In vitro antiprotozoal activities against *T. b. rhodesiense* (STIB900), *T. cruzi* (Tulahuen C2C4), *P. falciparum* (chloroquine resistant K1),[83] and *L. amazonensis* intracellular amastigotes,[82] cytotoxicities against L6 rat myoblast cells,[83] and in vivo activities against *T. b. rhodesiense* (STIB900)[85] and *L. donovani* (LV82)[82] were measured following established protocols. All protocols and procedures used in the current study were reviewed and approved by the local veterinary authorities of the Canton Basel-Stadt, Switzerland, or the Institutional Animal Care and Use Committee at The Ohio State University. The data in the *T. b. rhodesiense* model were generated at the time when the determination of survival was still accepted by the authorities.

Uncorrected melting points were measured on a Thomas-Hoover capillary melting point apparatus. ^{1}H NMR spectra were recorded in DMSO-d_6 on a Varian Gemini 2000 or Unity Plus 300 MHz spectrometer or a Varian Inova 400 MHz spectrometer. Spectra were recorded at 300 MHz unless the higher field strength is specified. ^{13}C NMR spectra were recorded in DMSO-d_6 on a Varian Unity Plus operating at 75 MHz. Anhydrous EtOH was distilled over Mg/I_2 immediately prior to use. Other anhydrous solvents were purchased from Aldrich Chemical Co., Milwaukee, WI, in Sure-seal containers and were used without further purification. Reaction mixtures were monitored by TLC on silica gel or by reverse phase HPLC. Organic layers of extraction mixtures were neutralized as necessary with acidic or basic washes, washed with saturated NaCl solution, and dried over $MgSO_4$ or Na_2SO_4 before being evaporated under reduced pressure. Normal phase gravity and flash column chromatography were performed using Davisil grade 633, type 60A silica gel (200−425 mesh). Reverse phase flash chromatography was performed as previously described.[41] Analytical HPLC chromatograms were recorded on a Hewlett-Packard 1090 series II or Agilent 1200 chromatograph using a Zorbax Rx C8 column (4.6 mm × 75 mm, 3.5 μm) maintained at 40 °C and UV photodiode array detection at 230, 254, 265, 290, and 320 nm. Area % values are reported at the wavelengths where the strongest signals of the products were observed. Mobile phases consisted of mixtures of acetonitrile (0−75%) or methanol (0−95%) in water containing formic acid (80 mM), ammonium formate (20 mM), and triethylamine (15 mM). Samples were eluted at appropriate gradients at a flow rate of 1.5 mL/min. Similar analyses were performed on a Hewlett-Packard 1100 system using a Zorbax SB C8 column (3.0 mm × 100 mm, 3.5 μm), eluting at 0.6 mL/min. Preparative reverse phase HPLC was performed on a Varian ProStar chromatography workstation configured with two PS-215 pumps fitted with 50 mL pump heads, a Dynamax Microsorb C18 (60 Å) column (41.4 cm × 25 cm, 8 μm), PS-320 variable wavelength UV−vis detector, and a PS-701 fraction collector. Mobile phases consisted of mixtures of acetonitrile (0−75%) or methanol (0−95%) in water containing formic acid (40 mM) and ammonium formate (10 mM). Flow rates were maintained at 40 mL/min. Select fractions were analyzed for purity by analytical HPLC as described above. Pooled purified fractions were evaporated under reduced pressure, reconstituted in water, and lyophilized on a VirTis BenchTop 2K or 6K lyophilizer. Low resolution ESI mass spectra were recorded on an Agilent Technologies 1100 series LC/MSD trap mass spectrometer or a VG analytical 70-SE spectrometer. Elemental analyses were performed by Atlantic Microlab, Norcross, GA, and, unless stated otherwise, were within ±0.4% of calculated values. CHN analyses were performed by combustion using a Perkin-Elmer 2400 or Carlo Erba 1108 automatic analyzer. Chlorine analyses were performed by flask combustion followed by ion chromatography. The compounds reported as salts were frequently analyzed correctly for fractional moles of water and/or other solvents; in each case ^{1}H NMR spectra

were consistent with the analysis. The purity of all final compounds was determined to be ≥95% by combustion analysis.

General Procedure for Amidines 1−4, 7−9, 12−16, and 19−21. The nitrile was added to a mixture of anhydrous EtOH and 1,4-dioxane that had been saturated with hydrogen chloride at 0 °C in a dry three-neck flask equipped with a gas inlet tube, a thermometer, and a drying tube. The reaction mixture was then sealed and stirred at ambient temperature until the nitrile was no longer detectable. The reaction mixture was diluted with ether. The crude imidate was filtered off, dried under high vacuum over KOH, and then reacted immediately with an excess of ammonia or the appropriate amine in EtOH. The reaction mixture was diluted with ether, and the crude product was filtered off. The product was purified by direct recrystallization or by reverse phase HPLC or flash chromatography followed by conversion to the dihydrochloride salt using aqueous or ethanolic HCl.

4,4″-Diamidino-*m*-terphenyl Dihydrochloride (1). **1** was prepared from nitrile **43** (0.56 g, 2.01 mmol) with ammonium carbonate used in place of ammonia. After purification by preparative HPLC, the product was recrystallized from ethanolic HCl−ether to give a white solid (346 mg, 44%): mp >350 °C; ^{1}H NMR δ 9.50 (br s, 3H), 9.24 (br s, 3H), 8.14 (t, J = 1.6 Hz, 1H), 8.10 (d, J = 8.7 Hz, 4H), 7.99 (d, J = 8.2 Hz, 4H), 7.87 (dd, J = 7.7 and 1.6 Hz, 2H), 7.68 (t, J = 7.7 Hz, 1H); ESI MS m/z 315.1 ([M + H]$^+$ of free base); HPLC 100 area %. Anal. ($C_{20}H_{18}N_4$·2HCl·0.7H_2O) C, H, N, Cl.

4,4″-Bis(*N*-isopropyl)amidino-*m*-terphenyl Dihydrochloride (2). **2** was prepared from nitrile **43** and isopropylamine. The product was purified by reverse phase flash chromatography and recrystallized from aqueous HCl to give a solid (690 mg, 61%): mp 253−254 °C; ^{1}H NMR δ 9.69 (d, J = 8.2 Hz, 2H), 9.57 (br s, 2 H), 9.21 (br s, 2H), 8.07 (m, 5H), 7.86 (m, 6H), 7.69 (t, J = 7.8 Hz, 1H), 4.13 (m, 2H), 1.31 (d, J = 6.4 Hz, 12H); ESI MS m/z 399.2 ([M + H]$^+$ of free base); HPLC 100 area %. Anal. ($C_{26}H_{30}N_4$·2HCl·1.4H_2O) C, H, N, Cl.

4,4″-Bis(imidazolin-2-yl)-*m*-terphenyl Dihydrochloride (3). **3** was prepared from nitrile **43** and ethylenediamine. The crude precipitated product was recrystallized from aqueous HCl to give a white solid (1.26g, 79%): mp >250 °C (dec); ^{1}H NMR δ 10.90 (br s, 3H), 8.22 (m, 5H), 8.16 (d, J = 8.7 Hz, 4H), 7.91 (dd, J = 7.8 and 1.7 Hz, 2H), 7.68 (t, J = 7.8 Hz, 1H), 4.04 (s, 8H); ESI MS m/z 367.2 ([M + H]$^+$ of free base); HPLC 99.0 area %. Anal. ($C_{24}H_{22}N_4$·2HCl·2.8H_2O) C, H, N, Cl.

4,4″-Bis[(5,5-dimethyl)-1,4,5,6-tetrahydropyrimidin-2-yl]-*m*-terphenyl Dihydrochloride (4). **4** was prepared from nitrile **43** (961 mg, 3.43 mmol) and 2,2-dimethylpropane-1,3-diamine. The product was recrystallized from aqueous HCl to give white granules (1.33 g, 74%): mp >350 °C (dec); ^{1}H NMR δ 10.39 br s, 3H), 8.14 (t, J = 1.7 Hz, 1H), 8.11 (d, J = 8.6 Hz, 4H), 7.97 (d, J = 8.6 Hz, 4H), 7.87 (dd, J = 7.7 and 1.6 Hz, 2H), 7.68 (t, J = 7.8 Hz, 1H), 3.24 (s, 8H), 1.07 (s, 12H); ESI MS m/z 451.2 ([M + H]$^+$ of free base); HPLC 99.0 area %. Anal. ($C_{30}H_{34}N_4$·2HCl·1.25H_2O) C, H, N, Cl.

4,4″-Bis(*N*′-hydroxy)amidino-*m*-terphenyl Dihydrochloride (5). Potassium *tert*-butoxide (8.42 g, 75.0 mmol) was added to a stirred solution of hydroxylamine hydrochloride (5.25 g, 75.6 mmol) in dry DMSO (45 mL). After 30 min nitrile **43** (2.11 g, 7.52 mmol) was added, and the mixture was stirred overnight. The reaction mixture was poured over ice−water, and the precipitated amidoxime base was filtered off (2.05 g, 79%): mp >215 °C (dec); ^{1}H NMR δ 9.71 (br s, 2H), 7.98 (s, 1H), 7.80 (s, 8H), 7.71 (d, J = 7.3 Hz, 2H), 7.57 (t, J = 7.7 Hz, 1H), 5.89 (br s, 4 H); HPLC 100 area %. Anal. ($C_{20}H_{18}N_4O_2$·0.1H_2O) C, H, N.

An aliquot of the base (478 mg, 1.38 mmol) was recrystallized from aqueous HCl to give a white solid (221 mg, 38%): mp >260° (dec); ^{1}H NMR δ 11.33 (br s, 2H), 9.16 (br s, 4H), 8.11 (s, 1H), 8.08 (d, J = 8.5 Hz, 4H), 7.87 (m, 6H), 7.67 (t, J = 7.7 Hz, 1H); ESI MS m/z 347.2 ([M + H]$^+$ of free base); HPLC 99 area %. Anal. ($C_{20}H_{18}N_4O_2$·2HCl) C, H, N, Cl.

4,4″-Bis(*N*′-methoxy)amidino-*m*-terphenyl Dihydrochloride (6). A mixture of amidoxime base **5** (1.56 g, 4.49 mmol) and potassium *tert*-butoxide (1.07 g, 9.53 mmol) in DMSO (20 mL) was stirred for 2 h followed by the addition of iodomethane (0.9 mL, 14 mmol). The reaction mixture was stirred overnight and poured over ice. The precipitated crude product was chromatographed on silica, eluting with $CHCl_3$/MeOH (20:1) and recrystallized twice from MeOH−H_2O to give white crystals (532 mg, 32%): mp 141−142 °C; ^{1}H NMR δ 8.04 (s, 1H), 7.96 (d, J = 8.3 Hz, 4H), 7.86 (d, J = 8.4 Hz, 4H), 7.79 (dd, J = 7.7 and 1.6 Hz, 2H), 7.03 (t, J = 8.1 Hz, 2H), 3.48 (s, 6H). Anal. ($C_{22}H_{22}N_4O_2$) C, H, N.

The base was converted to the HCl salt using aqueous HCl to give a white solid (570 mg, 87% from salt conversion, 28% from the amidoxime): mp 192 °C (dec); ^{1}H NMR δ 8.08 (m,1H), 8.01 (d, J = 8.5 Hz, 4H), 7.46 (d, J = 8.5 Hz, 4H), 7.82 (dd, J = 7.6 and 1.6 Hz, 2H), 7.65 (t, J = 7.7 Hz, 1H), 3.87 (s, 6H); ESI MS m/z 375.5 ([M + H]$^+$ of free base); HPLC 99 area %. Anal. ($C_{22}H_{22}N_4O_2$·1.95HCl·1.3H_2O) C, H, N.

4,4″-Diamidino-5′-chloro-*m*-terphenyl Dihydrochloride (7). **7** was prepared from nitrile **44** (1.03 g, 3.28 mmol). The product was purified by reverse phase flash chromatography and converted to the HCl salt using aqueous HCl to give a solid (532 mg, 53%): mp >250 °C (dec); ^{1}H NMR δ 9.52 (br s, 4H), 9.27 (br s, 4H), 8.16 (d, J = 8.5 Hz, 4H), 8.12 (t, J = 1.5 Hz, 1H), 8.00 (d, J = 8.5 Hz, 4H), 7.96 (d, J = 1.5 Hz, 2H); ESI MS m/z 349.2 ([M + H]$^+$ of free base); HPLC 99.4 area %. Anal. ($C_{20}H_{17}ClN_4$·2HCl·2.3H_2O) C, H, N, Cl.

4,4″-Diamidino-5′-nitro-*m*-terphenyl Dihydrochloride (8). **8** was prepared from nitrile **45** (1.64 g, 5.03 mmol). The product was purified by reverse phase flash chromatography and converted to the HCl salt using aqueous HCl to give a solid (929 mg, 42%): mp >350 °C (dec); ^{1}H NMR δ 9.58 (br s, 4H), 9.34 (br s, 4H), 8.62 (d, J = 1.5 Hz, 2H), 8.59 (t, J = 1.6 Hz, 1H), 8.25 (d, J = 8.6 Hz, 4H), 8.05 (d, J = 8.5 Hz, 4H); ESI MS m/z 360.1 ([M + H]$^+$ of free base); HPLC 100 area %. Anal. ($C_{20}H_{17}N_5O_2$·2.2HCl·1.9H_2O) C, H, N, Cl.

4,4″-Bis[(5,5-dimethyl)-1,4,5,6-tetrahydropyrimidin-2-yl]-5′-nitro-*m*-terphenyl Dihydrochloride (9). **9** was prepared analogously to **4** from nitrile **45** (1.66 g, 5.11 mmol), but the imidate intermediate was prepared in neat ethanolic HCl. The product was purified by preparative HPLC and converted to the HCl salt using ethanol HCl and ether to give an off-white solid (1.37g, 47%): mp >389 °C (dec); ^{1}H NMR δ 10.70 (br s, 4H), 8.61 (m, 3H), 8.27 (d, J = 8.5 Hz, 4H), 8.01 (d, J = 8.6 Hz, 4H), 3.25 (s, 8H), 1.08 (s, 12H); ESI MS m/z 496.4 ([M + H]$^+$ of free base); HPLC 99.0 area %. Anal. ($C_{30}H_{33}N_5O_2$·2HCl·H_2O) C, H, N, Cl.

4,4″-Diamidino-5′-amino-*m*-terphenyl Dihydrochloride (10). Nitro compound **8** (0.536 g, 1.24 mmol) was hydrogenated for 3 h at 60 psi over 10% Pd/C (90 mg, 0.055 mmol) in EtOH/H_2O (2:1, 150 mL). The reaction mixture was filtered through Celite and evaporated to a white solid. The product was recrystallized from EtOH−H_2O to give white crystals (401 mg, 80%): mp >250 °C (dec); ^{1}H NMR δ 9.48 (br s, 4H), 9.25 (br s, 4H), 7.97 (d, J = 9.1 Hz, 4H), 7.93 (d, J = 9.1 Hz, 4H), 7.22 (t, J = 1.5 Hz, 1H), 7.01 (t, J = 1.5 Hz, 2H), 5.53 (br s, 2H); ESI MS m/z 330.2 ([M + H]$^+$ of free base); HPLC 100 area %. Anal. ($C_{20}H_{19}N_5$·2HCl·2.7H_2O) C, H, N, Cl.

4,4″-Diamidino-5′-hydroxy-*m*-terphenyl Dihydrochloride (11). Dinitrile **46** (0.77 g, 2.6 mmol) was converted to 4,4″-bis(*N*′-hydroxy)amidino-5′-hydroxy *m*-terphenyl (free base) in 99% yield following the procedure for compound **5**: mp 160−163 °C; ^{1}H NMR δ 9.68 (br s, 3H), 7.76 (d, J = 9 Hz, 4H), 7.69 (d, J = 9 Hz, 4H), 7.37 (s, 1H), 7.05 (s, 2H), 5.84 (br s, 4H); ^{13}C NMR δ 158.4, 151.5, 141.5, 141.0, 131.6, 126.6, 126.2, 116.2, 112.9; MS (ESI) m/z 363 ([M + H]$^+$).

To a solution of the diamidoxime (0.36 g, 1 mmol) in glacial acetic acid (10 mL) was slowly added acetic anhydride (0.35 mL). After stirring overnight, the solvent was evaporated to dryness under reduced pressure and the oily residue obtained was used without further purification, where it was dissolved in absolute ethanol (25 mL) and glacial AcOH (10 mL) followed by addition of 10% palladium on carbon (80 mg). The mixture was hydrogenated on a Parr apparatus at 50 psi for 4 h at room temperature. The mixture was filtered through a filter aid and the filter pad washed with water. The filtrate was evaporated under reduced pressure and the residue was collected and washed with ether to give **11** as an acetate salt. The diamidine was purified by neutralization with Na_2CO_3 followed by filtration of the resultant solid and washing with water (3×). Finally,

the free base was stirred with ethanolic HCl overnight, diluted with ether, and the solid formed was filtered and dried to give the diamidine hydrochloride salt **11** (77%): mp >300 °C; ^{1}H NMR δ 10.12 (br s, 1H), 9.48 (br s, 4H), 9.26 (br s, 4H), 7.98 (d, J = 9 Hz, 4H), 7.95 (d, J = 9 Hz, 4H), 7.52 (s, 1H), 7.23 (s, 2H); ^{13}C NMR (DMSO-d_6) δ 165.19, 158.7, 145.1, 140.6, 128.8, 127.3, 126.9, 116.8, 114.2. HRMS calcd for $C_{20}H_{19}N_4O$ m/z 331.1559 ([M + H]$^+$ for free base); observed 331.1564. Anal. ($C_{20}H_{18}N_4O$·2.0HCl·0.8H_2O·0.5EtOH) C, H, N.

4,4″-Diamidino-5′-methoxy-*m*-terphenyl Dihydrochloride (12). **12** was prepared from nitrile **47** (1.01 g, 3.22 mmol). The product was purified by reverse phase flash chromatography and converted to the HCl salt using aqueous HCl to give a gray solid (960 mg, 71%): mp >225 °C (dec); ^{1}H NMR δ 9.51 (br s, 4H), 9.28 (br s, 4H), 8.11 (d, J = 8.5 Hz, 4H), 7.99 (d, J = 8.5 Hz, 4H), 7.71 (m, 1H), 7.40 (d, J = 1.3 Hz, 2H), 3.95 (s, 3H); ESI MS m/z 345.2 ([M + H]$^+$ of free base); HPLC 98.4 area %. Anal. ($C_{21}H_{20}N_4O$·2HCl·1.6H_2O) C, H, N, Cl.

3,3″-Diamidino-*m*-terphenyl Dihydrochloride (13). **13** was prepared from nitrile **48** (1.01 g, 3.60 mmol). The product was purified by preparative HPLC and converted to the HCl salt using aqueous HCl to give a solid (716 mg, 51%): mp >350 °C; ^{1}H NMR δ 9.69 (br s, 4H), 9.34 (br s, 4H), 8.48 (s, 1H), (8.37, s, 2H), 8.18 (d, J = 8.0 Hz, 2H), 7.88 (d, J = 7.8 Hz, 4H), 7.75 (t, J = 7.8 Hz, 2H), 7.67 (t, J = 2.8 Hz, 1H); ESI MS m/z 315.3 ([M + H]$^+$ of free base); HPLC 100 area %. Anal. ($C_{20}H_{18}N_4$·2HCl·0.6H_2O) C, H, N, Cl.

3,3″-Bis(*N*-isopropyl)amidino-*m*-terphenyl Dihydrochloride (14). An aliquot (0.95 g 2.13 mmol) of the imidate intermediate prepared from nitrile **48** was reacted with isopropylamine and purified analogously to **2** as a white solid (681 mg, 68%): mp >240 °C (dec); ^{1}H NMR δ 9.83 (d, J = 8.0 Hz, 2H), 9.68 (br s, 2H), 9.22 (br s, 2H), 8.50 (s, 1H), (8.23, s, 2H), 8.13 (d, J = 7.4 Hz, 2H), 7.86 (dd, J = 7.5 and 1.5 Hz, 2H), 7.78 (d, J = 7.8 Hz, 2H), 7.73 (t, J = 7.6 Hz, 2H), 7.67 (t, J = 7.7 Hz, 1H), 4.13 (m, 1H), 1.33 (d, J = 6.4 Hz, 12H); ESI MS m/z 398.3 ([M + H]$^+$ of free base); HPLC 98.7 area %. Anal. ($C_{26}H_{30}N_4$·2HCl·1.2H_2O) C, H, N, Cl.

3,3″-Bis(imidazolin-2-yl)-*m*-terphenyl Dihydrochloride (15). **15** was prepared from an aliquot of the imidate above (0.99 g, 2.22 mmol) and ethylenediamine. The product was purified by reverse phase flash chromatography and then converted to the HCl salt using ethanolic HCl–ether to give a white solid (775 mg, 79%): mp 325–327 °C (dec); ^{1}H NMR δ 11.04 (br s, 3H), 8.75 (s, 2H), 8.43 (s, 1H), 8.26 (d, J = 8.0 Hz, 2H), 8.08 (d, J = 7.9 Hz, 2H), 7.90 (dd, J = 7.5 and 1.5 Hz, 2H), 7.78 (t, J = 7.9 Hz, 2H), 7.67 (t, J = 7.8 Hz, 1H), 4.05 (s, 8H); ESI MS m/z 367.4 ([M + H]$^+$ of free base); HPLC 99.5 area %. Anal. ($C_{24}H_{22}N_4$·2HCl·1.6H_2O) C, H, N, Cl.

3,3″-Bis[(5,5-dimethyl)-1,4,5,6-tetrahydropyrimidin-2-yl]-*m*-terphenyl Dihydrochloride (16). **16** was prepared from nitrile **48** (1.02 g, 3.64 mmol) and 2,2-dimethylpropane-1,3-diamine. After purification by preparative HPLC, the crude HCl salt (prepared using aqueous HCl) was dissolved in water and treated with aqueous NaOH to precipitate the free base. This was converted to the HCl salt using a mixture of ethanolic HCl, dioxane, and ether to give a white solid (671 mg, 35%): mp >335 °C (dec); ^{1}H NMR δ 10.51 (br s, 4H), 8.58 (s, 1H), 8.37 (s, 2H), 8.16 (d, J = 8.0 Hz, 2H), 7.88 (dd, J = 8.7 and 1.6 Hz, 2H), 7.85 (d, J = 7.8 Hz, 2H), 7.75 (t, J = 7.8 Hz, 2H), 7.66 (t, J = 7.8 Hz, 1H), 3.52 (s, 8H), 1.07 (s, 12H); ESI MS m/z 451.3 ([M + H]$^+$ of free base); HPLC 100 area %. Anal. ($C_{30}H_{34}N_4$·2.3HCl·0.55H_2O) C, H, N, Cl.

3,3″-Bis(*N*′-hydroxy)amidino-*m*-terphenyl Dihydrochloride (17). **17** was prepared following the procedure for amidoxime **5** from nitrile **48** (2.81 g, 10.0 mmol). The amidoxime base was recrystallized from EtOH to give white crystals (3.57 g, 103%): mp 212–213 °C; ^{1}H NMR δ 9.70 (br s, 2H), 8.03 (t, J = 1.6 Hz, 2H), 8.01 (t, J = 1.5 Hz, 1H), 7.78 (dm, J = 7.7 Hz, 2H), 7.73 (m, 2H), 7.71 (m, 2H), 7.60 (dd, J = 8.4 and 7.9 Hz, 1H), 7.50 (t, J = 7.8 Hz, 2H), 5.98 (br s, 4H). Anal. ($C_{20}H_{18}N_4O_2$·0.9EtOH.) C, H, N.

An aliquot of the base (511 mg, 1.27 mmol) was converted to the HCl salt using ethanolic HCl–ether to give a white solid (546 mg, 88%): mp >110 °C (dec); ^{1}H NMR δ 11.32 (br s, 2H), 9.14 (br s, 4H), 8.33 (s, 1H), 8.21 (s, 2H), 8.14 (d, J = 7.5 Hz, 2H), 7.87 (dd, J = 7.7 and 1.6 Hz, 2H), 7.78 (dm, J = 7.8 Hz, 2H), 7.73 (t, J = 7.7 Hz, 2H), 7.67 (t, J = 7.8 Hz, 1H); ESI MS m/z 347.2 ([M + H]$^+$ of free base); HPLC 100 area %. Anal. ($C_{20}H_{18}N_4O_2$·2HCl·0.7H_2O·0.8EtOH) C, H, N, Cl.

3,3″-Bis(*N*′-methoxy)amidino-*m*-terphenyl Dihydrochloride (18). **18** was prepared from amidoxime base **17** either by the method employed for compound **6** or using dimethyl sulfate and aqueous NaOH in dioxane. The combined products from multiple experiments were chromatographed on silica, eluting with hexanes/EtOAc (2:1) and converted to the HCl salt using ethanolic HCl–ether to give a white solid (1.69 g, 88% from salt conversion, 21% from amidoxime): mp 235–237 °C (dec); ^{1}H NMR δ 8.78 (br s, 2H), 8.34 (s, 1H), 8.24 (s, 2H), 8.09 (d, J = 8.0 Hz, 2H), 7.85 (dd, J = 7.7 and 1.6 Hz, 2H), 7.80 (d, J = 8.0 Hz, 2H), 7.67 (m, 3H), 3.89 (s, 6H); ESI MS m/z 375.2 ([M + H]$^+$ of free base); HPLC 98.4 area %. Anal. ($C_{22}H_{22}N_4O_2$·2HCl·0.3H_2O) C, H, N, Cl.

3,3″-Diamidino-5′-chloro-*m*-terphenyl Dihydrochloride (19). **19** was prepared from nitrile **49** (973 mg, 3.09 mmol). The product was purified by reverse phase flash chromatography and converted to the HCl salt using aqueous HCl to give a white solid (469 mg, 26%): mp >350 °C; ^{1}H NMR δ 9.65 (br s, 4H), 9.32 (br s, 4H), 8.42 (s, 1H), 8.36 (s, 2H), 8.23 (d, J = 7.9 Hz, 2H), 7.99 (d, J = 1.4 Hz, 2H), 7.91 (d, J = 7.9 Hz, 2H), 7.76 (t, J = 7.8 Hz, 2H); ESI MS m/z 349.2 ([M + H]$^+$ of free base); HPLC 100 area %. Anal. ($C_{20}H_{17}ClN_4$·2HCl·0.75H_2O) C, H, N, Cl.

3,3″-Diamidino-5′-methoxy-*m*-terphenyl Dihydrochloride (20). **20** was prepared from nitrile **50** (1.00 g, 3.23 mmol). The product was purified by reverse phase flash chromatography and converted to the HCl salt using aqueous HCl to give a light gray solid (990 mg, 73%): mp >325 °C; ^{1}H NMR δ 9.64 (br s, 4H), 9.27 (br s, 4H), 8.32 (s, 2H), 8.18 (d, J = 7.8 Hz, 2H), 7.97 (s, 1H), 7.87 (d, J = 7.9 Hz, 2H), 7.74 (t, J = 7.8 Hz, 2H), 7.44 (d, J = 1.2 Hz, 2H), 3.95 (s, 3H); ESI MS m/z 345.2 ([M + H]$^+$ of free base); HPLC 100 area %. Anal. ($C_{21}H_{20}N_4O$·2HCl·1.3H_2O) C, H, N, Cl.

3,4″-Diamidino-*m*-terphenyl Dihydrochloride (21). **21** was prepared from nitrile **55** (1.00 g, 3.58 mmol). The crude product was recrystallized from aqueous HCl to give a white solid (1.18 g, 85%): mp >220 °C (dec); ^{1}H NMR δ 9.61 (br s, 2H), 9.52 (br s, 2H), 9.32 (br s, 2H), 9.27 (br s, 2H), 8.29 (m, 1H), 8.23 (m, 1H), 8.18 (dm, J = 8.0 Hz, 1H), 8.12 (d, J = 8.7 Hz, 2H), 8.00 (d, J = 8.7 Hz, 2H), 7.89 (m,3H), 7.75 (t, J = 7.8 Hz, 1H), 7.68 (t, J = 7.8 Hz, 1H); ESI MS m/z 315.1 ([M + H]$^+$ of free base); HPLC 97.5 area %. Anal. ($C_{20}H_{18}N_4$·2HCl·1.8H_2O) C, H, N, Cl.

3,4″-Diamidino-5′-chloro-*m*-terphenyl Dihydrochloride (22). Lithium bis(trimethylsilyl)amide (1 M solution in THF, 10 mL, 10 mmol) was added dropwise to a suspension of nitrile (1.00 g, 3.18 mmol) in dry THF (15 mL). The mixture was stirred overnight and then cooled to 0 °C (ice–salt bath) before the slow addition of saturated ethanolic HCl. After 2 h the stirred solution was diluted with ether to precipitate the crude product, which was purified by preparative HPLC. Conversion to the HCl salt using EtOH–aqueous HCl followed by recrystallization from water–acetone gave a white powder (750 mg, 56%): mp >260 °C (dec); ^{1}H NMR δ 9.50 (br s, 4H), 9.27 (br s, 4H), 8.30 (m, 1H), 8.23 (dm, J = 8.1 Hz, 1H), 8.20 (t, J = 1.5 Hz, 1H), 8.17 (d, J = 8.5 Hz, 2H), 8.00 (m, 3H), 7.95 (t, J = 1.7 Hz, 1H), 7.90 (dm, J = 8.3 Hz, 1H), 7.76 (t, J = 7.8 Hz, 1H); ESI MS m/z 349.1 ([M + H]$^+$ of free base); HPLC 100 area %. Anal. ($C_{20}H_{17}ClN_4$·2HCl·1.75H_2O) C, H, N, Cl.

General Procedure for 1,3-Dipyridylbenzenediamidines 23–25 and 29. A solution of the amidoxime (3–5 mmol) in acetic acid was treated with acetic anhydride (5 mL), giving a precipitate. The mixture was transferred to a hydrogenation bottle, and more AcOH and 10% Pd/C (10–20 mol %) were added. The mixture was hydrogenated at 60 psi until completion and filtered through Celite. The product was purified by preparative HPLC and converted to the HCl salt using aqueous HCl unless stated otherwise.

1,3-Bis(6-amidinopyridin-3-yl)benzene Dihydrochloride (23). **23** was prepared from amidoxime **63** (1.28 g, 3.65 mmol) as a white solid (668 mg, 47%): mp 342–343 °C; ^{1}H NMR δ 9.71 (br s,

4H), 9.50 (br s, 4H), 9.31 (d, J = 2.2 Hz, 2H), 8.68 (dd, J = 8.4 and 2.3 Hz, 2H), 8.52 (d, J = 8.4 Hz, 2H), 8.38 (m, 1H), 8.05 (dd, J = 7.8 and 1.7 Hz, 2H), 7.75 (t, J = 7.8 Hz, 1H); ESI MS m/z 317.1 ($[M + H]^+$ of free base); HPLC 100 area %. Anal. ($C_{18}H_{16}N_6 \cdot 2HCl \cdot 1.5H_2O$) C, H, N, Cl.

1,3-Bis(5-amidinopyridin-3-yl)benzene Trihydrochloride (24). **24** was prepared from amidoxime **64** (1.04 g, 2.97 mmol) as a white solid (542 mg, 42%): mp >300 °C; ^{1}H NMR δ 9.79 (br s, 4H), 9.42 (br s, 4H), 9.38 (d, J = 2.1 Hz, 2H), 9.04 (d, J = 2.1 Hz, 2H), 8.78 (t, J = 2.1 Hz, 2H), 8.57 (m, 1H), 8.04 (dd, J = 7.7 and 1.7 Hz, 2H), 7.56 (t, J = 7.8 Hz, 1H); ESI MS m/z 317.1 ($[M + H]^+$ of free base); HPLC 97.5 area %. Anal. ($C_{18}H_{18}N_6 \cdot 2.8HC \cdot 0.8H_2O$) C, H, N, Cl.

1,3-Bis(5-amidinopyridin-2-yl)benzene Trihydrochloride (25). **25** was prepared from amidoxime **69** (1.17 g, 3.35 mmol). The product was converted to the HCl salt using ethanolic HCl−ether to give a white solid (992 mg, 76%): mp >350 °C; ^{1}H NMR δ 9.71 (br s, 4H), 9.41 (br s, 4H), 9.15 (t, J = 1.1 Hz, 2H), 9.01 (s, 1H), 8.44 (d, J = 8.5 Hz, 2H), 8.40 (dd, J = 8.7 and 2.0 Hz, 2H), 8.37 (dd, J = 7.8 and 1.8 Hz, 2H), 7.75 (t, J = 7.8 Hz, 1H); ESI MS m/z 317.1 ($[M + H]^+$ of free base); HPLC 100 area %. Anal. ($C_{18}H_{16}N_6 \cdot 3HCl \cdot 0.6H_2O$) C, H, N, Cl.

1,3-Bis(5-amidinopyridin-2-yl)benzene Diacetate 26). **26** was prepared and chromatographed analogously to **25** from amidoxime **69** (700 mg, 2.01 mmol). The product was converted to the free base using aqueous NaOH. A mixture of the free base in H_2O (20 mL) and AcOH (2 mL) was heated and filtered, and the filtrate was lyophilized to give the acetate salt (319 mg, 36%): mp >227−230 °C; ^{1}H NMR δ 10.24 (br s, 8H), 9.10 (d, J = 1.4 Hz, 2H), 8.96 (t, J = 1.5 Hz 1H), 8.33 (m. 6H), 7.73 (t, J = 7.8 Hz, 1H), 1.79 (s, 6H); ESI MS m/z 317.1 ($[M + H]^+$ of free base); HPLC 100 area %. Anal. ($C_{18}H_{18}N_6 \cdot 2.25CH_3CO_2H \cdot 2H_2O$) C, H, N, Cl.

1,3-Bis-(5-*N*′-methoxyamidinopyridin-2-yl)benzene Tetrahydrochloride 27. To a suspension of diamidoxime **69** (348 mg, 1.00 mmol) in DMF (10 mL) was added LiOH·H_2O (252 mg, 6.01 mmol, in 3 mL of H_2O) which was followed by dimethyl sulfate (630 mg, 4.99 mmol). The reaction mixture was stirred overnight, after which it was poured onto ice−water and the precipitate was filtered, washed with water, and dried to give the free base of **27** in 77% yield: mp 157−158 °C; ^{1}H NMR δ 8.96 (s, 2H), 8.84 (s, 1H), 8.09−8.22 (m, 6H), 7.63 (t, J = 7.8 Hz, 1H), 6.30 (br s, 4H), 3.78 (s, 6H); ^{13}C NMR δ 156.1, 149.0, 146.8, 138.6, 134.3, 129.4, 127.5, 127.1, 124.7, 119.8, 60.7.

The free base (200 mg, 0.53 nM) was converted to the tetrahydrochloride salt by stirring overnight in ethanol saturated with HCl(g) to yield a pale yellow solid (205 mg, 69%): mp 196−197.5 °C; MS m/z 377 ($[M + H]^+$ of free base). Anal. ($C_{20}H_{20}N_6O_2 \cdot 4.0\ HCl \cdot 1.1H_2O \cdot 0.5EtOH$) C, H, N.

1,3-Bis[(5-[*N*′-dimethylaminoacetoxy]amidino)pyridin-2-yl]-benzene (28). To a stirred solution of diamidoxime **69** (348 mg, 1.00 mmol) and K_2CO_3 (966 mg, 7 mmol) in DMF (10 mL) was added dimethylaminoacetyl chloride hydrochloride (632 mg, 4 mmol). The reaction mixture was stirred overnight at room temperature and then poured onto brine solution. The precipitate was filtered, recrystallized from methanol to furnish **28** in a 79% yield: mp 156−157.5 °C; ^{1}H NMR (DMSO-d_6) δ 9.02 (s, 2H), 8.90 (s, 1H), 8.19−8.25 (m, 6H), 7.66 (m, 1H), 7.05 (s, 4H), 3.39 (s, 4H), 2.30 (s, 12H); ^{13}C NMR (DMSO-d_6) δ 167.9, 157.2, 154.8, 147.6, 138.4, 135.6, 129.5, 127.9, 126.3, 125.0, 119.9, 58.2, 44.5; MS m/z 519 ($[M + H]^+$ of free base). HRMS calcd for $C_{26}H_{31}N_8O_4$ $[M + H]^+$ 519.2468; observed 519.2457. Anal. ($C_{26}H_{30}N_8O_4 \cdot 1.25H_2O$) C, H, N.

1,3-Bis(4-amidinopyryidin-2-yl)benzene Dihydrochloride (29). **29** was prepared by the general procedure from amidoxime **70** (2.19 g,5.34 mmol). The product was converted to the HCl salt using ethanolic HCl with a trace of water to give a pale pink solid (1.22 g, 59%): mp 309−310 °C; ^{1}H NMR δ 9.92 (br s, 4H), 9.59 (br s, 4H), 9.14 (s,1H), 9.00 (d, J = 5.1 Hz, 2H), 8.64 (s, 2H), 8.35 (dd, J = 8.7 and 1.7 Hz, 2H), 7.84 (dd, J = 5.1 and 1.6 Hz, 2H), 7.75 (t, J = 7.8 Hz, 1H); ESI MS m/z 317.1 ($[M + H]^+$ of free base); HPLC 97.7 area %. Anal. ($C_{18}H_{16}N_6 \cdot 2.4HCl \cdot 1.1H_2O$) C, H, N, Cl.

3,3″-Bis(benzimidoylamino)-5′-chloro-*m*-terphenyl Dihydrochloride (30). A solution of 5′-chloro-3,3″-diamino-*m*-terphenyl (**72**) in THF (30 mL) was added dropwise to a mixture of sodium bis(trimethylsilyl)amide (2 M solution in THF, 6.0 mL, 12.0 mmol) and THF (6.0 mL). The mixture was stirred for 20 min and then split into two portions.

To the first aliquot was added a solution of benzonitrile (0.75 mL, 7.3 mmol), and the mixture was stirred for 3 days. More sodium bis(trimethylsilyl)amide solution (3.0 mL, 6.0 mmol) was added, and the reaction mixture was stirred an additional 3 h before being poured over ice and extracted into CH_2Cl_2. The product was purified by preparative HPLC and lyophilized. A solution of the lyophilized product in EtOH, water, and 1 N HCl was evaporated, dissolved in hot water, filtered, and lyophilized to give the HCl salt as a white powder (682 mg, 42%): mp >200 °C (dec); ^{1}H NMR (400 MHz) δ 11.72 (br s, 2H), 9.95 (br s, 2H), 9.18 (br s, 2H), 8.07 (s, 1H), 8.02 (s, 2H), 7.97 (m, 6H), 7.89 (s, 2H), 7.80 (t, J = 7.4 Hz, 2H), 7.70 (m, 6H), 7.53 (d, J = 7.9 Hz, 2H); ESI MS m/z 501.3 ($[M + H]^+$ of free base); HPLC 98.8 area %. Anal. ($C_{32}H_{25}ClN_4 \cdot 2HCl \cdot 1.5H_2O$) C, H, N, Cl.

3,3″-Bis(picolimidoylamino)-5′-chloro-*m*-terphenyl Dihydrochloride (31). **31** was prepared analogously to **30** using the second aliquot from above and 2-cyanopyridine (0.89 g, 8.55 mmol) in place of benzonitrile to give an off-white powder (661 mg, 41%): mp >170 °C; ^{1}H NMR (400 MHz) δ 11.94 (br s, 2H), 10.19 (br s, 2H), 9.46 (br s, 2H), 8.91 (d, J = 4.0 Hz, 2H), 8.55 (d, J = 7.9 Hz, 2H), 8.24 (t, J = 7.6 Hz, 2H), 8.08 (s, 1H), 8.02 (s, 2H), 7.96 (d, J = 7.7 Hz, 2H), 7.87 (m, 4H), 7.70 (t, J = 7.8 Hz, 2H), 7.54 (d, J = 7.7 Hz, 2H); ESI MS m/z 503.3 ($[M + H]^+$ of free base); HPLC 98.1 area %. Anal. ($C_{30}H_{23}ClN_6 \cdot 2HCl \cdot 2H_2O$) C, H, N, Cl.

3,4″-Bis(benzimidoylamino)-*m*-terphenyl Dihydrochloride (32). Triethylamine (1.5 mL, 10.8 mmol) was added to a stirred suspension of 3,4″-diamino-*m*-terphenyl dihydrochloride (**77**, 1.01 g, 3.03 mmol) in THF (50 mL). After 1.5 h benzonitrile (1.0 mL, 9.80 mmol) was added, followed by the slow addition of sodium bis(trimethylsilyl)amide (2 M solution in THF, 8.0 mL, 16.0 mmol). The reaction mixture was stirred for 3 days, poured over ice, and extracted into $CHCl_3$. The product was purified by preparative HPLC and lyophilized. A solution of the lyophilized product in EtOH and 1 N HCl was evaporated, dissolved in hot water, filtered, and lyophilized to give the HCl salt as a white powder (558 mg, 34%): mp 216 °C; ^{1}H NMR (400 MHz) δ 11.70 (br s, 2H), 9.92 (br s, 2H), 9.15 (br s, 2H), 8.07 (s, 1H), 7.98 (m, 7H), 7.91 (d, J = 7.3 Hz, 1H), 7.79 (m, 4H), 7.70 (m, 6H), 7.61 (d, J = 7.8 Hz, 2H), 7.51 (d, J = 7.3 Hz, 1H); ESI MS m/z 467.6 ($[M + H]^+$ of free base); HPLC 100 area %. Anal. ($C_{32}H_{26}N_4 \cdot 2HCl \cdot 1.5H_2O$) C, H, N, Cl.

3,4″-Bis(picolimidoylamino)-*m*-terphenyl Dihydrochloride (33). **33** was prepared analogously to **32** with 2-cyanopyridine used in place of benzonitrile as a yellow powder (1.04 g, 64%): mp 190 °C; ^{1}H NMR (400 MHz) δ 11.96 (br s, 1H), 11.95 (br s, 1H), 10.17 (br s, 1H), 10.15 (br s, 1H), 9.45 (br s, 1H), 9.39 (br s, 1H), 8.91 (s, 2H), 8.56 (d, J = 8.0 Hz, 1H), 8.52 (d, J = 8.1 Hz, 1H), 8.24 (m, 2H), 8.08 (s, 1H), 8.01 (d, J = 8.2 Hz, 2H), 7.97 (s, 1H), 7.92 (d, J = 7.7 Hz, 1H), 7.87 (m, 2H), 7.80 (m, 2H), 7.71 (t, J = 7.9 Hz, 1H), 7.76 (t, J = 7.8 Hz, 1H), 7.62 (d, J = 8.2 Hz, 2H), 7.52 (d, J = 7.8 Hz, 1H); ESI MS m/z 469.6 ($[M + H]^+$ of free base); HPLC 98.9 area %. Anal. ($C_{30}H_{24}N_6 \cdot 2HCl \cdot 1.9H_2O$) C, H, N, Cl.

3,4″-Bis(benzimidoylamino)-5′-chloro-*m*-terphenyl Dihydrochloride (34). To a solution of 5″-chloro-3,4″-diamino-*m*-terphenyl (**78**, 1.01 g, 3.42 mmol) and benzonitrile (1.10 g, 10.7 mmol) in THF (40 mL) was slowly added sodium bis(trimethylsilyl)-amide (2 M solution in THF, 7.0 mL, 14.0 mmol). The mixture was stirred for 3 days. Workup and purification were analogous to **32**. The final product was recrystallized from hot water to give a gray powder (954 mg, 49%): mp >200 °C (dec); ^{1}H NMR (400 MHz) δ 11.71 (br s, 2H), 9.95 (br s, 2H), 9.19 (br s, 1H), 9.17 (br s, 1H), 8.06 (m, 4H), 7.98 (m, 5H), 7.87 (d, J = 8.4 Hz, 2H), 7.80 (t, J = 7.3 Hz, 2H), 7.70 (m, 5H), 7.63 (d, J = 8.0 Hz, 2H), 7.53 (d, J = 7.7 Hz, 1H); ESI MS m/z 501.2 ($[M + H]^+$ of free base); HPLC 98.7 area %. Anal. ($C_{32}H_{25}ClN_4 \cdot 2HCl \cdot 2.4H_2O$) C, H, N, Cl.

3,4″-Bis(picolimidoylamino)-5′-chloro-*m*-terphenyl Dihydrochloride (35). **35** was prepared analogously to **34** with 2-cyanopyridine used in place of benzonitrile. The HCl salt was prepared using ethanolic HCl to give a yellow powder (668 mg, 34%): mp >190 °C (dec); ^{1}H NMR (400 MHz) δ 11.94 (br s, 2H), 10.18 (br s, 1H), 10.16 (br s, 1H), 9.47 (br s, 1H), 9.41 (br s, 1H), 8.92 (m, 2H), 8.54 (d, J = 8.0 Hz, 1H), 8.51 (d, J = 8.0 Hz, 1H), 8.24 (m, 2H), 8.06 (t, J = 7.5 Hz, 4H), 7.97 (d, J = 7.9 Hz, 1H), 7.89 (m, 2H), 7.86 (m, 2H), 7.71 (t, J = 7.9 Hz, 1H), 7.63 (d, J = 8.7 Hz, 2H), 7.54 (d, J = 7.9 Hz, 1H); ESI MS m/z 503.5 ([M + H]$^+$ of free base); HPLC 98.9 area %. Anal. ($C_{30}H_{23}ClN_6$·2.5HCl·1.5H_2O) C, H, N, Cl.

2-Isopropoxy-4-(picolimidoylamino)-5′-chloro-*m*-terphenyl Dihydrochloride (36). **36** was prepared analogously to **34** from 4-amino-5′-chloro-2-isopropoxy-*m*-terphenyl (**90**, 1.20 g, 3.55 mmol), 2-cyanopyridine (0.67 g, 6.44 mmol), and sodium bis(trimethylsilyl)-amide (2 M solution in THF, 3.0 mL, 6.0 mmol) in THF (60 mL). The product was converted to the HCl salt using ethanolic HCl and ether to give a solid (699 mg, 41%): mp >154 °C (dec); ^{1}H NMR (400 MHz) δ 11.88 (br s, 1H), 10.14 (br s, 1H), 9.38 (br s, 1H), 8.91 (d, J = 4.3 Hz, 1H), 8.50 (d, J = 8.0 Hz, 1H), 8.24 (td, J = 7.8 and 1.4 Hz, 1H), 7.87 (td, J = 7.4 and 4.8 Hz, 1H), 7.76 (m, 2H), 7.74 (s, 1H), 7.71 (d, J = 1.7 Hz, 1H), 7.68 (d, J = 8.1 Hz, 1H), 7.61 (t, J = 1.5 Hz, 1H), 7.52 (t, J = 7.5 Hz, 2H), 7.43 (tt, J = 7.3 and 2.1 Hz, 1H), 7.32 (s, 1H), 7.15 (dd, J = 8.1 and 1.4 Hz, 1H), 4.71 (septet, J = 6.0 H, 1H), 1.31 (d, J = 6.0 Hz, 6H); ESI MS m/z 442.8 ([M + H]$^+$ of free base); HPLC 100 area %. Anal. ($C_{27}H_{24}ClN_3O$·2HCl·0.25H_2O) C, H, N, Cl.

2-Isopropoxy-5-(picolimidoylamino)-5′-chloro-*m*-terphenyl Dihydrochloride (37). **37** was prepared analogously to **36** from 5-amino-5′-chloro-2-isopropoxy-*m*-terphenyl (**91**, 1.42 g, 4.20 mmol) to give a solid (1.01 g, 50%): mp 172–177 °C; ^{1}H NMR (400 MHz) δ 11.68 (br s, 1H), 10.03 (br s, 1H), 9.26 (br s, 1H), 8.89 (dd, J = 3.9 and 0.8 Hz, 1H), 8.45 (d, J = 8.0 Hz, 1H), 8.22 (td, J = 7.8 and 1.2 Hz, 1H), 7.85 (m, 2H), 7.75 (t, J = 7 1.6 Hz, 1H), 7.73 (s, 1H), 7.71 (t, J = 1.0 Hz, 1H), 7.67 (t, J = 1.7 Hz, 1H), 7.65 (d, J = 2.6 Hz, 1H), 7.51 (t, J = 7.5 Hz, 2H), 7.43 (m, 2H), 7.33 (d, J = 9.1 Hz, 1H), 4.76 (septet, J = 6.0 H, 1H), 1.31 (d, J = 6.0 Hz, 6H); ESI MS m/z 442.9 ([M + H]$^+$ of free base); HPLC 99.1 area %. Anal. ($C_{27}H_{24}ClN_3O$·2HCl·0.1H_2O) C, H, N, Cl.

General Suzuki Coupling Procedure for Cyano-Substituted Terphenyls and Biphenyls 43–45, 47–50, and 53–56. A solution of tetrakis(triphenylphosphine)palladium(0) (5–10 mol %) and the dibromobenzene (1 equiv) in DME (50 mL) was stirred for 15–30 min under Ar. The boronic acid (2.2–2.5 equiv for double couplings, 1–1.2 equiv for single couplings) was added, followed by Na_2CO_3 (10% solution, 75 mL). The mixture was refluxed until reaction was complete. The cooled reaction mixture was worked up by extraction into an appropriate solvent. The product was purified by chromatography on silica gel and recrystallization from an appropriate solvent.

4,4″-Dicyano-*m*-terphenyl (43). **43** was prepared from 1,3-dibromobenzene (**38**, 1.97 g, 8.35 mmol) and 4-cyanophenylboronic acid (2.61g, 17.8 mmol). Column chromatography by gradient elution using hexanes/EtOAc mixtures followed by recrystallization from EtOAc–hexanes gave an ivory colored solid (1.59 g, 68%): mp 199–203 °C; ^{1}H NMR δ 8.09 (t, J = 1.8 Hz, 1H), 8.04 (d, J = 8.5 Hz, 4H), 8.97 (d, J = 8.4 Hz, 4H), 7.84 (dd, (d, J = 7.7 and 1.5 Hz, 2H), 7.66 (t, J = 7.8 Hz, 1H); HPLC 100 area %. Anal. ($C_{20}H_{12}N_2$) C, H, N.

4,4″-Dicyano-5′-chloro-*m*-terphenyl (44). **44** was prepared from dibromobenzene **39** (1.62g, 6.00 mmol) and 4-cyanophenylboronic acid (2.21 g, 15.0 mmol). Column chromatography, eluting with $CHCl_3$ followed by recrystallization from toluene containing a trace of DMF, gave a white solid (1.48 g, 78%): mp 297–301 °C; ^{1}H NMR δ 8.09 (m, 5H), 7.98 (d, J = 8.4 Hz, 4H), 7.92 (d, J = 1.5 Hz, 2H). Anal. ($C_{20}H_{11}ClN_2$) C, H, N.

4,4″-Dicyano-5′-nitro-*m*-terphenyl (45). **45** was prepared from dibromobenzene **40** (1.69 g, 6.01 mmol) and 4-cyanophenylboronic acid (2.21g, 15.0 mmol). The reaction mixture was poured over ice to precipitate the crude product, which was recrystallized from DMF–EtOH to give a solid (1.18 g, 60%): mp 319–320 °C; ^{1}H NMR δ 8.58 (d, J = 1.5 Hz, 2H), 8.55 (t, J = 1.5 Hz, 1H), 8.18 (d, J = 8.3 Hz, 4H), 8.03 (d, J = 8.3 Hz, 4H). Anal. ($C_{20}H_{11}N_3O_2$·0.1H_2O) C, H, N.

4,4″-Dicyano-5′-hydroxy-*m*-terphenyl (46). To a stirred solution of 3,5-dibromophenol (**41**, 1.25 g, 5.0 mmol) and tetrakis(triphenylphosphine)palladium (200 mg) in toluene (10 mL) under a nitrogen atmosphere was added 5 mL of a 2 M aqueous solution of Na_2CO_3 followed by 4-cyanophenylboronic acid (0.37 g, 2.5 mmol) in methanol (5 mL). The vigorously stirred mixture was warmed to 80 °C for 12 h. The solvent was evaporated, and the precipitate was partitioned between methylene chloride (200 mL) and 2 M aqueous Na_2CO_3 (15 mL) containing 3 mL of concentrated ammonia. The organic layer was dried and then concentrated to dryness under reduced pressure to afford **46** as a white solid in 76% yield: mp 290–292 °C; ^{1}H NMR δ 10.00 (br s, 1H), 7.92–7.94 (m, 8H), 7.58 (s, 1H), 7.15 (s, 2H); ^{13}C NMR δ 158.5, 144.4, 140.5, 132.8, 127.8, 118.8, 116.9, 114.2, 110.3.

4,4″-Dicyano-5′-methoxy-*m*-terphenyl (47). **47** was prepared from dibromobenzene **42** (1.60 g, 6.03 mmol) and 4-cyanophenylboronic acid (2.21g, 15.0 mmol). Purification by column chromatography, eluting with C_2HCl_2/hexanes (4:1) followed by recrystallization from CH_3CN–H_2O, gave a solid (1.51 g, 81%): mp 239–241 °C; ^{1}H NMR δ 8.04 (d, J = 8.6 Hz, 4H), 7.95 (d, J = 8.5 Hz, 4H), 7.66 (t, J = 1.5 Hz, 1H), 7.37 (d, J = 1.5 Hz, 2H), 3.93 (s, 3H). Anal. ($C_{21}H_{14}N_2O_2$) C, H, N.

3,3″-Dicyano-*m*-terphenyl (48).[61] **48** was prepared from 1,3-dibromobenzene (**38**, 2.66 g, 11.3 mmol) and 3-cyanophenylboronic acid (3.75 g, 25.5 mmol). Column chromatography, eluting with hexanes/EtOAc (3:1) mixtures followed by recrystallization from CH_3CN, gave a white solid (2.38 g, 75%): mp 165–167 °C (lit.[61] 164–165°); ^{1}H NMR δ 8.37 (t, J = 1.5 Hz, 2H), 8.18 (ddd, J = 8.0, 1.9, and 1.1 Hz, 2H), 8.13 (t, J = 1.6 Hz, 1H), 7.87 (dt, J = 7.7 and 1.4 Hz, 2H), 7.82 (dd, J = 8.0 and 1.5 Hz, 2H), 7.71 (t, J = 7.8 Hz, 2H), 7.55 (t, J = 7.6 Hz, 1H). Anal. ($C_{20}H_{12}N_2$) C, H, N.

3,3″-Dicyano-5′-chloro-*m*-terphenyl (49). **49** was prepared from dibromobenzene **39** (1.63 g, 6.03 mmol) and 3-cyanophenylboronic acid (2.22 g, 15.1 mmol). Purification by column chromatography, eluting with $CHCl_3$ followed by recrystallization from DMF, gave a light gray solid (991 mg, 52%): mp 279–277 °C; ^{1}H NMR δ 8.43 (t, J = 1.6 Hz, 2H), 8.23 (dm, J = 8.0 Hz, 2H), 8.11 (t, J = 1.6 Hz, 1H), 7.93 (d, J = 1.6 Hz, 2H), 7.90 (dt, J = 7.9 and 1.3 Hz, 2H), 7.71 (t, J = 7.9 Hz, 2H). Anal. ($C_{20}H_{11}ClN_2$·0.1H_2O) C, H, N.

3,3″-Dicyano-5′-methoxy-*m*-terphenyl (50). **50** was prepared from dibromobenzene **42** (1.33 g, 5.01 mmol) and 3-cyanophenylboronic acid 1.84 g, 12.5 mmol). The product was chromatographed on silica, eluting with CH_2Cl_2/hexanes (4:1) and recrystallized from CH_3CN–H_2O to give a solid (1.32 g, 71%): mp 194–196 °C; ^{1}H NMR δ 8.38 (t, J = 1.5 Hz, 2H), 8.19 (dm, J = 8.7 Hz, 2H), 7.87 (dt, J = 7.8 and 1.3 Hz, 2H), 7.70 (t, J = 1.5 Hz, 1H), 7.69 (t, J = 7.7 Hz, 2H), 7.37 (d, J = 1.5 Hz, 2H), 3.93 (s, 3H). Anal. ($C_{21}H_{14}N_2O$) C, H, N.

3-Bromo-4′-cyanobiphenyl (53). **53** was prepared from iodobenzene **51** (3.06 g, 10.8 mmol) and 4-cyanophenylboronic acid (1.50 g, 10.2 mmol). The product was chromatographed on a silica column, eluting with hexanes/EtOAc (9:1) and recrystallized from toluene–hexanes to give white crystals (1.86 g, 71%): mp 56–57 °C; ^{1}H NMR δ 7.97 (t, J = 1.8 Hz, 1H), 7.95 (d, J = 8.5 Hz, 2H), 7.92 (d, J = 8.9 Hz, 2H), 7.77 (ddd, J = 7.7, 1.6, and 1.0 Hz, 1H), 7.66 (ddd, J = 8.1, 2.0, and 1.1 Hz, 1H), 7.48 (t, J = 8.0 Hz, 1H). Anal. ($C_{13}H_8BrN$) C, H, N.

3-Bromo-5-chloro-4′-cyanobiphenyl (54). **54** was prepared from iodobenzene **52** (868 mg, 2.73 mmol) and 4-cyanophenylboronic acid (402 mg, 2.73 mmol). The product was purified on a silica column, eluting with hexane/EtOAc (9:1) to give a solid (0.47 g, 59%): mp 128–129 °C; ^{1}H NMR δ 7.96 (m, 5H), 7.86 (m, 1H), 7.81 (m, 1H); HPLC 100 area %. Anal. ($C_{13}H_7BrClN$) C, H, N.

3,4″-Dicyano-*m*-terphenyl (55). **55** was prepared from bromobiphenyl **53** (2.59 g, 10.0 mmol) and 3-cyanophenylboronic acid (1.77 g, 12.1 mmol). The product was chromatographed on a silica column, eluting with $CHCl_3$ and recrystallized from CH_3CN–H_2O to give white crystals (2.35 g, 83%): mp 139–142 °C; ^{1}H NMR δ 8.37 (t, J =

1.5 Hz, 1H), 8.16 (dm, J = 8.0 Hz, 1H), 8.12 (t, J = 1.8 Hz, 1H), 8.06 (d, J = 8.7 Hz, 2H), 7.97 (d J = 8.7 Hz, 2H), 7.87 (dt, J = 7.8 and 1.3 Hz, 1H), 7.82 (m, 2H), 7.70 (t, J = 7.8 Hz, 1H), 7.64 (t, J = 7.7 Hz, 1H). Anal. ($C_{20}H_{12}N_2$) C, H, N.

5′-Chloro-3,4″-dicyano-*m*-terphenyl (56). **56** was prepared from **54** (1.20 g, 4.11 mmol) and 3-cyanophenylboronic acid (788 mg, 5.36 mmol). The reaction mixture was diluted with water to precipitate the product, which was then recrystallized from CH_3CN to give a solid (950 mg, 74%): mp 235−236 °C; ^{1}H NMR δ 8.42 (d, J = 1.6 Hz, 1H), 8.21 (ddd, J = 8.0, 1.8, and 1.1 Hz, 1H), 8.09 (m, 3H), 7.98 (d, J = 8.5 Hz, 2H), 7.94 (t, J = 1.7 Hz, 1H), 7.89 (m, 2H), 7.71 (t, J = 7.8 Hz, 1H); HPLC 97.1 area %. Anal. ($C_{20}H_{11}ClN_2$) C, H, N.

5-(4,4,5,5-Tetramethyl-1,3,2-dioxaborolan-2-yl)-picolinonitrile (59). A mixture of 5-bromopicolinonitrile (**57**, 2.93 g, 16.0 mmol), bis(pinacolato)diboron (4.50 g, 17.7 mmol), $PdCl_2{\cdot}CH_2Cl_2$ (401 mg, 0.191 mmol), and potassium acetate (4.75 g, 48.4 mmol) in DMSO (45 mL) was heated for 90 °C for 6 h. The reaction mixture was partitioned between water and toluene and then filtered through Celite, and the aqueous layer was extracted with toluene. The dried extracts were evaporated to a solid (3.11 g, 85%) which was used directly in the next step: ^{1}H NMR δ 8.88 (m, 1H), 8.22 (m, 1H), 8.04 (m, 1H), 1.33 (s, 12H).

5-(4,4,5,5-Tetramethyl-1,3,2-dioxaborolan-2-yl)-nicotinonitrile (60). **60** was prepared analogously to **59** from 5-bromonicotinonitrile (**58**, 5.16 g, 28.19 g) to give a solid (6.37 g, 98%) which was used directly in the next step: ^{1}H NMR δ 9.14 (d, J = 2.1 Hz, 1H), 8.99 (d, J = 1.5 Hz, 1H), 8.40 (t, J = 1.9 Hz,, 1H), 1.33 (s, 12H).

General Suzuki Coupling Procedure for Dipyridylbenzene Derivatives 61, 62, 67, and 68. A mixture of the appropriate aryl halide and boronic acid or ester, tetrakis(triphenylphosphine)-palladium(0) (0.05 equiv), and silver carbonate (2.5 equiv) was stirred in refluxing THF until reaction was complete (2−3 h). The reaction mixture was filtered through Celite, and the Celite pad was rinsed with hot THF. The evaporated filtrate was purified by column chromatography or by direct recrystallization.

1,3-Bis(6-cyanopyridin-3-yl)benzene (61). **61** was prepared from 1,3-diodobenzene (2.02 g, 6.12 mmol) and 5-(4,4,5,5-tetramethyl-1,3,2-dioxaborolan-2-yl)nicotinonitrile (**59**, 3.11 g, 13.5 mol). Column chromatography on silica, eluting with 2% MeOH in $CHCl_3$ followed by recrystallization of the crude product from CH_3CN−ether, gave a white solid (1.04 g, 60%): mp 233−236 °C; ^{1}H NMR δ 9.27 (d, J = 2.2 Hz, 2H), 8.53 (dd, J = 8.2 and 2.3 Hz, 2H), 8.30 (t, J = 1.8 Hz, 1H), 8.19 (d, J = 8.1 Hz, 2H), 7.98 (dd, J = 7.8 and 1.8 Hz, 2H), 7.83 (t, J = 7.8 Hz, 1H); HPLC 98.0 area %. Anal. ($C_{18}H_{10}N_4$) C, H, N.

1,3-Bis(5-cyanopyridin-3-yl)benzene (62). **62** was prepared from 1,3-diiodobenzene (1.65 g, 5.00 mmol) and boronate ester **60** (2.88 g, 12.5 mmol). The crude product was directly recrystallized from CH_3CN−ether to give a white solid (981 mg, 69%): mp 254−255 °C; ^{1}H NMR δ 9.37 (d, J = 2.3 Hz, 2H), 9.07 (d, J = 1.9 Hz, 2H), 8.86 (t, J = 2.2 Hz, 2H), 8.30 (t, J = 1.8 Hz, 1H), 7.97 (dd, J = 7.8 and 1.8 Hz, 2H), 7.71 (t, J = 7.8 Hz, 1H); HPLC 98.2 area %. Anal. ($C_{10}H_{10}N_4{\cdot}0.2H_2O$) C, H, N.

General Procedure for Amidoximes 63, 64, 69, and 70. Potassium *tert*-butoxide (10 equiv) was added to a solution of hydroxylamine hydrochloride (10 equiv) in DMSO (0.5−0.6 mL/mmol hydroxylamine hydrochloride). After 1 h the nitrile (1 equiv) was added and the reaction mixture was stirred overnight. The reaction mixture was poured over ice. The resulting precipitated product was filtered off and dried.

1,3-Bis(6-*N*′-hydroxyamidinopyridin-3-yl)benzene (63). **63** was prepared from nitrile **61** (1.03 g, 3.65 mmol) to give a white solid (1.28 g, 101%): ^{1}H NMR δ 10.06 (s, 2H), 9.02 (d, J = 2.3 Hz, 2H), 8.26 (dd, J = 8.4 and 2.3 Hz, 2H), 8.14 (t, J = 1.6 Hz, 1H), 7.96 (d, J = 8.4 Hz, 2H), 7.84 (dd, J = 7.7 and 1.6 Hz, 2H), 7.66 (t, J = 7.4 Hz, 1H), 5.91 (br s, 4H); HPLC 97.2 area %. The product was used in the next step without further purification.

1,3-Bis(5-*N*′-hydroxyamidinopyridin-3-yl)benzene (64). **64** was prepared from nitrile **62** (858 mg, 3.04 mmol) to give a light gray solid (1.07 g, 101%): ^{1}H NMR δ 9.92 (s, 2H), 9.02 (d, J = 2.2 Hz, 2H), 8.90 (d, J = 1.9 Hz, 2H), 8.38 (t, J = 2.0 Hz, 2H), 8.19 (m, 1H), 7.87 (dd, J = 7.8 and 1.5 Hz, 2H), 7.68 (t, J = 8.0 Hz, 1H), 6.14 (br s, 4H). The product was used in the next step without further purification.

1,3-Bis(5-cyanopyridin-2-yl)benzene (67). **67** was prepared analogously to **61** from bromopyridine **65** (2.02 g, 11.0 mmol) and 1,3-benzenediboronic acid (912 mg, 5.5 mmol). The product was purified on a column of silica, eluting with a gradient of 0−2% MeOH in $CHCl_3$ followed by recrystallization from CH_3CN to give a solid (976 mg, 63%): mp 241−242 °C; ^{1}H NMR δ 9.16 (dd, J = 2.0 and 0.9 Hz, 2H), 8.99 (t, J = 1.9 Hz, 1H), 8.46 (dd, J = 8.4 and 2.1 Hz, 2H), 8.37 (dd, J = 8.3 and 1.0 Hz, 2H), 8.33 (dd, J = 7.9 and 1.8 Hz, 2H), 7.73 (t, J = 7.8 Hz, 1H); HPLC 98.0 area %. Anal. ($C_{18}H_{10}N_4$) C, H, N.

1,3-Bis(4-cyanopyridin-2-yl)benzene (68). **68** was prepared analogously to **61** from bromopyridine **66** (4.50 g, 24.6 mmol) and 1,3-benzenediboronic acid (2.00 g, 12.1 mmol). After filtration of the reaction mixture through Celite, the filtrate was concentrated and diluted with ether to give a precipitate (2.98 g, 87%): mp 238−239 °C; ^{1}H NMR δ 8.96 (dd, J = 5.0 and 0.9 Hz, 2H), 8.91 (t, J = 1.7 Hz, 1H), 8.69 (t, J = 1.1 Hz, 2H), 8.32 (dd, J = 7.8 and 1.8 Hz, 2H), 7.88 (dd, J = 5.0 and 1.4 Hz, 2H), 7.71 (t, J = 7.8 Hz, 1H); HPLC 99.0 area %. Anal. ($C_{10}H_{18}N_4$) C, H, N.

1,3-Bis(5-*N*′-hydroxyamidinopyryidin-2-yl)benzene (69). **69** was prepared analogously to **63** from nitrile **67** (0.960 g, 3.40 mmol) to give a light gray solid (1.20 g, 101%): ^{1}H NMR δ 9.92 (s, 2H), 9.01 (dd, J = 1.8 and 1.2 Hz, 2H), 8.87 (t, J = 1.6 Hz, 1H), 8.20 (dd, J = 7.8 and 1.8 Hz, 2H), 8.15 (m, 4H), 7.68 (t, J = 7.8 Hz, 1H), 6.07 (br s, 4H); HPLC 98.5 area %. The product was used in the next step without further purification.

1,3-Bis(4-*N*′-hydroxyamidinopyryidin-2-yl)benzene (70). **70** was prepared analogously to **63** from nitrile **68** (1.51 g, 5.34 mmol). The sticky, filtered precipitate was dissolved in hot ethanol, and the solution was evaporated to a light gray solid (2.19 g, 118%, wet): ^{1}H NMR δ 10.12 (s, 2H), 8.88 (t, J = 1.6 Hz, 1H), 8.71 (d, J = 5.1 Hz, 2H), 8.30 (s, 2H), 8.21 (dd, J = 7.8 and 1.7 Hz, 2H), 7.66 (m, 3H), 6.20 (br s, 4H); HPLC 98.0 area %. The product was used in the next step without further purification.

Nitro-Substituted Terphenyl and Biphenyl Derivatives 71 and 73−76. Compounds **71** and **73−76** were prepared by Suzuki coupling reaction conditions analogous to those for compounds **43−45**, **47−50**, and **53−56**.

5′-Chloro-3,3″-dinitro-*m*-terphenyl (71). **71** was prepared from dibromide **39** (1.35 g, 5.00 mmol) and 3-nitrophenylboronic acid (1.85 g, 11.1 mmol). The reaction mixture was poured over ice, and the precipitated crude product was recrystallized from DMF as a gray solid (1.35 g, 76%): mp 242−243 °C; ^{1}H NMR δ 8.66 (t, J = 2.0 Hz, 2H), 8.34 (dm, J = 8.5 Hz, 2H), 8.29 (dm, J = 8.2 Hz, 2H), 8.16 (t, J = 1.6 Hz, 1H), 7.97 (d, J = 1.6 Hz, 2H), 7.81 (t, J = 8.0 Hz, 2H). Anal. ($C_{18}H_{11}ClN_2O_4{\cdot}0.2H_2O$) C, H, N.

5′-Chloro-3,3″-diamino-*m*-terphenyl (72). A mixture of dinitroterphenyl **71** (2.98 g, 8.40 mmol) and tin(II) chloride dihydrate (3 × 10.0 g portions, 133 mmol) in EtOH (100 mL) was refluxed for 3 h. The reaction mixture was diluted with water, neutralized by cautious addition of $NaHCO_3$, and extracted into CH_2Cl_2. Both layers were filtered through Celite, and the aqueous layer was extracted with CH_2Cl_2. Combined dried extracts were evaporated to a white solid (2.16 g, 87%), which was recrystallized from EtOH to give a white solid (1.24 g, 50%): mp 153−154 °C; ^{1}H NMR δ 7.65 (t, J = 1.6 Hz, 1H), 7.53 (d, J = 1.6 Hz, 2H), 7.13 (t, J = 7.8 Hz, 2H), 6.92 (t, J = 1.9 Hz, 2H), 6.86 (dd, J = 7.6 and 0.9 Hz, 2H), 6.62 (ddd, J = 8.0, 2.2, and 0.9 Hz, 2H), 5.20 (br s, 4H); ESI MS m/z 295.7 ($[M + H]^+$). Anal. ($C_{18}H_{15}ClN_2{\cdot}0.1H_2O$) C, H, N.

3-Bromo-4′-nitrobiphenyl (73). **73** was prepared from iodobenzene **51** (5.76 g, 20.4 mmol) and 4-nitrophenylboronic acid pinacol ester (5.04 g, 20.2 mmol). The product was purified on a column of silica, eluting with a gradient of 0−40% EtOAc in hexanes and recrystallized from EtOAc/hexanes to give yellow crystals (4.60 g, 82%): mp 88 °C; ^{1}H NMR δ 8.31 (d, J = 8.8 Hz, 2H), 8.01 (m, 3H),

7.87 (dm, J = 7.8 Hz, 1H), 7.69 (dm, J = 9.0 Hz, 1H), 7.50 (t, J = 7.9 Hz, 1H); HPLC 98.8 area %. Anal. ($C_{12}H_8BrN_2O$) C, H, N.

3-Bromo-5-chloro-4′-nitrobiphenyl (74). **74** was prepared from iodobenzene **52** (2.55 g, 8.04 mmol) and 4-nitrophenylboronic acid pinacol ester (2.00 g, 8.04 mmol). The product was purified on a column of silica, eluting with hexanes/EtOAc (19:1) and recrystallized from EtOAc–hexane to give white crystals (1.51 g, 60%): mp 147–148 °C; ^{1}H NMR δ 8.30 (d, J = 8.7 Hz, 2H), 8.06 (d, J = 8.8 Hz, 2H), 8.00 (t, J = 1.6 Hz, 1H), 7.92 (t, J = 1.7 Hz, 1H), 7.84 (t, J = 1.7 Hz, 1H); HPLC 100 area %.

3,4″-Dinitro-*m*-terphenyl (75). **75** was prepared from bromobiphenyl **73** (4.53 g, 16.3 mmol) and 3-nitrophenylboronic acid (2.82 g, 16.9 mmol). Column chromatography, eluting with a gradient from hexanes/EtOAc (4:1) to neat EtOAc followed by recrystallization from EtOH, gave a white solid (3.27 g, 63%): mp 188–189 °C; ^{1}H NMR δ 8.60 (t, J = 2.0 Hz, 1H), 8.34 (dm, J = 8.9 Hz, 2H), 8.28 (m, 2H), 8.17 (t, J = 1.7 Hz, 1H), 8.13 (dm, J = 8.9 Hz, 2H), 7.89 (m, 2H), 7.81 (t, J = 8.0 Hz, 1H), 7.69 (t, J = 7.7 Hz, 1H). Anal. ($C_{18}H_{12}N_2O_4 \cdot 0.05H_2O$) C, H, N.

5′-Chloro-3,4″-dinitro-*m*-terphenyl (76). **76** was prepared from bromobiphenyl **74** (2.09 g, 6.68 mmol) and 3-nitrophenylboronic acid (1.69 g, 8.33 mmol). The reaction mixture was diluted with water. The resulting precipitate was filtered off, dried, and purified by suspension in hot ethanol to give a light gray solid (2.18 g, 92%): mp 216–218 °C; ^{1}H NMR δ 8.64 (t, J = 2.0 Hz, 1H), 8.33 (m, 3H), 8.29 (ddd, J = 8.2, 2.2, and 0.9 Hz, 1H), 8.17 (d, J = 8.9 Hz, 2H), 8.14 (t, J = 1.6 Hz, 1H), 7.99 (t, J = 1.7 Hz, 1H), 7.95 (t, J = 1.7 Hz, 1H), 7.81 (t, J = 8.0 Hz, 1H); HPLC 100 area %. Anal. ($C_{18}H_{11}ClN_2O_4 \cdot 0.5H_2$).

3,4″-Diamino-*m*-terphenyl Dihydrochloride (77). A mixture of dinitroterphenyl **75** (3.00 g, 9.37 mmol) and 10% Pd/C (0.60 g, 0.56 mmol) in EtOH (300 mL) was hydrogenated at 60 psi. The reaction mixture was filtered through Celite. The filtrate was concentrated to a small volume, treated with saturated ethanolic HCl, and diluted with ether to give the hydrochloride salt as a white solid (2.24 g, 72%): mp >250 °C (dec); ^{1}H NMR δ 10.10 (br s, 4H), 7.89 (m, 1H), 7.85 (d, J = 8.5 Hz, 2H), 7.77 (dm, J = 7.8 Hz, 1H), 7.72 (m, 2H), 7.61 (m, 3H), 7.43 (d, J = 8.5 Hz, 2H), 7.36 (dm, J = 7.8 Hz, 1H). Anal. ($C_{18}H_{16}N_2 \cdot 2HCl \cdot 0.2H_2O$) C, H, N, Cl.

5″-Chloro-3,4″-diamino-*m*-terphenyl (78). Iron powder (3.60 g, 64.5 mmol) was added to a mixture of dinitroterphenyl **76** (2.19 g, 6.15 mmol) and ammonium chloride 1.02 g, 19.1 mmol) in refluxing EtOH/H_2O (2:1 mixture, 90 mL), and refluxing was continued for 2.5 h. The reaction mixture was cooled and filtered through Celite. The filtrate was diluted with water and extracted into ether. The extract was concentrated to ~50 mL and treated with saturated ethanolic HCl (3 mL) to precipitate the HCl salt (1.94 g, 85%). The salt was dissolved in hot water, filtered, and diluted with NaOH solution to precipitate the free base as a white solid (1.26 g, 69%) which was used directly in the next step: ^{1}H NMR δ 7.62 (t, J = 1.5 Hz, 1H), 7.51 (t, J = 1.7 Hz, 1H), 7.45 (d, J = 8.6 Hz, 2H), 7.39 (t, J = 1.7 Hz, 1H), 7.12 (t, J = 7.8 Hz, 1H), 6.91 (t, J = 1.9 Hz, 1H), 6.86 (d, J = 7.6 Hz, 1H), 6.65 (d, (t, J = 8.5 Hz, 2H), 6.60 (d, J = 7.9 Hz, 1H), 5.34 (br s, 2H), 5.17 (br s, 2H); HPLC 96.3 area %.

4-Amino-3-chlorobiphenyl (80). **80** was prepared analogously to compound **71** from 4-bromo-2-chloroaniline (**79**, 5.25 g, 25.4 mmol) and phenylboronic acid (3.75 g, 30.8 mmol). The product was chromatographed on a column of silica, eluting with 15–20% EtOAc in hexanes followed by recrystallization from hexanes to give a solid (3.62 g, 70%): mp 69–70 °C; ^{1}H NMR δ 7.56 (d, J = 7.3 Hz, 2H), 7.50 (d, J = 2.0 Hz, 1H), 7.38 (m, 3H), 7.25 (t, J = 7.3 Hz, 1H), 6.87 (d, J = 8.4 Hz, 1H), 5.48 (s, 2H); HPLC 100 area %. Anal. ($C_{12}H_{10}ClN$) C, H, N.

4-Amino-3-bromo-5-chlorobiphenyl (81). *N*-Bromosuccinimide (3.84 g, 21.6 mmol) was added to a solution of aminobiphenyl **80** (4.33 g, 21.3 mmol) in THF (60 mL) at 0 °C. After 1 h the reaction mixture was quenched with $NaHSO_3$ solution, neutralized with $NaHCO_3$ solution, and extracted into EtOAc. Column chromatography on silica, eluting with hexanes/EtOAc (9:1) followed by recrystallization from EtOAc–hexanes, gave crystals (5.00 g, 83%): mp 111–112 °C; ^{1}H NMR δ 7.71 (d, J = 2.1 Hz, 1H), 7.61 (t, J = 2.0 Hz, 2H), 7.59 (m, 1H), 7.41 (tm, J = 7.6 Hz, 2H), 7.30 (tm, J = 7.3 Hz, 1H), 5.54 (s, 2H); HPLC 100 area %. Anal. ($C_{12}H_9BrClN$) C, H, N.

3-Bromo-5-chlorobiphenyl (82). A solution of 4-amino-3-bromo-5-chlorobiphenyl (**81**, 4.51 g, 16.0 mmol) in EtOH (25 mL) was treated dropwise with H_2SO_4 (5 mL). Sodium nitrite (2.74 g, 39.7 mmol) was added, and the mixture was refluxed for 30 min. The reaction mixture was poured over ice and excess $NaHCO_3$ and then extracted into EtOAc. Column chromatography on silica, eluting with hexanes, gave a clear oil that solidified upon standing (4.52 g, 86%): mp 32–33 °C; ^{1}H NMR δ 7.85 (t, J = 1.5 Hz, 1H), 7.77 (t, J = 1.6 Hz, 1H), 7.73 (m, 3H), 7.49 (m, 2H), 7.43 (m, 1H); HPLC 99.5 area %. Anal. ($C_{12}H_8BrCl$) C, H, N.

(5-Chloro-biphenyl-3-yl)boronic Acid (83). Butyllithium (2.5 M/hexanes, 4.5 mL, 11.25 mmol) was added dropwise over 15 min to a solution of 3-bromo-5-chlorobiphenyl (**82**, 2.49 g, 9.31 mmol) in THF (150 mL) at −78 °C. The mixture was maintained for 1 h before the dropwise addition of triisopropyl borate (4.5 mL, 19.6 mmol). The mixture was maintained another hour at −78 °C before being warmed to ambient temperature. The reaction mixture was quenched with 1 N HCl (150 mL) and extracted with ether. The dried extract was evaporated to a white solid (2.12 g, 98%) which was used in the next step without further purification.

5′-Chloro-2-isopropoxy-4-nitro-*m*-terphenyl (88). **88** was prepared analogously to compounds **43–50** from bromobenzene **86** (1.35 g, 5.17 mmol) and boronic acid **83** (1.54 g, 6.62 mmol). The product was purified on a column of silica, eluting with hexanes/EtOAc (50:1) followed by recrystallization from EtOH to give yellow crystals (1.57 g, 82%): mp 100–101 °C; ^{1}H NMR δ 7.89 (m, 2H), 7.80 (t, J = 1.8 Hz, 1H), 7.76 (m, 4H), 7.63 (t, J = 1.7 Hz, 1H), 7.50 (tm, J = 7.4 Hz, 2H), 7.42 (tm, J = 7.3 Hz, 1H), 4.87 (septet, J = 6.0 Hz, 1H), 1.30 (d, J = 6.0 Hz, 6H); HPLC 96.2 area %. Anal. ($C_{21}H_{18}ClNO_3$) C, H, N.

5′-Chloro-2-isopropoxy-5-nitro-*m*-terphenyl (89). **89** was prepared analogously to compounds **43–50** from bromobenzene **87** (1.30 g, 5.01 mmol) and boronic acid **83** (1.50 g, 1.29 mmol). The product was purified on a column of silica, eluting with hexane/EtOAc (17:3) to give a white solid (1.68 g, 91%): mp 111 °C; ^{1}H NMR δ 8.28 (dd, J = 7.5 and 2.9 Hz, 1H), 8.26 (d, J = 2.9 Hz, 1H), 7.80 (t, J = 1.5 Hz, 1H), 7.77 (d, J = 1.4 Hz, 1H), 7.74 (t, J = 1.8 Hz, 2H), 7.63 (t, J = 1.7 Hz, 1H), 7.50 (t, J = 7.5 Hz, 2H), 7.41 (m, 2H), 4.91 (septet, J = 6.0 Hz, 1H), 1.32 (d, J = 6.0 Hz, 6H); HPLC 100%. Anal. ($C_{21}H_{18}ClNO_3$) C, H, N.

4-Amino-5′-chloro-2-isopropoxy-*m*-terphenyl (90). A solution of nitroterphenyl **88** (1.57 g, 4.26 mmol) in EtOH (75 mL) was brought to reflux. Tin(II) chloride dihydrate (5.18 g, 29.6 mmol) was slowly added via the condenser, and refluxing was continued for 1.5 h. The reaction mixture was portioned between ether and water basified with 1 N NaOH, and the aqueous layer was extracted twice with ether. Combined extracts were filtered through Celite. Column chromatography on silica, eluting with hexanes/EtOAc (3:2), gave a glass (1.20 g, 83%): ^{1}H NMR δ 7.70 (d, J = 7.2 Hz, 2H), 7.66 (t, J = 1.5 Hz, 1H), 7.48 (m, 4H), 7.40 (t, J = 7.3 Hz, 1H), 7.13 (d, J = 8.2 Hz, 1H), 6.34 (d, J = 2.0 Hz, 1H), 6.25 (dd, J = 8.2 and 2.0 Hz, 1H), 5.30 (s, 2H), 4.47 (septet, J = 6.1 Hz, 1H), 1.25 (d, J = 6.0 Hz, 6H). The product was used in the next step without further purification.

5-Amino-5′-chloro-2-isopropoxy-*m*-terphenyl (91). **91** was prepared analogously to compound **90** from nitroterphenyl **89** (1.64 g, 4.46 mmol). Column chromatography on silica, eluting with hexane/EtOAc (2:1), gave a glass (1.42 g, 94%): ^{1}H NMR δ 7.72 (m, 3H), 7.64 (t, J = 1.8 Hz, 1H), 7.51 (m, 3H), 7.41 (tm, J = 7.3 Hz, 1H), 6.84 (d, J = 8.7 Hz, 1H), 6.69 (d, J = 2.9 Hz, 1H), 6.57 (dd, J = 8.6 and 2.8 Hz, 1H), 4.79 (s, 2H), 4.15 (septet, J = 6.1 Hz, 1H), 1.11 (d, J = 6.0 Hz, 6H); HPLC 97.5 area %. The product was used in the next step without further purification.

AUTHOR INFORMATION

Corresponding Author

*Phone: 919-966-4294. Fax: 919-966-0704. E-mail: Tidwell@med.unc.edu.

Notes

The authors declare no competing financial interest.

ACKNOWLEDGMENTS

This work was supported by the Consortium for Parasitic Drug Development (CPDD), the Bill and Melinda Gates Foundation, and Medicines for Malaria Venture (MMV).

ABBREVIATIONS USED

AIA, arylimidamide; DMTHP, 5,5-dimethyl-1,4,5,6-tetrahydropyrimidin-2-yl; HAT, human African trypanosomiasis; NECT, nifurtimox−eflornithine combination therapy; pK_a, ionization constant; SI, selectivity index; VL, visceral leishmaniasis; WHO, World Health Organization

REFERENCES

(1) African trypanosomiasis (sleeping sickness). http://www.who.int/mediacentre/factsheets/fs259/en/ (accessed Mar 28, 2013).

(2) Malaria. http://www.who.int/mediacentre/factsheets/fs094/en/index.html (accessed Mar 28, 2013).

(3) Leishmaniasis. http://www.who.int/topics/leishmaniasis/en/ (accessed Mar 28, 2013).

(4) Chagas disease (American trypanosomiasis). http://www.who.int/mediacentre/factsheets/fs340/en/index.html (accessed Apr 26, 2012).

(5) Leishmaniasis. http://www.who.int/leishmaniasis/burden/en/ (accessed Mar 28, 2013).

(6) Legros, D.; Ollivier, G.; Gasteullu-Etchegorry, M.; Paquet, C.; Burri, C.; Jannin, J.; Buscher, P. Treatment of human African trypanosomiasis—present situation and needs for research and development. *Lancet Infect. Dis.* **2002**, *2*, 437−440.

(7) Astelbauer, F.; Walochnik, J. Antiprotozoal compounds: state of the art and new developments. *Int. J. Antimicrob. Agents* **2011**, *38*, 118−124.

(8) Cavalli, A.; Bolognesi, M. L. Neglected tropical diseases: multi-target-directed ligands in the search for novel lead candidates against *Trypanosoma* and *Leishmania*. *J. Med. Chem.* **2009**, *52*, 7339−7359.

(9) Alvar, J.; Aparicio, P.; Aseffa, A.; Den, B. M.; Canavate, C.; Dedet, J.-P.; Gradoni, L.; Ter, H. R.; Lopez-Velez, R.; Moreno, J. The relationship between leishmaniasis and AIDS: the second 10 years. *Clin. Microbiol. Rev.* **2008**, *21*, 334−359.

(10) Cruz, I.; Nieto, J.; Moreno, J.; Canavate, C.; Desjeux, P.; Alvar, J. Leishmania/HIV co-infections in the second decade. *Indian J. Med. Res.* **2006**, *123*, 357−388.

(11) Desjeux, P.; Alvar, J. Leishmania/HIV co-infections: epidemiology in Europe. *Ann. Trop. Med. Parasitol.* **2003**, *97* (Suppl. 1), 3−15.

(12) Lachaud, L.; Bourgeois, N.; Plourde, M.; Leprohon, P.; Bastien, P.; Ouellette, M. Parasite susceptibility to amphotericin B in failures of treatment for visceral leishmaniasis in patients coinfected with HIV type 1 and *Leishmania infantum*. *Clin. Infect. Dis.* **2009**, *48*, e16−e22.

(13) Pintado, V.; Lopez-velez, R. HIV-associated viseceral leishmaniais. *Clin. Microbiol. Infect.* **2003**, *7*, 291−300.

(14) Rabello, A.; Orsini, M.; Disch, J. Leishmania/HIV co-infection in Brazil: an appraisal. *Ann. Trop. Med. Parasitol.* **2003**, *97* (Suppl. 1), 17−28.

(15) Sinha, P. K.; van Griensven, J.; Pandey, K.; Kumar, N.; Verma, N.; Mahajan, R.; Kumar, P.; Kumar, R.; Das, P.; Mitra, G.; Flevaud, L.; Ferreyra, C.; Remartinez, D.; Pece, M.; Palma, P. P. Liposomal amphotericin B for visceral leishmaniasis in human immunodeficiency virus-coinfected patients: 2-year treatment outcomes in Bihar, India. *Clin. Infect. Dis.* **2011**, *53*, e91−e98.

(16) Wolday, D.; Berhe, N.; Akuffo, H.; Desjus, P.; Britton, S. Emerging leishmania/HIV co-infection in Africa. *Med. Microbiol. Immunol.* **2001**, *190*, 65−67.

(17) Anonymous. Human African trypanosomiasis (sleeping sickness): epidemiological update. *Wkly. Epidemiol. Rec.* **2006**, *81*, 71−80.

(18) Croft, S.; Barrett, M.; Urbina, J. Chemotherapy of trypanosomiases and leishmaniasis. *Trends Parasitol.* **2005**, *21*, 508−512.

(19) Delespaux, V.; de Koning, H. P. Drugs and drug resistance in African trypanosomiasis. *Drug Resist. Updates* **2007**, *10*, 30−50.

(20) Pepin, J.; Guern, C.; Milord, F.; Schechter, P. J. Difluoromethylornithine for arseno-resistant *Trypanosoma brucei gambiense* sleeping sickness. *Lancet* **1987**, *2*, 1431−1433.

(21) Rodriques, C. J.; de Castro, S. L. A critical review on Chagas disease chemotherapy. *Mem. Inst. Oswaldo Cruz* **2002**, *97*, 3−24.

(22) Murambiwa, P.; Masola, B.; Govender, T.; Mukaratirwa, S.; Musabayane, C. T. Anti-malarial drug formulations and novel delivery systems: a review. *Acta Trop.* **2011**, *118*, 71−79.

(23) Griensven, J. v.; Balasegaram, M.; Meheus, F.; Avlar, J.; lynen, L.; Boelaert, M. Combination therapy for visceral leishmaniasis. *Lancet Infect. Dis.* **2010**, *10*, 184−194.

(24) Olliaro, P. L.; Guerin, P. J.; Gerstl, S.; Haaskjold, A. A.; Rottingen, J.-A.; Sundar, S. Treatment options for visceral leishmaniasis: a systematic review of clinical studies done in India, 1980−2004. *Lancet Infect. Dis.* **2005**, *5*, 763−774.

(25) *Control of the Leishmaniasis*; WHO Technical Report Series No. 949; World Health Organization: Geneva, Switzerland, 2010.

(26) Sundar, S.; Chakravarty, J.; Agarwal, D.; Rai, M.; Murray, H. W. Single-dose liposomal amphotericin B for visceral leishmaniasis in India. *N. Eng. J. Med.* **2010**, *362*, 504−512.

(27) Sundar, S.; Jha, T. K.; Thakur, C. P.; Sinha, P. K.; Bhattacharya, S. K. Injectable paromomycin for visceral leishmaniasis in India. *N. Engl. J. Med.* **2007**, *356*, 2571−2581.

(28) Dorlo, T. P. C.; Balasegaram, M.; Beijnen, J. H.; de Vries, P. J. Miltefosine: a review of its pharmacology and therapeutic efficacy in the treatment of leishmaniasis. *J. Antimicrob. Chemother.* **2012**, *67*, 2576−2597.

(29) Das, B. P.; Boykin, D. W. Synthesis and antiprotozoal activity of 2,5-bis(4-guanylphenyl)furans. *J. Med. Chem.* **1977**, *20*, 531−536.

(30) Werbovetz, K. Diamidines as antitrypanosomal, antileishmanial and antimalarial agents. *Curr. Opin. Invest. Drugs* **2006**, *7*, 147−157.

(31) Boykin, D. W.; Kumar, A.; Hall, J. E.; Bender, B. C.; Tidwell, R. R. Anti-pneumocystis activity of bisamidoximes and bis-*O*-alkylamidoximes prodrugs. *Bioorg. Med. Chem. Lett.* **1996**, *6*, 3017−3020.

(32) Yeates, C. DB-289 Immtech International. *IDrugs* **2003**, *6*, 1086−1093.

(33) Yeramian, P.; Meshnick, S. R.; Krudsood, S.; Chalermrut, K.; Silachamroon, U.; Tangpukdee, N.; Allen, J.; Brun, R.; Kwiek, J. J.; Tidwell, R.; Looareesuwan, S. Efficacy of DB289 in Thai patients with *Plasmodium vivax* or acute, uncomplicated *Plasmodium falciparum* infections. *J. Infect. Dis.* **2005**, *192*, 319−322.

(34) Thuita, J. K.; Karanja, S. M.; Wenzler, T.; Mdachi, R. E.; Ngotho, J. M.; Kagira, J. M.; Tidwell, R.; Brun, R. Efficacy of the diamidine DB75 and its prodrug DB289, against murine models of human African trypanosomiasis. *Acta Trop.* **2008**, *108*, 6−10.

(35) Goldsmith, R. B.; Gray, D. R.; Yan, Z.; Generaux, C. N.; Tidwell, R. R.; Reisner, H. M. Application of monoclonal antibodies to measure metabolism of an anti-trypanosomal compound in vitro and in vivo. *J. Clin. Lab. Anal.* **2010**, *24*, 187−194.

(36) Bakunov, S. A.; Bakunova, S. M.; Bridges, A. S.; Wenzler, T.; Barszcz, T.; Werbovetz, K. A.; Brun, R.; Tidwell, R. R. Synthesis and antiprotozoal properties of pentamidine congeners bearing the benzofuran motif. *J. Med. Chem.* **2009**, *52*, 5763−5767.

(37) Bakunov, S. A.; Bakunova, S. M.; Wenzler, T.; Barszcz, T.; Werbovetz, K. A.; Brun, R.; Tidwell, R. R. Synthesis and antiprotozoal activity of cationic 2-phenylbenzofurans. *J. Med. Chem.* **2008**, *51*, 6927−6944.

(38) Bakunov, S. A.; Bakunova, S. M.; Wenzler, T.; Ghebru, M.; Werbovetz, K. A.; Brun, R.; Tidwell, R. R. Synthesis and antiprotozoal

activity of cationic 1,4-diphenyl-1*H*-1,2,3-triazoles. *J. Med. Chem.* **2010**, *53*, 254−272.
(39) Bakunova, S. M.; Bakunov, S. A.; Patrick, D. A.; Kumar, E. V. K. S.; Ohemeng, K. A.; Bridges, A. S.; Wenzler, T.; Barszcz, T.; Jones, S. K.; Werbovetz, K. A.; Brun, R.; Tidwell, R. R. Structure−activity study of pentamidine analogues as antiprotozoal agents. *J. Med. Chem.* **2009**, *52*, 2016−2035.
(40) Bakunova, S. M.; Bakunov, S. A.; Wenzler, T.; Barszcz, T.; Werbovetz, K. A.; Brun, R.; Hall, J. E.; Tidwell, R. R. Synthesis and in vitro antiprotozoal activity of bisbenzofuran cations. *J. Med. Chem.* **2007**, *50*, 5807−5823.
(41) Bakunova, S. M.; Bakunov, S. A.; Wenzler, T.; Barszcz, T.; Werbovetz, K. A.; Brun, R.; Tidwell, R. R. Synthesis and antiprotozoal activity of pyridyl analogues of pentamidine. *J. Med. Chem.* **2009**, *52*, 4657−4667.
(42) Branowska, D.; Farahat, A. A.; Kumar, A.; Wenzler, T.; Brun, R.; Liu, Y.; Wilson, W. D.; Boykin, D. W. Synthesis and antiprotozoal activity of 2,5-bis[amidinoaryl]thiazoles. *Bioorg. Med. Chem.* **2010**, *18*, 3551−3558.
(43) Chackal-Catoen, S.; Miao, Y.; Wilson, W. D.; Wenzler, T.; Brun, R.; Boykin, D. W. Dicationic DNA-targeted antiprotozoal agents: naphthalene replacement of benzimidazole. *Bioorg. Med. Chem.* **2006**, *14*, 7434−7445.
(44) Crowell, A. L.; Stephens, C. E.; Kumar, A.; Boykin, D. W.; Secor, W. E. Activities of dicationic compounds against *Trichomonas vaginalis*. *Antimicrob. Agents Chemother.* **2004**, *48*, 3602−3605.
(45) Czarny, A.; Wilson, W. D.; Boykin, D. W. Synthesis of mono-cationic and dicationic analogs of Hoechst 33258. *J. Heterocycl. Chem.* **1996**, *33*, 1393−1397.
(46) Ismail, M. A.; Brun, R.; Easterbrook, J. D.; Tanious, F. A.; Wilson, W. D.; Boykin, D. W. Synthesis and antiprotozoal activity of aza-analogues of furmadine. *J. Med. Chem.* **2003**, *46*, 4761−4769.
(47) Ismail, M. A.; Brun, R.; Wenzler, T.; Tanious, F. A.; Wilson, W. D.; Boykin, D. W. Dicationic biphenyl benzimidazole derivatives as antiprotozoal agents. *Bioorg. Med. Chem.* **2004**, *12*, 5405−5413.
(48) Kumar, A.; Zhao, M.; Wilson, W. D.; Boykin, D. W. Dicationic 2,4-diaryl pyrimidines as DNA selective binding agents. *Bioorg. Med. Chem. Lett.* **1994**, *4*, 2913−2918.
(49) Nguyen, B.; Tardy, C.; Bailly, C.; Colson, P.; Houssier, C.; Kumar, A.; Boykin, D. W.; Wilson, W. D. Influence of compound structure on affinity, sequence selectivity, and mode of binding to DNA for unfused aromatic dications related to furamidine. *Biopolymers* **2002**, *63*, 281−297.
(50) Patrick, D. A.; Bakunov, S. A.; Bakunova, S. M.; Kumar, E. V. K. S.; Chen, H.; Jones, S. K.; Wenzler, T.; Barzcz, T.; Werbovetz, K. A.; Brun, R.; Tidwell, R. R. Synthesis and antiprotozoal activities of dicationic bis(phenoxymethyl)benzenes, bis(phenoxymethyl)-naphthalenes, and bis(benzyloxy)naphthalenes. *Eur. J. Med. Chem.* **2009**, *44*, 3543−3551.
(51) Patrick, D. A.; Bakunov, S. A.; Bakunova, S. M.; Kumar, E. V. K. S.; Lombardy, R. J.; Jones, S. K.; Bridges, A. S.; Zhirnov, O.; Hall, J. E.; Wenzler, T.; Brun, R.; Tidwell, R. R. Synthesis and in vitro antiprotozoal activities of dicationic 3,5-diphenylisoxazoles. *J. Med. Chem.* **2007**, *50*, 2468−2485.
(52) Patrick, D. A.; Boykin, D. W.; Wilson, W. D.; Tanious, F. A.; Spychala, J.; Bender, B. C.; Hall, J. E.; Dykstra, C. C.; Ohemeng, K. A.; Tidwell, R. R. Anti-*Pneumocystis carinii* pneumonia activity of dicationic carbazoles. *Eur. J. Med. Chem.* **1997**, *32*, 781−793.
(53) Patrick, D. A.; Hall, J. E.; Bender, B. C.; McCurdy, D. R.; Wilson, W. D.; Tanious, F. A.; Saha, S.; Tidwell, R. R. Synthesis and anti-*Pneumocystis carinii* pneumonia activity of novel dicationic dibenzothiophenes and orally active prodrugs. *Eur. J. Med. Chem.* **1999**, *34*, 575−583.
(54) Wang, S.; Hall, J. E.; Tanious, F. A.; Wilson, W. D.; Patrick, D. A.; McCurdy, D. R.; Bender, B. C.; Tidwell, R. R. Dicationic dibenzofuran derivatives as anti-*Pneumocystis carinii* pneumonia agents: synthesis, DNA binding affinity, and anti-P. carinii activity in an immunosuppressed rat model. *Eur. J. Med. Chem.* **1999**, *34*, 215−224.
(55) Xiao, G.; Kumar, A.; Li, K.; Rigl, C. T.; Bajic, M.; Davis, T. M.; Boykin, D. W.; Wilson, W. D. Inhibition of the HIV-1 rev-RRE complex formation by unfused aromatic cations. *Bioorg. Med. Chem.* **2001**, *9*, 1097−1113.
(56) Das, B. P.; Boykin, D. W. Synthesis and antiprotozoal activity of 2,5-bis(4-guanylphenyl)thiophenes and -pyrroles. *J. Med. Chem.* **1977**, *20*, 1219−1221.
(57) Stephens, C. E.; Brun, R.; Salem, M. M.; Werbovetz, K. A.; Tanious, F.; Wilson, W. D.; Boykin, D. W. The activity of diguanidino and "reversed" diamidino 2,5-diarylfurans versus *Trypanosoma cruzi* and *Leishmania donovani*. *Bioorg. Med. Chem. Lett.* **2003**, *13*, 2065−2069.
(58) Stephens, C. E.; Tanious, F.; Kim, S.; Wilson, W. D.; Schell, W. A.; Perfect, J. R.; Franzblau, S. G.; Boykin, D. W. Diguanidino and "reversed" diamidino 2,5-diarylfurans as antimicrobial agents. *J. Med. Chem.* **2001**, *44*, 1741−1748.
(59) Wang, M. Z.; Zhu, X.; Srivastava, A.; Liu, Q.; Sweat, J. M.; Pandharkar, T.; Stephens, C. E.; Riccio, E.; Parman, T.; Munde, M.; Mandal, S.; Madhubala, R.; Tidwell, R. R.; Wilson, W. D.; Boykin, D. W.; Hall, J. E.; Kyle, D. E.; Werbovetz, K. A. Novel arylimidamides for treatment of visceral leishmaniasis. *Antimicrob. Agents Chemother.* **2010**, *54*, 2507−2516.
(60) Zhu, X.; Liu, Q.; Yang, S.; Parman, T.; Green, C. E.; Mirsalis, J. C.; Soeiro, M. d. N. C.; Souza, E. M. d.; Silva, C. F. d.; Batista, D. d. G. J.; Stephens, C. E.; Banerjee, M.; Farahat, A. A.; Munde, M.; Wilson, W. D.; Boykin, D. W.; Wang, M. Z.; Werbovetz, K. A. Evaluation of arylimidamides DB1955 and DB1960 as candidates against visceral leishmaniasis and chagas disease—in vivo efficacy, acute toxicity, pharmacokinetics and toxicology studies. *Antimicrob. Agents Chemother.* **2012**, *56*, 3690−3699.
(61) von der Saal, W.; Engh, R. A.; Eichinger, A.; Gabriel, B.; Kucznierz, R.; Sauer, J. Syntheses and selective inhibitory activities of terphenyl-bisamidines for serine proteases. *Arch. Pharm.* **1996**, *329*, 73−82.
(62) Hu, L.; Arafa, R. K.; Ismail, M. A.; Patel, A.; Munde, M.; Wilson, W. D.; Wenzler, T.; Brun, R.; Boykin, D. W. Synthesis and activity of azaterphenyl diamidines against *Trypanosoma brucei rhodesiense* and *Plasmodium falciparum*. *Bioorg. Med. Chem.* **2009**, *17*, 6651−6658.
(63) Hu, L.; Arafa, R. K.; Ismail, M. A.; Wenzler, T.; Brun, R.; Munde, M.; Wilson, W. D.; Nzimiro, S.; Samyesudhas, S.; Werbovetz, K. A.; Boykin, D. W. Azaterphenyl diamidines as antileishmanial agents. *Bioorg. Med. Chem. Lett.* **2008**, *18*, 247−251.
(64) Ismail, M. A.; Arafa, R. K.; Brun, R.; Wenzler, T.; Miao, Y.; Wilson, W. D.; Generaux, C.; Bridges, A.; Hall, J. E.; Boykin, D. W. Synthesis, DNA affinity, and antiprotozoal activity of linear dications: terphenyl diamidines and analogues. *J. Med. Chem.* **2006**, *49*, 5324−5332.
(65) Da Silva, C. F.; Da Silva, P. B.; Batista, M. M.; Daliry, A.; Tidwell, R. R.; Soeiro, M. d. N. C. The biological in vitro effect and selectivity of aromatic dicationic compounds on Trypanosoma cruzi. *Mem. Inst. Oswaldo Cruz* **2010**, *105*, 239−245.
(66) Daliry, A.; Da Silva, P. B.; Da Silva, C. F.; Batista, M. M.; De Castro, S. L.; Tidwell, R. R.; Soeiro, M. d. N. C. In vitro analyses of the effect of aromatic diamidines upon *Trypanosoma cruzi*. *J. Antimicrob. Chemother.* **2009**, *64*, 747−750.
(67) Chanteau, S. H.; Tour, J. M. Synthesis of anthropomorphic molecules: the NanoPutians. *J. Org. Chem.* **2003**, *68*, 8750−8766.
(68) Kajigaeshi, S.; Kakinami, T.; Inoue, K.; Kondo, M.; Nakamura, H.; Fujikawa, M.; Okamoto, T. Halogenation using quaternary ammonium polyhalides. VI. Bromination of aromatic amines by use of benzyltrimethylammonium tribromide. *Bull. Chem. Soc. Jpn.* **1988**, *61*, 597−599.
(69) Anbazhagan, M.; Saulter, J. Y.; Hall, J. E.; Boykin, D. W. Synthesis of metabolites of the prodrug 2,5-bis(4-*O*-methoxyamidinophenyl)furan. *Heterocycles* **2003**, *60*, 1133−1145.
(70) Sinclair, D. J.; Sherburn, M. S. Single and double Suzuki−Miyaura couplings with symmetric dihalobenzenes. *J. Org. Chem.* **2005**, *70*, 3730−3733.

(71) Pelter, M. W.; Pelter, L. S. W.; Colovic, D.; Strug, R. Microscale synthesis of 1-bromo-3-chloro-5-iodobenzene: an improved deamination of 4-bromo-2-chloro-6-iodoaniline. *J. Chem. Educ.* **2004**, *81*, 111−112.
(72) Ault, A.; Kraig, R. 1-Bromo-3-chloro-5-iodobenzene. An eight-step synthesis from benzene. *J. Chem. Educ.* **1966**, *43*, 213−214.
(73) Markevitch, D. Y.; Rapta, M.; Hecker, S. J.; Renau, T. E. An efficient synthesis of 5-bromopyridine-2-carbonitrile. *Synth. Commun.* **2003**, *33*, 3285−3289.
(74) Ishiyama, T.; Murata, M.; Miyaura, N. Palladium(0)-catalyzed cross-coupling reaction of alkoxydiboron with haloarenes: a direct procedure for arylboronic esters. *J. Org. Chem.* **1995**, *60*, 7508−7510.
(75) Chaumeil, H.; Le Drian, C.; Defoin, A. Efficient synthesis of substituted terphenyls by Suzuki coupling reaction. *Synthesis* **2002**, 757−760.
(76) Ramachandran, U.; Mital, A.; Bharatam, P. V.; Khanna, S.; Rao, P. R.; Srinivasan, K.; Kumar, R. C.; Singh, H. P.; Lal Kaul, C.; Raichur, S.; Chakrabartid, R. Studies on some glitazones having pyridine as the linker unit. *Bioorg. Med. Chem.* **2004**, *12*, 655−662.
(77) Zhang, N.; Thomas, L.; Wu, B. Palladium-catalyzed selective cross-coupling between 2-bromopyridines and aryl bromides. *J. Org. Chem.* **2001**, *66*, 1500−1502.
(78) Al-Saffar, F.; Berlin, S.; Musil, T.; Sivadasan, S. Process for Preparing Protected Amidines from Nitriles. WO2006090153A1, 2006.
(79) Lange, J. H. M.; van Stuivenberg, H. H.; Coolen, H. K. A. C.; Adolfs, T. J. P.; McCreary, A. C.; Keizer, H. G.; Wals, H. C.; Veerman, W.; Borst, A. J. M.; de Looff, W.; Verveer, P. C.; Kruse, C. G. Bioisosteric replacements of the pyrazole moiety of rimonabant: synthesis, biological properties, and molecular modeling investigations of thiazoles, triazoles, and imidazoles as potent and selective CB1 cannabinoid receptor antagonists. *J. Med. Chem.* **2005**, *48*, 1823−1838.
(80) Rix, D.; Clavier, H.; Coutard, Y.; Gulajski, L.; Grela, K.; Mauduit, M. Activated pyridinium-tagged ruthenium complexes as efficient catalysts for ring-closing metathesis. *J. Organomet. Chem.* **2006**, *691*, 5397−5405.
(81) Michrowska, A.; Bujok, R.; Harutyunyan, S.; Sashuk, V.; Dolgonos, G.; Grela, K. Nitro-substituted Hoveyda−Grubbs ruthenium carbenes: enhancement of catalyst activity through electronic activation. *J. Am. Chem. Soc.* **2004**, *126*, 9318−9325.
(82) Delfin, D. A.; Morgan, R. E.; Zhu, X.; Werbovetz, K. A. Redox-active dinitrodiphenylthioethers against *Leishmania*: synthesis, structure−activity relationships and mechanism of action studies. *Bioorg. Med. Chem.* **2009**, *17*, 820−829.
(83) Orhan, I.; Sener, B.; Kaiser, M.; Brun, R.; Tasdemir, D. Inhibitory activity of marine sponge-derived natural products against parasitic protozoa. *Mar. Drugs* **2010**, *8*, 47−58.
(84) Collar, C. J.; Zhu, X.; Werbovetz, K.; Boykin, D. W.; Wilson, W. D. Molecular factors governing inhibition of arylimidamides against *Leishmania*: conservative computational modeling to improve chemotherapies. *Bioorg. Med. Chem.* **2011**, *19*, 4552−4561.
(85) Wenzler, T.; Boykin, D. W.; Ismail, M. A.; Hall, J. E.; Tidwell, R. R.; Brun, R. New treatment option for second-stage African sleeping sickness: in vitro and in vivo efficacy of aza analogs of DB289. *Antimicrob. Agents Chemother.* **2009**, *53*, 4185−4192.
(86) Donkor, I. O.; Assefa, H.; Rattendi, D.; Lane, S.; Vargas, M.; Goldberg, B.; Bacchi, C. Trypanocidal activity of dicationic compounds related to pentamidine. *Eur. J. Med. Chem.* **2001**, *36*, 531−538.
(87) Donkor, I. O.; Huang, T. L.; Tao, B.; Rattendi, D.; Lane, S.; Vargas, M.; Goldberg, B.; Bacchi, C. Trypanocidal activity of conformationally restricted pentamidine congeners. *J. Med. Chem.* **2003**, *46*, 1041−1048.
(88) Ansede, J. H.; Anbazhagan, M.; Brun, R.; Easterbrook, J. D.; Hall, J. E.; Boykin, D. W. *O*-Alkoxyamidine prodrugs of furamidine: in vitro transport and microsomal metabolism as indicators of in vivo efficacy in a mouse model of *Trypanosoma brucei rhodesiense* infection. *J. Med. Chem.* **2004**, *47*, 4335−4338.
(89) Baker, B. R.; Cory, M. Irreversible enzyme inhibitors. CLXIV. Proteolytic enzymes. 14. Inhibition of guinea pig complement by meta-substituted benzamidines. *J. Med. Chem.* **1969**, *12*, 1049−1052.
(90) Basselin, M.; Badet-Denisot, M.-A.; Lawrence, F.; Robert-Gero, M. Effects of pentamidine on polyamine level and biosynthesis in wild-type, pentamidine-treated, and pentamidine-resistant *Leishmania*. *Exp. Parasitol.* **1997**, *85*, 274−282.
(91) Cory, M.; Tidwell, R. R.; Fairley, T. A. Structure and DNA binding activity of analogs of 1,5-bis(4-amidinophenoxy)pentane (pentamidine). *J. Med. Chem.* **1992**, *35*, 431−438.
(92) de Koning, H. P. Transporters in African trypanosomes: role in drug action and resistance. *Int. J. Parasitol.* **2001**, *31*, 512−522.
(93) Dykstra, C. C.; Tidwell, R. R. Inhibition of topoisomerases from *Pneumocystis carinii* by aromatic dicationic molecules. *J. Protozool.* **1991**, *38*, 78S−81S.
(94) Ghosh, A. K.; Bhattacharyya, F. K.; Ghosh, D. K. *Leishmania donovani*: amastigote inhibition and mode of action of berberine. *Exp. Parasitol.* **1985**, *60*, 404−413.
(95) Lanteri, C. A.; Trumpower, B. L.; Tidwell, R. R.; Meshnick, S. R. DB75, a novel trypanocidal agent, disrupts mitochondrial function in *Saccharomyces cerevisiae*. *Antimicrob. Agents Chemother.* **2004**, *48*, 3968−3974.
(96) Mathis, A. M.; Bridges, A. S.; Ismail, M. A.; Kumar, A.; Francesconi, I.; Anbazhagan, M.; Hu, Q.; Tanious, F. A.; Wenzler, T.; Saulter, J.; Wilson, W. D.; Brun, R.; Boykin, D. W.; Tidwell, R. R.; Hall, J. E. Diphenyl furans and aza analogs: effects of structural modification on in vitro activity, DNA binding, and accumulation and distribution in trypanosomes. *Antimicrob. Agents Chemother.* **2007**, *51*, 2801−2810.
(97) Moreno, S. N. J. Pentamidine is an uncoupler of oxidative phosphorylation in rat liver mitochondria. *Arch. Biochem. Biophys.* **1996**, *326*, 15−20.
(98) Stead, A. M. W.; Bray, P. G.; Edwards, I. G.; DeKoning, H. P.; Elford, B. C.; Stocks, P. A.; Ward, S. A. Diamidine compounds: selective uptake and targeting in *Plasmodium falciparum*. *Mol. Pharmacol.* **2001**, *59*, 1298−1306.
(99) Tidwell, R. R.; Jones, S. K.; Geratz, J. D.; Ohemeng, K. A.; Cory, M.; Hall, J. E. Analogs of 1,5-bis(4-amidinophenoxy)pentane (pentamidine) in the treatment of experimental *Pneumocystis carinii* pneumonia. *J. Med. Chem.* **1990**, *33*, 1252−1257.
(100) Werbovetz, K. A. Promising therapeutic targets for antileishmanial drugs. *Expert Opin. Ther. Targets* **2002**, *6*, 407−422.
(101) Zhu, W.; Zhang, Y.; Sinko, W.; Hensler, M. E.; Olson, J.; Molohon, K. J.; Lindert, S.; Cao, R.; Li, K.; Wang, K.; Wang, Y.; Liu, Y.-L.; Sankovsky, A.; de Oliveira, C. A. F.; Mitchell, D. A.; Nizet, V.; McCammon, J. A.; Oldfield, E. Antibacterial drug leads targeting isoprenoid biosynthesis. *Proc. Natl. Acad. Sci. U.S.A.* **2013**, *110*, 123−128.
(102) Bibler, M. R.; Chou, T. C.; Toltzis, R. J.; Wade, P. A. Recurrent ventricular tachycardia due to pentamidine-induced cardiotoxicity. *Chest* **1988**, *94*, 1303−1306.
(103) Biyah, K.; Molimard, M.; Naline, E.; Bazelly, B.; Advenier, C. Indirect muscarinic receptor activation by pentamidine on airway smooth muscle. *Br. J. Pharmacol.* **1996**, *119*, 1131−1136.
(104) Bouchard, P.; Sai, P.; Reach, G.; Caubarrere, I.; Ganeval, D.; Assan, R. Diabetes mellitus following pentamidine-induced hypoglycemia in humans. *Diabetes* **1982**, *31*, 40−45.
(105) Kempin, S. J.; Jackson, C. W.; Edwards, C. C. In vitro inhibition of platelet function and coagulation by pentamidine isethionate. *Antimicrob. Agents Chemother.* **1977**, *12*, 451−454.
(106) Murphey, S. A.; Josephs, A. S. Acute pancreatitis associated with pentamidine therapy. *Arch. Intern. Med.* **1981**, *141*, 56−58.
(107) Small, C. B.; Harris, C. A.; Friedland, G. H.; Klein, R. S. The treatment of *Pneumocystis carinii* pneumonia in the acquired immunodeficiency syndrome. *Arch. Intern. Med.* **1985**, *145*, 837−840.
(108) Western, K. A.; Schultz, M. G. Pentamidine nontoxicity. *Ann. Intern. Med.* **1969**, *70*, 234−234.

(109) Fidock, D. A.; Rosenthal, P. J.; Croft, S. L.; Brun, R.; Nwaka, S. Antimalarial drug discovery: efficacy models for compound screening. *Nat. Rev. Drug Discovery* **2004**, *3*, 509−520.
(110) Arnold, L.; Tyagi, R. K.; Meija, P.; Swetman, C.; Gleeson, J.; Perignon, J.-L.; Druilhe, P. Further improvements of the *P. falciparum* humanized mouse model. *PLoS One* **2011**, *6*, e18045.
(111) Langhorne, J.; Buffet, P.; Galinski, M.; Good, M.; Harty, J.; Leroy, D.; Mota, M. M.; Pasini, E.; Renia, L.; Riley, E.; Stins, M.; Duffy, P. The relevance of non-human primate and rodent malaria models for humans. *Malar. J.* **2011**, *10*, 23.
(112) Angulo-Barturen, I.; Jimenez-Diaz, M. B.; Mulet, T.; Rullas, J.; Herreros, E.; Ferrer, S.; Jimenez, E.; Mendoza, A.; Regadera, J.; Rosenthal, P. J.; Bathurst, I.; Pompliano, D. L.; de las Heras, F. G.; Gargallo-Viola, D. A murine model of *falciparum*-malaria by in vivo selection of competent strains in non-myelodepleted mice engrafted with human erythrocytes. *PLoS One* **2008**, *3*, e2252.
(113) Moreno, A.; Badell, E.; Van, R. N.; Druilhe, P. Human malaria in immunocompromised mice: new in vivo model for chemotherapy studies. *Antimicrob. Agents Chemother.* **2001**, *45*, 1847−1853.
(114) Moreno, A.; Perignon, J. L.; Morosan, S.; Mazier, D.; Benito, A. *Plasmodium falciparum*-infected mice: more than a tour de force. *Trends Parasitol.* **2007**, *23*, 254−259.

AAC Journals.ASM.org

In Vitro and *In Vivo* Evaluation of 28DAP010, a Novel Diamidine for Treatment of Second-Stage African Sleeping Sickness

Tanja Wenzler,[a,b] Sihyung Yang,[c] Donald A. Patrick,[d] Olivier Braissant,[b,e] Mohamed A. Ismail,[f] Richard R. Tidwell,[d] David W. Boykin,[f] Michael Zhuo Wang,[c] Reto Brun[a,b]

Medical Parasitology & Infection Biology, Swiss Tropical and Public Health Institute, Basel, Switzerland[a]; University of Basel, Basel, Switzerland[b]; Department of Pharmaceutical Chemistry, School of Pharmacy, The University of Kansas, Lawrence, Kansas, USA[c]; Department of Pathology and Laboratory Medicine, School of Medicine, University of North Carolina, Chapel Hill, North Carolina, USA[d]; Department of Urology, University Hospital of Basel, Basel, Switzerland[e]; Department of Chemistry, Georgia State University, Atlanta, Georgia, USA[f]

African sleeping sickness is a neglected tropical disease transmitted by tsetse flies. New and better drugs are still needed especially for its second stage, which is fatal if untreated. 28DAP010, a dipyridylbenzene analogue of DB829, is the second simple diamidine found to cure mice with central nervous system infections by a parenteral route of administration. 28DAP010 showed efficacy similar to that of DB829 in dose-response studies in mouse models of first- and second-stage African sleeping sickness. The *in vitro* time to kill, determined by microcalorimetry, and the parasite clearance time in mice were shorter for 28DAP010 than for DB829. No cross-resistance was observed between 28DAP010 and pentamidine on the tested *Trypanosoma brucei gambiense* isolates from melarsoprol-refractory patients. 28DAP010 is the second promising preclinical candidate among the diamidines for the treatment of second-stage African sleeping sickness.

African sleeping sickness, also known as human African trypanosomiasis (HAT), is a tropical disease that threatens millions of people living in sub-Saharan Africa (1). It is caused by two subspecies of the single-celled parasite *Trypanosoma brucei*, *Trypanosoma brucei gambiense* and *Trypanosoma brucei rhodesiense*. The protozoans are transmitted by the bite of infected tsetse flies. The disease is fatal without effective treatment. The burden of the disease has been reduced to some extent by increased control interventions, but the disease is still one of the most neglected tropical diseases, and it is estimated by the WHO that there are still 25,000 to 30,000 infected patients (2, 3).

HAT progresses in two stages. In the first stage, the parasites reside in the blood and the lymphatic system. In the second stage, the parasites cross the blood-brain barrier (BBB) and spread the infection to the central nervous system (CNS), leading to neurological and psychiatric disorders, including irregular and fragmented sleeping patterns, behavioral changes, motor weakness, coma, and ultimately death (4).

Patients can be cured only by effective and safe drugs. Vaccines are not available and are unlikely to be developed in the near future, and self-healing through the body's own immune system is also not possible due to antigenic variation of the surface glycoproteins of the parasites (5). The drugs currently available have serious disadvantages such as adverse effects, limited efficacy, complicated treatment schedules, and the need for parenteral administration. New drugs are therefore needed, especially for the second stage of the disease.

In the search for new drugs, aromatic diamidines are seen as promising candidates for use against HAT. These compounds are known to have a broad spectrum of antiprotozoal activities (6). Pentamidine has been in use since the 1940s for first-stage *T. b. gambiense* HAT and against leishmaniasis and *Pneumocystis jirovecii* pneumonia (7). Diminazene (8) and isometamidium (a monoamidine) are used to treat animal trypanosomiasis. Therefore, considerable effort has been put into the synthesis and investigation of novel aromatic diamidines with improved properties for use against HAT.

One problem with diamidines is that they are protonated at physiological pH and therefore do not easily cross the gastrointestinal tract and the BBB by diffusion. Their cationic nature was therefore believed to reduce their potential for use as oral drugs and to reduce their efficacy against second-stage HAT by any route of administration; therefore, much effort went into the design of prodrugs (6, 9). Prodrugs are inactive against trypanosomes *in vitro* but can be metabolized to the active diamidine molecules by host enzymes upon administration *in vivo* (10–12), thus serving as potentially orally active drugs. The prodrug approach worked well with regard to oral bioavailability in animal models (9, 13, 14) as well as in humans, in whom the prodrug DB289 (pafuramidine maleate) underwent clinical trials as the first oral drug for treatment of first-stage HAT patients (15, 16). Several other prodrugs have been tested in the second-stage mouse model, but few of them were able to cure CNS infections in mice (14, 17).

During a series of tests in our laboratory, we discovered that the diamidine DB829 was intrinsically active in second-stage animal models (14, 18). This was unexpected, as simple diamidines (amidines without substituents on either nitrogen atom) are thought to be unable to cross the BBB by diffusion due to their cationic

Received 25 October 2013 **Returned for modification** 12 January 2014
Accepted 14 May 2014
Published ahead of print 27 May 2014
Address correspondence to Tanja Wenzler, Tanja.Wenzler@unibas.ch.
Supplemental material for this article may be found at http://dx.doi.org/10.1128/AAC.02309-13.

doi:10.1128/AAC.02309-13

nature. For many years, DB829 remained the only diamidine that showed high CNS activity *in vivo* (14, 19).

Recently, we found that 28DAP010 (also known as CPD0905) and its close analogues 19DAP025 and 27DAP060 were highly active *in vitro* against *T. b. rhodesiense* and were curative in the stringent *T. b. rhodesiense* STIB900 first-stage mouse model at the low dose of 4 × 5 mg/kg of body weight (i.e., daily dose of 5 mg/kg given on 4 consecutive days) or as a single dose of 10 mg/kg by an intraperitoneal (i.p.) route of administration (20). In this paper, we present more data from our investigations of this new novel diamidine with high CNS activity *in vivo*, 28DAP010, and its analogues 19DAP025 and 27DAP060. We performed a full dose-response experiment in the STIB900 acute-stage mouse model to determine the minimal curative dose for the three compounds and evaluated their CNS activity in the GVR35 CNS mouse model. As 28DAP010 showed better efficacy than the analogues, we carried out a detailed biological characterization of this compound. We collected *in vitro* data on different *T. brucei* strains and subspecies, with a particular emphasis on trypanocidal activity on *T. b. gambiense*, as the majority (>98%) of African sleeping sickness patients are infected with *T. b. gambiense* (2). Additionally, we assessed the time to kill of 28DAP010 *in vitro* using microcalorimetry, a new method to measure drug activity on a real-time basis (21). This was important, because aromatic diamidines typically kill the trypanosomes rather slowly, with a time to kill of about 24 to 48 h after treatment (22). Among the diamidines, DB829 was one of the slowest-acting compounds, with a time to kill of >48 h (23). After having analyzed the pharmacokinetic properties of 28DAP010 in mice at a curative single dose, we assessed the parasite clearance time at an identical dose in mice infected with *T. b. rhodesiense* and *T. b. gambiense* strains.

MATERIALS AND METHODS

Materials. Pentamidine isethionate was purchased from Sigma-Aldrich (St. Louis, MO). Syntheses of 28DAP010 (CPD-0905) (20), 19DAP025 (20), 27DAP060 (20), DB829 (24), DB1244 (20) and deuterium-labeled DB75 (DB75-d8; deuterated phenyl rings; internal standard) (25), all isolated as their hydrochloride salts, have been previously reported.

Antitrypanosomal activities of 28DAP010 and pentamidine *in vitro*.
(i) Preparation of compounds. Compounds were dissolved in 100% dimethyl sulfoxide (DMSO) and finally diluted in culture medium prior to the *in vitro* assay. The DMSO concentration never exceeded 1% in the *in vitro* alamarBlue assays at the highest drug concentration. For microcalorimetry assays, the DMSO concentration was kept at 0.1% in all samples.

(ii) Parasites. The *T. brucei* strains used in this study are described in Table 1.

(iii) *In vitro* growth inhibition assays using *T. brucei* subspecies. The 50% inhibitory concentrations (IC_{50}s) were determined using the alamarBlue assay as described by Räz et al. (26), with a 3-day drug exposure and minor modifications as described previously (23). Assays were carried out at least three times independently and each time in duplicate. The IC_{50}s are the means of the independent assays. Coefficients of variation were less than 50%. Different culture and assay media were used for *T. b. gambiense* and *T. b. rhodesiense*, as previously described by Wenzler et al. (23).

(iv) Microcalorimetry studies using *T. brucei* subspecies. *In vitro* time of drug action was monitored using isothermal microcalorimetry. With this method, the time of drug action on a parasite population can be determined on a real-time basis (21, 23). The strain STIB900 was used as a representative for *T. b. rhodesiense* and STIB930 (and sometimes additionally ITMAP141267) for *T. b. gambiense*.

For experiments with continuous drug exposure, bloodstream trypanosomes (2 ml at 5 × 10^4/ml per ampoule) were spiked with different concentrations of 28DAP010, with a final DMSO concentration of 0.1% (vol/vol). Negative controls contained culture medium only. The heat flow was continuously measured (1 reading/second) at 37°C in the isothermal microcalorimetry instrument (thermal activity monitor, model 249 TAM III). Each experiment with continuous drug exposure was set up in triplicate and carried out a total of 3 times (21).

TABLE 1 *T. brucei* isolates used in this study

Trypanosome strain(s)[a]	Subspecies	Year of isolation	Origin	Reference
STIB900, STIB704	*T. b. rhodesiense*	1982	Tanzania	52
BS221, S427	*T. b. brucei*	1960	Uganda	42
BS221Δ*AT1*	*T. b. brucei*			42
GVR35, S10	*T. b. brucei*	1966	Serengeti	53
STIB930, STIB754	*T. b. gambiense*	1978	Côte d'Ivoire	54
ITMAP141267	*T. b. gambiense*	1960	DRC	55
130R	*T. b. gambiense*	2005	DRC	56
40R	*T. b. gambiense*	2005	DRC	56
45R	*T. b. gambiense*	2005	DRC	56
349R	*T. b. gambiense*	2006	DRC	56
DAL898R	*T. b. gambiense*	1985	Côte d'Ivoire	52
K03048	*T. b. gambiense*	2003	South Sudan	57

[a] Strains labeled with an "R" were isolated from patients after a relapse after melarsoprol treatment.

(v) Inoculum studies. For studies of the drug effect on different parasite densities in the inoculum, the parasite density was reduced to 1 × 10^4/ml of bloodstream trypanosomes and supplemented with 28DAP010 at the desired concentrations. Inhibition of growth and viability was compared with that in the samples containing the standard inoculum of 5 × 10^4/ml of bloodstream trypanosomes and the same drug concentrations (23). Each experiment was set up in triplicate and repeated once.

(vi) Drug wash-out experiments. For the 24-h exposure experiment, trypanosomes (*T. b. rhodesiense* strain STIB900 and *T. b. gambiense* strain STIB930) were incubated with 28DAP010 for 24 h at 37°C and then washed twice to remove the compound. Subsequently, the washed trypanosomes were resuspended in drug-free culture medium, transferred to ampoules, and inserted into the isothermal microcalorimetry instrument. The drug-free control samples (drug free, wash-out) were washed identically to the drug-containing samples. Each 24-h exposure experiment was set up in triplicate and repeated once (23).

(vii) Analysis of microcalorimetry heat flow data. To facilitate further calculations, the recorded data were resampled to obtain an effective sampling frequency of 1 data point per 1.5 min, using the manufacturer's software (TAM assistant version v1.2.4.0), and exported to a spreadsheet. Forty-five minutes was added to the time data to account for the preparation of the ampoules and the transfer from the bench to the calorimeter. Resulting data were plotted as heat flow (in μW) over time. Each single curve for heat flow (in watts) over time was analyzed using the R statistical package (27). Data were smoothed using a cubic spline (smooth.spline function) in the R statistical software (27–30). The time to onset of drug action was determined as the time at which a divergence between the heat flow of the drug-free controls and the drug-containing specimens could be observed. The time to peak was determined as the time point at which the highest heat flow was measured for each samples. The time to kill the parasite population was defined as the time point when the heat production was reduced to the level of the sterile medium control (base level) (23).The growth rate (μ) of each culture was calculated using the heat-over-time data (integrated heat flow data over time). For this calculation, the Gompertz growth model was fitted over the whole curve using R software and the Grofit package as described previously (23, 31). The growth rate calculated based on the heat released by the metabolic activity

in the culture is considered only as a proxy for the growth rate calculated from the exponential growth phase by conventional approaches, since lysis and chemical processes due to the nature of the medium might also contribute to the overall heat signal (23, 31).

***In vivo* studies. (i) Efficacy and time to kill in mice.** The efficacy and time-to-kill experiments were performed at the Swiss Tropical and Public Health Institute. Adult female NMRI (Naval Medical Research Institute) mice were obtained from Janvier, France, or from Harlan, the Netherlands. They weighed between 20 and 25 g at the beginning of the study and were housed under standard conditions with food pellets and water *ad libitum*. All protocols and procedures were reviewed and approved by the veterinary authorities of Canton Basel-Stadt, Switzerland. For experiments with mice, the compounds were dissolved in DMSO and further diluted with distilled water to a final DMSO concentration of 10% prior to administration to the animals.

(ii) Efficacy in an acute-stage *T. b. rhodesiense* STIB900 mouse model. The STIB900 acute-stage mouse model mimics the first (hemolymphatic) stage of HAT. Experiments were performed as previously reported (23). Briefly, four female NMRI mice per group were infected intraperitoneally (i.p.) with 5×10^3 STIB900 bloodstream forms. Drug administration (i.p.) began 3 days after infection. A control group was infected but remained untreated. All mice were monitored for parasitemia by microscopic examination of tail blood twice a week until day 30, followed by once a week until 60 days after infection. The time to parasite relapse was recorded to calculate the mean relapse time in days after infection. Mice were euthanized after parasitemia relapse detection. Mice were considered cured if they survived and were aparasitemic until day 60.

(iii) Efficacy in acute-stage *T. b. gambiense* mouse models. Experiments were performed as previously reported (23). Briefly, four female NMRI mice per group were immunosuppressed with 200 mg/kg of cyclophosphamide (Endoxan, Baxter, Deerfield, IL) 2 days prior to infection with 10^5 bloodstream forms with one of the four *T. b. gambiense* strains (i.e., ITMAP141267, STIB930, 130R, or 45R). Immunosuppression with cyclophosphamide followed every second week until the end of the experiment. Drug administration (i.p.) began 3 days after infection. A control group was infected but remained untreated. Mice were monitored for parasitemia twice a week until day 30 and then once a week until 90 days after infection. Mice were considered cured if they survived and were aparasitemic until day 90.

(iv) Efficacy in a CNS stage *T. b. brucei* GVR35 mouse model. The GVR35 mouse CNS model mimics the second stage of the disease. GVR35 is a less virulent strain than STIB900 and crosses the BBB of mice around 7 days after infection (32). Experiments were performed as previously reported (14), with minor modifications. Five female NMRI mice per experimental group were used. Each mouse was inoculated i.p. with 2×10^4 bloodstream forms. The drug administration was i.p. for diamidines and *per os* (p.o.) for prodrugs on five consecutive days from day 17 to 21 after infection. Some experimental groups were treated for 10 consecutive days (day 17 to 26 after infection). A negative-control group was treated on day 17 with a single dose of diminazene aceturate at 40 mg/kg of body weight i.p., which is subcurative since it clears the trypanosomes only from the hemolymphatic system and not from the CNS, leading to a subsequent reappearance of trypanosomes in the blood (33). Parasitemia was monitored twice a week from the time after treatment until day 50 after infection, followed by once a week until 180 days after infection. Mice were considered cured when there was no parasitemia relapse detected over the 180-day observation period. Surviving and aparasitemic mice were euthanized on day 180.

(v) *In vivo* time to kill. Infection with *T. b. rhodesiense* and *T. b. gambiense* and immunosuppression for *T. b. gambiense*-infected mice were carried out as described for the efficacy experiments. In different mouse models the parasite load varied, an observation that was also made in the efficacy experiments. Mice were treated with a single dose of 20 mg/kg i.p. 3 days postinfection. The first microscopic examination of blood was done 24 h after treatment, and examination was done subsequently twice per day until all parasites had disappeared. When microscopy was not sensitive enough to detect any parasites, a hematocrit buffy coat examination was performed. The first time point at which no trypanosomes were detected on the microscopic slide or in the buffy coat was considered the clearance time (or time to kill) in mice. The detection limit by buffy coat examination was <100 trypanosomes/ml of blood. Mice were kept and further observed by tail blood examination until the end of the experiment to verify whether the administered dose was curative in the infected mice (23).

Pharmacokinetic studies. (i) Animals for PK studies. The pharmacokinetic (PK) studies were performed at the University of Kansas. Protocols for the animal studies were approved by the Institutional Animal Care and Use Committee of the University of Kansas. Male Swiss Webster mice (weighing 20 to 25 g) were purchased from the Charles River Laboratories (O'Fallon, MO). Mice were housed in a clean room under filtered, pathogen-free air, in a 12-h light/dark cycle, and with food pellets and water available *ad libitum*. Although a different strain and sex of mice were used in our PK studies compared to efficacy studies, we did not expect that diamidine PK would differ significantly between different strain and sex of mice.

(ii) Pharmacokinetics and brain exposure in mice. The single-dose pharmacokinetics of 28DAP010 was evaluated in mice (in triplicate) after intravenous (i.v.) and i.p. administration. 28DAP010 was dissolved in sterile saline. The doses were 7.5 μmol/kg (approximately 2.4 mg/kg) for i.v. administration and 65 μmol/kg (approximately 21 mg/kg) for i.p. administration, which was the dose used in the *in vivo* time-to-kill study. The dose volume was 5 ml/kg. No overt adverse effects were observed in mice at these dose levels. Blood sampling occurred at 0.25, 0.5, 1, 2, 4, 6, 8, 12, 24, 48, and 72 h postdose. Additional earlier sampling times, at 0.0167 and 0.083 h, were included for the i.v. administration. Blood was collected via the submandibular vein (~0.04 ml per bleed) or heart (~0.8 ml) into lithium heparin-coated Microvette tubes (Sarstedt Inc., Newton, NC). Terminal blood and brain samples were collected at 4, 12, and 72 h postdose. Plasma was obtained by centrifugation. Excised mouse brain samples were quickly rinsed with distilled water, blotted dry with tissue paper, and weighed. All samples were stored at −20°C until further processing for quantification by ultrahigh-performance liquid chromatography-tandem mass spectrometry (UPLC-MS/MS).

(iii) Plasma and tissue binding assays. Binding of 28DAP010 to mouse plasma and brain was evaluated by the equilibrium dialysis method using a rapid equilibrium dialysis device (Thermo Scientific Pierce, Rockford, IL) as previously described (34). Briefly, blank (untreated and uninfected) mouse brains were collected and homogenized in 2 volumes (vol/wt) of water (3-fold dilution). 28DAP010 was spiked into blank plasma or brain homogenates to yield a final drug concentration of 1 μM. Spiked plasma or brain homogenates (in triplicate) were added to the dialysis device and dialyzed against phosphate-buffered saline (PBS) for 6 h at 37°C to reach equilibrium between the plasma/tissue compartment and the buffer compartment. At the end of incubation, samples from the plasma/tissue compartment and the buffer compartment were collected and analyzed for total and unbound concentrations by UPLC-MS/MS. Unbound fractions in the mouse brain ($f_{u,\,brain}$) were calculated by correcting for dilution (35).

(iv) UPLC-MS/MS analysis. (*a*) Sample preparation. Plasma samples (2 μl) were mixed with 200 μl of 7:1 (vol/vol) methanol-water containing 0.1% trifluoroacetic acid and an internal standard (1 nM DB75-d8) and then vortex mixed for 30 s, followed by centrifugation (2,800 × *g*) to pellet proteins. The supernatant was transferred to a new tube and dried using a 96-well microplate evaporator (Apricot Designs Inc., Covina, CA) under N_2 at 50°C and reconstituted with 100 μl of 15% methanol containing 0.1% trifluoroacetic acid.

(*b*) Determination of drug concentration. The reconstituted samples (5-μl injection volume) were analyzed for drug concentration using a Waters Xevo TQ-S mass spectrometer (Foster City, CA) coupled with a Waters Acquity UPLC I-Class system. Compounds were separated on a

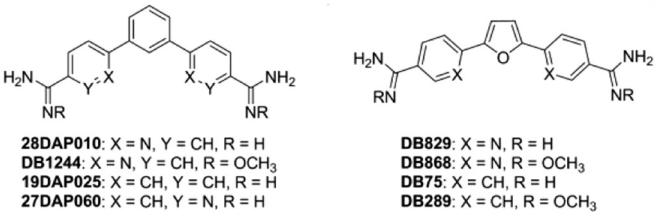

FIG 1 Chemical structures of 28DAP010, its prodrug DB1244, and its analogues.

Waters UPLC BEH C_{18} column (2.1 mm by 50 mm by 1.7 μm) equilibrated at 50°C. UPLC mobile phases consisted of water containing 0.1% formic acid (solution A) and methanol containing 0.1% formic acid (solution B). After a 0.15-min initial holding period at 10% solution B, mobile phase composition started with 10% solution B and was increased to 80% solution B over 2.2 min with a flow rate of 0.4 ml/min. Then the column was washed with 90% solution B for 0.5 min and was reequilibrated with 5% solution B for 1.1 min before injection of the next sample. The characteristic single reaction monitoring (SRM) transition for 28DAP010 and DB75-d8 were *m/z* 317.1→283.1 and 313.2→296.3, respectively, under positive electrospray ionization mode. The calibration curves for 28DAP010 ranged from 0.5 nM to 50 μM. The intraday coefficient of variation (CV) and accuracy were determined by measuring the same preparation of three standards three times on the same day. At concentrations of 5, 1,000, and 25,000 nM, the intraday CV and average accuracy of 28DAP010 quantification were 11.2% and 103%, 5.33% and 104%, and 0.70% and 106%, respectively.

(v) Pharmacokinetic analysis. The total area under the plasma concentration-time curve (AUC), terminal elimination half-life ($t_{1/2}$), maximum plasma drug concentration (C_{max}), time to reach C_{max} (T_{max}), clearance (CL), steady-state volume of distribution (V_{ss}), and mean residence time (MRT) were calculated using the trapezoidal rule-extrapolation method and noncompartmental analysis (WinNonlin version 5.0; Pharsight, Mountain View, CA).

RESULTS

Acute-stage *T. b. rhodesiense* mouse model. 28DAP010 and its two analogues 19DAP025 and 27DAP060 (Fig. 1) are highly active *in vitro* as well as *in vivo* against African trypanosomes (20). Within this study we analyzed the minimal curative dose in the stringent STIB900 acute-stage mouse model. All three compounds showed superior activity, curing all mice at 4 × 5 mg/kg i.p. or at single doses of 10 mg/kg i.p. (28DAP010 and 19DAP025) or 5 mg/kg i.p. (27DAP060) (20) (Table 2). Pentamidine cured only 1/4 mice at 4 × 5 mg/kg i.p. (23). *In vivo* efficacies of 28DAP010 and 19DAP025 were comparable. Cure rates of 3/4 or 2/4 mice were attained at a daily dose of 5 mg/kg i.p. or 1 mg/kg administered on 4 consecutive days. 27DAP060 was slightly more effective than 28DAP010 and 19DAP025. With the low dose of 4 × 0.25 mg/kg i.p., none of the 3 compounds were able to cure any of the mice, and the parasitemia relapses were detected already around 4 days after the last drug administration. 28DAP010 and its dipyridylfuran analogue DB829 showed similar efficacies in the STIB900 acute-stage mouse model (Table 2).

TABLE 3 *In vivo* antitrypanosomal activity of 28DAP010 in mice with GVR35 CNS infections

Dose regime (no. of doses × mg/kg[e])	No. of mice cured/no. infected				
	28DAP010	19DAP025	27DAP060	DB1244	DB829 or diminazene
5 × 25 i.p.	2/5, 5/6[a]	0/1[d]			4/5,[b] 6/6[a,b]
10 × 10 i.p.	0/5, 1/6[a]				
10 × 20 i.p.	5/5	0/1[d]	0/4		
5 × 100 p.o.				0/5	
1 × 40 i.p.					0/5[c]

[a] Cure obtained in a previous experiment.
[b] Result for DB829.
[c] Result for diminazene.
[d] Several mice died or were euthanized due to compound toxicity.
[e] No. of doses × mg/kg, one daily dose administered on consecutive days.

CNS *T. b. brucei* mouse model. The high efficacies in the acute-stage mouse model showed that the compounds merited further testing in the GVR35 CNS mouse model. 28DAP010 was the most potent compound among the three diamidines, curing all infected mice at 10 × 20 mg/kg i.p. (Table 3). The high CNS activity is exceptional, having been observed so far with only one other diamidine, DB829 (14).

The two analogues of 28DAP010—19DAP025 and 27DAP060—were both less effective and did not achieve any cures. Additionally, 19DAP025 was toxic and killed most of the mice at the dosages administered. 28DAP010 was also tested at 25 mg/kg for only 5 days and was almost as potent as DB829. This is only a slightly higher total dose than 10 mg/kg i.p. administered for 10 days but was clearly more effective (Table 3). 28DAP010 was well tolerated in NMRI mice at 5 × 25 mg/kg and 10 × 20 mg/kg i.p., without any overt toxicity observed.

The prodrug DB1244 is a methamidoxime derivative of 28DAP010 (analogous to DB868 being the methamidoxime derivative of DB829). It has been tested orally at 100 mg/kg administered on 5 consecutive days. At identical oral doses, DB1244 was

TABLE 2 *In vivo* antitrypanosomal activities of 28DAP010 and its analogues 19DAP010 and 27DAP060 (along with dipyridylfuran analogue DB829) in mice with acute-stage STIB900 *T. b. rhodesiense* infections[a]

Dose regime (no. of doses × mg/kg)	28DAP010 (*in vitro* IC_{50} [nM], 17 ± 4)		19DAP025 (*in vitro* IC_{50} [nM], 4 ± 1)		27DAP060 (*in vitro* IC_{50} [nM], 6 ± 1)		DB829 (*in vitro* IC_{50} [nM], 20 ± 4)	
	No. of mice cured/no. infected	MRD	No. of mice cured/no. infected	MRD	No. of mice cured/no. infected	MRD	No. of mice cured/no. infected	MRD
1 × 5 i.p.	3/4	17	2/4	17	4/4		2/4	53.5
1 × 10 i.p.	4/4		4/4		ND		4/4	
4 × 0.25 i.p.	0/4	12	0/4	9.25	0/4	13	0/4	14.75
4 × 1 i.p.	3/4	14	2/4	19	4/4		3/4	14
4 × 5 i.p.	4/4		4/4		4/4		4/4	

[a] DB1244, the methamidoxime prodrug of 28DAP010, cured 2/4 mice at 4 × 25 mg/kg p.o. (20). IC_{50}s are from references 20 and 23 and are expressed as means ± standard deviations. No. of doses × mg/kg, one daily dose administered on consecutive days; MRD, mean relapse day; ND, not determined.

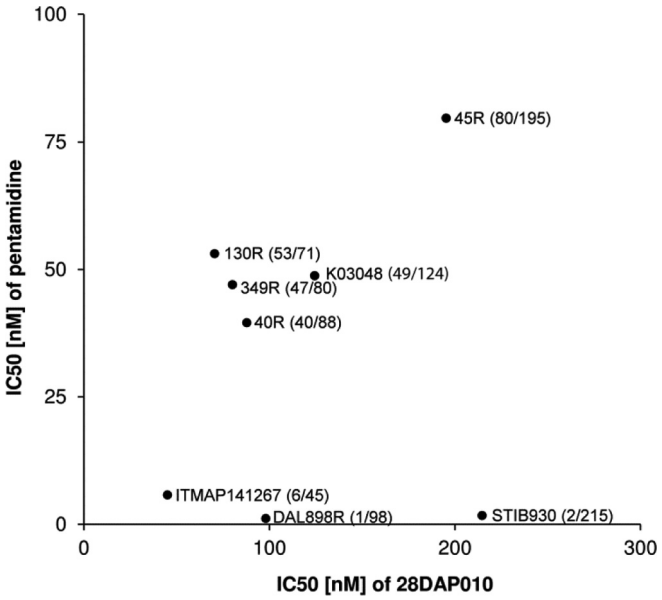

FIG 2 *In vitro* activities of pentamidine versus 28DAP010 against different *T. b. gambiense* strains. Symbols represent the average IC_{50} of at least three independent determinations. The first number in each set of parentheses represents the IC_{50} for pentamidine and the second number that for 28DAP010. No significant correlation was observed between pentamidine and 28DAP010 activities ($r^2 = 0.019$).

less potent in the CNS mouse model (no cures [Table 3]) than DB868 (5/5 mice cured) (14).

***In vitro* activity against different trypanosome strains.** We analyzed the *in vitro* activity of 28DAP010 against different trypanosome isolates in the alamarBlue viability assay. As most sleeping sickness patients suffer from *T. b. gambiense* infections, we tested 28DAP010 against several *T. b. gambiense* field isolates. The strains and culture conditions were identical to those used to determine the trypanocidal activity of DB829 (23), so the IC_{50}s of 28DAP010 and DB829 can therefore directly be compared. The *in vitro* IC_{50}s of 28DAP010 were higher for all tested *T. b. gambiense* isolates (IC_{50} = 45 to 215 nM [Fig. 2]) than for *T. b. rhodesiense* strain STIB900 (IC_{50} = 17 nM) and *T. b. brucei* strain BS221 (IC_{50} = 25 nM). Among the *T. b. gambiense* strains, there was no clear correlation between isolates from patients suffering from a relapse after melarsoprol treatment (strains whose name includes "R") and reduced potency of 28DAP010 (Fig. 2), whereas pentamidine appeared to be less active against strains that had been recently isolated (since 2003), which has also previously been shown (23). 28DAP010 was more active against the four "R" strains (130R, 349R, 40R, and DAL898R) than against the reference melarsoprol-sensitive strain STIB930. ITMAP141267 was the oldest isolate tested in this study (isolated in 1960 from the Democratic Republic of the Congo [DRC]), and it was the strain most sensitive to 28DAP010 and among those most sensitive to pentamidine (Fig. 2). However, no correlation in reduced trypanocidal activity among *T. b. gambiense* strains was observed between 28DAP010 and pentamidine (r^2 = 0.019) or with the isolates from melarsoprol-refractory patients.

We additionally studied the dependency of the P2 transporter for the uptake of 28DAP010 into trypanosomes using BS221Δ*AT1*, a P2 knockout strain (IC_{50} = 400 nM), and its corresponding wild type, BS221 (IC_{50} = 25 nM), by comparing the IC_{50}s determined in the alamarBlue assay. The resistance factor (RF) obtained with 28DAP010 on the P2 knockout strain (RF = 16) was comparable to the RF obtained by DB829 (14), suggesting that both compounds are taken up primarily by the P2 transporter.

***In vivo* mouse models with acute-stage infection with different *T. b. gambiense* isolates.** We assessed the efficacy of 28DAP010 in mice against four different *T. b. gambiense* isolates and compared the activity with that against *T. b. rhodesiense* STIB900 (Table 4). This was a crucial experiment since *in vitro*, 28DAP010 had been shown to be less active against the tested *T. b. gambiense* isolates than against *T. b. rhodesiense* strain STIB900 and *T. b. brucei* strain BS221. However, in *in vivo* experiments in mice, 28DAP010 was at least as efficacious for *T. b. gambiense* strains as for *T. b. rhodesiense* STIB900. 28DAP010 was curative at 1 × 20 mg/kg i.p. and at 4 × 5 mg/kg i.p. in STIB900-infected mice as well as in mice infected with either of the four *T. b. gambiense* strains (ITMAP141267, STIB930, 130R, and 45R), two of which (130R and 45R) were isolated from melarsoprol relapse patients. At a single dose of 5 mg/kg i.p., 28DAP010 cured 3/4 STIB900-infected mice, whereas all mice were cured of infection with the *T. b. gambiense* strains ITMAP141267 and STIB930 at the identical dose (Table 4). A group given a dose of 1 × 5 mg/kg i.p. was not included in the *in vivo* experiments with 130R and 45R, as the high efficacy with a 100% cure rate at a single dose of 20 mg/kg i.p. had not been expected prior to the experiment.

Time course of drug action *in vitro*. The time course of drug action of 28DAP010 *in vitro* versus the *T. b. rhodesiense* strain STIB900 and the two *T. b. gambiense* strains STIB930 and ITMAP141267 was recorded using isothermal microcalorimetry. Drug action was studied at different drug concentrations in 10-fold dilution steps ranging from 2 to 20,000 nM concentrations against the *T. b. rhodesiense* strain STIB900 or from 20 to 20,000 nM against the two *T. b. gambiense* strains. Four parameters were

TABLE 4 *In vitro* and *in vivo* antitrypanosomal activities of 28DAP010 against different *T. brucei* strains[a]

28DAP010 dose regime (no. of doses × mg/kg)	No. of mice cured/no. infected				
		T. b. gambiense			
	T. b. rhodesiense STIB900 (*in vitro* IC_{50} [nM], 17 ± 4)	ITMAP141267 (*in vitro* IC_{50} [nM], 45 ± 6)	STIB930 (*in vitro* IC_{50} [nM], 215 ± 56)	130R (*in vitro* IC_{50} [nM], 71 ± 33)	45R (*in vitro* IC_{50} [nM], 195 ± 50)
1 × 5 i.p.	3/4	4/4	3/3	ND	ND
1 × 20 i.p.	4/4	3/3	4/4	4/4	4/4
4 × 5 i.p.	4/4	4/4	4/4	4/4	4/4

[a] IC_{50}s are expressed as means ± standard deviations. No. of doses × mg/kg, one daily dose administered on consecutive days; ND, not determined.

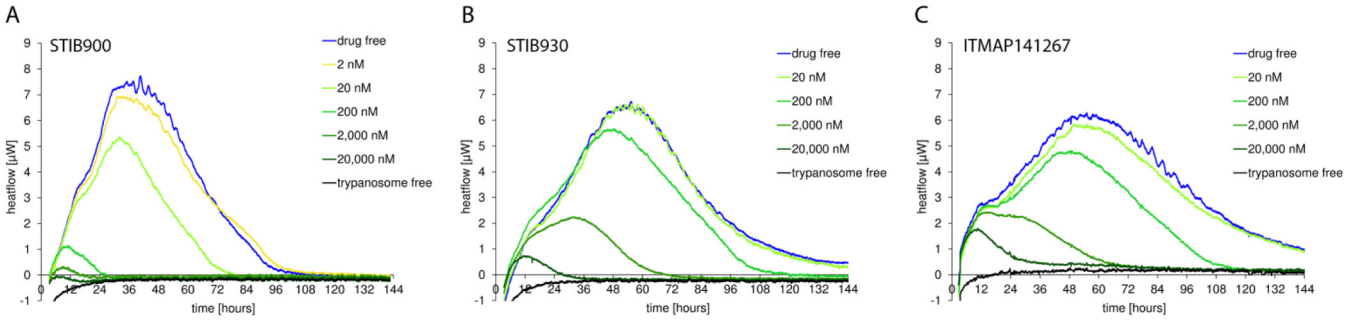

FIG 3 Microcalorimetry heat flow profiles of *T. b. rhodesiense* strain STIB900 (A) and *T. b. gambiense* strains STIB930 (B) and ITMAP141267 (C) in the presence of various concentrations of 28DAP010. Drug-free samples included parasites (5×10^4/ml inoculum) without drug treatment, and trypanosome-free experiment did not include any parasites or drug. Each curve represents the mean of three samples.

calculated from the curves for heat flow over time to describe the time course of drug action quantitatively: (i) the onset of drug action, (ii) the time to peak, (iii) the time to kill, and (iv) the growth rate (μ) and hence the level of growth inhibition ($1 - \mu_{drug}/\mu_{drug\ free}$) (23).

The time of drug action of 28DAP010 was concentration dependent (Fig. 3). The higher the concentration, the faster 28DAP010 acted and killed the parasites (in contrast to DB829, with which saturation was observed at ≥2,000 nM [23]). The onset of drug action on *T. b. rhodesiense* strain STIB900 ranged from <4 to 16 h, and the time to kill the parasite culture ranged from 24 to 92 h at concentrations of 20,000 to 20 nM (Table 5). At the highest tested drug concentration of 20,000 nM, drug action was so strong that not all parameters could be calculated. Also, the inhibition of the growth rate (μ) was dependent on the drug concentration, ranging from 7% at 2 nM up to >93% at the highest tested concentration of 20,000 nM.

Drug action of 28DAP010 *in vitro* was slower for *T. b. gambiense* strains ITMAP141267 and STIB930 (Fig. 3; Table 5) than for *T. b. rhodesiense* strain STIB900. This is consistent with the reduced activity (higher IC_{50}s) of 28DAP010 observed for *T. b. gambiense* in the alamarBlue assay. Growth of the two *T. b. gambiense* strains was also slightly slower in drug-free control cultures (μ = 0.018 to 0.024 h^{-1}, time to peak = 53 to 58 h, and time to overgrowth = 144 to 172 h) than that of *T. b. rhodesiense* strain STIB900 (μ = 0.029 h^{-1}, time to peak = 34 h, and time to overgrowth = 111 h) at identical trypanosome inocula of 5×10^4 trypanosomes/ml (Table 5). The onset of drug action for the two *T. b. gambiense* strains ranged from 5 to 30 h and the time to kill ranged from 46 to 126 h (2 to 5 days) at effective concentrations of 200 to 20,000 nM 28DAP010. Also, the inhibition of the growth rate (μ) was dependent on the drug concentration, ranging from 0.6 to 4% at 20 nM up to >82% at 20,000 nM for both *T. b. gambiense* strains (Table 5).

An inoculum effect is a phenomenon that has previously been observed with several diamidines. We studied the effect of two

TABLE 5 Drug action analysis of 28DAP010 by isothermal microcalorimetry

T. brucei strain[c]	Concn (nM)	Onset of action, mean (SD) (h)	Time to peak, mean (SD) (h)	Time to kill, mean (SD) (h)	Growth rate (μ), mean (SD) (h^{-1}/1,000)	Inhibition (%)[d]
STIB900	None (drug free)		34 (4)	111 (10)	29 (1)	
	2[a]	NM[e]	32 (8)	113 (7)	27 (1)	7
	20[a]	16 (3)	30 (7)	92 (5)	22 (2)	24
	200	7 (1)	10 (2)	49 (17)	7 (4)	76
	2,000	≤5[b]	10 (1)	32 (10)	3 (2)	>90
	20,000[b]	<4[b]	<9[b]	24 (7)	2[b]	>93
STIB930	None (drug free)		53 (2)	144 (8)	24 (2)	
	20[a]	NM	53 (2)	146 (5)	24 (1)	0.6
	200	30 (9)	50 (1)	126 (8)	23 (1)	4
	2,000	9 (2)	36 (3)	90 (8)	11 (2)	52
	20,000[b]	5[b]	13 (5)	46 (9)	4[b]	>82
ITMAP141267	None (drug free)		58 (4)	172 (11)	18 (3)	
	20[a]	NM	57 (4)	172 (7)	17 (3)	4
	200	21 (6)	47 (3)	124 (12)	16 (3)	11
	2,000	11 (4)	18 (6)	79 (7)	8 (1)	55
	20,000	6 (1)	10 (1)	47 (19)	3 (1)	85

[a] Inhibition is too small to recover parameters from every experiment performed accurately.
[b] Inhibition is too strong to recover parameters from every experiment performed accurately.
[c] Initial inoculum density was 5×10^4 trypanosomes/ml.
[d] Inhibition was determined as follows: $(1 - \mu_{drug}/\mu_{drug\ free}) \times 100$.
[e] NM, not measurable.

TABLE 6 Effects of inoculum and drug wash-out on drug action of 28DAP010 by isothermal microcalorimetry

T. brucei strain and inoculum	Concn (nM)	Onset of action, mean (SD) (h)	Time to peak, mean (SD) (h)	Time to kill, mean (SD) (h)	Growth rate (μ), mean (SD) (×1,000) (h^{-1})	Inhibition[e] (%)
STIB900						
5×10^4/ml	None (drug free)		38 (3)	118 (7)	27 (2)	
	20	14 (2)	33 (1)	93 (4)	22 (2)	19
	200	6 (1)	12 (1)	37 (3)	5 (1)	81
1×10^4/ml (low inoculum)	None (drug free)		50 (3)	125 (5)	27 (1)	
	20	12 (7)	29 (2)	59 (2)	4 (1)	85
	200[b]	9[b]	13[b]	25[b]	NM[a,b]	>98
5×10^4/ml, wash-out	None (drug free)		55 (4)	132 (11)	26 (2)	
	200	<30	45 (7)	82 (19)	6 (2)	77
STIB930						
5×10^4/ml	None (drug free)		50 (2)	148 (9)	24 (2)	
	200	26 (4)	50 (1)	121 (8)	23 (1)	6
	2,000	8 (2)	36 (3)	85 (7)	10 (2)	58
1×10^4/ml (low inoculum)	None (drug free)		68 (1)	160 (10)	24 (2)	
	200	27 (3)	52 (5)	100 (11)	12 (2)	51
	2,000[b]	<15[b]	31 (5)	60 (3)	2[b]	>93
5×10^4/ml, wash-out	None (drug free)		64 (5)	154 (11)	21 (1)	
	200[c]	<30	61 (2)	128 (9)	21 (1)	0
	2,000[d]	<30	60 (4)	130 (12)	15 (2)	28

[a] NM, not measurable.
[b] Inhibition is too strong to recover parameters from every experiment performed accurately.
[c] Only two independent experiments were performed (in triplicate).
[d] Only one independent experiment was performed (in triplicate).
[e] Inhibition was determined as follows: $(1 - \mu_{drug}/\mu_{drug\ free}) \times 100$.

different initial parasite densities (5×10^4/ml and 1×10^4/ml) on the sensitivity to 28DAP010 by isothermal microcalorimetry (see Fig. S1 in the supplemental material). With an inoculum of 5×10^4/ml, the growth rate of *T. b. rhodesiense* strain STIB900 was inhibited by 19% at 20 nM and 81% at 200 nM (Table 6). Considerably stronger inhibition was observed at the lower inoculum of 1×10^4/ml. The parasite culture was inhibited by 85% at 20 nM and >98% at 200 nM (Table 6; see also Fig. S1). In contrast, onset of drug action and time to peak of the heat flow curves remained similar with the different inocula (Table 6). The same phenomenon was observed in the experiments with *T. b. gambiense* strain STIB930. With an initial inoculum of 5×10^4/ml, parasite growth rate was inhibited by 6% at a drug concentration of 200 nM and by 58% at 2,000 nM. Stronger inhibitions were observed at the lower inoculum, with 51% at 200 nM and >93% at 2,000 nM (Table 6). The other two parameters, onset of action and time to peak of the heat flow curves, remained again similar at the different inocula. No clear inoculum effect was observed at 2 nM 28DAP010 (see Fig. S1).

Diamidines are normally taken up rapidly into trypanosomes, but parasite death is usually delayed. We tested whether continuous drug exposure is required for 28DAP010 to kill the trypanosomes or if an exposure of 24 h is sufficient to kill the parasites at a later time point. Inhibition of trypanosome cultures that were incubated for 24 h with 28DAP010 and then washed was monitored in drug-free culture medium by microcalorimetric analysis. The heat flow of preexposed trypanosome samples in drug-free culture medium was compared with that of parasites continuously exposed to the drug. The wash-out experiments were performed with two strains (STIB900 and STIB930).

The time to peak of the washed, drug-free samples was delayed by 14 to 17 h compared to the drug-free samples that were not washed (Table 6; see also Fig. S2 in the supplemental material). This delay was attributed to loss of some trypanosomes during the washing steps since both samples were set up and run simultaneously. The trypanosome culture was still alive, as seen by heat flow rate above baseline at the 24-h time point, and heat production did increase in the wash-out samples after any drug was removed. This indicates that the cells were still multiplying after the drug preexposure at a 200 or 2,000 nM concentration. However, the cultures in the drug-free medium did die after some time (see Fig. S2). The times to kill after drug wash-out were delayed compared to those with continuous drug exposure (82 versus 37 h) for *T. b. rhodesiense* strain STIB900 at 200 nM and for *T. b. gambiense* strain STIB930 (130 versus 85 h) at 2,000 nM (Table 6). However, the 24-h exposure was sufficient to kill STIB900 at 200 nM and STIB930 at 2,000 nM at the later time, which confirms that lethal concentrations were taken up within the first 24 h. With lower drug concentrations, a revival of the parasite culture after wash-out was observed in some cases: with STIB900 at 20 nM and with STIB930 at 200 nM (data not shown).

Pharmacokinetics and brain exposure of 28DAP010 after i.v. and i.p. administration in mice. The mean plasma concentration-time profiles of 28DAP010 were determined after a single i.v. dose of 7.5 μmol/kg (2.4 mg/kg) or a single i.p. dose of 65 μmol/kg (21 mg/kg) (Fig. 4). Both profiles exhibited at least a biphasic decline with an initial distribution phase and a terminal elimination phase. Pharmacokinetic outcomes were determined using noncompartmental analysis (Table 7). Following i.v. administration, the average plasma concentration of 28DAP010 reached 70.2 μM about 1 min after i.v. administration, but it quickly decreased, to below 1 μM by 2 h postdose and below 0.1 μM by 8 h postdose (Fig. 4A). The steady-state volume of distribution was 15 liters/kg, markedly greater than the physiologic fluid volume. The

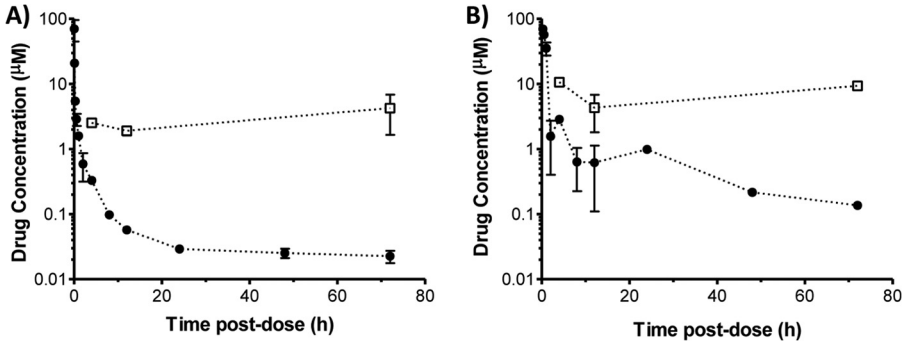

FIG 4 Plasma (filled circles) and brain (open squares) concentration-time profiles of 28DAP010 following intravenous (A) and intraperitoneal (B) administration to uninfected mice. The doses were 7.5 μmol/kg (or 2.4 mg/kg) for i.v. administration and 65 μmol/kg (or 21 mg/kg) for i.p. administration. Symbols and error bars represent means and standard errors of triplicate determinations, respectively.

average brain concentration of 28DAP010 was 4.2 μM at 72 h postdose, approximately 190-fold higher than the corresponding plasma concentration (Table 7). Following i.p. administration, 28DAP010 was rapidly absorbed into blood circulation, reaching a plasma C_{max} of 69.6 μM at 15 min postdose. The average plasma concentration of 28DAP010 decreased below 1 μM by 8 h postdose but remained above 0.1 μM for at least 72 h after injection (Fig. 4B). The average brain concentration of 28DAP010 was 9.3 μM at 72 h postdose, approximately 69-fold higher than the corresponding plasma concentration (Table 7).

The nonspecific binding of 28DAP010 to mouse plasma proteins and brain tissues was determined (Table 7). 28DAP010 showed moderate binding to mouse plasma ($f_{u,\ plasma}$ = 26.3%) but bound avidly to brain tissues ($f_{u,\ brain}$ = 0.69%).

TABLE 7 Pharmacokinetic parameters of 28DAP010 after i.v. and i.p. administration to uninfected mice

Compartment	Parameter[a]	Value for dosing route	
		i.v.	i.p.
Plasma	Dose, μmol/kg (mg/kg)	7.5 (2.4)	65 (21)
	$C_{5\ min}$, μmol/liter	20.8 ± 0.7[b]	NC[c]
	C_{max}, μmol/liter	70.2[d]	69.6
	T_{max}, h	NC	0.25
	$AUC_{0-\infty}$, μmol/liter · h	15	102
	$t_{1/2}$, h	68	26
	CL, liter/h/kg	0.50	NC
	V_{ss}, liters/kg	15	NC
	MRT, h	30	NC
	$f_{u,\ plasma}$, %	26.3 ± 2.2[b]	
Brain	C_{brain_72h}, μmol/liter	4.2 ± 4.5[b]	9.3 ± 0.5[b]
	AUC_{brain_0-72h}, μmol/liter · h	202	469
	B/P at 72 h	190	69
	$f_{u,\ brain}$, %	0.69 ± 0.07[b]	

[a] $C_{5\ min}$, plasma concentration at 5 min postdose; C_{max}, maximum plasma concentration; T_{max}, time to reach C_{max}; $AUC_{0-\infty}$, area under the plasma concentration-time curve from time zero to infinitity; $t_{1/2}$, terminal elimination half-life; CL, clearance; V_{ss}, steady-state volume of distribution; MRT, mean residence time; C_{brain_72h}, brain concentration at 72 h postdose; AUC_{brain_0-72h}, area under the brain concentration-time curve from time zero to 72 h postdose; B/P, brain-to-plasma concentration ratio; f_u, drug unbound fraction; $C_{5\ min}$, plasma concentration at 5 min postdose; B/P, brain-to-plasma concentration ratio.
[b] Mean ± standard deviation of triplicate determinations.
[c] NC, not calculated.
[d] Plasma concentration at 1 min postdose.

Time of drug action *in vivo*. The time of drug action of 28DAP010 *in vivo* was determined following a single i.p. dose of 20 mg/kg to mice infected with *T. b. rhodesiense* strain STIB900 or the *T. b. gambiense* strains ITMAP141267 and STIB930. The *in vivo* time to kill (parasite clearance time) of 28DAP010 was determined in the same experiment as the previously reported data for DB829 (23). Typically, diamidines are rather slow-acting compounds, especially DB829. Therefore, the first blood sample collected was 24 h after treatment. This time point is close to the parasite clearance time of 28DAP010, as in each group one mouse (STIB930 and ITMAP141267) or three of four mice (STIB900 infected) were already parasite free 24 h after drug administration.

The parasite clearance time was, on average, 26 h (24 to 32 h) when mice were infected with the *T. b. rhodesiense* strain STIB900 (Table 8). This is in the range of the *in vitro* time to kill at 2,000 to 20,000 nM concentrations (24 to 32 h [Table 5]). The time to kill for the *T. b. gambiense* strain ITMAP141267 was, on average, 42 h (24 to 56 h); that in STIB930-infected mice was 40 h (24 to 48 h) (Table 8), which is slightly faster than the *in vitro* time to kill at the two highest concentrations of 2,000 and 20,000 nM (Table 4).

DISCUSSION

Our studies of the diamidine 28DAP010 and its two analogues 27DAP060 and 19DAP025 showed that they are highly active against African trypanosomes *in vivo*. In the STIB900 acute-stage mouse model, the mice were cured by a single i.p. dose (Table 2) (20). However, among the three analogues, only 28DAP010 cured mice with second-stage infections in the GVR35 CNS mouse model (Table 3).

The availability of more efficacy data for a number of diami-

TABLE 8 *In vivo* time to kill (parasite clearance time) in infected mice after 28DAP010 treatment

T. brucei strain	Time to kill (h), mean (range)[a]
STIB900	26 (24–32)
ITMAP141267	42 (24–56)
STIB930	40 (24–48)

[a] 28DAP010 was given as a single dose at 20 mg/kg i.p. 3 days after infection. Values are means of four mice per group; ranges represents the time when the first and last mouse became aparasitemic.

dines makes it possible to consider some structure-activity relationships. 28DAP010 is chemically closely related to DB829 (Fig. 1). In the present study, 19DAP025 was less CNS potent and more toxic than its diaza analogue 28DAP010 (Table 3). Most of the infected mice died during or shortly after treatment with 19DAP025 at 5 × 25 mg/kg or 10 × 20 mg/kg i.p. A similar comparison can be made between furamidine and DB829 (14). 27DAP060, a regioisomer of 28DAP010, was highly active *in vivo* in the acute-stage mouse model (Table 2) but less CNS active than 28DAP010 (Table 3). This has been observed in previous experiments with aza analogues of furamidine (DB75) (24), in which only DB829 cured CNS-infected mice (14). The two pyridyl nitrogen atoms introduced in DB75 decreased the pK_a value of DB829 by only 1 unit, and it was still above physiological pH (36). The higher BBB penetration can therefore not be attributed to an effect on pK_a alone. The identical positions of the nitrogen atoms in the outer pyridine rings in both DB829 and 28DAP010 (Fig. 1) may play a crucial role in CNS potency and in the recognition of the molecules by a presumed transporter protein located at the BBB, which supports the penetration of 28DAP010 and DB829 into the brain. The CNS mouse model results for these two molecules confirm that certain diamidines do indeed have potential for curing not only first-stage but also second-stage HAT by the parenteral administration route.

There is still some interest in the use of prodrugs, particularly because of their potential for oral administration. Since the analogue DB868, the methamidoxime prodrug of DB829, cured mice showing CNS infection after oral administration (14), we analyzed the potency of DB1244, which is a methamidoxime prodrug of 28DAP010, in the GVR35 CNS mouse model at the same dosage. However, DB1244 was much less CNS active than DB868 (Table 3) (14), although its acute-stage mouse model activity was similar (Table 2) (14, 20). Further metabolism and pharmacokinetic studies of DB1244 are needed to explain the observed efficacy difference. When DB868 was tested by the oral route in vervet monkeys with second-stage infections, the therapeutic window was smaller for the prodrug DB868 than for its active diamidine DB829 (18). Measurement of the efficacy of 28DAP010 in the second-stage vervet monkey model will be needed for comparison with DB829.

Our greatest concern was to test the susceptibilities of different *T. b. gambiense* isolates to 28DAP010, as >98% of all HAT cases are due *T. b. gambiense* infections (2). Most of our strains were isolated from patients from the Democratic Republic of the Congo (DRC), the country harboring most HAT patients (1). We observed considerable reduction in the *in vitro* activity of 28DAP010 against the different *T. b. gambiense* strains compared to *T. b. rhodesiense* and *T. b. brucei* strains. This phenomenon has been observed previously with DB829 (against all tested *T. b. gambiense* isolates) and with pentamidine against recent isolates (K03048, 40R, 45R, 130R, and 349R) that were derived from patients within the last 10 years (23). However, our *in vivo* experiments with *T. b. gambiense* infections with four different isolates (ITMAP141267, STIB930, 130R, and 45R) were encouraging. 28DAP010 proved to be highly active against *T. b. gambiense* as well as *T. b. rhodesiense* isolates. The *T. b. gambiense*-infected mice were cured at doses comparable to, or even lower than, those used for mice infected with *T. b. rhodesiense* STIB900 (Table 4). The reduced *in vitro* activities of 28DAP010 and DB829 may be the result of factors that do not influence activity *in vivo*. They could be due to the slower growth of *T. b. gambiense* isolates or be the result of different culture conditions leading, for example, to a downregulation of a diamidine uptake transporter(s) (37) and thus to a reduced susceptibility of the *T. b. gambiense* isolates *in vitro* (23).

Cross-resistance between pentamidine and melamine-based arsenicals such as melarsoprol is a well-known phenomenon (38–40) involving the P2 transporter (41, 42). Therefore, we were concerned about a possible cross-resistance between 28DAP010 and these drugs or the possible development of more resistant trypanosome strains. Tests using a P2 knockout (KO) *T. brucei* strain indicated that the uptake of 28DAP010 is dependent on the P2 transporter. We observed a resistance factor ($IC_{50\ P2\text{-}KO}/IC_{50\ wild\ type}$) of 16, which was similar to that for DB829 and diminazene in the 72-h alamarBlue assay (14). Recently another transporter, aquaporin 2 (AQP2), was identified which is also involved in drug uptake and the development of resistance to pentamidine and melarsoprol (40, 43, 44). However, cross-resistance seems to be limited to the two diamidines pentamidine and 28DAP010, as the IC_{50}s of the two diamidines for different *T. b. gambiense* field isolates do not correlate ($r^2 = 0.019$) (Fig. 2). A similar effect was observed between pentamidine and diminazene (44). Analysis of *T. b. gambiense* field isolates with reduced susceptibility to pentamidine did reveal rearrangements of the *TbAQP2/TbAQP3* locus accompanied by *TbAQP2* gene loss (44). The mutant *T. b. gambiense* field isolates were less susceptible to pentamidine and melarsoprol but still susceptible to diminazene (44) and DB829 (23) and, as can be seen in Fig. 2, also to 28DAP010. Additionally, 28DAP010 was able to cure mice that were infected with recent *T. b. gambiense* isolates that were less susceptible to pentamidine *in vitro* (Table 4). Lack of AQP2 dependency for uptake of 28DAP010 and DB829 would explain why the recent *T. b. gambiense* isolates that were less susceptible to pentamidine were still sensitive to 28DAP010 and DB829.

An understanding of the pharmacokinetics and pharmacodynamics of drugs is necessary to develop effective treatment schedules. The time of drug action on trypanosomes can be determined *in vitro* using isothermal microcalorimetry (21). This method is based on the heat production of metabolically active parasites and thus allows studying the growth of cultures in the presence and absence of drugs (21, 23). It is simple to use and offers constant monitoring of a parasite population on a real-time basis (21).We analyzed the time of drug action of 28DAP010 at different concentrations on 3 different trypanosome strains. The time course of drug action was concentration dependent. No saturation could be observed with 28DAP010, whereas in experiments with DB829, saturation was found above 2,000 nM (23). This was probably due to saturation of the P2 transporter with DB829 (23, 37). It is possible that 28DAP010 is taken up by an additional high-capacity, low-affinity transporter at high drug concentrations, leading to a stronger drug action at concentrations above 2,000 nM.

We studied the inoculum effect of 28DAP010 by using identical drug concentrations but different initial parasite densities (inocula), 1×10^4/ml and 5×10^4/ml (see Fig. S1 in the supplemental material). We observed a strong inoculum effect on the growth rate (μ) and on the time to kill. However, the onset of drug action and the time to peak were less affected at the different trypanosome starting densities at identical drug concentrations, as can be observed at 20 and 200 nM concentrations with STIB900 or at 200 and 2,000 nM concentrations with STIB930 (Table 6). This indi-

cates that the drug action starts almost concurrently at the different starting densities using the same drug concentration. This phenomenon has been previously observed with DB829 and pentamidine in microcalorimetric studies (23). The major reason for the inoculum effect *in vitro* seems to be the concurrent onset of drug action, which appears at a much lower trypanosome density at the lower inoculum. Therefore, the inhibition of these compounds is more pronounced than for the drug-free control samples at the lower inoculum than at the higher inoculum.

The time taken to kill parasites is an important parameter to measure treatment efficacy. It has been shown that several diamidines (such as pentamidine, DB75, and DB829) are rapidly taken up by African trypanosomes; however, trypanosome death occurred much later (9, 23, 45, 46). We studied the drug action at effective concentrations (200 nM for STIB900 and 2,000 nM for STIB930) for an exposure time of 24 h, after which the drug was washed out (see Fig. S2 in the supplemental material). Growth was followed by isothermal microcalorimetry. After the drug had been washed out from the trypanosome culture, the parasites seemed to grow for at least one more day (see time to peak in Table 6). The trypanosomes were finally killed as a consequence of the 24-h drug exposure, but death occurred almost 2 days later than in continuously exposed trypanosomes (Table 6; see also Fig. S2). Microcalorimetric studies with multiple concentrations of 28DAP010 and multiple time points would be needed to examine this phenomenon in detail, but this was beyond the scope of this study. The performed wash-out experiments suggest that the high maximum drug concentration in plasma (C_{max}) after i.p. administration (Table 7) resulted in the high *in vivo* efficacy observed after a single i.p. dose with 28DAP010. The great *in vivo* efficacy in *T. b. rhodesiense*- and *T. b. gambiense*-infected mice (Tables 2 and 4) is not surprising considering the high C_{max} combined with the long half-life of 28DAP010.

28DAP010 showed a high brain-to-plasma concentration (B/P) ratio at 72 h postdose (Table 7), suggesting good CNS penetration. The high B/P ratio appears to be largely driven by the more extensive binding of 28DAP010 to brain tissue than to plasma ($f_{u,\ plasma}/f_{u,\ brain}$). However, it has been previously observed using fluorescence microscopy that DB75 did not distribute into brain parenchyma but sequestered within endothelial cells lining the BBB and blood-cerebrospinal fluid barrier. It is unknown whether 28DAP010 was also sequestered within the endothelial cells or distributed more extensively into brain parenchyma. Nonetheless, the observed high B/P ratio and efficacy in the CNS *T. b. brucei* mouse model support 28DAP010 as a CNS-active trypanocide.

The speed at which drugs act is of varying clinical importance. Fast elimination of the parasite is not as vital for HAT patients as it is for patients infected with some other parasites, like malaria parasites, which cause much more rapid death. However, fast-acting drugs are of advantage to minimize the risk of resistant parasite selection in the patient and to reduce the hospitalization time. *In vitro* as well as *in vivo*, 28DAP010 was faster acting than DB829. However, a short exposure to 28DAP010 or to DB829 (23) was sufficient to kill the trypanosomes in a delayed manner (Table 6). High drug levels therefore do not need to be maintained over the entire parasite clearance time *in vivo*.

More problematic than a relatively slow speed of action are undesirable side effects such as hepatotoxicity or nephrotoxicity. Such effects have been observed for pentamidine (47) and DB289 (pafuramidine) (15, 16, 48), and the nephrotoxicity of pafuramidine actually led to the termination of the clinical studies (16). It is encouraging that studies with rats and mice indicate that nephrotoxicity is not clearly class related (49). DB829 (resulting from DB868 administration) accumulated less in liver and kidneys than did DB75 (after pafuramidine administration) (16). The toxicity profile of 28DAP010 may also differ from that observed for pafuramidine.

Second-stage efficacy of DB829 has been demonstrated in the mouse (14) and monkey (18) models. In the present study, 28DAP010 revealed similar efficacies in mouse models. Both molecules are able to cure both disease stages and infections with both studied subspecies, *T. b. gambiense* and *T. b. rhodesiense*, at low and tolerated doses. Extensive toxicity studies of 28DAP010 and DB829 side by side are still needed. Drug tolerability will be an important criterion for choosing the better of these two diamidines for further drug development.

There is a continuing discussion about the relative advantages and disadvantages of prodrugs and intrinsically active compounds. The use of an orally active prodrug to cure second-stage HAT could be helpful in resource-poor settings. However, parenteral administration also has advantages. The use of an active diamidine will simplify the pharmacokinetic and toxicity analyses that will be needed if the drug is to be used, and treatment with one of the backup compounds, 28DAP010 or DB829, could be short and simple. Treatment duration of 5 days or less for second stage could well be feasible and could be tested for further development for HAT on the basis of the favorable pharmacokinetics after parenteral administration.

A sustained drug development pipeline will increase the chance of getting a new and improved treatment into the market (19). This will help to control, and eventually to eliminate, the disease (50, 51). With 28DAP010, we have found a new promising backup diamidine as a preclinical candidate for the treatment of first- and second-stage African sleeping sickness.

ACKNOWLEDGMENTS

We thank Pati Pyana and Anne Clarisse Lekane Likeufack for collecting *T. b. gambiense* strains from patients in the Democratic Republic of the Congo, Guy Riccio and Christiane Braghiroli for carrying out experiments for *in vivo* efficacy and time to kill in mice, and Kirsten Gillingwater for help with the time-to-kill experiments in mice. We also thank Jennifer Jenkins for critical reading and input to the manuscript.

This work was supported by the Bill and Melinda Gates Foundation through the Consortium for Parasitic Drug Development (CPDD) and by the Swiss Tropical and Public Health Institute.

REFERENCES

1. **Simarro PP, Cecchi G, Franco JR, Paone M, Fèvre EM, Diarra A, Postigo JAR, Mattioli RC, Jannin JG.** 2011. Risk for human African trypanosomiasis, Central Africa, 2000–2009. Emerg. Infect. Dis. **17:**2322–2324. http://dx.doi.org/10.3201/eid1712.110921.
2. **WHO.** 2014. Trypanosomiasis, human African (sleeping sickness). Fact sheet no. 259. WHO, Geneva, Switzerland.
3. **Brun R, Don R, Jacobs RT, Wang MZ, Barrett MP.** 2011. Development of novel drugs for human African trypanosomiasis. Future Microbiol. **6:**677–691. http://dx.doi.org/10.2217/fmb.11.44.
4. **Blum J, Schmid C, Burri C.** 2006. Clinical aspects of 2541 patients with second stage human African trypanosomiasis. Acta Trop. **97:**55–64. http://dx.doi.org/10.1016/j.actatropica.2005.08.001.
5. **Brun R, Blum J, Chappuis F, Burri C.** 2010. Human African trypanosomiasis. Lancet **375:**148–159. http://dx.doi.org/10.1016/S0140-6736(09)60829-1.

6. **Soeiro MNC, de Castro SL, de Souza EM, Batista DGJ, Silva CF, Boykin DW.** 2008. Diamidine activity against trypanosomes: the state of the art. Curr. Mol. Pharmacol. **1:**151–161. http://dx.doi.org/10.2174/1874467210801020151.
7. **Sands M, Kron MA, Brown RB.** 1985. Pentamidine: a review. Rev. Infect. Dis. **7:**625–634. http://dx.doi.org/10.1093/clinids/7.5.625.
8. **Peregrine AS, Mamman M.** 1993. Pharmacology of diminazene: a review. Acta Trop. **54:**185–203. http://dx.doi.org/10.1016/0001-706X(93)90092-P.
9. **Werbovetz K.** 2006. Diamidines as antitrypanosomal, antileishmanial and antimalarial agents. Curr. Opin. Investig. Drugs **7:**147–157.
10. **Wang MZ, Saulter JY, Usuki E, Cheung Y-L, Hall M, Bridges AS, Loewen G, Parkinson OT, Stephens CE, Allen JL, Zeldin DC, Boykin DW, Tidwell RR, Parkinson A, Paine MF, Hall JE.** 2006. CYP4F enzymes are the major enzymes in human liver microsomes that catalyze the O-demethylation of the antiparasitic prodrug DB289 [2,5-bis(4-amidinophenyl)furan-bis-O-methylamidoxime]. Drug Metab. Dispos. **34:**1985–1994. http://dx.doi.org/10.1124/dmd.106.010587.
11. **Wang MZ, Wu JQ, Bridges AS, Zeldin DC, Kornbluth S, Tidwell RR, Hall JE, Paine MF.** 2007. Human enteric microsomal CYP4F enzymes O-demethylate the antiparasitic prodrug pafuramidine. Drug Metab. Dispos. **35:**2067–2075. http://dx.doi.org/10.1124/dmd.107.016428.
12. **Saulter JY, Kurian JR, Trepanier LA, Tidwell RR, Bridges AS, Boykin DW, Stephens CE, Anbazhagan M, Hall JE.** 2005. Unusual dehydroxylation of antimicrobial amidoxime prodrugs by cytochrome b5 and NADH cytochrome b5 reductase. Drug Metab. Dispos. **33:**1886–1893. http://dx.doi.org/10.1124/dmd.105.005017.
13. **Midgley I, Fitzpatrick K, Taylor LM, Houchen TL, Henderson SJ, Wright SJ, Cybulski ZR, John BA, McBurney A, Boykin DW, Trendler KL.** 2007. Pharmacokinetics and metabolism of the prodrug DB289 (2,5-bis[4-(n-methoxyamidino)phenyl]furan monomaleate) in rat and monkey and its conversion to the antiprotozoal/antifungal drug DB75 (2,5-bis(4-guanylphenyl)furan dihydrochloride). Drug Metab. Dispos. **35:**955–967. http://dx.doi.org/10.1124/dmd.106.013391.
14. **Wenzler T, Boykin DW, Ismail MA, Hall JE, Tidwell RR, Brun R.** 2009. New treatment option for second-stage African sleeping sickness: in vitro and in vivo efficacy of aza analogs of DB289. Antimicrob. Agents Chemother. **53:**4185–4192. http://dx.doi.org/10.1128/AAC.00225-09.
15. **Burri C.** 2010. Chemotherapy against human African trypanosomiasis: is there a road to success? Parasitology **137:**1987–1994. http://dx.doi.org/10.1017/S0031182010001137.
16. **Paine MF, Wang MZ, Generaux CN, Boykin DW, Wilson WD, De Koning HP, Olson CA, Pohlig G, Burri C, Brun R, Murilla GA, Thuita JK, Barrett MP, Tidwell RR.** 2010. Diamidines for human African trypanosomiasis. Curr. Opin. Investig. Drugs **11:**876–883.
17. **Hu L, Patel A, Bondada L, Yang S, Wang MZ, Munde M, Wilson WD, Wenzler T, Brun R, Boykin DW.** 2013. Synthesis and antiprotozoal activity of dicationic 2,6-diphenylpyrazines and aza-analogues. Bioorg. Med. Chem. **21:**6732–6741. http://dx.doi.org/10.1016/j.bmc.2013.08.006.
18. **Thuita JK.** 2013. Biological and pharmacological investigations of novel diamidines in animal models of human African trypanosomiasis. Ph.D. thesis. University of Basel, Basel, Switzerland.
19. **Mäser P, Wittlin S, Rottmann M, Wenzler T, Kaiser M, Brun R.** 2012. Antiparasitic agents: new drugs on the horizon. Curr. Opin. Pharmacol. **12:**562–566. http://dx.doi.org/10.1016/j.coph.2012.05.001.
20. **Patrick DA, Ismail MA, Arafa RK, Wenzler T, Zhu X, Pandharkar T, Jones SK, Werbovetz KA, Brun R, Boykin DW, Tidwell RR.** 2013. Synthesis and antiprotozoal activity of dicationic m-terphenyl and 1,3-dipyridylbenzene derivatives. J. Med. Chem. **56:**5473–5494. http://dx.doi.org/10.1021/jm400508e.
21. **Wenzler T, Steinhuber A, Wittlin S, Scheurer C, Brun R, Trampuz A.** 2012. Isothermal microcalorimetry, a new tool to monitor drug action against *Trypanosoma brucei* and *Plasmodium falciparum*. PLoS Negl. Trop. Dis. **6:**e1668. http://dx.doi.org/10.1371/journal.pntd.0001668.
22. **Wilson WD, Tanious FA, Mathis A, Tevis D, Hall JE, Boykin DW.** 2008. Antiparasitic compounds that target DNA. Biochimie **90:**999–1014. http://dx.doi.org/10.1016/j.biochi.2008.02.017.
23. **Wenzler T, Yang S, Braissant O, Boykin DW, Brun R, Wang MZ.** 2013. Pharmacokinetics, Trypanosoma brucei gambiense efficacy, and time of drug action of DB829, a preclinical candidate for treatment of second-stage human African trypanosomiasis. Antimicrob. Agents Chemother. **57:**5330–5343. http://dx.doi.org/10.1128/AAC.00398-13.
24. **Ismail MA, Brun R, Easterbrook JD, Tanious FA, Wilson WD, Boykin DW.** 2003. Synthesis and antiprotozoal activity of aza-analogues of furamidine. J. Med. Chem. **46:**4761–4769. http://dx.doi.org/10.1021/jm0302602.
25. **Stephens CE, Patrick DA, Chen H, Tidwell RR, Boykin DW.** 2001. Synthesis of deuterium-labelled 2,5-bis(4-amidinophenyl)furan, 2,5-bis[4-(methoxyamidino)phenyl]furan, and 2,7-diamidinocarbazole. J. Labelled Comp. Radiopharm. **44:**197–208. http://dx.doi.org/10.1002/jlcr.444.
26. **Räz B, Iten M, Grether-Bühler Y, Kaminsky R, Brun R.** 1997. The Alamar Blue assay to determine drug sensitivity of African trypanosomes (*T. b. rhodesiense* and *T. b. gambiense*) in vitro. Acta Trop. **68:**139–147. http://dx.doi.org/10.1016/S0001-706X(97)00079-X.
27. **Development Core Team R.** 2013. R: a language and environment for statistical computing. R Foundation for Statistical Computing, Vienna, Austria.
28. **Chambers JM, Hastie TJ.** 1992. Statistical models in S. Chapman & Hall/CRC, Boca Raton, FL.
29. **Hastie TJ, Tibshirani RJ.** 1990. Generalized additive models. Chapman & Hall, New York, NY.
30. **Legendre P, Legendre LFJ.** 1998. Numerical ecology. Elsevier, Amsterdam, Netherlands.
31. **Braissant O, Bonkat G, Wirz D, Bachmann A.** 2013. Microbial growth and isothermal microcalorimetry: growth models and their application to microcalorimetric data. Thermochim. Acta **555:**64–71. http://dx.doi.org/10.1016/j.tca.2012.12.005.
32. **Wang Y, Utzinger J, Saric J, Li JV, Burckhardt J, Dirnhofer S, Nicholson JK, Singer BH, Brun R, Holmes E.** 2008. Global metabolic responses of mice to *Trypanosoma brucei brucei* infection. Proc. Natl. Acad. Sci. U. S. A. **105:**6127–6132. http://dx.doi.org/10.1073/pnas.0801777105.
33. **Jennings FW, McNeil PE, Ndung'u JM, Murray M.** 1989. Trypanosomiasis and encephalitis: possible aetiology and treatment. Trans. R. Soc. Trop. Med. Hyg. **83:**518–519. http://dx.doi.org/10.1016/0035-9203(89)90272-1.
34. **Yan GZ, Brouwer KLR, Pollack GM, Wang MZ, Tidwell RR, Hall JE, Paine MF.** 2011. Mechanisms underlying differences in systemic exposure of structurally similar active metabolites: comparison of two preclinical hepatic models. J. Pharmacol. Exp. Ther. **337:**503–512. http://dx.doi.org/10.1124/jpet.110.177220.
35. **Kalvass JC, Maurer TS.** 2002. Influence of nonspecific brain and plasma binding on CNS exposure: implications for rational drug discovery. Biopharm. Drug Dispos. **23:**327–338. http://dx.doi.org/10.1002/bdd.325.
36. **Yang S, Wenzler T, Miller PN, Wu H, Boykin DW, Brun R, Wang MZ.** 5 May 2014. Mechanisms underlying the differential efficacy of cationic diamidines against first and second stage human African trypanosomiasis: a pharmacokinetic comparison. Antimicrob. Agents Chemother. http://dx.doi.org/10.1128/AAC.02605-14.
37. **Ward CP, Wong PE, Burchmore RJ, de Koning HP, Barrett MP.** 2011. Trypanocidal furamidine analogues: influence of pyridine nitrogens on trypanocidal activity, transport kinetics, and resistance patterns. Antimicrob. Agents Chemother. **55:**2352–2361. http://dx.doi.org/10.1128/AAC.01551-10.
38. **Williamson J, Rollo IM.** 1959. Drug resistance in trypanosomes; cross-resistance analyses. Br. J. Pharmacol. Chemother. **14:**423–430. http://dx.doi.org/10.1111/j.1476-5381.1959.tb00946.x.
39. **Bernhard SC, Nerima B, Mäser P, Brun R.** 2007. Melarsoprol- and pentamidine-resistant *Trypanosoma brucei rhodesiense* populations and their cross-resistance. Int. J. Parasitol. **37:**1443–1448. http://dx.doi.org/10.1016/j.ijpara.2007.05.007.
40. **Baker N, de Koning HP, Mäser P, Horn D.** 2013. Drug resistance in African trypanosomiasis: the melarsoprol and pentamidine story. Trends Parasitol. **29:**110–118. http://dx.doi.org/10.1016/j.pt.2012.12.005.
41. **Mäser P, Sütterlin C, Kralli A, Kaminsky R.** 1999. A nucleoside transporter from *Trypanosoma brucei* involved in drug resistance. Science **285:**242–244. http://dx.doi.org/10.1126/science.285.5425.242.
42. **Matovu E, Stewart ML, Geiser F, Brun R, Mäser P, Wallace LJM, Burchmore RJ, Enyaru JCK, Barrett MP, Kaminsky R, Seebeck T, de Koning HP.** 2003. Mechanisms of arsenical and diamidine uptake and resistance in *Trypanosoma brucei*. Eukaryot. Cell **2:**1003–1008. http://dx.doi.org/10.1128/EC.2.5.1003-1008.2003.
43. **Baker N, Glover L, Munday JC, Aguinaga Andrés D, Barrett MP, de Koning HP, Horn D.** 2012. Aquaglyceroporin 2 controls susceptibility to melarsoprol and pentamidine in African trypanosomes. Proc. Natl. Acad. Sci. U. S. A. **109:**10996–11001. http://dx.doi.org/10.1073/pnas.1202885109.

44. **Graf FE, Ludin P, Wenzler T, Kaiser M, Brun R, Pyana PP, Büscher P, de Koning HP, Horn D, Mäser P.** 2013. Aquaporin 2 mutations in *Trypanosoma brucei gambiense* field isolates correlate with decreased susceptibility to pentamidine and melarsoprol. PLoS Negl. Trop. Dis. **7:**e2475. http://dx.doi.org/10.1371/journal.pntd.0002475.
45. **Mathis AM, Bridges AS, Ismail MA, Kumar A, Francesconi I, Anbazhagan M, Hu Q, Tanious FA, Wenzler T, Saulter J, Wilson WD, Brun R, Boykin DW, Tidwell RR, Hall JE.** 2007. Diphenyl furans and aza analogs: effects of structural modification on in vitro activity, DNA binding, and accumulation and distribution in trypanosomes. Antimicrob. Agents Chemother. **51:**2801–2810. http://dx.doi.org/10.1128/AAC.00005-07.
46. **Berger BJ, Carter NS, Fairlamb AH.** 1995. Characterisation of pentamidine-resistant *Trypanosoma brucei brucei*. Mol. Biochem. Parasitol. **69:**289–298. http://dx.doi.org/10.1016/0166-6851(94)00215-9.
47. **Turner PR, Denny WA.** 1996. The mutagenic properties of DNA minor-groove binding ligands. Mutat. Res. **355:**141–169. http://dx.doi.org/10.1016/0027-5107(96)00027-9.
48. **Harrill AH, Desmet KD, Wolf KK, Bridges AS, Eaddy JS, Kurtz CL, Hall JE, Paine MF, Tidwell RR, Watkins PB.** 2012. A mouse diversity panel approach reveals the potential for clinical kidney injury due to DB289 not predicted by classical rodent models. Toxicol. Sci. Off. J. Soc. Toxicol. **130:**416–426. http://dx.doi.org/10.1093/toxsci/kfs238.
49. **Wolf KK, DeSmet K, Bridges A, Tidwell R, Paine MF, Hall JE, Watkins PB.** 2012. Two structurally similar anti-parasitic prodrugs differ markedly in toxicity profilesabstr ID2928. Soc. Toxicol. Annu. Meet. Abstr. Suppl.
50. **Simarro PP, Diarra A, Ruiz Postigo JA, Franco JR, Jannin JG.** 2011. The Human African Trypanosomiasis Control and Surveillance Programme of the World Health Organization 2000–2009: the way forward. PLoS Negl. Trop. Dis. **5:**e1007. http://dx.doi.org/10.1371/journal.pntd.0001007.
51. **Maurice J.** 2013. New WHO plan targets the demise of sleeping sickness. Lancet **381:**13–14. http://dx.doi.org/10.1016/S0140-6736(13)60006-9.
52. **Brun R, Schumacher R, Schmid C, Kunz C, Burri C.** 2001. The phenomenon of treatment failures in human African trypanosomiasis. Trop. Med. Int. Health **6:**906–914. http://dx.doi.org/10.1046/j.1365-3156.2001.00775.x.
53. **Jennings FW, Gray GD.** 1983. Relapsed parasitaemia following chemotherapy of chronic *T. brucei* infections in mice and its relation to cerebral trypanosomes. Contrib. Microbiol. Immunol. **7:**147–154.
54. **Felgner P, Brinkmann U, Zillmann U, Mehlitz D, Abu-Ishira S.** 1981. Epidemiological studies on the animal reservoir of *gambiense* sleeping sickness. Part II. Parasitological and immunodiagnostic examination of the human population. Tropenmed. Parasitol. **32:**134–140.
55. **Likeufack ACL, Brun R, Fomena A, Truc P.** 2006. Comparison of the in vitro drug sensitivity of *Trypanosoma brucei gambiense* strains from West and Central Africa isolated in the periods 1960–1995 and 1999–2004. Acta Trop. **100:**11–16. http://dx.doi.org/10.1016/j.actatropica.2006.09.003.
56. **Pyana PP, Ngay Lukusa I, Mumba Ngoyi D, Van Reet N, Kaiser M, Karhemere Bin Shamamba S, Büscher P.** 2011. Isolation of *Trypanosoma brucei gambiense* from cured and relapsed sleeping sickness patients and adaptation to laboratory mice. PLoS Negl. Trop. Dis. **5:**e1025. http://dx.doi.org/10.1371/journal.pntd.0001025.
57. **Maina N, Maina KJ, Mäser P, Brun R.** 2007. Genotypic and phenotypic characterization of *Trypanosoma brucei gambiense* isolates from Ibba, South Sudan, an area of high melarsoprol treatment failure rate. Acta Trop. **104:**84–90. http://dx.doi.org/10.1016/j.actatropica.2007.07.007.

General Discussion and Conclusion

This PhD thesis was embedded in the international and nonprofit 'Consortium for Parasitic Drug Development' (CPDD) with the aim to discover new treatments for second stage human African trypanosomiasis.

We focused on the discovery of novel aromatic diamidines. Lead optimization efforts resulted in compounds that cured trypanosome-infected animals by the oral route and animals with second stage disease by an oral or parenteral route of administration without overt toxicity. These two achievements are great advances in the diamidine research since the mother molecule pentamidine has to be administered parenterally and only cures the first stage of the disease.

In this thesis we characterized in vitro and in vivo the most promising novel diamidines and prodrugs thereof and finally were able to identify two new preclinical candidates, DB829 and 28DAP010, for a parenteral treatment of second stage and one preclinical candidate, DB868, for oral treatment of first stage sleeping sickness.

Stimulated by the poor oral bioavailability of diamidines, we searched for prodrugs that are neutral, in contrast to their parent diamidines, which contain charged amidine groups. Especially the di-O-methylamidoxime (methamidoxime) prodrug derivatives exhibited enhanced oral activity and reduced acute toxicity in animal models for trypanosomiasis (Ansede et al., 2004). A prodrug is a precursor molecule that shows no in vitro activity. After oral absorption it is converted by host enzymes to its active form, the parent diamidine (Saulter et al., 2005; Werbovetz, 2006). The prodrug approach was successful with regard to oral bioavailability in animal models (Chapters 3 and 4; Hu et al., 2013; Midgley et al., 2007; Wenzler et al., 2009; Werbovetz, 2006) as well as in humans, where the prodrug DB289 (pafuramidine maleate) underwent clinical trials as the first oral drug for treatment of first stage HAT patients (Burri, 2010; Paine et al., 2010).

During the clinical trials with pafuramidine, drug discovery of diamidines and their prodrugs continued. We screened over 2000 molecules in vitro and found almost 500 compounds that had IC_{50}s below 100 nM against the *T. b. rhodesiense* strain STIB900 and an in vitro selectivity index (SI) >1000 versus L6 cells, a rat myoblast cell line. Thus diamidines were highly potent in vitro and selective against the parasite.

The most active diamidines in vitro and their prodrugs were tested for efficacy in mouse models for African trypanosomiasis. Several backup compounds were identified that were more potent orally than pafuramidine and could serve as second-generation diamidine prodrugs (Chapters 3, 4 and 8; Hu et al., 2013; Patrick et al., 2013; Wenzler et al., 2009). Two of the new prodrugs, DB844 and DB868, were particularly superior to pafuramidine in CNS infected mice. The blood-brain-barrier (BBB) is a membrane that hinders diamidines from penetrating into the brain which is a prerequisite for CNS activity. Both CNS potent prodrugs were aza analogues of pafuramidine (Chapter 3; Wenzler et al., 2009).

Safety and second stage efficacy of DB844 was additionally studied in a vervet monkey model of CNS stage HAT (Thuita et al., 2012). DB844 efficacy was superior to pentamidine and pafuramidine which were both non-curative in the same monkey model. Unfortunately, toxicity was higher than that of pafuramidine and thus the therapeutic window not large enough to follow up on DB844 as a new preclinical drug candidate for the treatment of HAT (Thuita et al., 2012).

The most promising prodrug for HAT is currently DB868. Its safety was assessed in two different monkey species and DB868 was tolerated in vervet monkeys up to a dose of 30 mg/kg per day for 10 days (Thuita et al., 2013). Plasma biomarkers indicative of liver injury were not significantly altered by drug administration and kidney-mediated alterations in creatinine and urea concentrations were not observed either. Follow-up efficacy experiments demonstrated that DB868 is capable to cure all infected monkeys with *T. b. rhodesiense* infection during first stage disease at a cumulative dose 14-fold lower than the maximum tolerated dose (Thuita et al., 2013). However, only one out of

four infected monkeys with second stage disease were cured at both 10 and 20 mg/kg p.o. per day for 10 days (Thuita, 2013). Since DB868 is significantly better tolerated, cures infected monkeys at lower doses, and has thus a larger therapeutic window than pafuramidine, DB868 can be considered a backup clinical candidate for a new and safe oral treatment of first stage HAT.

We tested many other diamidine prodrugs in the GVR35 CNS mouse model by the oral administration route. However, only very few showed CNS activity and none exceeded that of DB844 and DB868 (Chapters 3 and 4; Hu et al., 2013; Wenzler et al., 2009). The third most potent compound was the curved 2,6-diarylpyrazine diamidine prodrug DB1227 (compound 12 in (Chapter 4; Hu et al., 2013)) in the highly stringent GVR35 mouse model of CNS stage HAT (Figure 1). It cured two out of five infected mice at 100 mg/kg p.o. per day administered on 5 consecutive days and three out of four infected mice when administered for 10 days. This compound merits further evaluation for an oral treatment of HAT (second to DB868).

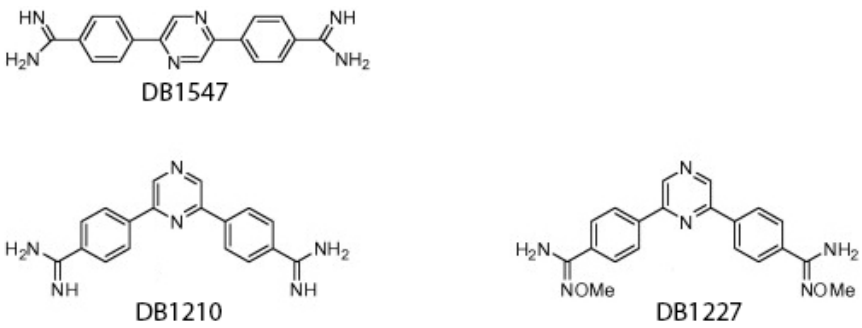

Figure 1: Chemical structures of the 2,5-diphenyl pyrazine diamidine DB1547 and the 2,6-diphenyl pyrazine diamidine DB1210 and its methamidoxime prodrug DB1227. Figure adapted from (Hu et al., 2013).

These examples show that the prodrug approach was successful. It improved *in vivo* efficacy by the oral route and in some cases even cured second stage HAT in animal models, implying good absorption across the intestinal barrier and sometimes even across the BBB (Chapters 3 and 4; Hu et al., 2013; Wenzler et al., 2009).

The DNA binding to the minor groove was higher for DB1210 (ΔT_m = 15.1°C) (compound 10 in (Chapter 4; Hu et al., 2013)), the parent diamidine of DB1227 (Figure 1), than for the linear 2,6-diarylpyrazine diamidine DB1547 (ΔT_m = 8.0°C), probably due to the crescent shape of DB1210 that fits better to the DNA curvature. The DNA binding of the linear compound DB1547 was probably achieved by incorporation of water molecules to form a complex with the DNA minor groove (Chapter 4; Hu et al., 2013; Miao et al., 2005). Not only the DNA binding but also the in vitro and in vivo activity was improved with the curved 2,6-diarylpyrazine diamidine DB1210 compared to its linear 2,5 isomer (Chapter 4; Hu et al., 2013). This is another example were DNA binding correlates with trypanocidal activity, which has been observed in many instances but not all, indicating that binding to kDNA or binding to genomic DNA is an important part of the mode of action of these diamidines.

CNS activity of the parent diamidine DB1210 was studied in the GVR35 CNS mouse model by a intraperitoneal (i.p.) route at 20 mg/kg per day administered on 10 consecutive days that cured one out of three infected mice (unpublished data). This compound is more active than expected by a cationic diamidine but its CNS activity is still not sufficient for considering it as a new lead for a parenteral treatment for second stage HAT.

Several other parent diamidines were tested by the i.p. route not only in the STIB900 acute mouse model which mimics the first stage of HAT but also in the GVR35 CNS mouse model. As hypothesized, most of them were inactive, as these compounds are protonated at physiological pH. However, one diamidine, DB829 (CPD0801) was able to cure CNS infected mice at 20 mg/kg i.p. per day administered for 10 days (Chapter 3; Wenzler et al., 2009) or 25mg/kg i.p. per day for 5 days (Chapter 9; Wenzler et al., 2013a). This was unexpected. For several years this was the only diamidine - a singleton - that was able to cure CNS infected mice. Just recently we identified another diamidine with CNS activity which is 28DAP010 (CPD0905) (Chapters 8 and 9; Patrick et al., 2013; Wenzler et al., 2013a). Interestingly, both are chemically highly related compounds (Figure 2). Our data confirm that certain diamidines can indeed cross the BBB and be

CNS active. We hypothesize that a transporter located at the BBB recognizes these two structurally highly related compounds and transports them actively across the BBB into the brain since passive diffusion across the BBB is unlikely.

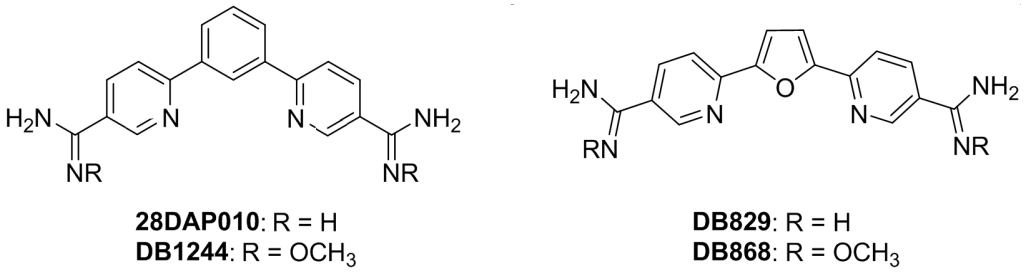

28DAP010: R = H
DB1244: R = OCH_3

DB829: R = H
DB868: R = OCH_3

Figure 2: Chemical structures of the diamidines 28DAP010 and DB829 and their methamidoxime prodrugs DB1244 and DB868. Figure adapted from Wenzler et al.,(2013a).

DB1244, the methamidoxime prodrug of 28DAP010 was similarly active in the STIB900 acute mouse model as DB868 the methamidoxime prodrug of DB829. Both prodrugs cured two out of four mice at 25 mg/kg p.o. when administered for 4 days (Chapters 3 and 8; Patrick et al., 2013; Wenzler et al., 2009). However, DB1244 was less active in the GVR35 CNS mouse model, resulting in no cures at the same dose at which DB868 was curative (Chapters 3 and 9; Wenzler et al., 2013a, 2009). DB1244 is bioconverted to 28DAP010 as indicated by the high efficacy of DB1244 in the STIB900 acute mouse model. It is therefore more likely that the level of plasma protein- and tissue-binding of the prodrug or metabolites determine whether the compound is CNS active or inactive than differences in bioconversion.

Membrane transporters at the trypanosome cell surface that recognize diamidine compounds as a substrate are important for the selective uptake. The P2 transporter, encoded by the gene *TbAT1,* has been identified in 1999 (Mäser et al., 1999). It is involved in drug uptake of diamidines and melamine-based arsenicals and causes cross-resistance between pentamidine and melarsoprol which are both used to treat HAT. *TbAT1* gene deletion or mutated P2 transporters with impaired function were described in drug resistant strains induced in the laboratory or in trypanosome isolates from the field

(Baker et al., 2013). Recent studies revealed that there is another transporter, aquaglyceroporin 2 (AQP2), that is involved in cross-resistance between melarsoprol and pentamidine (Baker et al., 2012).

The selective uptake improves the selectivity of these compounds towards the parasite. However, genetic changes (unless deleterious to the parasite) can lead to altered and reduced drug uptake and thus to drug resistance. A big threat for a new compound is its potential of cross-resistance with current drugs. Especially since the novel diamidines are chemically analogous to pentamidine, an understanding of the mechanism underlying drug resistance is of help to estimate its potential for cross-resistance.

AQP2-related resistance to melarsoprol and pentamidine has been observed in laboratory-induced resistant trypanosomes (Baker et al., 2012). We investigated if AQP2 impairments also occur in the field and analyzed twelve *T. b. gambiense* field isolates, among which eight were from melarsoprol-refractory patients. We found that six of the analyzed *T. b. gambiense* strains isolated from melarsoprol relapse patients carried a chimeric *TbAQP2/3* gene in both or at least in one allele (Chapter 5; Graf et al., 2013). These six strains had a significantly lower in vitro susceptibility to pentamidine and melarsoprol than the *TbAQP* 'wild-type' isolates. This demonstrates that rearrangements of *TbAQP2 - TbAQP3* locus occur also in the field and are not just an artificial laboratory product.

Interestingly, the occurrence of the chimeric *TbAQP2/3* genes correlated with reduced in vitro susceptibility to pentamidine and melarsoprol but not with reduced susceptibility to diminazene (Chapters 5 and 9; Graf et al., 2013; Wenzler et al., 2013a). Diminazene, in contrast to pentamidine and melarsoprol, is taken up exclusively by the P2-transporter (de Koning et al., 2004). Therefore it is not unexpected, that diminazene uptake is independent of AQP2. Additionally, Baker et al. (2012) showed that deletion of *AQP2* caused only resistance to pentamidine and melarsoprol but not to other diamidines such as diminiazene or the monoamidine isometamidium.

We have tested DB829 and 28DAP010 in a *TbAT1*-KO cell line and observed a resistance factor (RF = IC_{50} AT1-KO / IC_{50} wild type) of 16 to 18 which is comparable to that of DB75 and diminazene (Chapters 3 and 9; Wenzler et al., 2013a, 2009). This suggests that DB829 and 28DAP010 are both also taken up primarily by the P2 transporter. This bears some risk of cross-resistance to melarsoprol. However, we do not know whether loss of *TbAT1* really causes treatment failures nor how well trypanosomes with P2 deletions are transmitted by the tsetse fly. Eighteen *T. b. gambiense* isolates have been collected from patients in South Sudan from an area where a high melarsoprol treatment failure rate (20%) was reported with the aim to identify drug resistant isolates or *TbAT1*(resistant)-type alleles (Maina et al., 2007). However, no evidence for an impaired P2 transporter was found. The strains were collected in the year 2003. Interestingly, the first-line drug for the second stage disease had been switched from melarsoprol to eflornithine already in 2001 (Maina et al., 2007). If resistance based on mutated P2 transporters existed in that area, they might have been acquired but carried some fitness cost negatively affecting the transmission. A similar result has been observed at the Omugo focus in North Western Uganda (Kazibwe et al., 2009). In Omugo, base-line genotypes were available when melarsoprol treatment failure was prevalent and could be compared with the data several years after melarsoprol had been withdrawn. The mutant *TbAT1* alleles found in isolates from melarsoprol relapse patients in the year 1998 have disappeared in 2006, suggesting that drug pressure is responsible for circulating trypanosomes with impaired P2 transporters (Kazibwe et al., 2009).

The AQP2 mediated uptake may have a greater impact on the cross-resistance of pentamidine and melarsoprol than the P2 transporter (Baker et al., 2013). The resistance factor in *TbAT1* null mutants is only slightly increased in vitro to melarsoprol and pentamidine (RF = 2 to 5) (Chapter 3; Matovu et al., 2003; Wenzler et al., 2009) whereas resistance in *TbAQP2* null mutants is more pronounced, especially to pentamidine (RF > 15) (Baker et al., 2012).

The *T. b. gambiense* field isolates from melarsoprol refractory patients that contained a chimeric *TbAQP2* gene (40R, 45R, 130R, 349R and K03048; IC_{50}s = 47 to 81 nM) were

all 8 to 80-fold less sensitive to pentamidine than trypanosomes with a wild type *TbAQP2* gene (STIB930, ITMAP141267 and DAL898R; IC_{50}s = 1 to 6 nM) (Chapters 5, 7 and 9; Graf et al., 2013; Wenzler et al., 2013a, 2013b). Interestingly, loss of resistance did not correlate to the same extent to DB829 or 28DAP010 (Chapters 7 and 9; Wenzler et al., 2013a, 2013b). We suppose based on these data that the AQP2 of *T. brucei* does not mediate DB829 and 28DAP010 uptake and conclude that the AQP2 is unlikely a source for potential cross-resistance of melarsoprol or pentamidine with one of the novel diamidines DB829 or 28DAP010. Further analysis to determine the resistant factor for DB829 and 28DAP010 with a *TbAQP2* null mutant and herewith the final evidence for our hypothesis will probably be done in other laboratories (e.g. Horn et al).

The potential for cross-resistance is not only related to drug uptake as e.g. was observed for diamidines and melarsoprol via P2 or AQP2. The activation of the prodrugs fexinidazole and nifurtimox rely on the same enzyme (a parasite type I nitroreductase) for its activation (R. Wilkinson et al., 2011). This could also bear some risk of cross-resistance development.

Time of drug action of diamidines is often long and the parasite clearance time or its dependency on drug concentrations important to know to predict clinical outcome and to optimize dosing regimens. Time to kill analyses are particular time- and labor-intensive or expensive with conventional laboratory methods. Within this thesis we established a new method to determine time of drug action, in particular the time to kill pathogenic protozoans in vitro (Chapter 6; Wenzler et al., 2012). We exploited the capacity of viable cells to produce heat. The highly sensitive microcalorimeters are able to measure heat flow, which correlates with the density of viable cells in a culture (Figure 3). The main advantages of this method are that microcalorimetry is simple to use, the samples do not need any fluorescence or other kind of labeling, and it measures the heat flow of the parasite culture on a real time basis (1 measurement per second) (Chapter 6; Wenzler et al., 2012). Heat flow measurements are unspecific. Onset of drug action by a small change in the heat flow can be detected already by a reduced metabolic activity of drug treated cells, which can be detected earlier than by standard viability measurements.

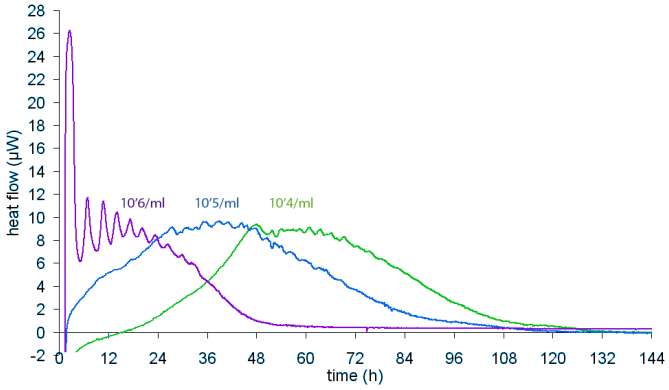

Figure 3: Microcalorimetric heat flow measurements of *T. b. rhodesiense* at different initial parasite densities of 10^6 cells, 10^5 cells and 10^4 cells / ml (Wenzler et al., 2012).

One drawback of this methodology is the sample numbers. A typical calorimeter e.g. TAM III from TA instruments, contains 48 channels. The throughput is therefore significantly lower compared to conventional viability analysis in the 96- or 384-well format. Routine drug screening to measure inhibition (e.g. IC_{50}s) of a large number of diverse compounds will most likely continue with established methods such as the Resazurin / Alamar blue assay. However, microcalorimetry is a promising tool for gathering extra information for lead compounds, such as onset of drug action and time to kill of the parasite culture (Chapter 6; Wenzler et al., 2012).

We applied this method to analyze time of drug action of our two most promising diamidines DB829 and 28DAP010. Both diamidines were similarly potent in vitro against the *T. b. rhodesiense* strain STIB900, the *T. b. brucei* strain BS221, against several *T. b. gambiense* strains, and in vivo models of acute and CNS infection (Chapters 3, 7 and 9; Wenzler et al., 2013a, 2013b, 2009). Nevertheless, we could distinguish these two compounds based on their time of drug action. 28DAP010 was acting significantly faster than DB829 in vitro especially at concentrations above 10x IC_{50}s. The clearance time in vivo was also faster in mice treated with 28DAP010 (1 to 2 days) than with DB829 (3 to 5 days) and more homogenous versus the different trypanosome strains STIB900 (26h / 78h), STIB930 (40h / 62h), and ITMAP141267 (42h / 102h) (Chapters 7 and 9; Wenzler et al., 2013a, 2013b).

We observed a saturation at concentrations above 2,000 nM of DB829 in our microcalorimetry results (Chapter 7; Wenzler et al., 2013b). Up to 2,000 nM, the inhibition increased dose-dependently, whereas above 2,000 nM no further inhibition was observed versus any of the three trypanosome strains. This is likely related to the saturation of the P2 transporter. In a P2 transporter-mediated uptake assay, the Michaelis-Menten constant, K_m, of DB829 was 1.1 μM (Ward et al., 2011), indicating that the maximum uptake rate is almost reached around 2 μM and therefore no significantly higher inhibition can be expected at higher drug concentrations (Chapter 7; Wenzler et al., 2013b).

Interestingly, no such saturation was observed with 28DAP010 (Chapter 9; Wenzler et al., 2013a). In addition to P2, there may be a low affinity - high capacity transporter involved in drug uptake of 28DAP010 but not of DB829, and this hypothetical additional transporter increases drug import at high 28DAP010 concentrations.

DB829 showed some efficacy by the oral route. We have tested DB829 in the acute mouse model and found that it cured three out of four mice at 50 mg/kg p.o. when administered for 4 days, which is more than 10-fold higher than what is required by an i.p. route (Chapters 3 and 7; Wenzler et al., 2013b, 2009). 28DAP010 has not yet been tested orally but a similar effect can be expected. Interestingly another diamidine, Synthalin, a previous anti-diabetic drug, was also active orally (Synthalin and Insulin, 1927). This shows that certain diamidines have better intestinal absorption than others. Oral bioavailability increased from DB75 (0.2%) to DB820 (0.4%) to DB829 with the highest oral bioavailability of 1.2% (personal communication Michael Wang). However, the oral bioavailability of DB829 would be far too low to cure CNS infections. Therefore, to maximize efficacy, this compound still needs to be administered by a parenteral route.

One issue of diamidines is the hepato- and nephrotoxicity that was observed with several diamdines such as synthalin, pentamidine and pafuramidine (Burri, 2010; Harrill et al., 2012; Paine et al., 2010; Turner and Denny, 1996). Especially problematic is the delayed-onset of renal insufficiency observed in an expanded Phase I study, which resulted in the

cancellation of pafuramidine development. Interestingly, the novel aza analog DB829 accumulated in rat kidney cells more than ten-times less than furamidine after a single intravenous dose of 10 μmol/kg (Brun et al., 2011; Paine et al., 2010). The low kidney exposure with DB829 may provide the necessary safety margin that is required to develop this CNS-active diamidine to a second stage HAT medication.

Variations in uptake rate, accumulation, oral bioavailability, pharmacokinetics, and BBB penetration show that diamidines have different characteristics. Discarding the entire class of compounds from the HAT pipeline because several diamidines have a small therapeutic window because of the risk of hepato and renal toxicity, may not be sensible. Fexinidazole was a similar case (Tweats et al., 2012). This compound was dropped in the 80s because of potential mutagenicity but was recollected by DNDi almost 30 years later and it is now one of the most promising clinical candidates for the treatment of HAT. We propose a careful toxicity evaluation of DB829 and 28DAP010 instead of discarding the entire diamidine class from the HAT pipeline.

A pharmacological effect can persist beyond the time trypanocidal drug concentrations are detectable in the plasma. It has been shown that several diamidines are taken up to high concentrations (mM) into African trypanosomes within minutes or hours but trypanosome death occurred up to days later (Mathis et al., 2007; Werbovetz, 2006; Wilson et al., 2008). We performed a wash-out experiment with DB829 and 28DAP010 with a 24 hours drug exposure time (i) because a single curative dose of 20 mg/kg i.p. gave a high and long exposure with plasma levels after 24 h of 0.483 μM for DB829 and 0.982 μM for 28DAP010 (Chapters 7 and 9; Wenzler et al., 2013a, 2013b) and (ii) because the uptake rate of DB829 is slower than that of pentamidine, DB75, or DB820 (Ward et al., 2011). Using microcalorimetry, we studied drug action on pre-exposed trypanosome cultures after the drug had been removed and observed that concentrations of 200 nM for STIB900 (Figure 4) and 2,000 nM for STIB930 were sufficient to kill the parasite culture in vitro 2.5 to 4.5 days after the drug was removed (Chapters 7 and 9; Wenzler et al., 2013a, 2013b). The accumulated drug in the parasite was killing the

parasites in a delayed manner. Our data show that the plasma drug levels do not need to be maintained until all the parasites are killed.

Activity and time of drug action of different diamidines was thought to correlate with uptake (Ward et al., 2011). The time to peak and the time to kill were comparable after drug washout for DB829 and 28DAP010 at 200 nM on STIB900 (Figure 3) or at 2,000 nM on STIB930 (Chapters 7 and 9; Wenzler et al., 2013a, 2013b). The same killing kinetics may indicate same mechanism of action and the faster time to kill at high 28DAP010 concentrations could indeed be related due to a higher uptake rate only.

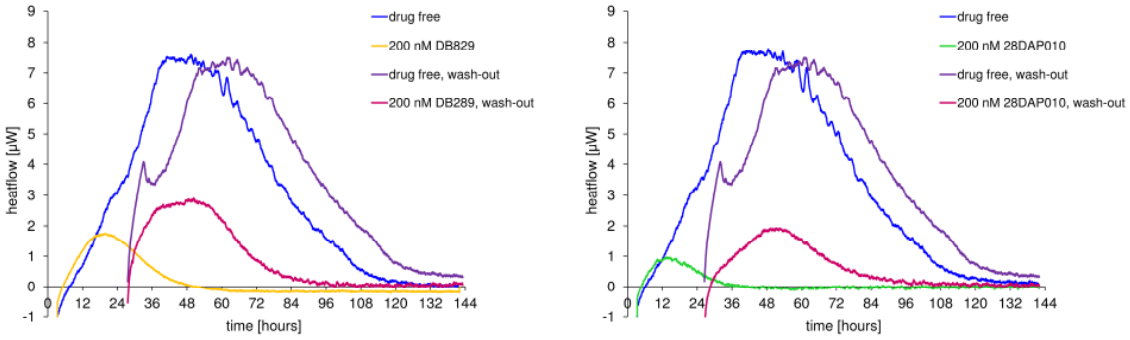

Figure 4: Effect of drug washout after a 24 hours exposure with DB829 and 28DAP010 at 200 nM on the *T. b. rhodesiense* strain STIB900. Parasites were still viable after 24 hours of exposure. The heat flow further increased for 1 additional day after drug wash-out, and then the parasite culture died off and was killed around 3 days after the drug was washed out.

With these studies we have shown that DB829 and 28DAP010 are highly active in vivo against the human pathogenic *T. brucei* subspecies and that both are highly active on either disease stage. Whether one of the two could be used for HAT patients without the need of staging is still unclear. However, treatment for the first stage disease is likely to be shorter than the one for second stage disease. The question remains whether parenteral application would be accepted for first stage infections.

Interindividual differences in patients' response have been observed in the clinical development for pafuramidine. Bioconversion to the active diamidine, which involved different activation steps, varied between patients (personal communication Christian

Burri). Administration of an active diamidine itself, rather than a prodrug, will simplify pharmacokinetic predictions and will help to select the optimal dosage for a safe and effective treatment (Chapters 7 and 9; Wenzler et al., 2013a, 2013b).

A well-tolerated drug is desired that cures first as well as second stage by an oral route and with a short treatment, preferably single dose. The current drugs, however, are far from that. Finally, great advancements have been made and the pipeline has been filled up with new HAT drug candidates (Chapter 1; Mäser et al., 2012). Fexinidazole has entered clinical trials Phase II/III to investigate safety and efficacy of a 10 days oral treatment, and development of the oxaborole compound SCYX-7158 for second stage HAT has been initiated with a Phase I study with a single oral dose. Whether one of these two compounds will make it to the market is not yet clear. Statistically, two compounds entering the clinical trials are not sufficient to ensure a new treatment option for HAT. We have experienced with pafuramidine, how fast a compound can drop out from clinical development. Pafuramidine had looked highly promising until the delayed renal toxicity was observed in mid-phase III, which instantly terminated the development program (Burri, 2010; Harrill et al., 2012; Paine et al., 2010).

Most likely, the development of a third compound will not be funded as long as fexinidazole and SCYX-7158 are under clinical testing. Otherwise, a parenteral treatment may be still acceptable in particular for the severe second stage of the disease. A treatment with DB829 or 28DAP010 will be cheaper, and simpler to administer than the NECT therapy which is already an improvement over current drugs on the market. Furthermore, DB829 and 28DAP010 will cure by shorter treatment duration. A single dose for first stage and a 5-day treatment for second stage disease can be realistically considered for the clinical development for the treatment of HAT.

A safe and effective treatment is a prerequisite for the control and elimination of African sleeping sickness. With DB829 and 28DAP010 we identified promising preclinical backup candidates for the development of a new treatment of 2nd stage HAT.

References

Ansede, J.H., Anbazhagan, M., Brun, R., Easterbrook, J.D., Hall, J.E., Boykin, D.W., 2004. O-alkoxyamidine prodrugs of furamidine: in vitro transport and microsomal metabolism as indicators of in vivo efficacy in a mouse model of Trypanosoma brucei rhodesiense infection. J. Med. Chem. 47, 4335–4338.

Baker, N., de Koning, H.P., Mäser, P., Horn, D., 2013. Drug resistance in African trypanosomiasis: the melarsoprol and pentamidine story. Trends Parasitol. 29, 110–118.

Baker, N., Glover, L., Munday, J.C., Aguinaga Andrés, D., Barrett, M.P., de Koning, H.P., Horn, D., 2012. Aquaglyceroporin 2 controls susceptibility to melarsoprol and pentamidine in African trypanosomes. Proc. Natl. Acad. Sci. U. S. A. 109, 10996–11001.

Brun, R., Don, R., Jacobs, R.T., Wang, M.Z., Barrett, M.P., 2011. Development of novel drugs for human African trypanosomiasis. Future Microbiol. 6, 677–691.

Burri, C., 2010. Chemotherapy against human African trypanosomiasis: is there a road to success? Parasitology 137, 1987–1994.

De Koning, H.P., Anderson, L.F., Stewart, M., Burchmore, R.J.S., Wallace, L.J.M., Barrett, M.P., 2004. The trypanocide diminazene aceturate is accumulated predominantly through the TbAT1 purine transporter: additional insights on diamidine resistance in african trypanosomes. Antimicrob. Agents Chemother. 48, 1515–1519.

Graf, F.E., Ludin, P., Wenzler, T., Kaiser, M., Brun, R., Pyana, P.P., Büscher, P., de Koning, H.P., Horn, D., Mäser, P., 2013. Aquaporin 2 Mutations in Trypanosoma brucei gambiense Field Isolates Correlate with Decreased Susceptibility to Pentamidine and Melarsoprol. PLoS Negl Trop Dis 7, e2475.

Harrill, A.H., Desmet, K.D., Wolf, K.K., Bridges, A.S., Eaddy, J.S., Kurtz, C.L., Hall, J.E., Paine, M.F., Tidwell, R.R., Watkins, P.B., 2012. A mouse diversity panel approach reveals the potential for clinical kidney injury due to DB289 not predicted by classical rodent models. Toxicol. Sci. Off. J. Soc. Toxicol. 130, 416–426.

Hu, L., Patel, A., Bondada, L., Yang, S., Wang, M.Z., Munde, M., Wilson, W.D., Wenzler, T., Brun, R., Boykin, D.W., 2013. Synthesis and antiprotozoal activity of dicationic 2,6-diphenylpyrazines and aza-analogues. Bioorg. Med. Chem. 21, 6732–6741.

Kazibwe, A.J.N., Nerima, B., de Koning, H.P., Mäser, P., Barrett, M.P., Matovu, E., 2009. Genotypic Status of the TbAT1/P2 Adenosine Transporter of Trypanosoma brucei gambiense Isolates from Northwestern Uganda following Melarsoprol Withdrawal. PLoS Negl Trop Dis 3, e523.

Maina, N., Maina, K.J., Mäser, P., Brun, R., 2007. Genotypic and phenotypic characterization of Trypanosoma brucei gambiense isolates from Ibba, South Sudan, an area of high melarsoprol treatment failure rate. Acta Trop. 104, 84–90.

Mäser, P., Sütterlin, C., Kralli, A., Kaminsky, R., 1999. A nucleoside transporter from Trypanosoma brucei involved in drug resistance. Science 285, 242–244.

Mäser, P., Wittlin, S., Rottmann, M., Wenzler, T., Kaiser, M., Brun, R., 2012. Antiparasitic agents: new drugs on the horizon. Curr. Opin. Pharmacol.

Mathis, A.M., Bridges, A.S., Ismail, M.A., Kumar, A., Francesconi, I., Anbazhagan, M., Hu, Q., Tanious, F.A., Wenzler, T., Saulter, J., Wilson, W.D., Brun, R., Boykin, D.W., Tidwell, R.R., Hall, J.E., 2007. Diphenyl Furans and Aza Analogs: Effects of Structural Modification on In Vitro Activity, DNA Binding, and Accumulation and Distribution in Trypanosomes. Antimicrob. Agents Chemother. 51, 2801–2810.

Matovu, E., Stewart, M.L., Geiser, F., Brun, R., Mäser, P., Wallace, L.J.M., Burchmore, R.J., Enyaru, J.C.K., Barrett, M.P., Kaminsky, R., Seebeck, T., de Koning, H.P., 2003. Mechanisms of arsenical and diamidine uptake and resistance in Trypanosoma brucei. Eukaryot. Cell 2, 1003–1008.

Miao, Y., Lee, M.P.H., Parkinson, G.N., Batista-Parra, A., Ismail, M.A., Neidle, S., Boykin, D.W., Wilson, W.D., 2005. Out-of-shape DNA minor groove binders: induced fit interactions of heterocyclic dications with the DNA minor groove. Biochemistry (Mosc.) 44, 14701–14708.

Midgley, I., Fitzpatrick, K., Taylor, L.M., Houchen, T.L., Henderson, S.J., Wright, S.J., Cybulski, Z.R., John, B.A., McBurney, A., Boykin, D.W., Trendler, K.L., 2007. Pharmacokinetics and Metabolism of the Prodrug DB289 (2,5-Bis[4-(N-Methoxyamidino)phenyl]furan Monomaleate) in Rat and Monkey and Its Conversion to the Antiprotozoal/Antifungal Drug DB75 (2,5-Bis(4-Guanylphenyl)furan Dihydrochloride). Drug Metab. Dispos. 35, 955–967.

Paine, M.F., Wang, M.Z., Generaux, C.N., Boykin, D.W., Wilson, W.D., De Koning, H.P., Olson, C.A., Pohlig, G., Burri, C., Brun, R., Murilla, G.A., Thuita, J.K., Barrett, M.P., Tidwell, R.R., 2010. Diamidines for human African trypanosomiasis. Curr. Opin. Investig. Drugs Lond. Engl. 2000 11, 876–883.

Patrick, D.A., Ismail, M.A., Arafa, R.K., Wenzler, T., Zhu, X., Pandharkar, T., Jones, S.K., Werbovetz, K.A., Brun, R., Boykin, D.W., Tidwell, R.R., 2013. Synthesis and Antiprotozoal Activity of Dicationic m-Terphenyl and 1,3-Dipyridylbenzene Derivatives. J. Med. Chem. 56, 5473–5494.

R. Wilkinson, S., Bot, C., M. Kelly, J., S. Hall, B., 2011. Trypanocidal Activity of Nitroaromatic Prodrugs: Current Treatments and Future Perspectives. Curr. Top. Med. Chem. 11, 2072–2084.

Saulter, J.Y., Kurian, J.R., Trepanier, L.A., Tidwell, R.R., Bridges, A.S., Boykin, D.W., Stephens, C.E., Anbazhagan, M., Hall, J.E., 2005. Unusual dehydroxylation of antimicrobial amidoxime prodrugs by cytochrome b5 and NADH cytochrome b5 reductase. Drug Metab. Dispos. Biol. Fate Chem. 33, 1886–1893.

Synthalin and Insulin, 1927. Science 65, x.

Thuita, J.K., 2013. Biological and pharmacological investigations of novel diamidines in animal models of human African trypanosomiasis. PhD thesis. University of Basel, Basel, Switzerland.

Thuita, J.K., Wang, M.Z., Kagira, J.M., Denton, C.L., Paine, M.F., Mdachi, R.E., Murilla, G.A., Ching, S., Boykin, D.W., Tidwell, R.R., Hall, J.E., Brun, R., 2012. Pharmacology of DB844, an Orally Active aza Analogue of Pafuramidine, in a Monkey Model of Second Stage Human African Trypanosomiasis. PLoS Negl. Trop. Dis. 6, e1734.

Thuita, J.K., Wolf, K.K., Murilla, G.A., Liu, Q., Mutuku, J.N., Chen, Y., Bridges, A.S., Mdachi, R.E., Ismail, M.A., Ching, S., Boykin, D.W., Hall, J.E., Tidwell, R.R., Paine, M.F., Brun, R., Wang, M.Z., 2013. Safety, pharmacokinetic, and efficacy studies of oral DB868 in a first stage vervet monkey model of human African trypanosomiasis. PLoS Negl. Trop. Dis. 7, e2230.

Turner, P.R., Denny, W.A., 1996. The mutagenic properties of DNA minor-groove binding ligands. Mutat. Res. 355, 141–169.

Tweats, D., Bourdin Trunz, B., Torreele, E., 2012. Genotoxicity profile of fexinidazole--a drug candidate in clinical development for human African trypanomiasis (sleeping sickness). Mutagenesis.

Ward, C.P., Wong, P.E., Burchmore, R.J., de Koning, H.P., Barrett, M.P., 2011. Trypanocidal furamidine analogues: influence of pyridine nitrogens on trypanocidal activity, transport kinetics, and resistance patterns. Antimicrob. Agents Chemother. 55, 2352–2361.

Wenzler, T., Boykin, D.W., Ismail, M.A., Hall, J.E., Tidwell, R.R., Brun, R., 2009. New treatment option for second-stage African sleeping sickness: in vitro and in vivo efficacy of aza analogs of DB289. Antimicrob. Agents Chemother. 53, 4185–4192.

Wenzler, T., Patrick, D.A., Yang, S., Braissant, O., Ismail, M.A., Tidwell, R.R., Boykin, D.W., Wang, M.Z., Brun, R., 2013a. In vitro and in vivo evaluation of 28DAP010, a novel diamidine for the treatment of second stage African sleeping sickness. Antimicrob. Agents Chemother. submitted.

Wenzler, T., Steinhuber, A., Wittlin, S., Scheurer, C., Brun, R., Trampuz, A., 2012. Isothermal microcalorimetry, a new tool to monitor drug action against Trypanosoma brucei and Plasmodium falciparum. PLoS Negl. Trop. Dis. 6, e1668.

Wenzler, T., Yang, S., Braissant, O., Boykin, D.W., Brun, R., Wang, M.Z., 2013b. Pharmacokinetics, T. b. gambiense efficacy and time of drug action of DB829, a preclinical candidate for treatment of second stage human African trypanosomiasis. Antimicrob. Agents Chemother. 57, 5330–5343.

Werbovetz, K., 2006. Diamidines as antitrypanosomal, antileishmanial and antimalarial agents. Curr. Opin. Investig. Drugs Lond. Engl. 2000 7, 147–157.

Wilson, W.D., Tanious, F.A., Mathis, A., Tevis, D., Hall, J.E., Boykin, D.W., 2008. Antiparasitic compounds that target DNA. Biochimie 90, 999–1014.

Acknowledgements

I am very grateful to Professor Reto Brun for giving me the opportunity to do this PhD thesis in his unit, the parasite chemotherapy and for his generous and continuous support and confidence. I also would like to express my gratitude to Professor Marcel Tanner, Professor Pascal Mäser, Professor James Ed. Hall for their support and Professor Pascal Mäser and Professor Simon Croft for joining my PhD committee.

Warm thanks to all present and former members of the parasite chemotherapy group in particular also Christiane Braghiroli and Guy Riccio for their technical help of the extensive in vivo experiments, Sonja Bernhard for information about the clinical outcomes of pafuramidine, and the members of the Consortium for Parasitic Drug Development (CPDD) for support and interesting and helpful discussions.

I am thankful to the Bill and Melinda Gates Foundation who funded this project through the Consortium for Parasitic Drug Development (CPDD) and the Swiss Tropical and Public Health Institute for any additional financial support of the current work.

And finally, I would like to thank all my friends especially Nicole Rathfelder for care and encouragement.

Curriculum Vitae

Name	Tanja Wenzler
Date and place of birth	22. 10. 1975, Wangen i. A. , Germany (D)
Nationality	German
Address	Rheinländerstrasse 17, 4056 Basel, Switzerland (CH)
Telephone	M: +41 78 829 83 84 W: +41 61 284 81 65
E-mail	tanja.wenzler@unibas.ch

Work experience (Biology)

Since 06/2003 Scientist at the Swiss Tropical & Public Health Institute in the department Medical Parasitology & Infectious Biology (MPI) in Basel, CH. Focus: Drug Discovery for African sleeping sickness.

In vitro and in vivo evaluation of diamidines for 2nd stage human African trypanosomiasis. Responsible for in vitro screening against different parasitic protozoa (*T. b. rhodesiense, T. b. brucei, T. b. gambiense. T. cruzi, P. falciparum*) and cytotoxicity studies. Organized in vivo screening using mouse models with different trypanosome infections; project management of novel aromatic diamidines, dihydroquinolines and other scaffolds for testing against African Sleeping Sickness (in vitro and in vivo), contacts to collaborating international scientists.

Grand Challenges Explorations: drug-induced differentiation of trypanosomes leads to elimination of infection. Established a trypanosome differentiation assay and organized screening of 7,500 compounds in the differentiation MTS within the Grand Challenge Explorations Phase I Project by BMGF.

Implemented a trypanosome differentiation HTS at GSK, Spain and screened 350,000 compounds within the Grand Challenge Explorations Phase II Project by BMGF.

Established a new methodology to monitor time of drug action on trypanosomes on a real time basis using isothermal micorcalorimetry.

Teaching activities

Held a 10 days trypanosome workshop at CDRI, India. Knowledge transfer of screening methods to Asian Institutes (Kitasato Insitute Japan, Institute Pasteur Korea, FRIM Malaysia, MIPN Malaysia, CDRI India) in the frame of Pan-Asian Screening Network sponsored by Drugs for Neglected Diseases initiative (DNDi). Student training at SwissTPH. Block course support and lecture in "Drug Discovery and Development for Parasitic Diseases"

Education (Biology)	Since 2010 **Cell Biology**, **PhD** at SwissTPH / University of Basel, in CH.
	09/2010 – 01/2014 PhD student at SwissTPH, MPI department, Parasite Chemotherapy unit in Basel, CH. Thesis title: In vitro studies and in vivo evaluation of novel diamidines for 2nd stage sleeping sickness.
	2009 – 2010 **Infection Biology**, **MSc** at SwissTPH / University of Basel, CH.
	09/2009 – 09/2010 MSc student at SwissTPH, MPI department in Basel. Thesis title: Pharmacophore model for pentamidine analogs active against *Plasmodium falciparum*.
	1998 – 2003 **Biotechnology**, **Dipl. Ing.** (FH) Engineering Diploma (MSc equivalent) at Mannheim University of Applied Sciences, in D.
	09/2002 – 05/2003 diploma student at Hoffmann La Roche, Dyslipidemia department in Basel, in CH. Thesis title: Functional analysis of the NBDs of the ABCA1 transporter.
	09/2000 – 03/2001 trainee at Scottish Crop Research Institute (SCRI), Virology department in Dundee, in U.K. Topic: Application of phage – display technology to immunoassay to the detection of a plant virus disease. 07/1999 – 09/1999 trainee at staatlichen Lehr- und Forschungsanstalt für Landwirtschaft, Weinbau und Gartenbau in Green Genetic Engineering, D.
Courses	Essentials in Drug Development & Clinical Trials. Radiation Protection course. GMP (Good Manufacturing Practice) in pharmaceutical quality assurance.
Work experience & Education (Grafics)	1995 – 1997 at Druck-Team-Lang and at Desk Top Publishing & Fotosatz GmbH, in Linau in D 1992 – 1995 apprenticeship as Druckvorlagenherstellerin (preparing printing materials), in the reproretouch area at BGSD Color Reproduktion GmbH, and at DGS Berg GmbH, in D.
Research Publications	43 peer reviewed publications in scientific journals
Research Presentations	8 poster and 18 oral presentations outside SwissTPH / University of Basel Poster price award at the congress Medicine and Health in the Tropics, in France (2005)
Research Conferences	Attended 9 international congresses and 8 specialized trypanosomatid meetings.